UNCLASSIFIED

AD 426290

DEFENSE DOCUMENTATION CENTER

FOR

SCIENTIFIC AND TECHNICAL INFORMATION

CAMERON STATION, ALEXANDRIA, VIRGINIA

UNCLASSIFIED

DEVELOPMENT OF MECHANICAL FITTINGS
● PHASES I AND II ●

Air Force Flight Test Center
Air Force Rocket Propulsion Laboratory
Edwards Air Force Base, California

Project No. 6753, Task No. 675304

NOTICES

Qualified requesters may obtain copies of this report from DDC.

DDC release to OTS is authorized.

FOREWORD

This report summarizes the research activities performed under USAF Contract No. 04(611)-8176, from April 1, 1962, to July 31, 1963. The research was performed by Battelle Memorial Institute under the auspices of the Air Force Rocket Propulsion Laboratory, Air Force Flight Test Center, Edwards Air Force Base, with Lt. P. Olekszyk and Mr. Roy A. Silver serving as project monitors. The principal investigators were J. W. Adam, J. C. Gerdeen, and B. Goobich, Research Engineers; E. C. Rodabaugh, Senior Research Engineer; W. A. Spraker, Staff Mechanical Engineer; and T. M. Trainer, Group Director.

ABSTRACT

The purpose of this program was to develop a family of improved lightweight mechanical fittings for service with rockets' fluid systems under stringent environmental and operating conditions. The work consisted of (1) a review of the design and use of present fittings for missiles, (2) a review of candidate materials for the required operating conditions, (3) the establishment of recommended classifications for improved fittings, (4) the development of a design procedure for flanged fittings, and the preparation of typical designs, and (5) the design, fabrication, and laboratory evaluation of a 1/2-inch threaded fitting. Three major conclusions were drawn from this program: (1) the reconnectable union should be either threaded or flanged; (2) the connection between the tube and the fitting should be a permanent joint made independent of the seal mechanism or the reconnectable union, and (3) a helium-tight disconnectable fitting which incorporates a yielding radial seal can be achieved in tubing sizes of 1-inch diameter and less.

The following recommendations were made for future work: (1) the comparative features of the outward-acting and the inward-acting radial seals should be investigated further, and the performance of the lightweight 1/2-inch threaded fitting made of René 41 should be evaluated; (2) a line of threaded René 41 fittings – unions, tees, elbows, and crosses – should be designed, fabricated, and evaluated; (3) 1/2-inch threaded fittings of a low-strength material, probably Type 347 stainless steel, should be designed, fabricated, and evaluated; (4) typical threaded fittings should be designed for two or three other materials and for a few combinations of likely materials; (5) selection criteria for threaded fittings should be established.

TABLE OF CONTENTS

TABLE OF CONTENTS
(Continued)

TABLE OF CONTENTS
(Continued)

TABLE OF CONTENTS
(Continued)

LIST OF FIGURES

vii

Page

LIST OF FIGURES
(Continued)

Page

LIST OF FIGURES
(Continued)

LIST OF FIGURES
(Continued)

LIST OF FIGURES
(Continued)

LIST OF TABLES

LIST OF TABLES
(Continued)

DEVELOPMENT OF MECHANICAL FITTINGS

INTRODUCTION

The need to develop reliable lightweight mechanical fittings for service with rocket and missile fluid systems has become important because of the severe problems of vibration, temperature, and chemical activity encountered in the present missiles. Future requirements will be even more severe and it is estimated that operating temperatures may be as high as 3000 F. The fittings currently in general use were developed specifically for use in aircraft hydraulic systems. Although the original designs have been significantly upgraded, the present fittings have not proven sufficiently reliable and it is recognized that a new generation of fittings must be developed. To achieve this end, the Air Force Rocket Propulsion Laboratory initiated a program whose objectives were (1) to design, develop, and fabricate a family of lightweight mechanical fittings that could effectively seal helium, and (2) to provide and prepare specifications, drawings, and test requirements for the fitting in such manner that military standards may be published.

Because no one connector design can satisfy the requirements of the complete range of temperatures, pressures, and fluids encountered in advanced missile systems, a basic requirement of this program was to identify and develop families and classes of fittings. It was also required that the designs considered should be new and unique where applicable and not restricted to modifications of present designs. This goal was to be attained through

(1) Use of new and unique concepts

(2) New methods of joining tubing and fittings

(3) Optimum combination of materials

(4) Effective use of manufacturing techniques.

In performing the required research, Battelle has developed new design procedures and new design concepts. The threaded-fitting concept as demonstrated in the laboratory promises to be a major contribution to the improvement of threaded fittings. Because of the general interest of the design community, Rocket Propulsion Laboratories invites the readers and reviewers of this report to make comments and to assist in further advancing the state of the art.

SCOPE AND OBJECTIVES OF PHASES I AND II

Phase I was to consist of an investigation of parameters such that classes and types of fittings could be chosen and preliminary designs could be initiated. The investigation was to begin with a literature survey of present technology and a materials review for determination of the most suitable materials.

Investigations were to be made of (a) satisfactory methods of joining tubing and fittings, (b) forces required to tighten and seal, (c) effects of thread form on torque relaxation, (d) effect of thread lubricant on sealing, thread galling, and torque relaxation, (e) the use of computer techniques to evaluate design criteria, and (f) methods to alleviate or eliminate the chances of human error in the assembly of fittings.

The preliminary design of proposed connectors was to begin concurrently or on conclusion of these investigations. A stress analysis was to be made of each type of fitting. Optimum operational service ranges were to be determined showing crossover points between threaded and flanged fittings. Maximum strength under operational conditions versus minimum weight was to serve as a major criterion.

Phase II was to consist of the detailed design of a representative fitting as established in Phase I, and a laboratory evaluation of its performance capabilities. It was mutually agreed with the project monitor that the laboratory evaluation would be conducted with a 1/2-in. threaded fitting designed for 2000-psi service with temperature extremes of -320 F and 600 F. The laboratory tests were to determine proof pressure, tightening allowance, temperature, repeated assembly, and operational capabilities. In addition, a section on the design of flanged connections was to be prepared for the Fluid Component Designers' Handbook being completed by Space Technology Laboratories.

REPORT ORGANIZATION

The preparation of this report constituted a considerable problem because of the large quantity of information that was assembled and created and because of the interrelation of many of the design areas. The format finally selected is an arrangement of subjects such that the reader can best understand the proposed concepts, the detailed designs, and the laboratory evaluation.

The first part, "Determination of Fitting Classes", outlines the requirements which determined the selection of candidate fitting materials, details the reasons for selecting the three recommended materials, and describes how the characteristics of the three selected fitting materials combined with certain operational and handling requirements define the recommended fitting classes. The fitting classifications affect many of the subsequent design decisions.

The next three parts discuss in detail the design thinking on improved mechanical fittings. Early in Phase I it was concluded that a reconnectable mechanical fitting could be made to seal helium satisfactorily only if the seal were not a part of the tubing, as is the case with the present flared and flareless fittings. The reasons for this conclusion are given elsewhere in the report. As a result of this decision, the fitting design was divided into three elements. While these elements were not entirely independent of each other, their aspects were sufficiently unique that during much of Phase I they were considered to be separate design problems. The three elements, as shown in Figure 1, are

- **The fitting-to-fitting connection,** a reconnectable union in the fitting which provides the necessary structural integrity

- **The tube-to-fitting connection,** a permanent transition connection between the fitting and the piping.

- The **seal,** a metallic disposable seal independent of the structural connections except for the seal seating surface.

The design thinking is presented in this report in terms of these individual elements for two reasons: (1) they provide excellent means of discussing the many design aspects of the fitting in a systematic manner, and (2) the conclusions and recommendations concerning each element are different and more easily formulated when considered independently.
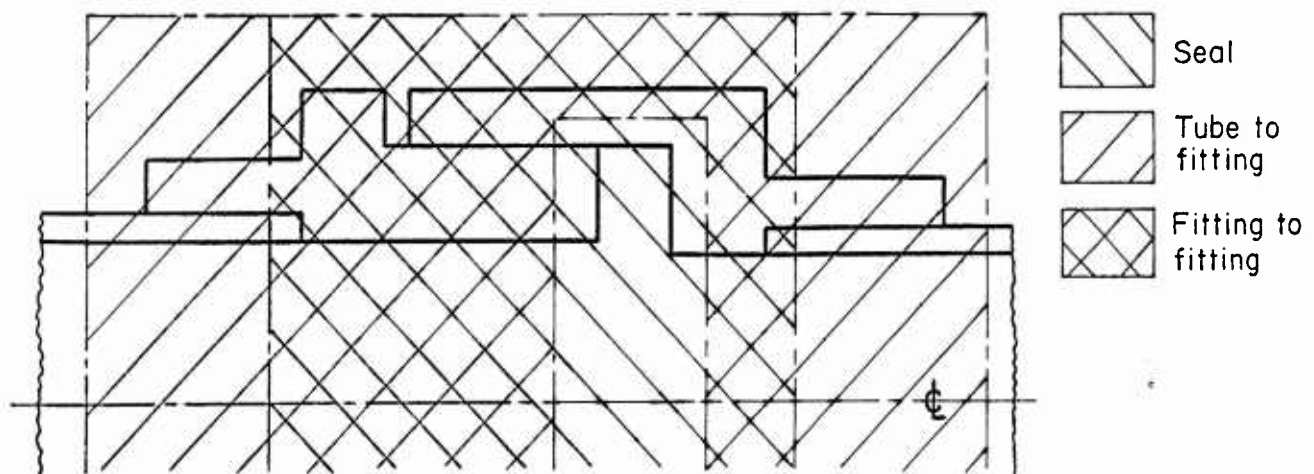
A-43889

FIGURE 1. DESIGN ELEMENTS OF A TOTAL FITTING

The fitting-to-fitting design is discussed first of the three because it provides the opportunity also to discuss many of the design problems which affect two or all three elements. This part also presents recommended design procedures and detailed designs for flanged and threaded connections. The tube-to-fitting design is discussed next because many of the loads described for the fitting-to-fitting connection apply also to the tube-to-fitting problem. Finally, the seal-design discussion is given. While the section on the seal design is the most important design section, it is presented last because the sealing problems can best be appreciated and the recommended seal designs best understood after the other aspects of the fitting have been discussed.

The fifth part of the report contains a description of the 1/2-inch threaded fitting which was fabricated, and the laboratory evaluation of its performance capabilities.

The final part of the body of the report is the "Summary of Recommendations". Although many specific conclusions and recommendations are presented in most of the major sections, the more important ones are summarized at the end of the report for convenience.

Nine appendixes contain important and pertinent information of two types: (1) information which is back-up material for discussions in the report body, and (2) selected detailed information pertaining to the program.

DETERMINATION OF FITTING CLASSES

General Service Requirements

Materials Selection

Assembly Torque

Recommended Fitting Classes

References

DETERMINATION OF FITTING CLASSES

To achieve minimum weight in a missile piping system, each fitting and component should be designed on the basis of the exact operating requirements for that particular component. Even if these requirements were known at every point in the system, such a procedure would be impractical because of the excessive expenditure of time and money. Fortunately, if the smaller fittings are designed within certain ranges of selected parameters, the production and logistics problems are reduced considerably, and the weight penalty is small. The most significant parameters considered in determining the recommended fitting classes were (1) general service requirements, (2) materials selection, and (3) assembly torque.

General Service Requirements

The general service requirements applicable to missiles' and rockets' fluid systems are shown in Table 1. It was agreed between Air Force Rocket Propulsion Laboratory and Battelle that the problems of developing a satisfactory fitting for up to 1500 F were sufficiently difficult that the upper design temperature at least for Phase I would be limited to 1500 F.

TABLE 1. GENERAL SERVICE REQUIREMENTS

Service	Pressure Range, psi	Temperature Range, F	Dimensional Range, inches
Propellant	0 to 1,500	-425 to 200	1 to 16
Pneumatic	0 to 2,000	-425 to 200	1/8 to 1
	0 to 10,000	-425 to 600	
	0 to 4,000	-425 to 1500	
Hot Gas	0 to 1,500	1000 to 3000	1 to 3

As presented in the table, the breakdown by fluids established natural "families" of fittings. However, within each family further classification was necessary. This was especially true for propellant and hot-gas systems where operating pressures may be much less than the maximum values stipulated.

Materials Selection

The selection of the fitting materials was determined largely by the mechanical properties of the materials and by the compatibility of the materials with the fluid media. In a few cases other considerations, such as machinability, governed. Since it would be impractical to review all of the candidate materials in detail, the characteristics of the classes of materials that were considered are discussed in general terms. The selected materials are subsequently described in some detail.

Materials Considered

General groupings of candidate materials and the major characteristics of the groups are discussed below.

Low-Density Materials. The low-density materials include the aluminum, magnesium, and titanium alloys. Even though the aluminum and magnesium alloys have a very low density, the low strengths and their tendency to lose strength drastically as temperature is increased above about 300 F, make them undesirable. Compatibility with missile propellants is also a severe limitation.

Titanium, which has good mechanical properties up to about 600 F, is generally not acceptable for service with oxidizers.

300 Series Stainless Steels. The 300 series stainless steels are easy to machine and fabricate, and are almost universally compatible with the fluids considered. However, because of their relatively low yield strength-to-density ratio it is not possible to design a lightweight fitting which can satisfy the operational limits specified in Table 1. Strength can be increased to some degree by cold working, but this increase is marginal when the final strength is compared with that of the age-hardenable stainless steels and other alloys discussed below. At temperature conditions exceeding 1000 F, the 300 series alloys are too sensitive to creep to be practical for this application.

400 Series Stainless Steels. The 400 series stainless steels have a good combination of physical properties over the temperature range of interest. They are easily fabricated, and are available in production quantities. However, the heat treatment required includes an oil or water quench, or at least a rapid cool, from temperatures of 1760 to 1850 F. This procedure causes distortions in the fitting that could be detrimental to the sealing surface.

High-Strength Tool Steels. The high-strength tool steels of the H-11 type, such as Potomac M, are difficult to weld and have poor corrosion resistance. Hence, they are not considered candidate materials.

Maraging Steels. The 18Ni-Co-Mo maraging steels possess extremely high strengths. However, these steels are still under development. Most work to date has emphasized ambient applications, and no compatability data are available. Also, because they are new, their availability is limited. For these reasons, they have not been considered further.

Nickel- and Cobalt-Base Metals. This category includes materials such as Haynes 25, Inconel "X", and René 41, all of which are considered possible choices. Of this group, René 41 has the best combination of properties over the temperature range of interest.

Age-Hardenable Stainless Steels. The precipitation-hardenable stainless steels include 17-7PH, PH 15-7 Mo, AM-350, 17-4PH, AM-355, and A-286. Of these, 17-7PH, PH 15-7 Mo, and AM-350 are not available as bar stock or plate and hence cannot be considered. 17-4PH, AM-355, and A-286 are available as plate and bar stock.
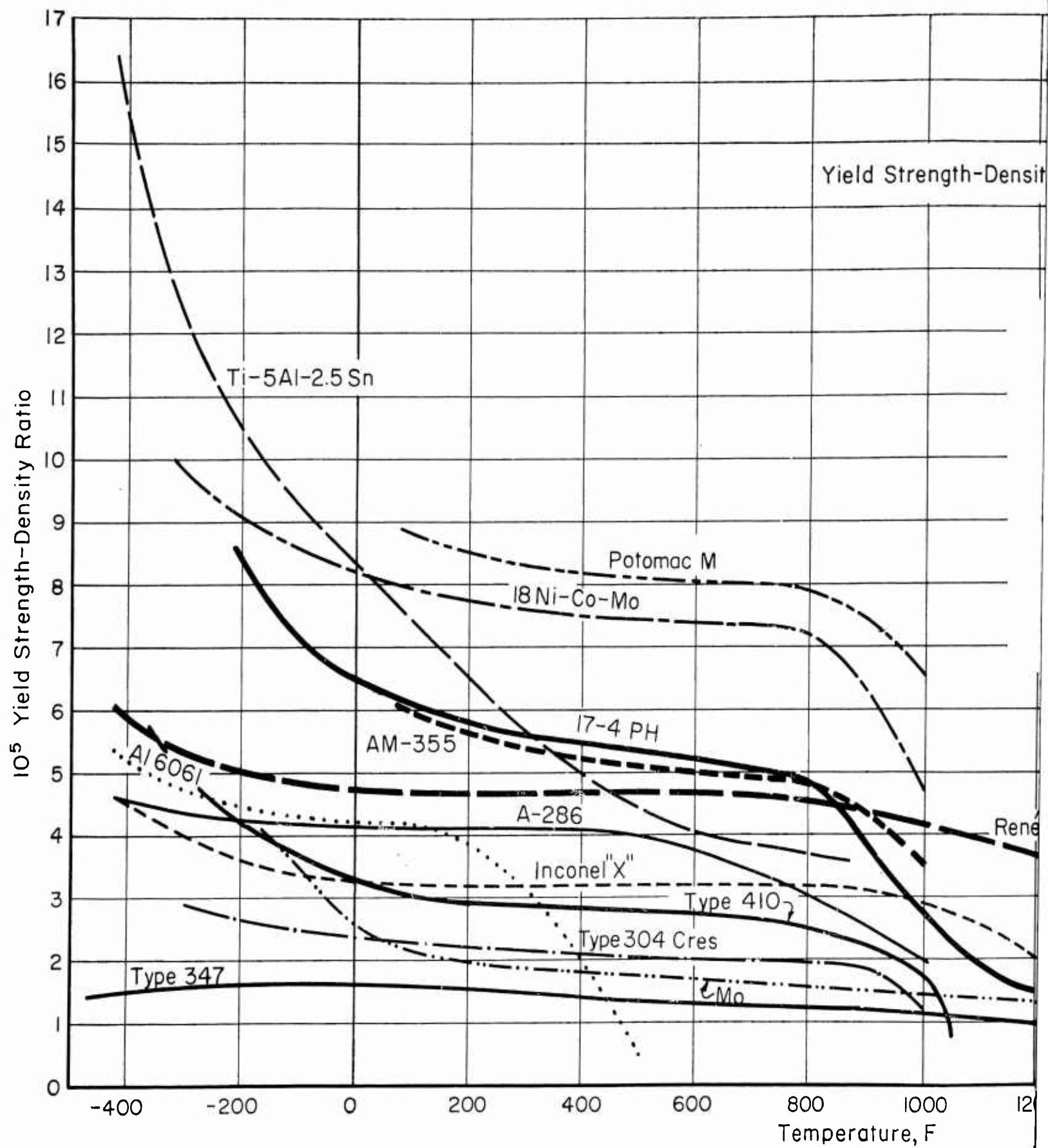
FIGURE 2. YIELD STRENGTH-DENSITY RATIO OVER SERVICE TEMPERATURE
RANGE

Yield Strength-Density Ratio = $\dfrac{0.2\% \text{ Offset Yield Strength, psi}}{\text{Density, lb/cu in.}}$

Legend

Material Group	Material
Low-density alloys	Al 6061, Ti-5Al-2.5Sn
300 series stainless steels	Type 347
	Type 304 Cres
400 series stainless steels	Type 410
High-strength tool steel	Potomac M
Maraging steel	18 Ni-Co-Mo
Ni-Co alloys	René 41, Inconel "X"
Age hardening	A-286, AM-355, 17-4PH
Refractory	Mo

tomac M

PH

René 41

Type 410

304 Cres

Mo

Temperature, F

600   800   1000   1200   1400   1600   1800   2000   2200

C-43890

TEMPERATURE
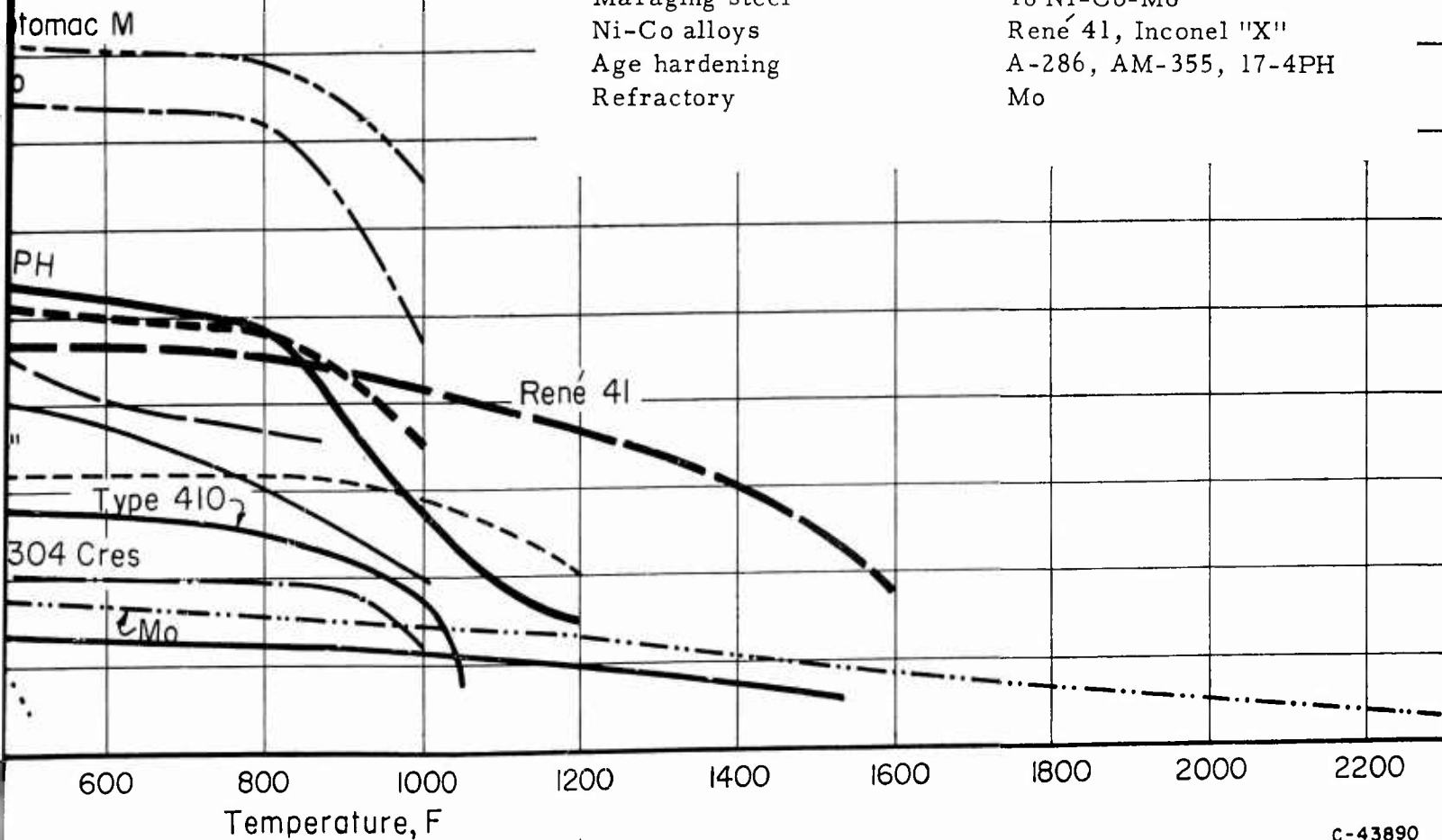
One important characteristic for design purposes is a low thermal expansion. Because of the martensitic structure of 17-4PH and AM-355 in the hardened condition, their coefficient of thermal expansion is approximately 60 per cent of the coefficient of the austenitic types such as A-286, 17-10P, and HNM.

The high strength/density ratio available over the temperature span of interest and the extensive experience developed by the aircraft and missile industries in the use of 17-4PH and AM-355 also help to make these alloys good choices.

Refractory Metals. Refractory metals such as tungsten, molybdenum, and tantalum are brittle, heavy, and hard to fabricate. Even so, the refractory metals are the best metals available for use at 1800 to 3000 F. However, they must be coated for oxidation and embrittlement protection. Except for applications at extremely high temperatures, they do not appear as promising as the other materials listed above.

Materials Selected

The three materials chosen as being most applicable are René 41, AM-355, and 17-4PH. Although there are a few fluids with which these materials are not compatible, they are considered to have the best combination of properties over the temperature range considered. They are produced by several companies; availability is not a problem. Considerable interest in these materials by the aircraft and missile industries in the last few years has resulted in much experience and data that can be used for design purposes.

These materials are harder to weld and fabricate than the 300 series stainless steels, but several companies are presently developing acceptable welding procedures.

Mechanical Properties

Materials used in mechanical fittings should have (1) a high yield strength-to-density ratio as a function of temperature, (2) creep resistance at elevated temperatures, and (3) low notch-sensitivity at cryogenic temperatures. In general, the yield strength, tensile strength, and elastic modulus of a given alloy decrease as temperature increases. As the temperature decreases, these properties increase, but the ductility and fracture toughness tend to decrease.

Yield Strength-to-Density Ratio. When weight is important, the yield strength-to-density ratio versus temperature curve is a major design criterion. Figure 2 shows these curves for the materials selected. Also, curves for some of the other materials considered are included for comparison.

The effect of the strength-to-density ratios on fitting weight can be illustrated by a simple example in which bending loads are not considered. If it is assumed that a missile contains 300 fittings having an average weight of 1 pound each when made from A-286, the total weight per missile would be 300 pounds. As shown in Figure 2, the yield-strength-to-density ratio at 200 F for Inconel "X", A-286, René 41, and 17-4PH is 3.2, 4.1, 4.7, and 5.8 x 10^5 respectively. Fabricating the 300 fittings from Inconel "X"

would increase the total weight to 383 pounds. When fabricated from René 41 and 17-4PH the total weight would decrease to 262 and 212 pounds respectively. The total fitting weight therefore could be reduced by more than 29 per cent if 17-4PH were used instead of A-286. At high temperatures, above 800 F, the comparison of yield strength-to-density ratio is also important even though the strength of materials decreases markedly as temperature increases, because the change is different for each metal.

Creep. Although the creep rate of metals is generally disregarded at temperatures less than 800 F, it increases rapidly as temperatures exceed 800 F. For most materials there is some temperature at which the creep resistance or stress-to-rupture strength becomes less than the tensile yield strength, and hence the creep resistance rather than the yield strength must be used as the design basis.

Because the factors governing tubing design in a fluid system also are major factors governing the design of a fitting for that system, the time and temperature dependency of the fitting weight can be illustrated by considering the time and temperature dependency of the tubing. The curve in Figure 3, tube weight versus temperature, is based on a 2-inch length of 2-inch outside-diameter tube of René 41 for a pressure of 1500 psi and a life of 1000 hours. The creep strength for René 41 becomes the controlling strength factor at about 1100 F, as evidenced by the change in slope. The curve in Figure 4 represents tube weight versus time for a 2-inch length of 2-inch outside diameter tubing of René 41 for a pressure of 1500 psi and a temperature of 1500 F. From these curves it is apparent that either a decrease in temperature or a decrease in service-life requirement would result in a significant weight saving. Thus, it is important that the expected service temperature and desired life be known to achieve an optimum design.

Creep and stress-to-rupture data at elevated temperatures are commonly available for all of the materials listed in the preceding section. The two best materials are René 41 and Inconel "X". AM-355 and 17-4PH are likely to become embrittled when kept at temperatures above 700 F and hence should be restricted to 600 F service for missile fittings.

Notch Sensitivity. At cryogenic temperatures, one of the most important considerations is the material's fracture toughness or its ability to fail in a ductile manner when notches are present. This property, which can be measured by impact tests or by center-notch tensile tests, decreases rapidly with decreasing temperatures.

Because of the high stress levels dictated when designing for minimum weight, and because of the importance of fracture toughness, the effects of intrinsic defects (flaws, inclusions) and manufacturing defects (surface scratches, designed notches, welds) must be considered at cryogenic temperatures, even though such imperfections do not cause problems at "normal" temperatures. An Air Force technical manual[1]* states that "metals with a minimum impact resistance of 15 ft-lb Charpy keyhole notch, or 18 ft-lb Izod V-notch are generally suitable for cryogenic service". However, there are many versions of impact tests; specifications have not been established to govern the evaluation at cryogenic temperatures, and minimum acceptable values have not been established for each of the various tests.

*References are listed on page 22.

10
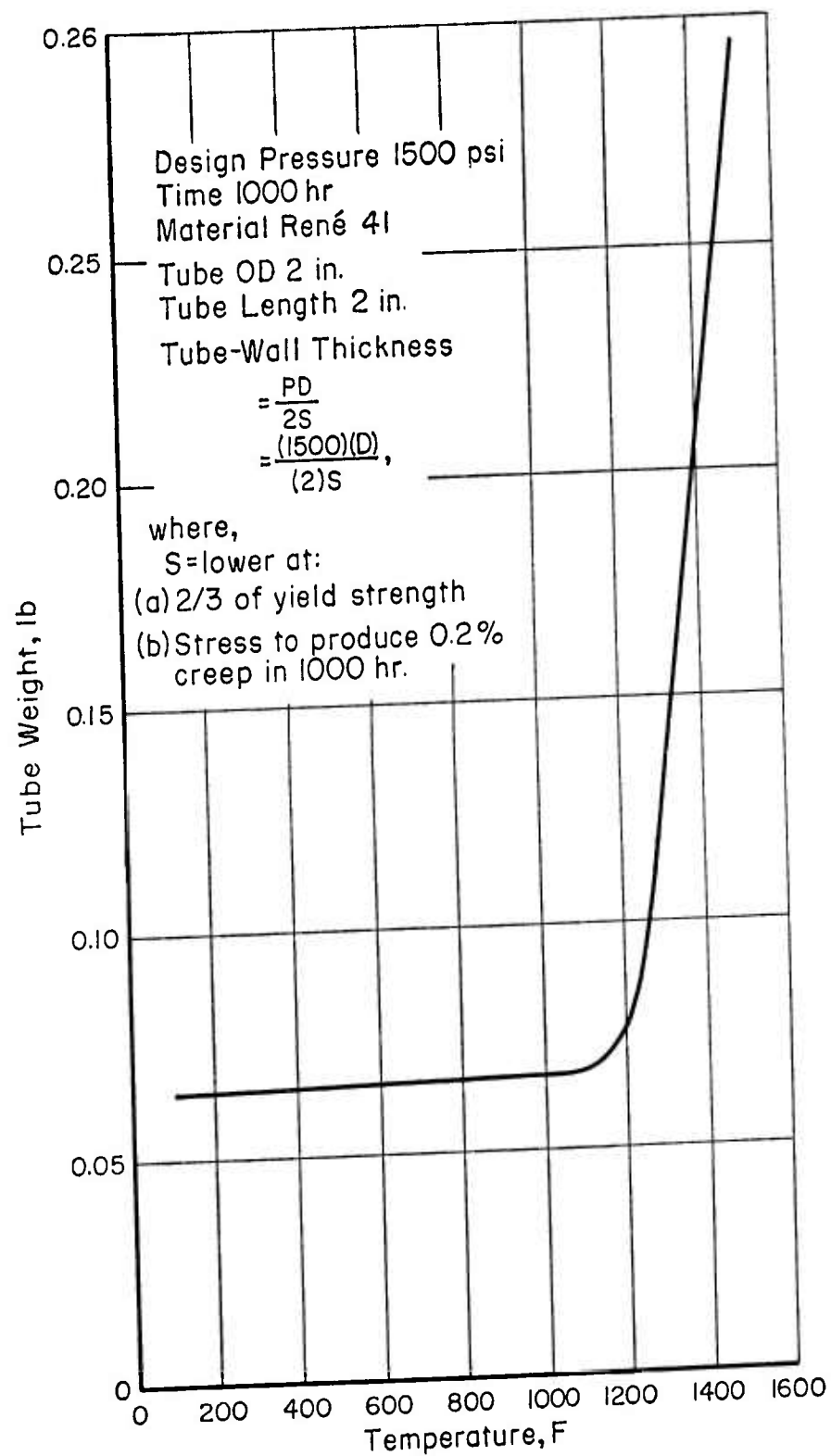
FIGURE 3. TUBE WEIGHT VS. TEMPERATURE

11
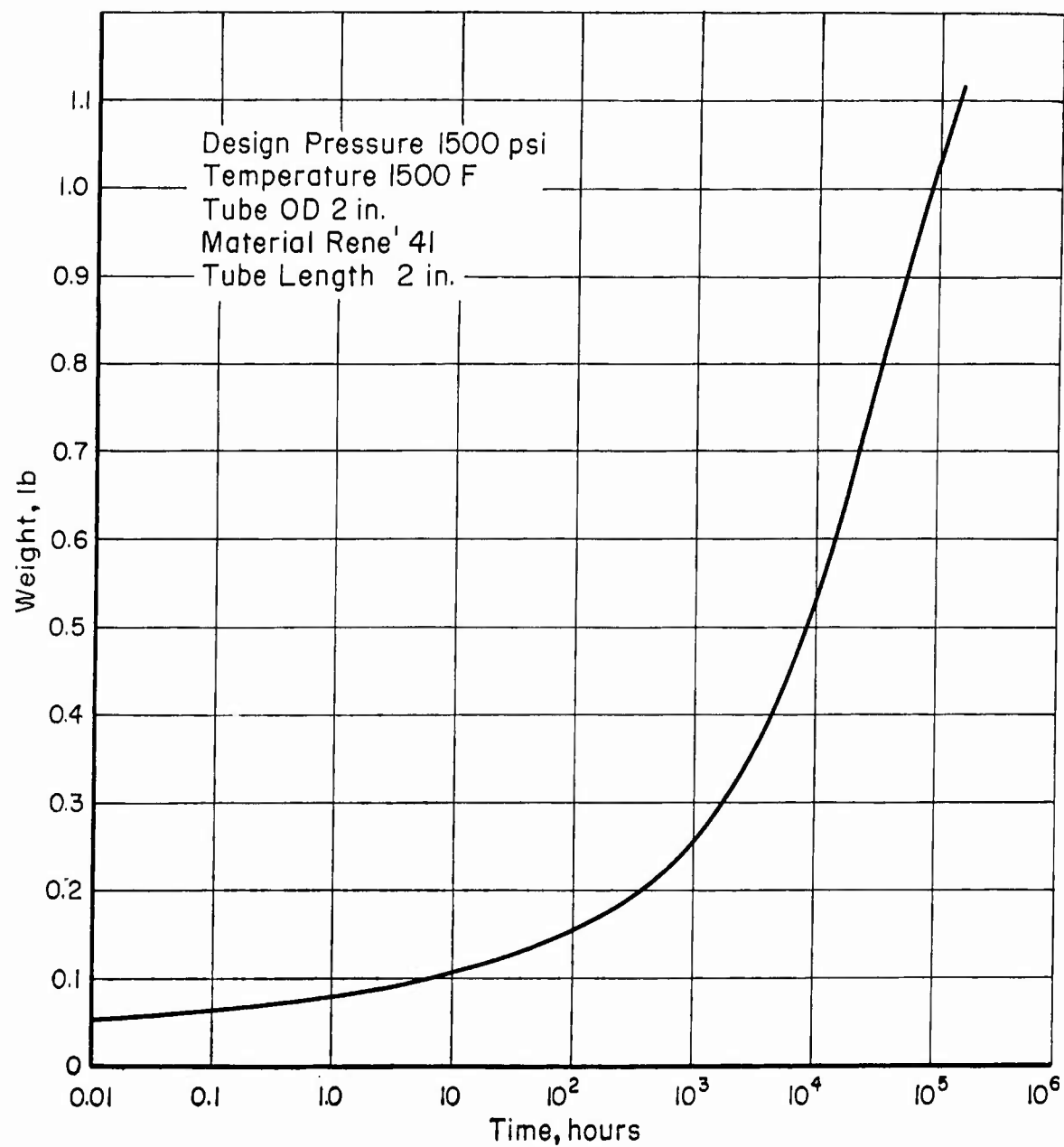
FIGURE 4. TUBE WEIGHT VS. TIME

The notched/unnotched tensile ratio-vs.-temperature curves given in Figure 5 show a sharp decrease in the notched/unnotched ratio below -100 F for AM-355 as compared to an almost constant value for René 41. The tendency for the notched-unnotched tensile ratio to drop rapidly as temperatures are decreased is typical for martensitic materials. It appears on the basis of available data that this is true of 17-4PH as well. On the basis of this curve, and because there is a lack of definitive data specifying minimum acceptable values, the lower service temperature for AM-355 and for the comparable material 17-4PH has been set at -100 F.

Fluid Compatibility

The fluids considered in this program and their useful temperature ranges are shown in Figure 6. As shown by Figure 6, the fluids could be divided into two groups on the basis of minimum service temperature. It was noted that the lower temperature extreme for Group A was approximately equal to the lower design-temperature (-100 F) limit for AM-355 and 17-4PH.

A summary of the compatibility data found for the compatibility of AM-355, 17-4PH, and René 41 with the fluids is given in Table 2. Compatibility data for these three materials with propellants are generally scarce and are nonexistent for some combinations. Also, many of the available data are contradictory. Therefore, estimates of the compatibility with some fluids have been extrapolated on the basis of data for other materials with similar chemical compositions. The following conclusions can be made on the basis of the data in Table 2:

(1) AM-355 is acceptable for general service with the majority of fluids.

(2) 17-4PH is acceptable for general service with the majority of fluids. It is unsatisfactory for use with hydrazine and MMH at all temperatures.

(3) René 41 is acceptable for general service with the exception that no data were found for hydrazine, 50 UDMH/50 hydrazine mixtures, and MMH. It is unsatisfactory for use with hydrogen peroxide.

Other data collected during the program indicate that the 18-8 type stainless steels are possible materials of construction for use with UDMH, UDMH/hydrazine mixtures, MMH, and hydrogen peroxide, as are many of the aluminum alloys.

Conclusions

Three materials were selected for minimum-weight fittings. René 41 can be used for the entire temperature range, -423 to +1500 F, whereas AM-355 and 17-4PH are restricted to the limits of -100 and 600 F. Within the narrower range, use of AM-355 or 17-4PH would result in a lighter fitting than would use of René 41. Also, both AM-355 and 17-4PH are more readily available and cost less than René 41. Although Type 347 stainless steel is widely used in this limited temperature range, a comparison of the yield strength-to-density ratio of Type 347 with that of AM-355 or 17-4PH (Figure 2) shows that a weight penalty might result if it were used. It is recognized that Type 347 is more readily available, is more easily machined, and has excellent compatibility. However minimum weight is considered to be a more critical selection criterion when designing for missile applications. Therefore, when considering the choice of materials three temperature service ranges are identifiable and three materials appear to be the best choice for these temperature ranges:

13
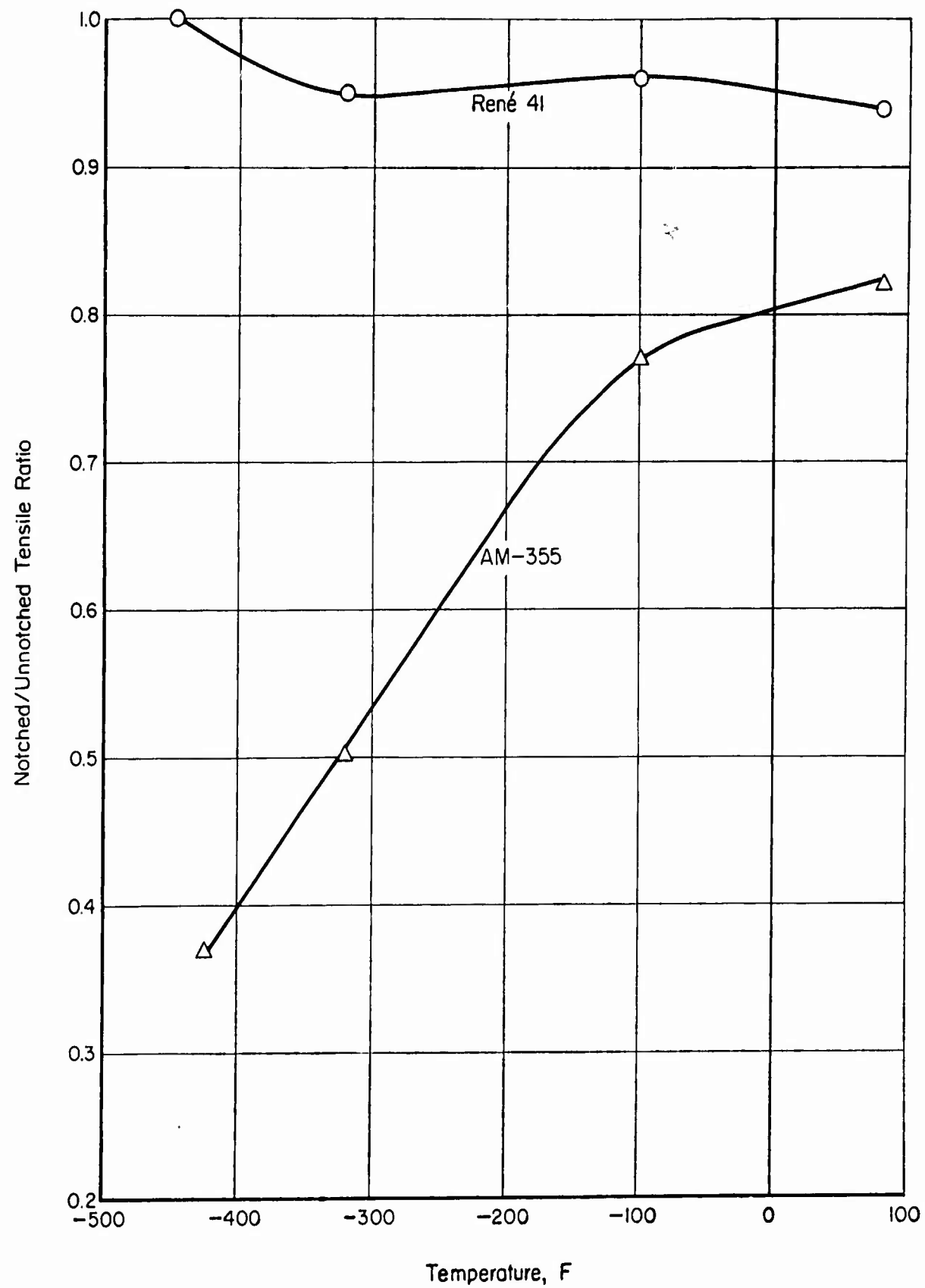
FIGURE 5. NOTCHED (K_t=6.3)/UNNOTCHED TENSILE RATIO VS. TEMPERATURE (TRANSVERSE)

Source: References (2) and (3).

14
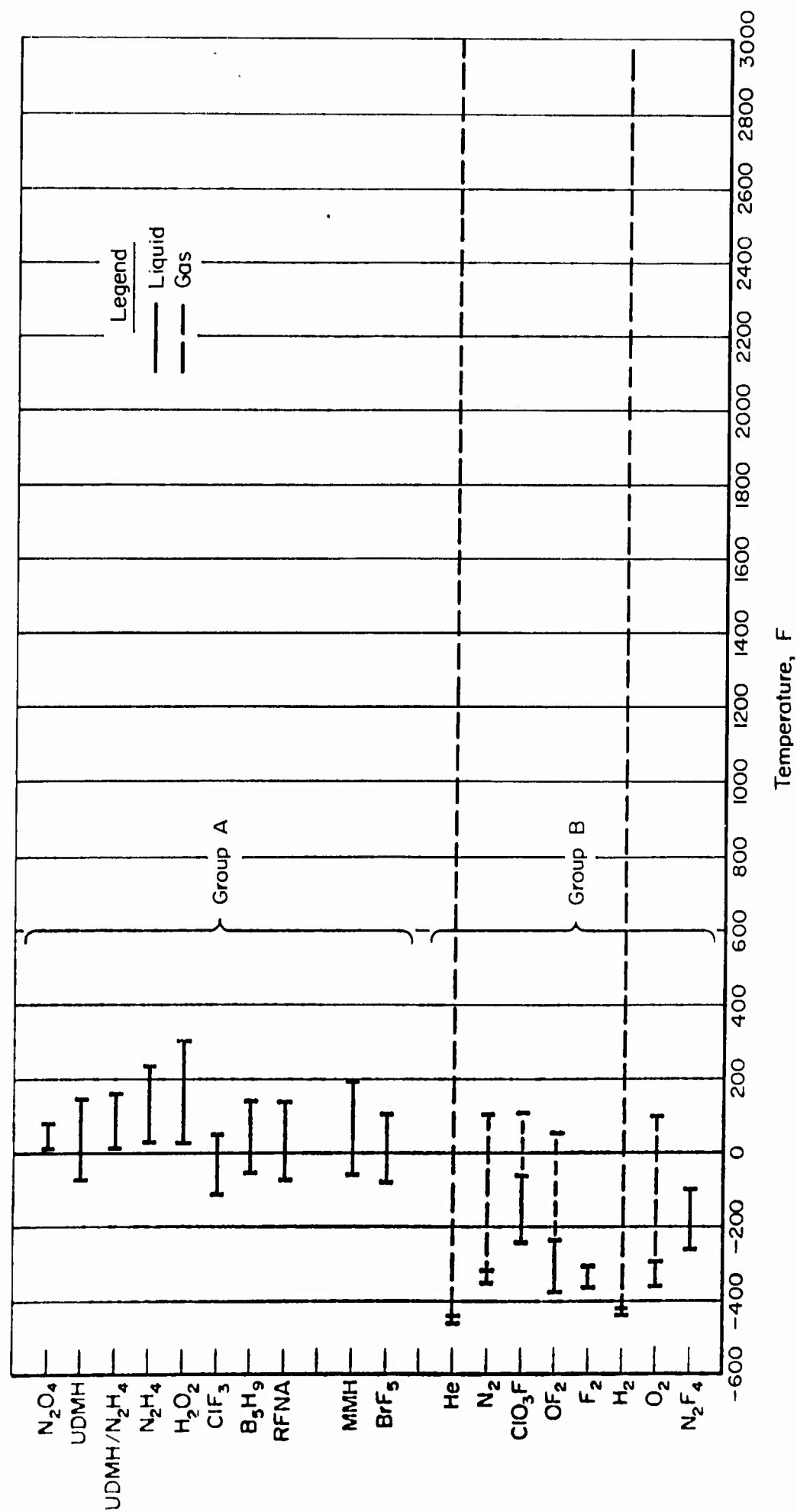
FIGURE 6. USEFUL TEMPERATURE RANGES OF FLUIDS

15

TABLE 2. SUMMARY OF FLUID-COMPATIBILITY DATA

Propellants	AM-355	17-4PH	René 41
		Group A	
N_2O_4	General service at 100 F[4] General service at 65 F[5] General service[6]	General service at 100 F[4] General service at 65 F[5] General service[6]	General service based on Inconel, nickel, and stainless steels if the N_2O_4 is dry[5]
UDMH	General service at ambient temperature[7]; limited service below 160 F[6]	General service at ambient temperature[7]; limited service[6]	Limited service at ambient temperature[7]; general service up to 85 F[8]
N_2H_4	Limited service below 160 F[6]	Unsatisfactory[6]	No data
50 UDMH/50 N_2H_4	Not usable at >160 F[7] General service at 160 F[4] General service at 160 F[5] Limited service below 160 F[6]	Limited service at 160 F[7] General service below 160 F[4] General service below 160 F[5] Limited service[6]	No data
H_2O_2	Limited service[7] Limited service 151 F[9]	Limited service 151 F[9]	Unsatisfactory based on other nickel- and Mo-containing alloys[8]
ClF_3	General service at ambient temperature based on AM-350 and mild steel	General service at ambient temperature based on AM-350 and mild steel	General service[6] General service at 80 F[10]
RFNA	Unsatisfactory above 130 F, based on 17-7PH[10]	Unsatisfactory above 130 F, based on 17-7PH[10]	Probably unsatisfactory at all temperatures[10]
WFNA	No data	No data	Unsatisfactory at all temperatures[10]

16

TABLE 2. (Continued)

Propellants	AM-355	17-4PH	René 41
MMH	Metals containing 0.5% Mo, Cu, limited service below 160 F[6]	Alloys cannot be used[7] Unsatisfactory[6]	No data
BrF_5	Probably the same as ClF_3	Probably the same as ClF_3	General service[6] General service[10]
RP_1	General service	General service	General service
		Group B	
O_2	General service down to -100 F based on mechanical properties	General service down to -100 F based on mechanical properties	General service in liquid oxygen[7]
NF_3	General service, liquid, based on stainless steel[7]	General service, liquid, based on stainless steel[7]	General service, liquid and vapor, based on compatibility with nickel and carbon steel[7]
PB	No metals are known to be incompatible at room temperatures and pressures[7]		
He	General service to 1500 F[a]	General service to 1500 F[a]	General service to 1500 F
N_2	General service to about 1300 F, at which temperature nitriding may be severe, depending upon exposure time[11][a]	General service to about 1300 F at which temperature nitriding may be severe, depending on exposure time[11][a]	General service to 1500 F[12]
ClF_3	General service to 160 F, based on stainless steel and mild steel[10]	General service to 160 F, based on stainless steel and mild steel[10]	General service to 160 F, based on nickel and nickel alloys[10]

17

TABLE 2. (Continued)

Propellants	AM-355	17-4PH	René 41
OF$_2$	General service at ambient temperature based on stainless steel and mild steel; probably general service at higher temperatures(13)	General service at ambient temperature based on stainless steel and mild steel; probably general service at higher temperatures(13)	General service at ambient temperature based on stainless steel and nickel; probably general service at higher temperatures(13)
F$_2$	General service to 400 F based on 300 and 400 series stainless steels(10)	General service to 400 F based on 300 and 400 series stainless steels(10)	General service to 600 F based on 300 series stainless steel and nickel
H$_2$	Not usable in liquid H$_2$(7) General service above -100 F (based on mechanical properties)	Not usable in liquid H$_2$(7) General service above -100 F, based on mechanical properties	General service, liquid H$_2$

(a) Temperatures specified pertain to fluid compatibility only. For recommended operating temperatures see Table 3.

18

(1) -100 to 600 F: Recommended materials: AM-355 and 17-4PH

(2) -425 to 600 F: Recommended material: René 41

(3) -425 to 1500 F: Recommended material: René 41

Above 1500 F it will probably be necessary to use a refractory material, although René 41 can be used for short-life fittings up to 1800 F.

Assembly Torque

A torque of 2000 in-lb has been chosen as a reasonable limit for individual threaded assemblies whether they are threaded connectors or nut-and-bolt assemblies. Torque is determined by the amount of preload needed to assure the sealing and structural integrity of the fitting during the expected service life. Preliminary analysis summarized in a later discussion, indicates that all propellant and hot-gas fittings should be flanged connections. Threaded connections can be used up to 1-in. size for pneumatic service up to 2000 psi and 600 F. For service at 10,000 psi - 600 F, or 4000 psi - 1500 F, the apparent limit for threaded connections is the 3/4-in. size.

Recommended Fitting Classes

Based on the above considerations, five fitting classes are recommended, as shown in Table 3.

TABLE 3. RECOMMENDED FITTING CLASSES

Class	Temperature, F	Maximum Design Pressure, psi	Size, in.	Service	Type of Connection	Material
Ia	-100 to 600	2000	1/8 to 1	Pneumatic	Threaded	AM-355 or
b[b]	-100 to 200	1500	1 to 16	Propellants A[a]	Flanged	17-4PH
IIa	-425 to 600	2000	1/8 to 1	Pneumatic	Threaded	René 41
b[b]	-425 to 200	1500	1 to 16	Propellants A and B	Flanged	René 41
IIIa	-425 to 600	10,000	1/8 to 3/4	Pneumatic	Threaded	René 41
b	-425 to 600	10,000	3/4 to 1	Pneumatic	Flanged	René 41
IVa[c]	-425 to 1500	4000	1/8 to 3/4	Pneumatic	Threaded	René 41
b	-425 to 1500	4000	3/4 to 1	Pneumatic	Flanged	René 41
V	1000 to 3000	1500	1 to 3	Hot gas	Flanged	Refractory

(a) The propellants are distinguished by two groups, as given in Figure 6.

(b) For large sizes where true maximum operating pressure is less than 1500 psi, a design on the basis of actual service pressure would result in a significant weight savings. Designs presented in this report are rated at maximum pressures.

(c) Fittings operating at higher temperatures (above 800 F) must be further qualified according to service life.
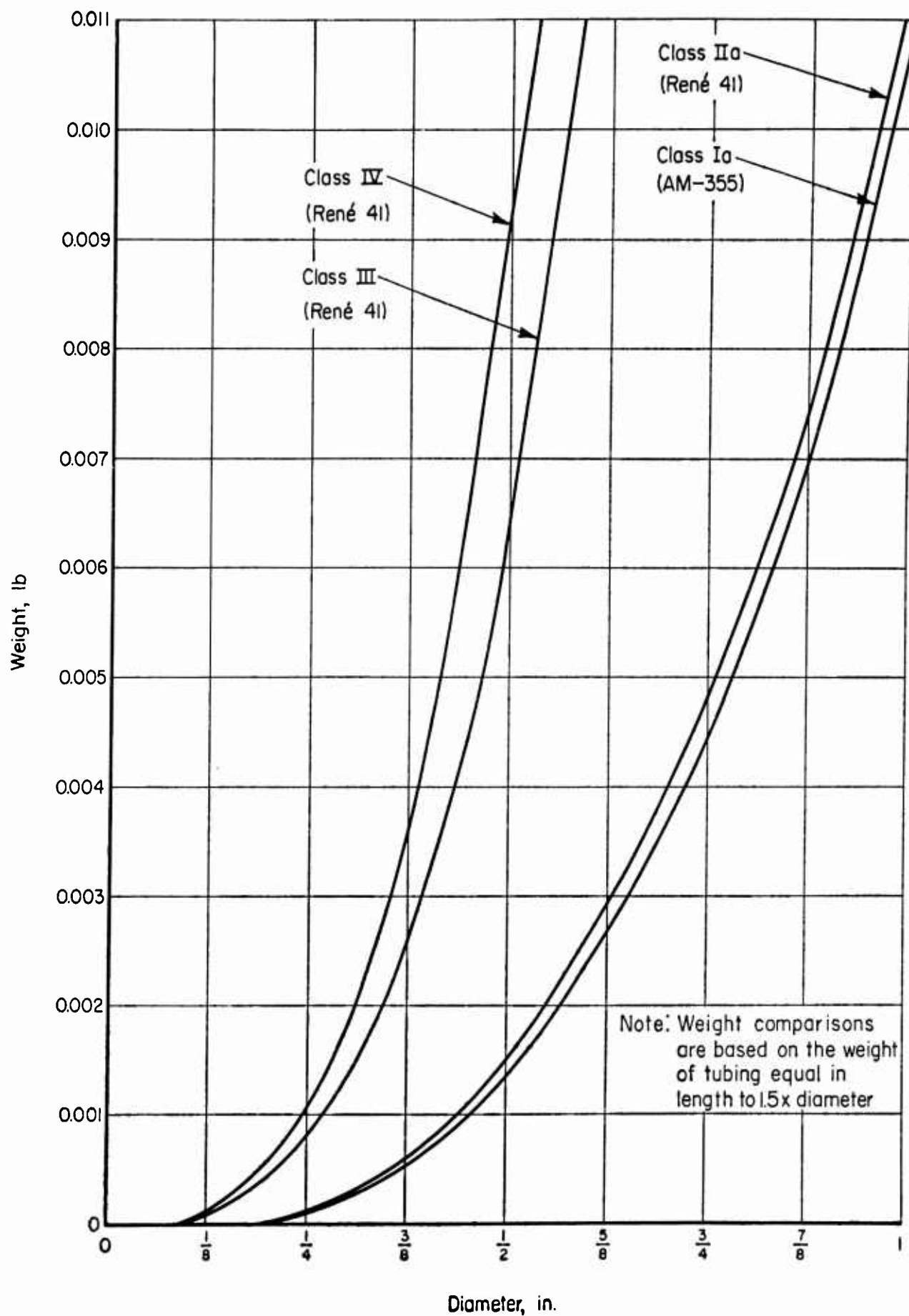
FIGURE 7. WEIGHT COMPARISON OF THREADED FITTING CLASSES

Class I is distinguished from Class II by the lower temperature limit, which allows for use of AM-355 or 17-4PH alloys. The high-pressure and high-temperature fittings are separated into Classes III and IV, on the basis of maximum service temperature. The Class IV fittings must be designed for a specified service life because of creep. Weight comparisons based on equivalent tube lengths (Figure 7) show that a 1/2-in. Class IV fitting may be 46.5 per cent heavier than a 1/2-in. Class III fitting. A 1-in. Class IIa fitting may be 4.7 per cent heavier than a 1-in. Class Ia fitting. However, the total weight increase per fitting may amount to less than 0.01 pound. Therefore, a class simplification is possible if these additional weights are not considered to be a severe penalty.

Classes III and IV are subdivided because of the 2000 in-lb torque limitation. It does not appear possible to overcome this limiting factor since the torque requirement for the 3/4 to 1-in. range is beyond a reasonable expectation of a man's capability with reasonable wrench lengths.

Although Classes Ib and IIb are designated, it is not recommended that discrete classes be established for large fittings. Instead a rigorous design procedure based on specific types of flanges should be developed as the controlling design specification. The flanges to be considered as the basis for this design procedure should be of the types illustrated in Figure 8. It may appear that this will complicate the logistics problem, but it should be noted that only a few large pipe fittings are used on each missile and that they vary significantly with missile type. Once a fitting is designed for a particular missile system, that fitting will probably be assigned a specific part number and can be ordered and stocked in appropriate quantities by that part number.

a Weld · Neck Flange   b. Ring Flange   A-44362
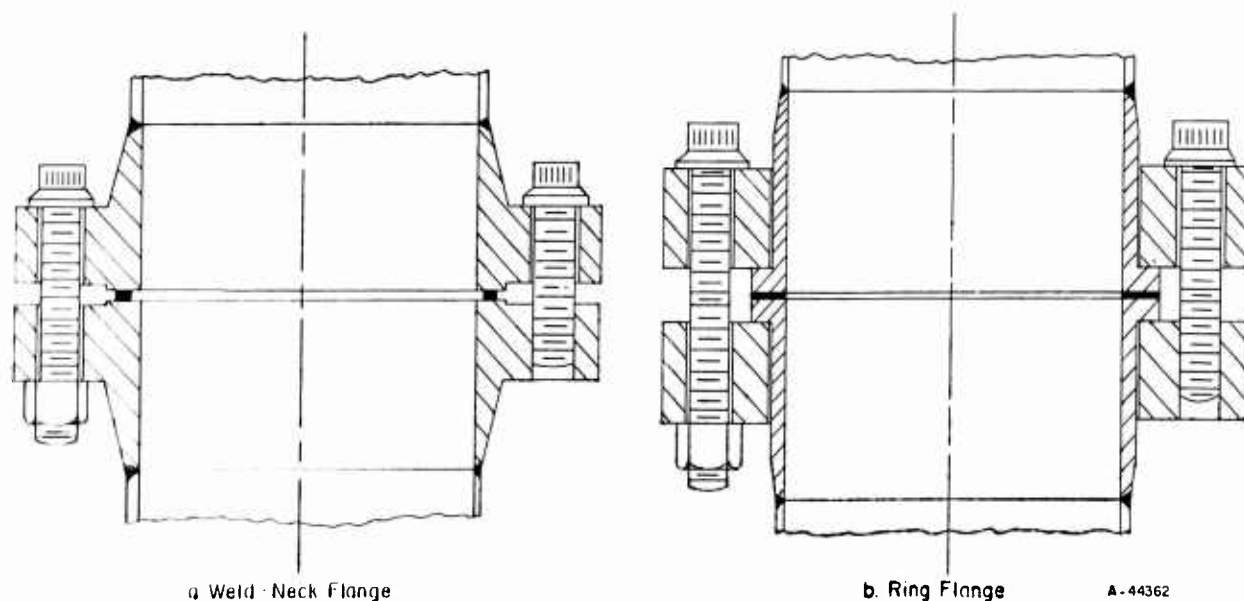
FIGURE 8. TYPES OF FLANGES CONSIDERED FOR RECOMMENDED
FLANGE DESIGN PROCEDURE

References

(1) "Integrated Pressure Systems and Components (Portable and Installed)", Air Force Technical Manual T.O. 00-25-223 (February 1, 1962).

(2) Churchill, J. L., and Watson, J. F., "Properties of R-41 Sheet, A Vacuum-Melted, Nickel Based Alloy", Rept MGR-164, Convair Astronautics Division of General Dynamics Corporation (June 19, 1960).

(3) Christian, J. L., "Physical and Mechanical Properties of Pressure Vessel Materials for Application in a Cryogenic Environment", ASD-TDR-62-258 (March 1962).

(4) Liberto, Ralph R., "Storable Propellant Data for the Titan II Program", Bell Aerospace Systems Company, Contract No. AF 04(694)-72 (March 1962).

(5) Liberto, Ralph R., "Storable Propellant Data for the Titan II Program", Bell Aerospace Systems Company, Report No. AFBMD-TR-61-55, Contract No. AF 04(647)-846 (July, 1961).

(6) Headquarters Office Instruction Data Sheets, HOI 74-30-1 through HOI 74-30-13, 6593 Test Group Development, Edwards Air Force Base, California.

(7) Liquid Propellants Manual, Liquid Propellants Information Agency, Contract NORD 7386.

(8) "Compatibility of Materials With Demazine", Food Machinery and Chemical Corp., Inorganic Research and Development Department.

(9) Bloom, Ralph, Weeks, Loren E., and Raleigh, Charles W., "Materials for Construction of Equipment in Use with Hydrogen Peroxide", Becco Chemical Division, Food Machinery and Chemical Corp. (1959).

(10) Boyd, W. K., and White, E. L., "Compatibility of Rocket Propellants With Materials of Construction", Defense Metals Information Center, Memorandum No. 65 (September 15, 1960).

(11) Private communication from Herbert J. Wagner and Carl Lund, Battelle Memorial Institute.

(12) Baughman, R. A., "Gas Atmosphere Effects on 32367 Metals", General Electric Company Interim Progress Report No. 3R59AGT 137, Contract AF 33(616)-5667 (February 15, 1959).

(13) "Oxygen Difluoride (OF_2)", Product Data Sheet, Product Development Department, General Chemical Division, Allied Chemical Corporation (November, 1962).

FITTING-TO-FITTING CONNECTION

FITTING-TO-FITTING CONNECTION

During the course of Phase I many methods of assembling a mechanical connection in a pressurized piping system were studied. Evaluation of these concepts, however, made it apparent that none could compete in simplicity, ruggedness, and reliability with the conventional attachments consisting of either a threaded nut mated with a threaded stub end, in small sizes, or bolted-flanged connections in larger sizes. The recommended threaded and bolted fitting-to-fitting connections developed during Phase II and described in this section contain a number of unique features in which lightweight, ruggedness, and reliability are achieved by use of high-strength materials and suitable design procedures.

The following discussion is presented in four sections:

● Design Parameters

● Designs Considered

● Proposed Threaded-Fitting Design

● Design Procedure for Bolted Fittings

In the first section the significant design parameters involved in designing a mechanical connection are discussed in general terms. Graphs and equations are given to indicate the approximate magnitude and significance of the effect of each parameter on the final design. The parameters discussed are applicable to both threaded and bolted fittings.

In the "Designs Considered" section a few of the methods of securing the fitting-to-fitting connection which were evolved in the early stages of Phase I are described.

The third section presents a discussion of the systematic design procedure which Battelle developed for the design of improved aerospace threaded fittings. The procedure is clarified by the discussion of the design of the experimental 1/2-inch fitting which was evaluated during Phase II. The results of the evaluation are described in a later section of this report.

The fourth section includes much of the material prepared for inclusion in the Fluid Designers' Handbook, plus a discussion of creep design procedure. As in the previous section, an example is presented for clarity.

Design Parameters

The general discussion of design parameters presented below enumerates and explains the effects on the structural components of the fitting-to-fitting connection of such factors as structural loads, seal seating loads, preload, temperature, and fatigue. Also, the interactions between the seal, the tube-to-fitting joint, and the fitting-to-fitting structure are briefly discussed.

Structural Loads

The structure of a mechanical connection must be designed to withstand several types of load, which may be imposed individually or in combinations. These loads are shown in Figure 9.

A-43896
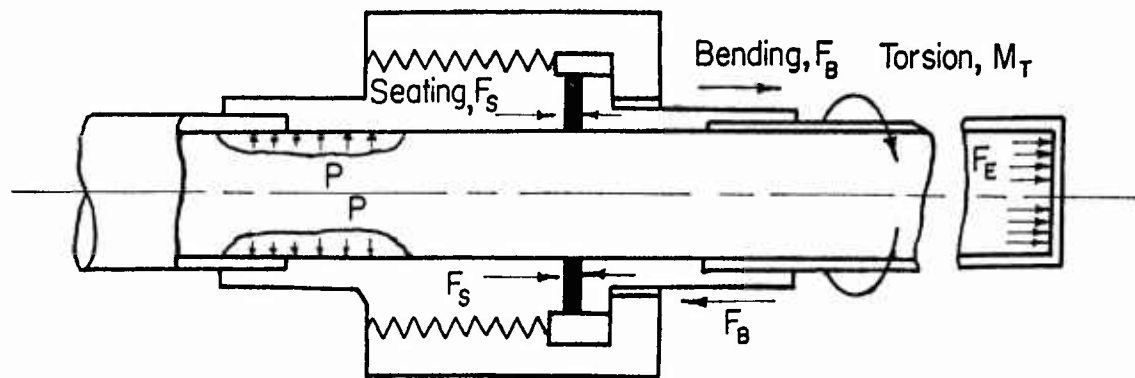
FIGURE 9. TYPICAL LOADS IMPOSED ON FITTINGS

Hoop Stresses From Internal Pressure. In the design of a tube for internal pressure, the hoop stresses are largest and control the design. In design of a fitting, however, the structure necessary to transfer axial loads requires an increase in wall thickness, so hoop stress from internal pressure becomes a secondary consideration.

Pressure End Load. The pressure end load acting on the structure is equal to

$$F_E = \frac{\pi}{4} G^2 P, \tag{1}$$

where

F_E = pressure end load, lb

G = effective seal diameter, in.

P = internal pressure, psi

Figure 10 shows values of the end load, F_E, for the maximum internal pressures of Fitting Classes I through V based on the approximation that G is equal to 1.1 the

24
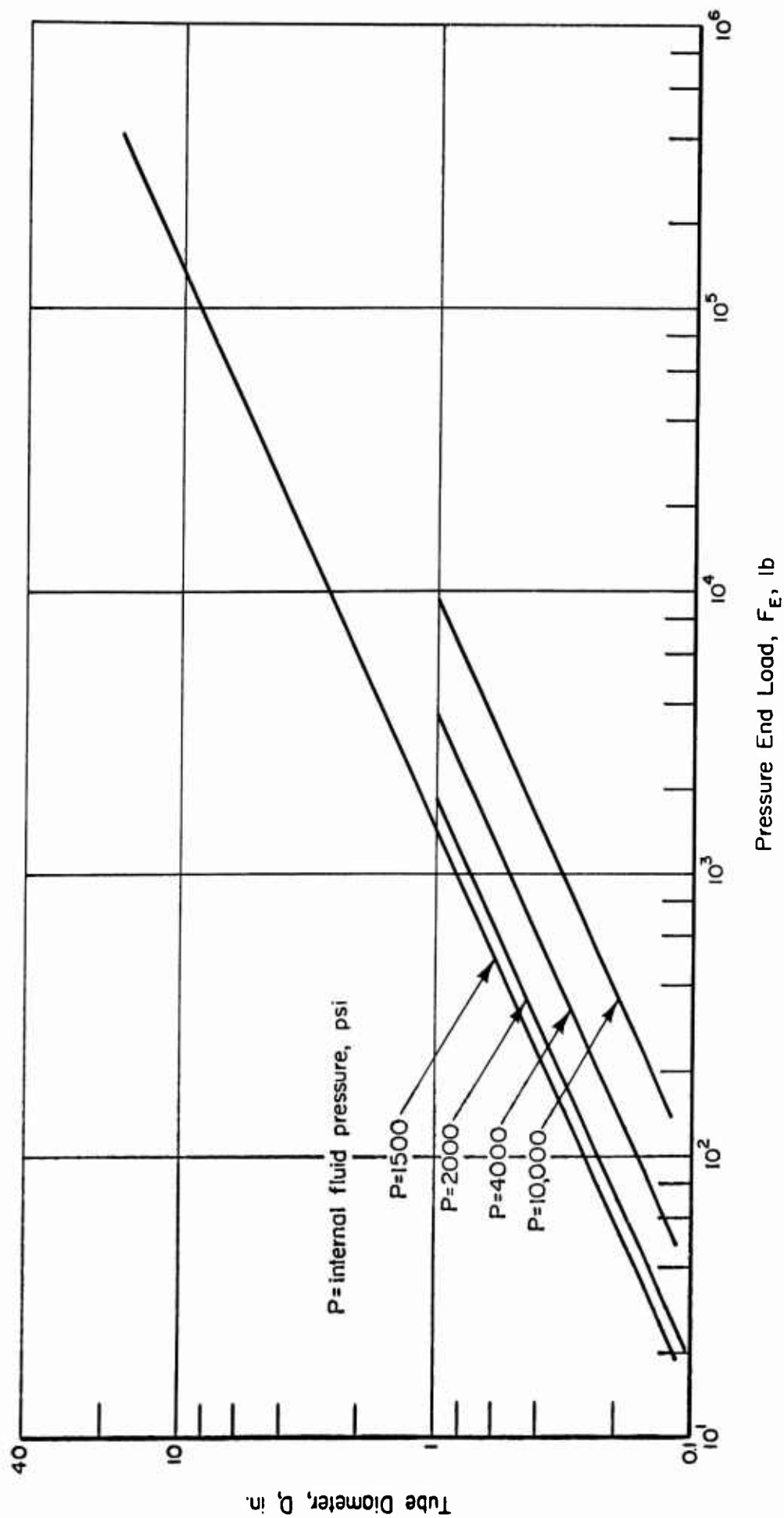
FIGURE 10.   PRESSURE END LOAD ACTING ON FITTINGS AS A FUNCTION OF TUBE DIAMETER AND DESIGN PRESSURE

25

tubing diameter. For the larger sizes, this load becomes very high: 360,000 lb for a 16-in. fitting withstanding 1500-psi internal fluid pressure.

In some systems, the pressure end load may be absorbed primarily by anchors or clamps rather than transmitted through the fitting. In such systems, it may be possible to use lighter fittings. However, for general use fittings must be designed to withstand the total pressure end-load.

Bending Moments. A bending moment, M, producing bending loads, F_B, may be present because of tubing misalignment, thermal expansion or contraction of the tubing system, vibrations, displacements of anchors, or acceleration forces. Bending moments imposed on a fitting in a tubing system cannot be determined in advance, since these moments depend upon the specific tubing system, its operating conditions and the location of the fitting in the system. However, some limits, even if arbitrary, must be established to make design possible. For the fitting designs presented in this report the design limits are based on (1) the strength of the tube in the system and (2) the strength of equipment (compressors, pumps, pressure vessels, etc.) to which the tubing system is attached.

The maximum bending moment that can be applied to a fitting through the attached tubing is given by the equation

$$M = SZ,$$

(2)

where

S = limiting stress of tube material, psi

Z = section modulus of tube cross section, in.^{3}.

Since both S and Z in Equation (2) depend on the material used for the tubing and its wall thickness, the bending moment, M, can be established only after the tube is selected. In the following, a procedure for establishing the design moment is shown for an assumed tube material and related wall thickness. Analogous bending moments for other tubing can readily be established by the same procedure.

It is assumed for illustrations of the procedure that the tube will be made of AM-350 stainless steel. This material is being used to some extent in missiles and, because of its high yield strength, a lightweight tube would be possible. The pertinent properties of AM-350 are:

Yield Strength at 70 F[1]*, psi   150,000

Fatigue Strength at 70 F[2], psi

10^5 cycles	95,000
10^6 cycles	85,000
10^7 cycles	84,000

On the basis of the yield strength, S in Equation (2) could be as high as 150,000 psi. However, considering the requirement that the fitting, and therefore the tubing must be designed to withstand 200,000 cycles of reversed bending,** it is apparent that the fatigue strength rather than the yield strength will control.

*Numbers in parentheses denote references listed on page 109.

**Paragraph III 2 g (page 5) Exhibit A "Technical Requirements, Development of Mechanical Fittings", Contract AF No. 04(611)-8176, March 13, 1962.

The fatigue strength of AM-350 for 200,000 cycles is about 90,000 psi. This, of course, is based on a smooth-specimen fatigue tests. In tubing systems there will be points of stress intensification at clamps and at curved tube sections. The stress-intensification factors may be of the order of two or larger. Accordingly, a fatigue stress limit of 50,000 psi has been used in computing the bending moment limit from Equation (2).

To compute the design bending moment by Equation (2), it is also necessary to determine the tube wall thickness, since the section modulus of the tube depends upon its thickness. Tube thickness can be computed with the following equation (based on hoop stresses):

$$t = \frac{PD}{2S_h} = \frac{PD}{200,000} \geq .005, \tag{3}$$

where

    t = tube-wall thickness, in.

    P = internal pressure, psi

    D = tube diameter, in.

    S_h = design stress, taken as two-thirds of the yield
        strength of AM-350 at 70 F

The thickness computed from Equation (3) can be very small, e.g., .001 in. for 1/8-in. tubing at 1500 psi. It is improbable that such very thin-walled tubing will be used. Accordingly, a minimum thickness of 0.005 in. has been used as the lower limit for tube thickness, t, in cases when Equation (3) gives values smaller than this limit.

For thin-walled tubing, the section modulus can be closely approximated by

$$Z = \frac{\pi D^2 t}{4}. \tag{4}$$

By substituting the value $S = 50,000$ and the expressions $t = \frac{PD}{200,000}$ and $Z = \frac{\pi D^2 t}{4}$ in Equation (2), the bending moment can be determined as

$$\begin{aligned} M &= 0.197\ PD^3 \\ t &> .005 \end{aligned} \tag{5}$$

When $t = 0.005$, the bending moment is

$$M = 197 D^2. \tag{6}$$

In smaller fittings for lower pressures the design will be controlled by the seal-seating load (discussed in the next section); hence, there will be a substantially larger bending-moment allowance than indicated directly by Equations (5) and (6). The approximate bending-moment allowance for small fittings is shown on Figure 11, along with bending-moment requirements implied by MIL-F-18280A[3], Par. 4.3.3.3.3 for comparison.

27
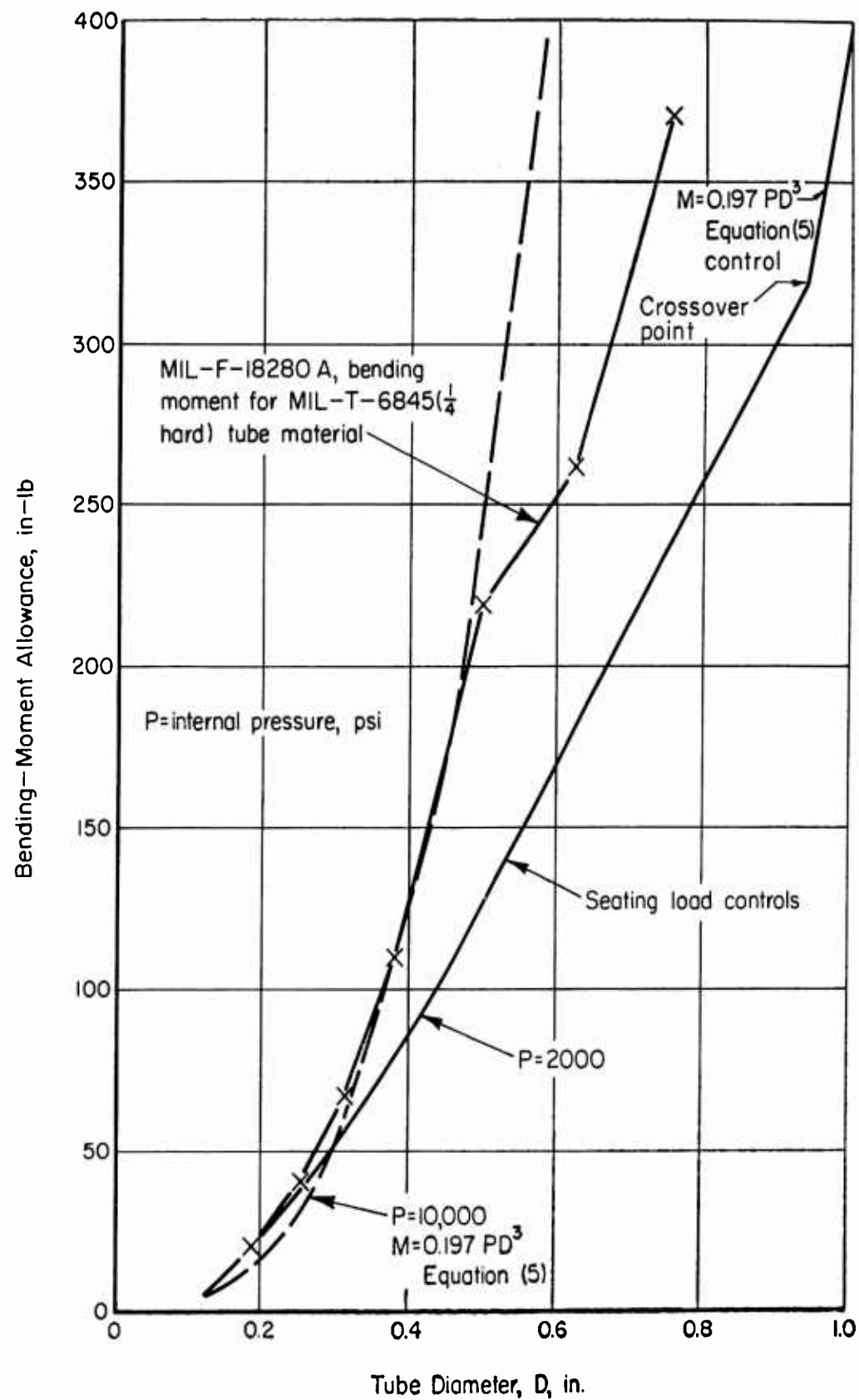
FIGURE 11. COMPARISON OF BENDING-MOMENT ALLOWANCE FOR
SMALL FITTINGS

28

While Equations (5) and (6) provide a reasonable design basis for small fittings, the bending moments calculated may be unnecessarily high for large fittings. The limitations on bending moments which can be applied to equipment to which the tubing is attached are not known; however, some indication of the limits may be obtained from the bending moments permitted on the piping connections to steam turbines[4], as shown on Figure 12. It is apparent that, even for equipment as heavily constructed as power-plant steam turbines, the bending-moment allowance is substantially less than that given by Equation (5).

Another general indication of typical bending moments on flanged joints given by Rossheim and Markl[5] is

$$M = 60 (D + 3)^3 \text{ in-lb.} \tag{7}$$

Equation (7) was originally developed as part of a review of a large number of stress calculations on piping systems. It may be considered as a typical bending moment that may occur in piping systems in power plants, chemical process plants, and oil refineries. Equation (7) is also plotted on Figure 12.

Design bending moments obtained from the larger of the moments from Equations (5) and (6), but not exceeding the moment obtained from Equation (7), are shown on Figure 13. These are the moments proposed for use in designing the fitting-to-fitting structure.

External Axial and Torsional Loads. External axial and torsional loads arise from the same causes as do bending loads. External axial loads are usually minor and can be discounted. Torsional loads are basically limited to three-dimensional tubing systems and may be a problem if sufficiently large to cause rotation of one part of the joint with respect to the other. Rotation could cause leakage, in either threaded or bolted fittings, because the seal is disturbed. It could also cause back-off and preload relaxation in a threaded joint. A torsional resistance of the fitting equal to that which can be safely imposed on the fitting by the attached tube is suggested as a design basis.

Seal-Seating Load

Quite independent of the structural load, the fitting structure must also be designed to withstand those loads required to produce intimate mating between the fitting's seal-contact faces and the seal. The factors involved are discussed on pages 129 through 132. For the purpose of fitting-to-fitting design, it has been assumed that an initial seating load of 1000 lb per linear in. of gasket length is required. The seal-seating load, F_G, is given by the equation

$$F_G = 1000 \, \pi G \text{ (lb)}, \tag{8}$$

where G = effective seal diameter. For preliminary evaluation, G may be taken as 1.1 D, where D is the tube size, giving

$$F_G = 3460 \, D \text{ (lb).} \tag{9}$$

29
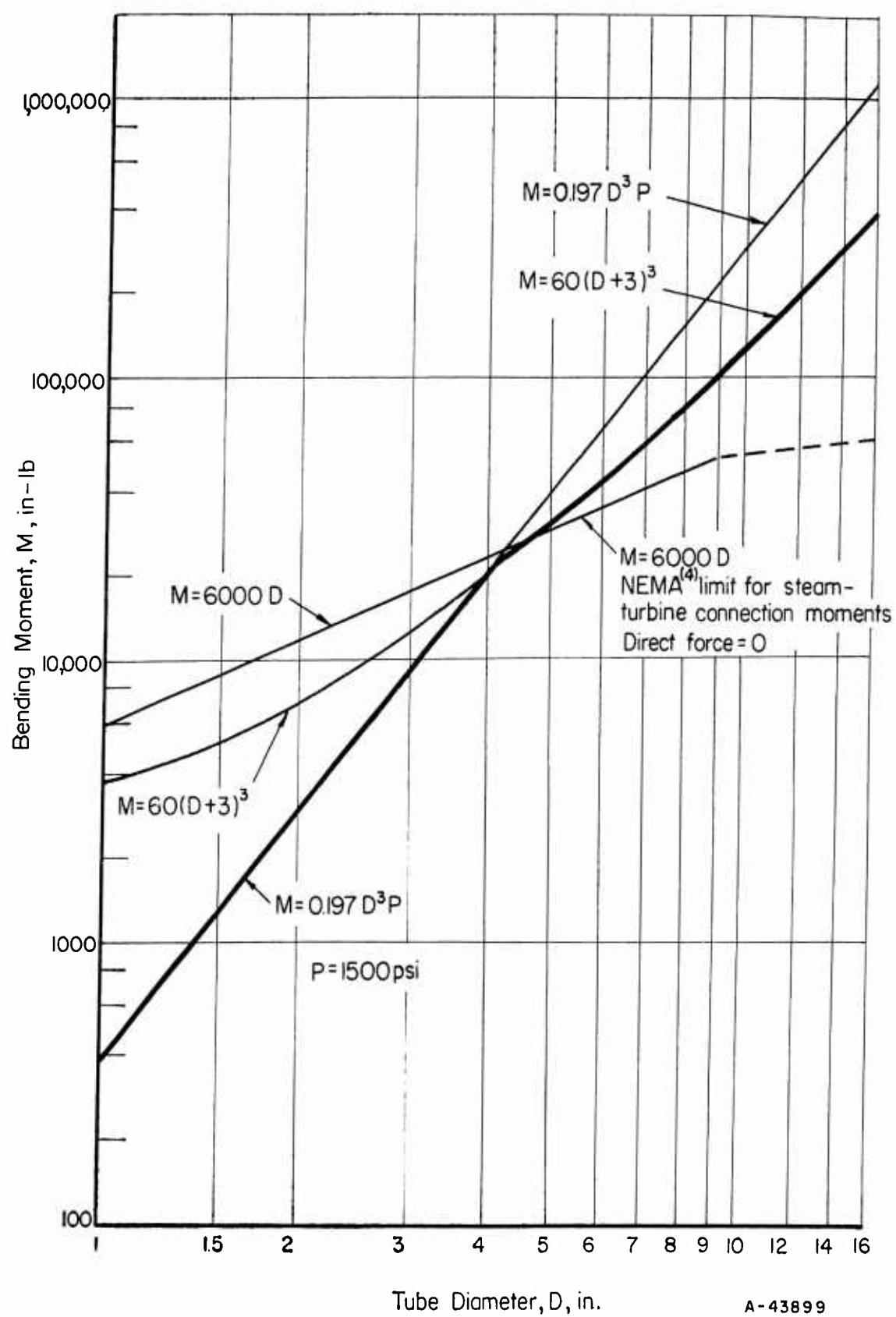
FIGURE 12. BENDING-MOMENT-LIMITED COMPARISON FOR LARGE FITTINGS, DESIGN PRESSURE AT 1500 PSI

30
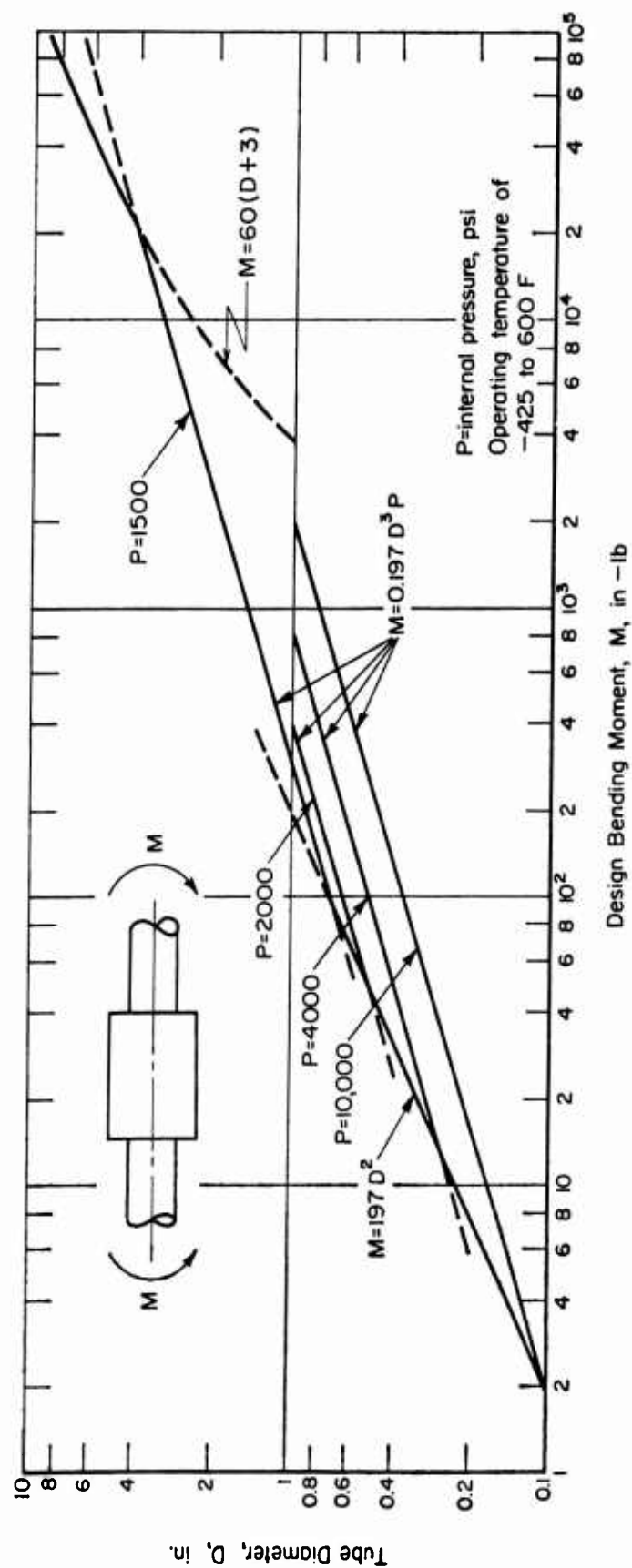
FIGURE 13.   PROPOSED DESIGN BENDING MOMENTS FOR FITTINGS

A-43900

31

Design Loads

The structural load applied by internal pressure is an axially symmetric load with respect to the fitting structure, since the fitting structure, in the design concepts proposed, is itself symmetric about the longitudinal axis of the tube. Although an analysis of axially symmetric structures similar to the configurations used in the fittings is quite complex, theoretical methods are available which make possible a fairly precise engineering design of axially symmetric loads such as that produced by internal pressure.

The structural load applied by bending, however, is not symmetrical. In the following, a pressure, P_B, equivalent to the bending moment, will be derived. The equivalent pressure, P_B, can then be handled in the same way as the actual pressure, P, i.e., by using theoretical methods for axially symmetric loads.

When a bending load is imposed on the fitting through the piping, a maximum tensile stress will exist at one point on the circumference. A diametrically opposed maximum compressive stress will arise simultaneously. However compressive failure is not likely to occur since the cumulative sum of the tensile stresses due to bending and the pressure end load is greater. In any case, the minimum strength of the fitting is equal to or greater than the maximum strength of the tubing under conditions where compressive failure might occur. The maximum tensile stress will be given by the equation

$$S_B = \frac{M}{Z} , \tag{10}$$

where

S_B = maximum bending stress in tube, psi

M = design bending load, in-lb (From Figure 13)

Z = section modulus of tube, in^3.

While this tensile stress exists at only one point on the circumference, it can be conservatively assumed that the fitting may be designed as if S_B, the maximum bending stress, existed uniformly all around the tube circumference. With this assumption, it is possible to express the bending load as an equivalent internal pressure, P_B, which is given by the equation

$$P_B = \frac{4 S_B t}{D} , \tag{11}$$

where

P_B = equivalent internal pressure, psi, from design moment, M.

S_B = maximum bending stress in tube, psi

t = tube-wall thickness, in.

D = outside diameter of tube, in.

If it is assumed that a tubing material such as AM-350 precipitation-hardening stainless steel with a design stress of 100,000 psi is used, the required tube-wall thickness can be determined by Equation (3). The equivalent axial load, F_B, in terms of P_B is

$$F_B = P_B \frac{\pi}{4} G^2 . \tag{12}$$

Figure 14 shows F_B as a function of size and pressure.

32
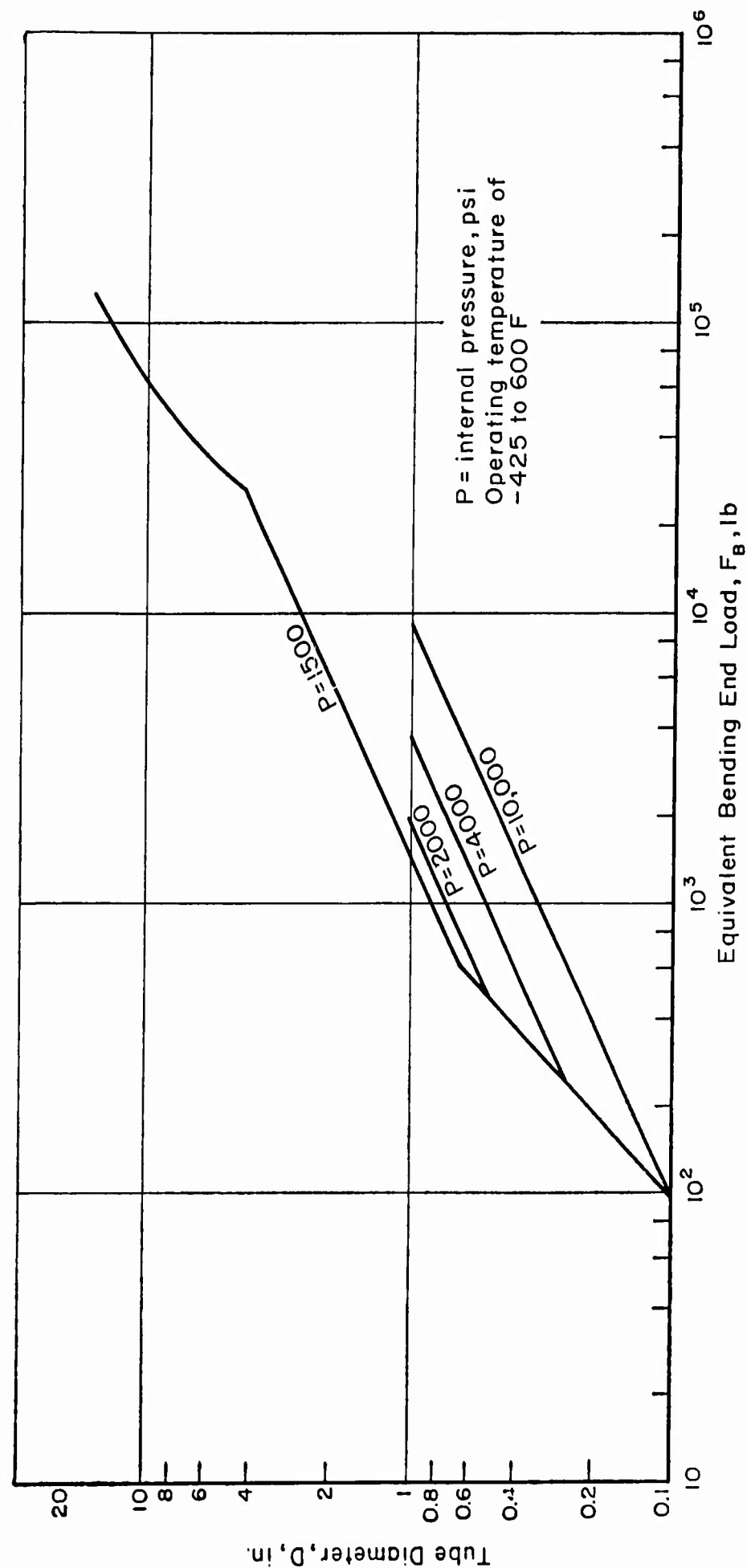
FIGURE 14. EQUIVALENT BENDING END LOAD AS A FUNCTION OF TUBE DIAMETER AND DESIGN PRESSURE
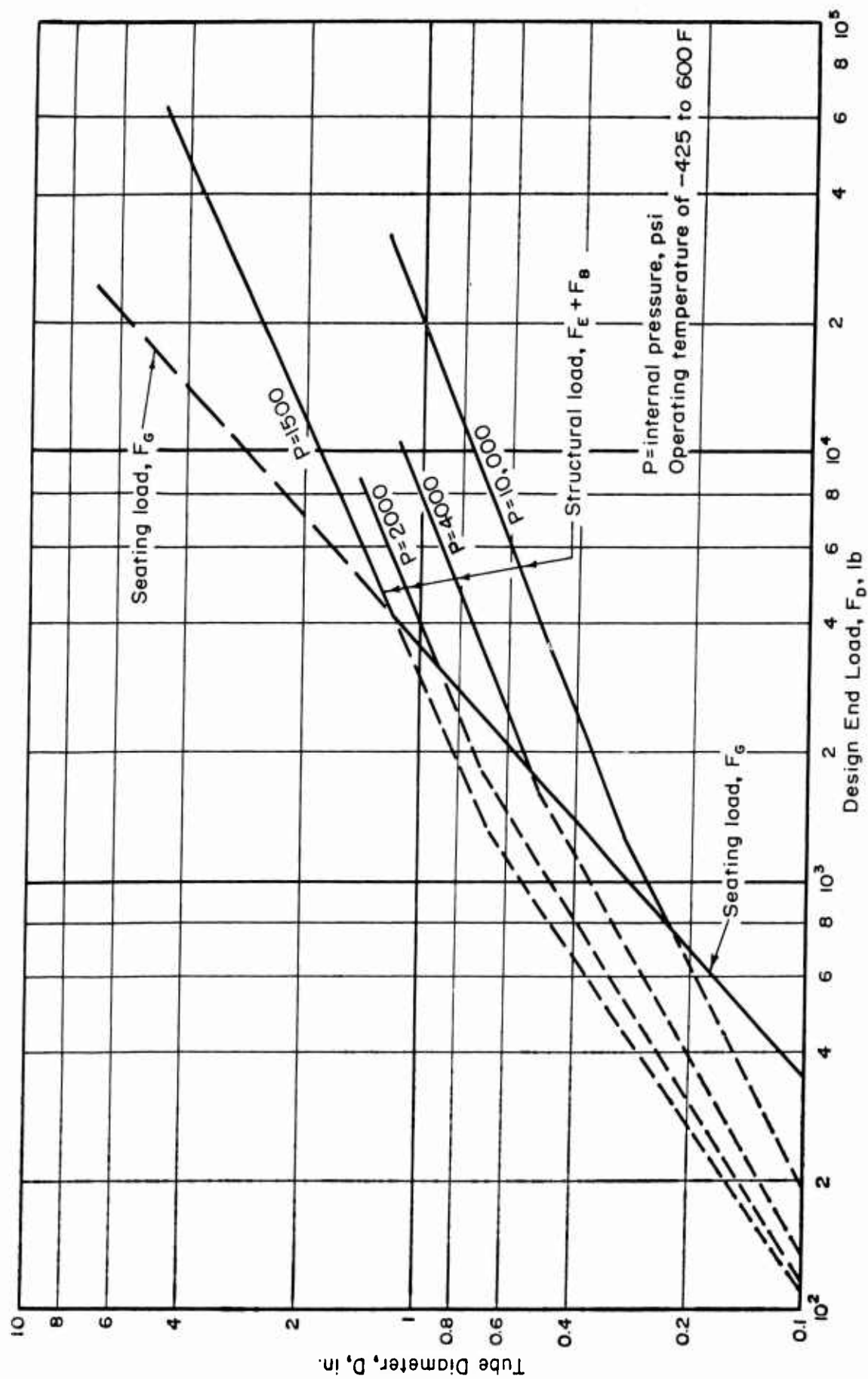
FIGURE 15. DESIGN END LOADS (GREATER OF F_G OR $F_E + F_B$) AS A FUNCTION OF TUBE DIAMETER AND DESIGN PRESSURE

34

The total structural load the fitting must carry is at least equal to the sum of the pressure end load and the pressure equivalent of the bending loads. However, the total structural load may not be the controlling design load since the load required to seat the gasket may be greater. The load required to seat the gasket given by Equation (9) and the total structural load are plotted in Figure 15. Figure 15 shows approximately the crossover point where either seating load or structural loads control the design. As an example, for a 3/8-in. fitting (D = 0.375), the seating and structural loads for different internal pressures are given in Table 4. The design load for each pressure is

TABLE 4. DESIGN LOADS FOR 3/8-IN. FITTING

(-425 to 600 F Operating Temperature)

Design Pressure, psi	Seating Load, lb	Structural Load, lb
1,500	1,300	600
2,000	1,300	750
4,000	1,300	1,000
10,000	1,300	2,100

underlined. For the 3/8-in. fitting the seating load is greater for design pressures of 1500, 2000, or 4000 psi, and only for a design pressure of 10,000 psi is the structural load the controlling factor.

Preload

Mechanical connections in a piping system are usually tightened so that an axial preload force in excess of the design structural load is created. In flanged connections, determination and control of the preload is accomplished more easily than in threaded connection. In threaded fittings the need for attaining a desired or required preload is often neglected although the principles involved apply as well to threaded connections as to flanged connections.

In service the action of the imposed axial loads is to "pull" the mating parts of the fitting apart. Any degree of separation generally will lead to early failure. Therefore in order to counteract this action it is necessary to prestress the flange members of the fitting in compression an amount greater than the expected strain relaxation caused by the tensile axial loads. Of course, preloading causes an initial tensile stress in the bolts or threaded nuts. This tensile stress may increase when the service loads are applied, and a balance must be achieved between a preload which is sufficient to prevent flange separation and a preload so large as to cause eventual tensile stress failure of the bolt or threaded nut. The factors that must be considered in determining the required preload are: (1) the spring constants of the compression and tension members, (2) the minimum compressive load on the flange members needed to prevent leakage, (3) the maximum allowable stress in the tensile members, (4) the magnitude of the structural loads, and (5) the effects of the thermal gradients.

The problem of a preloaded joint is statically indeterminate; hence, it must be solved on the basis of displacements of the structure. Calculations of displacements become quite complex where stretching and bending of structural parts, changes in moment arms, and radial effects of internal pressure are involved. A basic

understanding of the problem, however, can be obtained by disregarding the effects of moment-arm changes and the radial components of internal pressure. The following discussion is therefore limited to a simple case analogous to that shown in Figure 16, where only tensile and compressive displacements are considered.

In threaded fittings, the nut is the tension member, analogous to the bolt in Figure 16. The stub ends and seal are the compression members analogous to the rings and seal of Figure 16. In flanged fittings, the bolts are analogous to the bolt and the flanges and seal are analogous to the rings and seal of Figure 16.
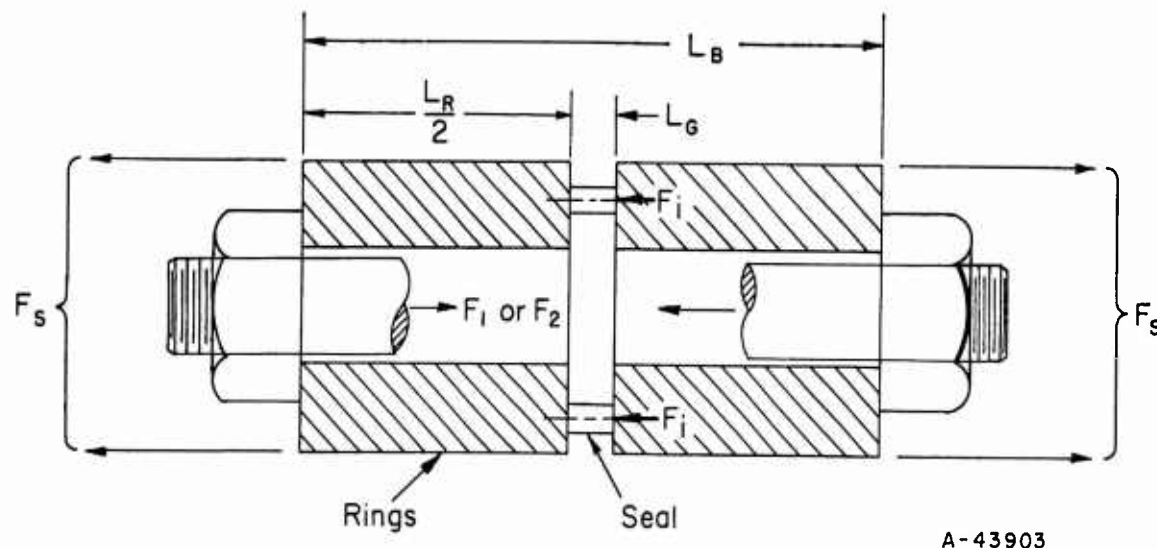
FIGURE 16. MODEL OF SIMPLIFIED PRELOAD THEORY

When the nut on the bolt is tightened, there will be an increase in bolt length and a decrease in the length of the rings and seal, given by

$$\delta_B = \frac{F_1 L_B}{E_B A_B} \ , \ \ \delta_R = \frac{F_1 L_R}{E_R A_R} , \ \ \delta_G = \frac{F_1 L_G}{E_G A_G} \ ,$$

where subscripts B, R, and G refer to the bolt, rings, and seal, respectively, and

F_1 = initial bolt axial force, lb E = modulus of elasticity, psi

L = free axial length, in. A = cross-sectional area, in.^{2}

When a load F_s is applied (as from the attached tube in the actual fitting), the force in the bolt in Figure 16 changes to F_2 and

$$\delta_{B2} = \frac{F_2 L_B}{E_B A_B} \ , \ \ \delta_{R2} = (F_2 \cdot F_s) \ \frac{L_R}{E_R A_R}, \ \ \delta_{G2} = (F_2 - F_s) \ \frac{L_G}{E_G A_G} \ .$$

The change in length of the bolt must remain equal to the combined changes in lengths of the rings and gasket:

$$\delta_{B2} - \delta_B = (\delta_R + \delta_G) - (\delta_{R2} + \delta_{G2}) \tag{13}$$

or

$$(F_2 - F_1) \ \frac{L_B}{E_B A_B} = (F_1 - F_2 + F_s) \left(\frac{L_R}{E_R A_R} + \frac{L_G}{E_G A_G} \right). \tag{14}$$

36

Defining $\dfrac{L_B}{E_B A_B} = R_B$ and $\dfrac{L_R}{E_R A_R} + \dfrac{L_G}{E_G A_G} = R_G$ as the spring constants (in. /lb), and collecting terms in Equation (14),

$$F_2(R_B + R_G) = F_1(R_B + R_G) + F_s R_G, \tag{15}$$

or

$$F_1 = F_2 - \frac{F_s}{1 + \dfrac{R_B}{R_G}} \quad . \tag{16}$$

If F_2, the maximum allowable load, and R_B and R_G, the spring constants, can be determined or closely approximated, the analytical determination of F_1 the preload is relatively simple by means of Equation (16). However, this simple case, if changed into a graphical representation, can be handled more easily when thermal effects are subsequently introduced. In a later discussion of the proposed fitting-to-fitting connections, the graphical presentation has been used extensively.
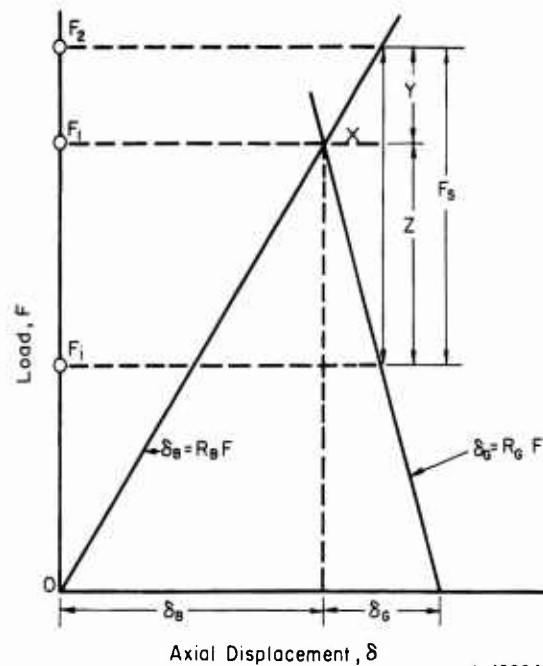
FIGURE 17. GRAPHICAL ILLUSTRATION OF SIMPLIFIED PRELOAD THEORY

The graphical representation of the basic relationships is shown in Figure 15. A line is drawn from the origin with a slope $\dfrac{\delta_B}{F} = R_B$. A second line, with slope $\dfrac{\delta_G}{F} = R_G$, is drawn to intersect the first line at $F = F_1$. The force applied, F_s, is drawn between the two intersecting lines as shown in the figure. As can be seen in the construction, $F_2 = F_1 + Y$. Since $\dfrac{X}{Y} = R_B$ and $\dfrac{X}{Z} = R_G$ and $Y + Z = \dfrac{X(R_B + R_G)}{R_B R_G} = F_s$:

$$X = \frac{F_s R_B R_G}{R_B + R_G}, \text{ and with } Y = \frac{X}{R_B}$$

37

$$F_2 = F_1 + Y = F_1 + \frac{R_G F_s}{R_B + R_G} = F_1 + \frac{F_s}{1 + \dfrac{R_B}{R_G}} \quad .$$

Accordingly, the construction shown by Figure 17 is a graphical presentation of Equation (16).

The load existing at the gasket, F_i, can be obtained from static equilibrium:

$$F_i = F_2 - F_s \ . \tag{17}$$

From a fitting-design standpoint, it is necessary that the average stress on the seal contact area be at least equal to the internal pressure to prevent leakage.[*] This stress is simply the load at the seal, F_i, divided by the seal contact area. Equations (16) and (17) give means of calculating the required preload, F_1, in order to maintain a required residual seal load, F_i, after application of the structural load, F_s. Equations (16) and (17) may be combined to give

$$F_1 = F_i + \frac{\dfrac{R_B}{R_G}}{1 + \dfrac{R_B}{R_G}} \ F_s \quad . \tag{18}$$

In the preceding discussion, the seal has been considered as not pressure energized. When considering a typical metal pressure-energized seal, reduction of F_i to a low value has a different but equally significant implication in the fitting design. A characteristic of many metal pressure-energized seals is that in order for the seal to be flexible enough to give any appreciable seal follow-up from internal pressure, its flexibility is such that it will withstand only a negligible amount of preload; almost all of the preload is supported by the fitting faces adjacent to the seal, or, in some designs, by a rigid part of the seal itself. With this type of seal, reduction of F_i to zero implies a separation of the fitting interface. In this case, leakage may not result under static conditions because of pressure-generated seal follow-up; however, vibration of the tube system may produce sufficient movement to cause flexing of the metal seal, thus possibly leading to leakage by abrasion of the sealing surfaces, or fatigue failure of the metal seal. Accordingly, even with a pressure-energized seal, the lower limit on F_i is an important design consideration.

In actual fitting design, other factors which influence the preload requirements are:

(1) Rotation of flanges

(2) Moment-arm changes as the load is transferred from the seal to the tube

(3) Radial effect of internal pressure.

---

[*]This is a theoretical lower limit on residual seal-contact-area stress and presumes a "perfect match" between sealing surfaces. This "perfect match" between sealing surfaces is, in practice, never really achieved but may be approached by adequate seal-seating load.

An equation for calculating F_2, including these factors, is

$$F_2 = F_1 + \alpha P, \tag{19}$$

where

P = internal pressure, psi

$$\alpha = \frac{\pi h_G}{4Q}\left\{\left[\frac{q_G}{h_G} - 2q_F(h_T - h_G)\right]G^2 - 2q_F B^2(h_D - h_T) - \frac{8}{\pi}q_r\right\}.$$

Equation (19) and the definition of α are taken from Wesstrom and Bergh[6] and Rodabaugh[7]. Symbols used are defined in Appendix I. The definition of α is directly applicable to a flanged fitting in which the flanges are identical. It may readily be adapted to a flanged fitting in which the two flanges are not identical. It may also be adapted to design of threaded fittings.

Equation (19), of course, reduces to Equation (16) when only tensile and compressive deformations are considered. Equation (17) can be used with Equation (19) to determine the relationship between F_1, F_s, and F_i.

Temperature Effects

In the preceding sections only design loads essentially at ambient temperature were discussed. When the effects of temperature change are considered, the design problem becomes more complex.

Creep or Relaxation. At high temperatures, the strain in a metal part under stress cannot be considered as independent of time. In a mechanical connection, where creep produces a reduction in preload and in turn a reduction in stress, the problem becomes one of relaxation with variable stress.

An accurate theoretical method for calculating the performance of a threaded or flanged fitting under creep or relaxation conditions has not been developed insofar as the authors are aware. The problem is very complex because of the variable stress field in the structure, nonlinear relationships that are a result of elastic-plastic deformations, and the introduction of time as an additional parameter.

In view of the necessity for design under creep or relaxation conditions, an approximate theoretical design procedure has been established, as shown and discussed in Appendix II. This design method has the virtue of relative simplicity and is believed to be conservative.

Thermal Gradients. If a cold fluid, like liquid oxygen, is suddenly introduced into a piping system, the temperatures of metal parts in direct contact with the fluid will decrease rapidly. The temperatures of those parts not in direct contact, such as the nut of a threaded fitting or the bolts of a bolted fitting, change less rapidly because of the air-film resistance between parts. Accordingly, there is a period during which the average temperature of the interior parts of the fitting is lower than the average

39

temperature of the exterior parts. During this time effective preload decreases because of the relative thermal expansion of the fitting nut or bolts.

When a hot fluid is introduced into a piping system the internal parts may become hotter than the external parts. This increases the preload, since a relative thermal contraction of the nut or bolts occurs. However, there is also the possibility of yielding of some member of the fitting, and if temperature equality were later re-established, the preload might be partially or completely removed, with consequent leakage.

The temperature difference is a function of the fluid properties and flow velocity, as well as the properties of the fitting and its material; hence, a numerical value for this temperature difference can be calculated only for each specific case. To facilitate fitting design, the following limits have been set for the permissible temperature gradients:

Service Temperature, F	Maximum Design Temperature Difference*, F
-100 to 600	100
-425 to 1500	400

A relatively thin-wall tube will change in temperature more rapidly than will the more massive fitting parts. Therefore, the tube will exert either a radially inward or outward force on the flanges or stub ends, depending on whether cooling or heating is occurring. In either case a consequent tendency for parts to rotate relative to each other will be a design factor. Although this factor has not been evaluated in the preliminary design, it should be considered when final designs are established.

A nonsymmetrical temperature condition exists when some types of hot or cold fluids are introduced into a horizontal pipeline. The colder liquid tends to flow along the bottom half of the tube while the relatively warm vapor is near the top. This heterogeneous flow pattern causes "bowing" of the pipeline, with resulting high bending moments transmitted to the mechanical fitting. This condition is specific to a given piping system and when it is present its effect should be considered by the designer as a bending moment which should be held within the bending-moment limits established previously.

Modulus of Elasticity. When the temperature of a fitting changes, there is a corresponding change in the modulus of elasticity and in the effective preload, F_1, to a new value, $(F_1)_T$. For AM-355 and René 41 in the temperature range under consideration, this effect is shown in Table 5.

With decreasing temperatures, the structure must retain a sufficient strength margin to prevent overstress by the consequent load increase. For the two materials considered, the yield strength increases more rapidly than does the modulus of elasticity and, therefore, the change in preload is not a design problem. However, for increasing temperatures, the structure must be endowed with extra preload to maintain an adequate residual load at temperature. As an example, for AM-355 for service at 600 F, this requires about 11 per cent extra preload.

*If in actual service the design limits are exceeded, use of a thermal shield is suggested. This could be simply a cylindrical sleeve at the bore of the fitting which provides a stagnant space between it and the fitting bore to retard heat transfer from the fluid to the fitting.

40

TABLE 5. CHANGE IN EFFECTIVE PRELOAD AS FUNCTION OF TEMPERATURE

	$(F_1)_T/F_1$ at Indicated Temperature				
	-425 F	-100 F	70 F	600 F	1500 F
AM-355	(a)	1.00	1.00	0.90	(a)
René 41	1.10	1.03	1.00	0.92	0.75

(a) Not used at these temperatures.

Threaded Versus Bolted Fittings

Considering pipe and tubing systems in general, threaded fittings are generally used in small sizes (1/8 to 1/2 in.). There is an overlapping size range of about 1/2 to 4 in. in which selection of threaded or bolted fittings depends upon the detailed service requirements of pressure, temperature, reliability, and installation conditions. For sizes larger than 4 in., bolted fittings are generally used.

Perhaps the most significant factor involved in the choice between threaded or bolted fittings is the torque required for preloading. In contrast to threaded fittings, in which the preload is applied by tightening a single threaded element, the preload is applied to bolted fittings by means of several comparatively small threaded elements, so while the preload is approximately the same, the required assembly torque is much lower for bolted fittings of comparable size and rating. The torque required to preload threaded fittings may be approximated by the equation

$$T = 0.2 \, dF_1, \tag{20}$$

where

T = required preload torque, in-lb

d = nominal thread size, in.

F_1 = required preload, lb.

For preliminary evaluation purposes, d may be taken to be 1.30 D. As discussed in the next sections on design procedures, F_1 can be established only after detailed dimensions of the fitting are selected. However, for preliminary evaluation of torque requirements, F_1 may be taken as equal to F_D. The design load, F_D, is shown in Figure 15. With these assumptions, torque requirements have been calculated and are plotted in Figure 18.

The torque that can be applied to a fitting depends on numerous factors; e.g., the type of tool being used, the precision with which torque must be applied, the space around the fitting as initially installed and, as might be the condition for subsequent disassembly and reassembly, the space for a workman to stand and brace himself while applying the torque. Obviously, in designing a line of fittings for general use, any maximum torque limit is necessarily somewhat arbitrary. However, based on general experience with pipe and tube fittings, an upper limit of 2000 in-lb of torque appears
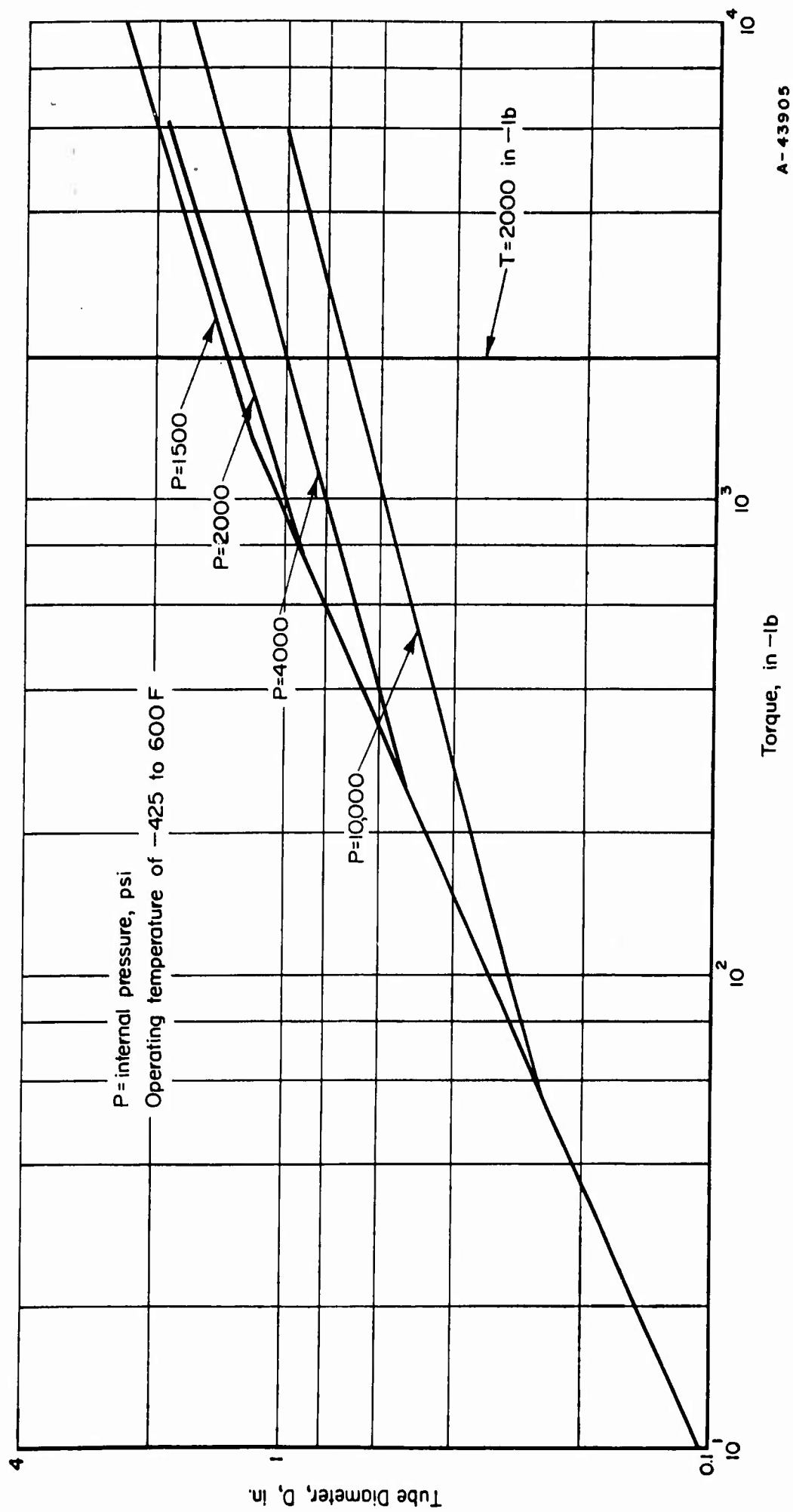
FIGURE 18. PRELIMINARY ESTIMATE OF PRELOAD TORQUE FOR THREADED FITTINGS

A-43905

42

reasonable. This torque limit, when transferred to Figure 18, subdivides the fittings into threaded and bolted as shown in Table 6.

TABLE 6. DIVISION OF FITTINGS INTO THREADED AND BOLTED, BASED ON A MAXIMUM TORQUE OF 2000 IN-LB

(-425 to 600 F Operating Temperature)

Design Pressure, psi	Threaded-Fitting Sizes, in.	Bolted-Fitting Sizes, in.
1,500	1/8 through 1-1/4	1-1/2 and larger
2,000	1/8 through 1	(a)
(4,000)[b]	1/8 through 1	(a)
10,000	1/8 through 3/4	3/4 through 1

(a) Larger sizes are not included in these pressure classes.

(b) The design pressure of 4000 psi is shown for information only. Fittings for 4000 psi and 30-minute life at 1500 F will probably be similar to the 10,000 psi-fittings at 600 F.

A more detailed analysis, in which actual fitting geometry is established, will shift this division, but Table 6 may be taken as a preliminary indication of the division between threaded and flanged fittings based on torque requirements. Table 3 shows slightly smaller-size divisions between threaded and bolted fittings in Classes I and II than shown in Table 6, reflecting an anticipation that preloads (F_1) will be somewhat higher than design loads (F_D).

Fatigue

In general, tube or pipe fittings are subject to fatigue damage due to cyclic bending (vibration) of the piping system. When the fitting is properly preloaded, the cyclic stress in the fitting-to-fitting structure will be low and fatigue failure of the fitting-to-fitting is not anticipated. Fatigue failure, with cyclic bending of the attached pipe, is more likely to occur at the tube-to-fitting juncture. With the details shown later herein, and assuming an adequate brazed or welded tube-to-fitting joint, fatigue failure will occur first in the tube at the end of the hub socket. The stress-intensification factor at this juncture, however, will be fairly low if the socket wall thickness is not too large; i.e., the change in crosssection is not too great. The stress-intensification factors can be further reduced by tapering the end of the socket.

43

Seal Interaction

The requirements for the fitting structure are dependent on the type of seal. For example, an axial seal such as a flat metal ring gasket will impose more stringent requirements on the structure than does a radial seal which is described in later sections of this report.

Tube-to-Fitting Interaction

Insofar as fitting-to-fitting design is concerned, the tube-to-fitting connection should be such that it does not distort the fitting structure, particularly the seating surface for the seal. Distortions produced at the tube-to-fitting connection can be prevented from distorting the sensitive parts of the fitting structure, such as threads in threaded fittings or seal-seating surfaces in both threaded and flanged fittings, by using a sufficiently long, relatively thin hub on the fitting stub ends (threaded fittings) or on flanges (flanged fittings). The hub length required will depend upon the details of the tube-to-fitting joining process and the magnitude and type of distortions produced. The distortions produced by the joining process will be particularly harmful if they are of an axially nonsymmetric type.

Designs Considered

During the early stages of Phase I many possible methods of securing the fitting-to-fitting connection were considered. These ranged from exotic concepts like "Chinese finger grips" to the simple and everyday nut and bolt. Four methods which were considered worthy of consideration were (1) ring clamps, (2) snap or overcenter clamps, (3) differential threads, and (4) ball-and-socket joints.

Ring Clamps

Ring clamps were devised in an attempt to duplicate a flanged connection without using a great number of bolts. Generally the ring clamp is made of two mating flanges with tapered outer surfaces. A split hoop whose inside surfaces are tapered at the same angle as the flanges is fitted over the mating flanges. Small projections with bolt holes are provided where the two halves of the hoop are mated. Generally only two bolts are used. When these bolts are tightened a clamping force normal to the tapered faces is imposed. The axial component of the clamping force is the only force available for sealing and preloading. A typical ring clamp is shown in Figure 19a. This type of clamp is used extensively for many commercial applications and has been used in missile systems. Three major considerations ruled out this type of flange for an improved fitting.

(1) It is difficult to attain the required preload and it is also difficult to control initial preload within the limits necessary for the proposed service conditions.

(2) The weight of a fitting of this type would far exceed that of standard-type flanges for high-pressure applications.

(3) It is exceedingly difficult to secure this type of joint when the tubing is misaligned.

44

a. Ring Clamp

Open

Closed
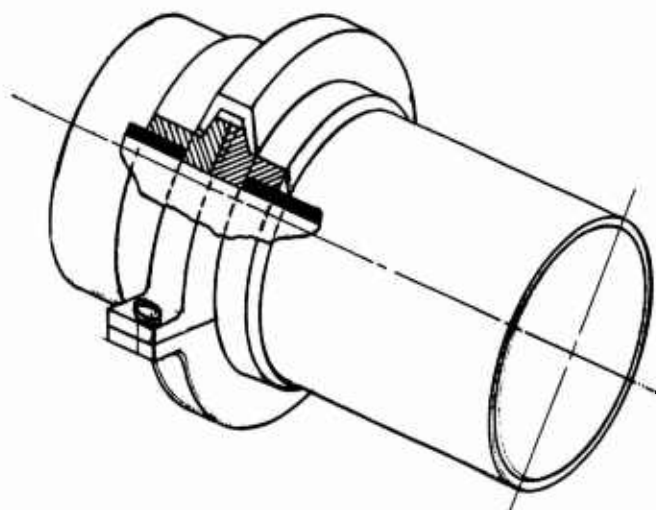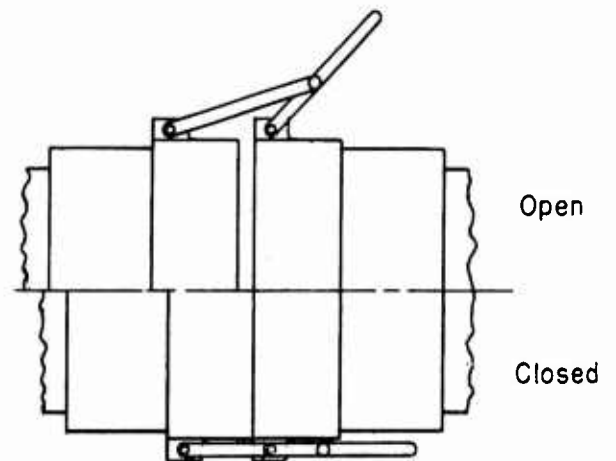
b. Snap on Overcenter Clamp

C

A

B
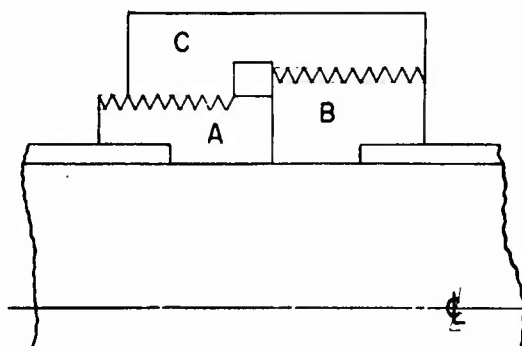
c. Differential Threads
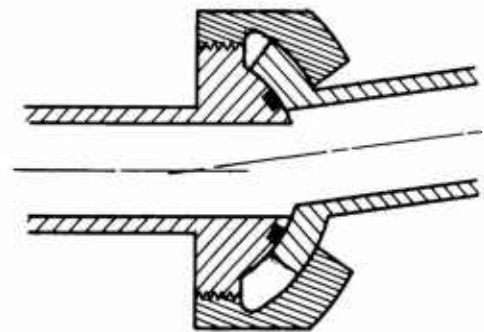
d. Ball and Socket Joint

FIGURE 19. FITTING-TO-FITTING DESIGNS CONSIDERED

Snap Clamps

Snap clamps, or overcenter clamps, like those in Figure 19b, would be placed circumferentially around the tube and would act like a circle of bolts. However, unlike bolts, snap clamps once closed cannot be further tightened unless a take-up screw is provided. Such a clamp would be complex in construction and would be less reliable than a simple bolt-and-nut arrangement. Snap clamps cannot compensate for misalignment, cannot be readily preloaded, and are subject to early fatigue failure due to working of the parts.

Differential Threads

The coupling shown in Figure 19c is a typical application of a differential thread. Because the threads on parts A and B have a different pitch, each will travel a different linear distance relative to coupling C as the coupling is rotated. An arrangement of this type can produce high preload forces but it is difficult to assemble, it is heavy, and it is susceptible to thread seizure.

Ball and Socket

A ball-and-socket-type joint (Figure 19d) is probably the most widely accepted means of joining two misaligned tubes. Because this type of joint can be made rugged, a design which can operate reliably is possible. However, in order to accommodate the seal in any angular position within the range of misalignment specified, it is probable that the seal would have to be placed at the ball-and-socket interface. Probably the best approach would be to machine a seal-retaining cavity in the ball and to make the socket sufficiently large that it could overlap the seal in any given position. A joint of this type is necessarily large and heavy because of the oversized socket and the oversized nut. This type of joint should not be used unless it is absolutely essential that the fitting compensate for misalignment. Although initial misalignment can be overcome with the ball-and-socket joint, bending moments due to vibration will still exist during operation. This type of joint is more likely to fail due to these bending moments.

Threaded and Bolted Flange Connections

Threaded and bolted flange connections have been used so universally that too often they are taken for granted. Many times when structural failures occur in threaded or bolted fittings it is concluded too rapidly that the failure can be ascribed to the method of connection. Rather, the failure is more probably the result of "insufficient" design; i.e., the fitting was not designed to take full advantage of the interacting physical phenomena inherent in the design. Battelle's choice of threaded and bolted flange connections as the best means at present of securing the fitting-to-fitting connection is based on the following:

(1) Preloading of the connection, which is considered essential for successful operation of the system, is easily attained.

(2) The effects of transient thermal gradients can be overcome by judicious choice of the spring constants R_B and R_G* in conjunction with the preload phenomena.

---

*See pages 35 through 39.

(3) Although assembly of the connection requires care, the technique is definitely within the capabilities of the average mechanic and the completed joint can be easily reassembled many times.

(4) In terms of load capability, the connection is probably lighter than other comparable designs.

(5) The reliability of threaded and bolted connections has been demonstrated conclusively.

It is recognized that such considerations as a torque relaxation and preload control by means of torque-wrench readings are two disadvantages inherent in these connections, especially with threaded fittings. However, because of the vast amount of experimental work already accomplished in these areas it is possible to adequately overcome the ambiguity these factors introduce into the design process.

Proposed Threaded-Fitting Design

The general procedure for designing a threaded fitting consists of the following steps:

(1) Establish design values based on service requirements

(2) Establish the location and magnitude of sealing loads

(3) Determine structural loads

(4) Design a fitting structure which satisfies the requirements of (1), (2), and (3).

The interrelationship of the decisions in each of the steps results in a relatively specific detailed design procedure for each type of fitting. This report section describes the design procedure and the design concept which Battelle developed for a unique proposed threaded-fitting configuration. The 1/2-inch experimental fitting evaluated during Phase II will be used to illustrate the discussion.

Design Values Based on Service Requirements

Some service requirements for threaded fittings are established by the fluid and vehicle systems, while others are estimated by the fitting designer. The following important design values, based on service requirements, are discussed in detail in previous sections of this report and on page 68.

(1) Tube diameter, material, and wall thickness

(2) Maximum and minimum operating pressure

(3) Maximum and minimum operating temperature

(4) Material compatibility requirements

47

(5) Required service life

(6) External loads

A seventh design requirement is the permissible leakage rate which varies with fluid density, fluid pressure, and mission life. Generally permissible leakage is designated simply as "zero leakage" which is not really an acceptable value for design purposes. As indicated in Table 7 a specific leakage rate of 7×10^{-7} atm cc/sec H_e is designated.

During a discussion with the project monitor at the end of the Phase I, a 1/2-inch, Class II threaded fitting was selected as a representative fitting for experimental verification of the design procedures developed during Phase I. Because the lowest temperature readily attained in the laboratory was -320 F (the boiling point of liquid nitrogen), the experimental fitting was designed for this low-temperature limit. Design values for the 1/2-inch experimental fitting, based on Class II service (see p 19), are given in Table 7.

TABLE 7. DESIGN VALUES BASED ON SERVICE REQUIREMENTS FOR 1/2-INCH EXPERIMENTAL FITTING

Tube Diameter, OD	0.500 inch
Tube Material (Class II Specifications)	René 41
Tube Wall Thickness (Equation 3)	0.0075 inch
Alternate Tube Material[a]	18-8 annealed stainless steel
Alternate Tube Wall Thickness[a]	0.035 inch
Operating Pressure (Class II Specifications)	0 to 2000 psi
Proof Pressure (1-1/2 times operating pressure)	3000 psi
Operating Temperature (Modified Class II Specifications)	-320 to 600 F
Fitting Material (Class II Specifications)	René 41
Material Compatibility	See p 13
Service Life (Estimated)	10,000 hours
External Loads – Limited by Tubing Strength	See pp 26-29
Permissible Leak Rate for Helium	7×10^{-7} atm cc/sec

(a) An alternate tube material and size were selected on the basis of MIL-F-18280A because of the current problems of obtaining René 41 tubing.

For convenience, the design properties of René 41 are given in Table 8.

TABLE 8. DESIGN PROPERTIES OF RENÉ 41

Temperature, F	Yield Stress, 1000 psi	Modulus of Elasticity 10^7 psi	Thermal Coefficient of Expansion, in./in./F
-425	190	3.2	7.5×10^{-6}
70	155	3.1	7.5×10^{-6}
600	150	2.9	7.5×10^{-6}

Sealing Load

The seal imposes two loads on the structural elements of the fitting. A detailed discussion of the seal, its development, and its sealing action is presented in a later section, "Seal Design". The more significant one is the radial sealing load. As shown in Figure 20, this load is applied along the circumferential interfaces between the seal and the two stub ends. The magnitude of this load is approximately 900 lb/linear inch.

The second load is that axial load required to assemble the seal. Experimentally this was determined to be approximately 1200 lb.

Structural-Load Determination

The structural load, F_S, which a fitting must carry is equal to the sum of the pressure end load and the axial load equivalent of the bending load. The methods for calculating these loads are given by Equations (1) and (12), respectively, in the "Design Parameters" section.

For the experimental fitting, the pressure end load, F_E, was calculated using an internal pressure of 2000 psi and an effective seal diameter of 0.820 in. F_E was found to be 1584 lb. To calculate the equivalent axial load, F_B, it was necessary to select a maximum tube bending stress, S_B. This was made two-thirds the yield stress of René 41, or 100,000 psi. F_B was found to be 1178 lb. Thus, F_S was $F_E + F_B$, or 2762 lb.

In the subsequent discussion, F_S will be used as a major design value for the fitting structure. However, if the axial load required by the seal had been greater, as may be the case with some seal configurations, the larger axial seal force would have been used instead of F_S. This is discussed in more detail on page 35.

Fitting-Structure Design

With the determination of the design values described in the above three parts, the completion of the fitting structure design consists essentially of three types of activities: (1) the selection of a means of joining the tube ends to the fitting parts, (2) the tentative selection of certain fitting dimensions as indicated by the seal requirements, and (3) the calculation of two nut dimensions to assure the proper operation of the fitting assembly under certain critical operating conditions.

Dimensions Established by Tube-to-Fitting Connection. The selection of a tube-to-fitting connection is a major design decision. A detailed discussion of the aspects of the problem and of the decisions made on the program is presented in the next section of the report, entitled "Tube-to-Fitting Connection". The procedure selected is the TIG-welded connection developed by North American Aviation. The general configuration of the connection for joining the fitting to tubing is shown in Figure 20. The OD and ID of the hubs of the stub ends are identical with the tubing OD and ID. The welding sleeves are placed such that clearance is allowed between the end of one welding sleeve and the end flange, and between the end of the other welding sleeve and the wrench flats. Because the nut must pass over the welding sleeve on each disassembly of the fitting, the end flange OD is determined by the welding sleeve OD and the necessary clearance.

49
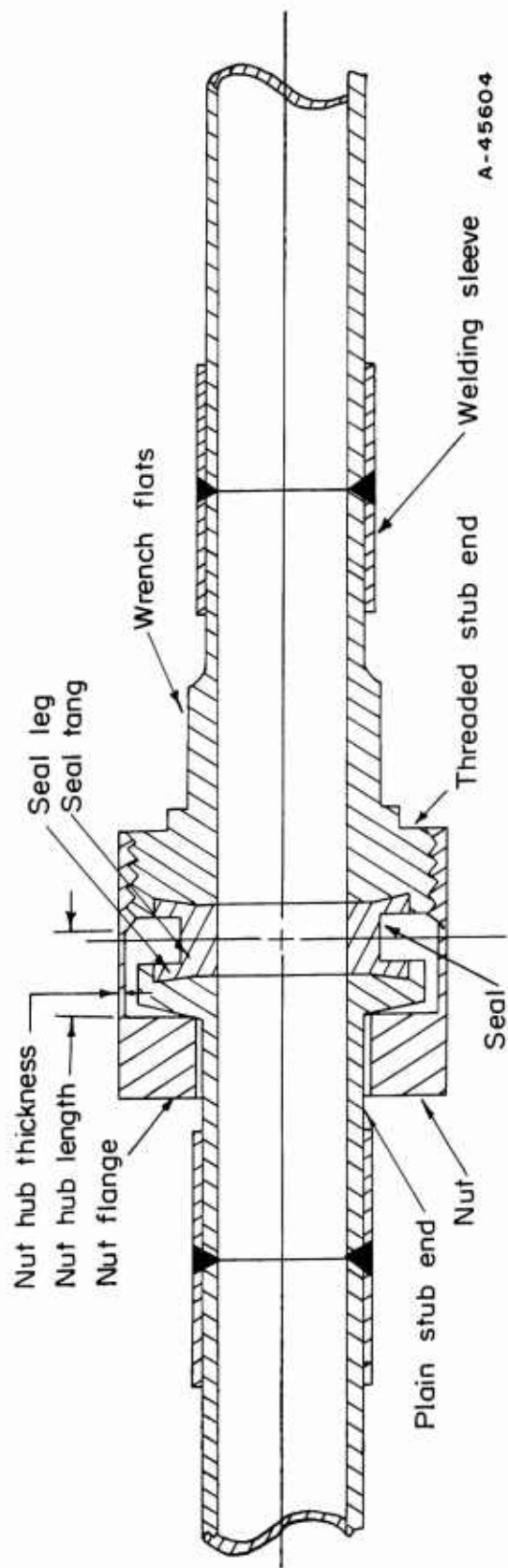
FIGURE 20. PROPOSED THREADED CONNECTION

The dimensions for the experimental fitting when used with stainless steel tubing are shown in Figure 21.

Dimensions Established by Seal. Because the seal is a replaceable element and because of the nature of the sealing action, it is necessary for the two stub end flanges to provide a cavity in which the seal can be nested. The dimensions of this cavity are given in Figure 22a.

A radial force, F_R, of 900 lb/linear inch is applied outwardly along circumferential surfaces A. This force develops a bending moment on each flange as shown in Figure 22b and induces a hoop stress in the flange rim. The rim thickness must be sufficient to prevent overstressing of the flange. If a 1-inch 20 UNEF, 75 per cent thread is used and if 0.010-inch radial clearance is provided between the OD of the plain stub end flange and the thread minor diameter on the nut, the resulting rim thickness is 0.056 inch. This value is adequate. The next smaller thread size possible would be a 15/16-20 UNEF. The rim thickness for this size thread is only 0.017 inch, which is inadequate.

When the flange was analyzed as a flat circular plate with the inside edge rigidly supported and with a bending moment applied at the outside edge, the maximum stress in the plain stub end flange was only 16,000 psi when the flange was 0.070 inch thick. A thickness of 0.070 inch was chosen because it is the thinnest, most lightweight design considered practical for manufacturing.

The threaded stub end was made 0.250 inch thick to provide a thread engagement of five full threads. The dimensions thus established for the threaded stub end were more than ample to resist the radial-seal load.

Selection of Nut Dimensions. With the selection of the seal and major stub-end dimensions, it is possible to select tentatively all but two of the nut dimensions. As explained later, the dimensions which cannot be selected, the nut hub thickness and the nut flange thickness (see Figure 20) are the most important in determining the deflection characteristics of the nut.

(1) Nut Flange Inside Diameter. The inside diameter of the nut flange is determined by the clearance needed for the welding sleeve. With an outside tube diameter of 0.500 inch and a welding sleeve thickness of 0.031 inch, the inside diameter of the experimental nut flange was selected as 0.570 inch to provide a diametral clearance of 0.008 inch.

(2) Nut Thread. The nut thread was determined as described immediately above. To assure the engagement of five threads while allowing reasonable machining tolerances, a thread length of 0.290 inch was selected.

(3) Nut Hex. To keep the nut as small and as lightweight as possible (using standard hex stock material), a hex of 1-1/16 inches across flats was chosen.

(4) Nut Hub Length. As shown in Figure 20, the nut hub length was determined by the seal dimensions and by the configuration of the plain stub end. Thus established, the nut hub length was 0.255 inch.

51
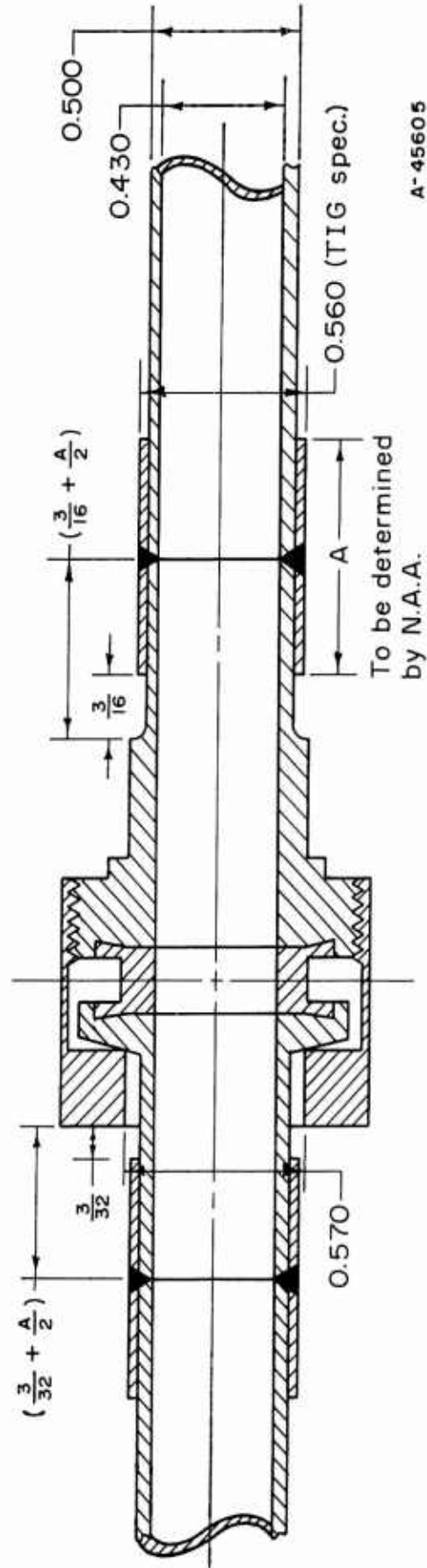
FIGURE 21. FITTING DIMENSIONS ESTABLISHED BY SELECTED
TUBE-TO-FITTING CONNECTION

52
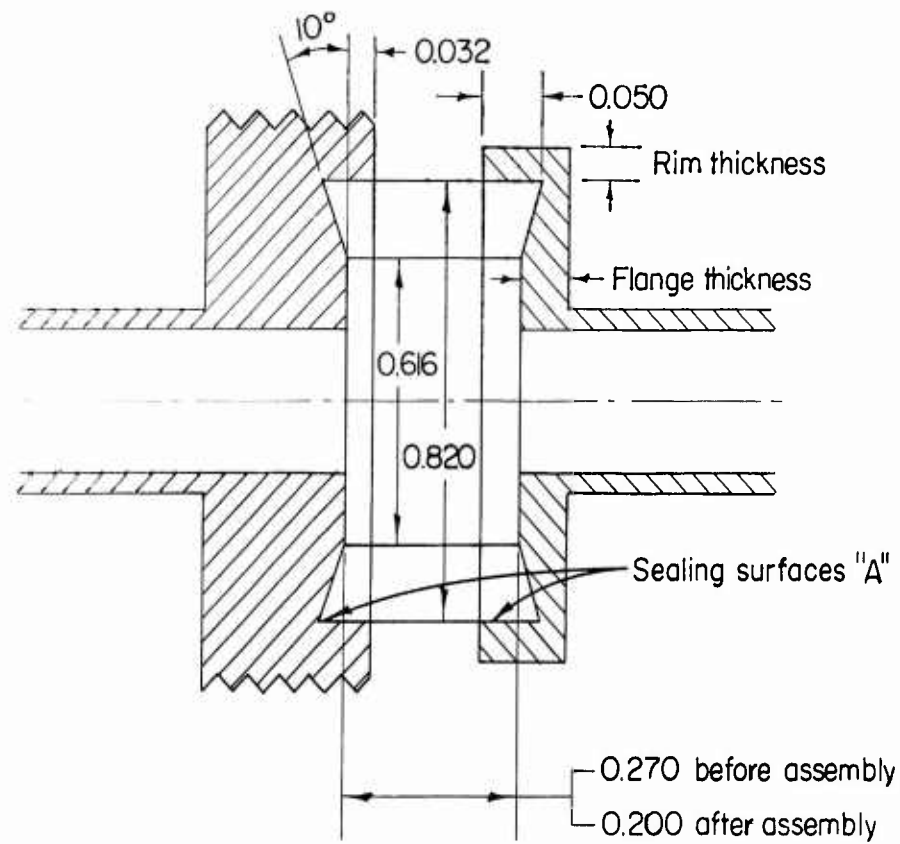
a. Dimensions of the Seal Cavities
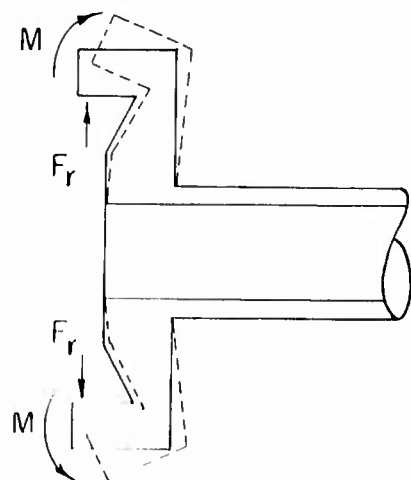
A-45606

b. Forces Applied by Seal

FIGURE 33   EFFECTS OF SEAL ON FLANGE DESIGN

Calculation of Two Nut Dimensions. As discussed in the "Design Parameters" section, the nut of a threaded fitting acts as a tension spring to press the stub ends and the seal together. The nut must clamp the compression parts satisfactorily during internal pressure variations, external load fluctuations, and changes in fitting component dimensions as a result of internal temperature variations. With several of the nut dimensions established (see above), the load-deflection characteristic of the nut is varied by changes in the nut hub thickness and the nut flange thickness. The significance of these dimensions is discussed in detail in Appendix V.

The calculations which establish the best combination of the two nut dimensions are complicated. They require the use of a preload diagram as a design tool, the iteration of incremental values of the two nut dimensions in several equations to determine stress and load-deflection limitations, and the manual comparison of candidate nuts to determine the best nut dimensions. The discussion to describe this lengthy and critical procedure is presented in the following steps:

(1) Explanation of the general graphical-design procedure

(2) Determination of the spring constant of the compression members

(3) Determination of the thermal-gradient displacements

(4) Description of the iterative design procedure

(5) Determination of the maximum allowable fitting load

(6) Determination of the desired nut spring constant

(7) Determination of the actual nut spring constant and selection of the best nut

(8) Determination of the preload limits for the selected nut.

(1) General Graphical-Design Procedure

The use of the following graphical-design procedure enables the designer to understand the relationship of several design factors for the nut. The construction of the diagram also enables the designer to (1) determine the desired load-deflection characteristic of an arbitrarily selected nut, and (2) establish the desired preload for the selected nut.

Figure 23 without KC_{cold}, F_S (cold), KC_{hot}, and F_S(hot) is a typical preload diagram (see p 37). The vertical axis indicates the axial fitting load between the nut flange and the plain stub end resulting in compression in the compression members and tension in the tension members. A preload diagram is usually used to determine the effect of an external load on the tension and compression members. Movement to the right on the X-axis indicates an increase in displacement of the tension member and a decrease in displacement for the compression members. Thus, an additional structural load at room temperature, F_S(RT), will increase the nut deflection and decrease the deflection of the compression members. The slopes of KT_{RT} and KC_{RT} are the spring rates of the tension and compression members respectively, expressed in lb/in. These values are the inverse of the spring constants (see p 37) which are expressed in in./lb.

54
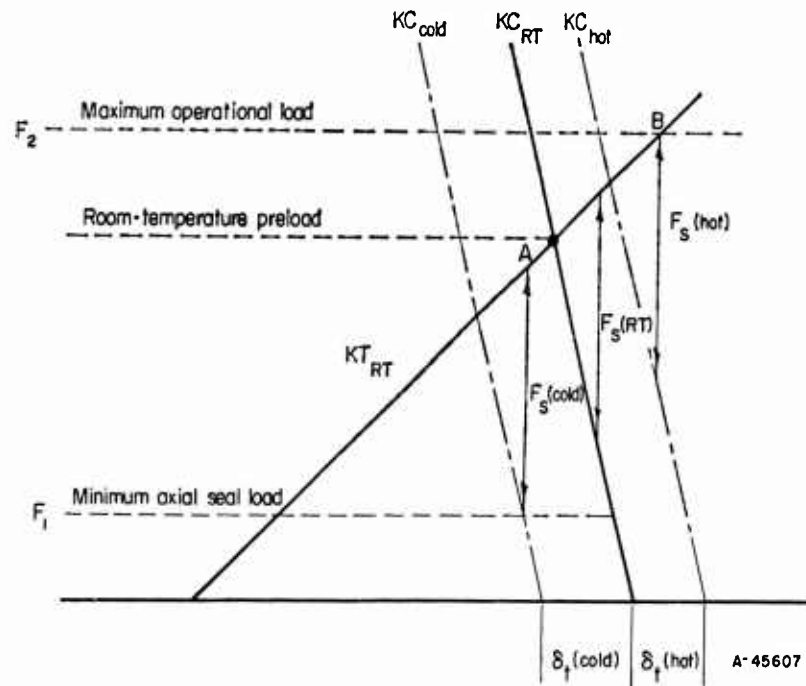
FIGURE 23. GRAPHICAL SOLUTION FOR KT
AND REQUIRED PRELOAD

To use a preload diagram as a design tool for the threaded fitting, the spring constant of the compression members is first calculated for room-temperature conditions and plotted as KC_{RT}. Next, the effects of thermal gradients in the fitting are added to the preload diagram. When a hot fluid is suddenly introduced into the fitting, an elongation, δ_t (hot), of the compression member occurs before the nut elongates. This momentarily shifts KC_{RT} to the right (KC_{hot}) in respect to the room temperature location of KT_{RT}. Similarly, a thermal gradient caused by a sudden flow of cold fluid causes a momentary shift of KC_{RT} to the left (KC_{cold}). For either condition, as the nut approaches the temperature of the compression members, the room-temperature preload is approached. However, the locations of KC_{hot} and KC_{cold} establish the performance required of the nut for the maximum temperature differences in the fitting.

The minimum axial seal load required for proper functioning of the seal, F_1, is added to the diagram. The maximum operational load at the maximum operating temperature, F_2, is calculated for a nut configuration resulting from an arbitrary selection of the nut hub thickness and the nut flange thickness. F_2 is added to the preload diagram.

The slope and location of KT_{RT}, the desired spring rate of the arbitrarily selected nut, is established by determining the location of two points. First, a vertical line, F_S, equal in length to the maximum expected structural load, is drawn up from the intersection of F_1 and KC_{cold}. This establishes Point A. Point B is established by drawing a second vertical line, F_S, to fit between F_2 and KC_{hot}. Point B is located on F_2. The desired spring rate of the arbitrarily selected nut, KT_{RT}, is then equal to a line drawn through Points A and B, and extended to intersect the displacement axis. The actual spring constant of the arbitrarily selected nut is then calculated to determine whether the nut will function satisfactorily. The proper room temperature or installation preload for the selected nut is determined by the intersection of KT_{RT} and KC_{RT}.

(2) Spring Constant of the Compression Members

The total spring constant of the compression members, i.e., deflection in inches per unit load, is the sum of the spring constants for the individual compression members. The general expression for calculation of displacements in parts subjected to tension or compression is given in Appendix I. The compression members of the experimental fitting consist of the plain stub end, the seal tang, and the threaded stub end. Pertinent dimensions for the individual compression members are given in Table 9. The axial length used for the threaded stub end was one-half the thread length. This was a somewhat arbitrary estimate of the portion of the threaded stub end under compression.

TABLE 9. DIMENSIONS OF COMPRESSION MEMBERS DETERMINING
COMPRESSION SPRING CONSTANTS

Compression Member	Axial Length, in.	Radial Thickness, in.	Average Diameter, in.
Flanged stub end	0.080	0.210	0.695
Seal tang	0.200	0.095	0.532
Threaded stub end	0.145	0.241	0.726

With these dimensions, the total spring constant of the compression members, KC_{RT}, was 0.585×10^{-7} in-lb. This value was used with the 276-lb minimum axial seal load to begin the preload diagram. The completed diagram for the 1/2-inch experimental fitting is shown in Figure 24.
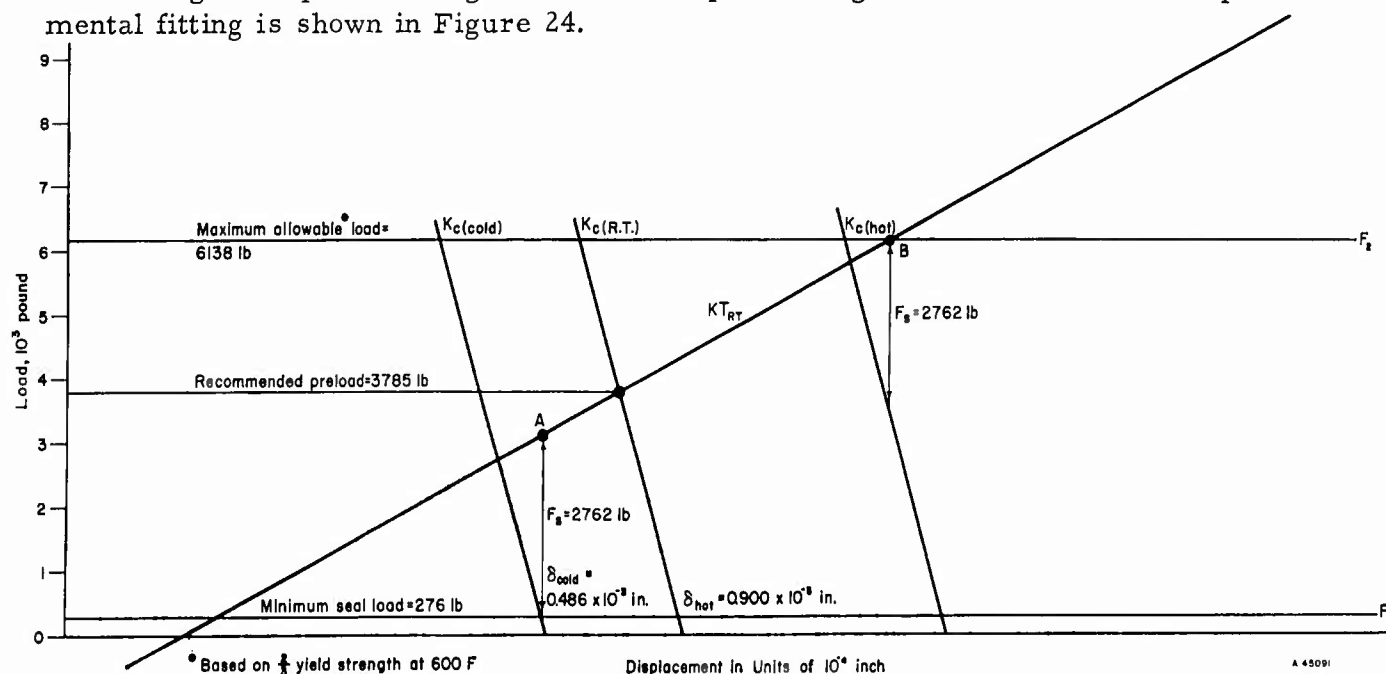
FIGURE 24. PRELOAD DIAGRAM FOR EXPERIMENTAL NUT

(3) Thermal-Gradient Displacements

The thermal-gradient displacements, as discussed previously, are the displacements due to unequal expansions or contractions caused by a temperature difference between the compression and tension members of the fitting. Thermal-gradient tests, which are described in Appendix IV, were conducted to determine the magnitude of the temperature differences. The cold thermal gradient was found to be -162 F, while the hot thermal gradient was 276 F.

One method of designing for creep in threaded fittings is to increase the hot thermal gradient by an amount which would cause a displacement equivalent to the amount of creep expected. Because the creep rate is dependent on both time and stress levels, this may be an excessively conservative design method. However, for the experimental fitting, the thermal gradients used were the same as those measured in the thermal-gradient tests, with an arbitrary 24 F added to the hot thermal gradient for creep. The displacements caused by these temperature differences can be calculated by the following equation:

$$\delta = \alpha L \Delta T \quad , \tag{21}$$

where

$$\alpha = \text{coefficient of thermal expansion,} \\ \text{in. /in. /F}$$

$$\Delta T = \text{temperature difference, F}$$

$$L = \text{length, in.}$$

For the experimental fitting, the length was taken to be the nut hub length plus one-half the nut thread length. The displacements caused by the temperature differences were then 0.486×10^{-3} and 0.900×10^{-3} inch for the cold and hot thermal gradients, respectively. The displacement of KC_{RT} for these conditions on the preload diagram is shown in Figure 24.

(4) Iterative Design Procedure

Because F_S is known (see page 49), the values needed to complete the preload diagram are the maximum operational load for the fitting and the spring constant of the tension member (the nut). The maximum operational load on the fitting is determined by the maximum allowable load on the nut. Both the maximum allowable nut load and the nut spring constant are established largely by the two nut dimensions as yet undetermined — the nut flange thickness and the nut hub thickness.

The design procedure now becomes an iterative one consisting of the following steps:

(1) Dimensions are selected for the nut hub thickness and the nut flange thickness

(2) The maximum load capability of the resultant nut configuration is calculated (see the following page)

57

(3) The spring constant desired for the resultant nut is determined (see below).

(4) The actual spring constant of the resultant nut is calculated (see below)

(5) A comparison of the spring constants is made. If the actual spring constant is equal to or greater than the desired spring constant, the nut will function satisfactorily

(6) a. If the nut is not satisfactory, Steps 1-5 are repeated

　　b. If the nut is satisfactory, the weight of the nut is calculated

(7) Steps 1 through 6 are repeated in an effort to find the lightest possible acceptable nut.

(5) <u>Maximum Allowable Load</u>

For any selected nut hub thickness and nut flange thickness, the maximum allowable nut load is the load at which the highest stress in the nut is equal to the maximum allowable stress of the nut material. For the 1/2-inch fitting, two-thirds of the yield stress (two-thirds of 150,000 psi) was selected as the maximum allowable stress. Six types of stresses are of concern in the nut: (1) the longitudinal hub stress, (2) the radial ring stress, (3) the tangential ring stress, (4) the thread shear stress, (5) the tensile stress in the nut hub, and (6) the tensile stress in the nut thread section. Methods of calculating these stresses are discussed in Appendix I. The type of stress which is limiting depends not only on the absolute values of the two unknown nut dimensions, but on their comparative values as well.

Normally a large number of nut flange thickness and nut hub thickness dimensions must be investigated. The method of selecting the optimum nut will be discussed later. For convenience, the nut flange thickness and nut hub thickness used for discussion will be 0.246 inch and .0253 inch, respectively. These dimensions are the dimensions of the experimental nut which were found to be optimum after repeated application of the design procedure. These dimensions were also used for the fabrication of the nut which was evaluated in Phase II. With these dimensions, the controlling stress was the tangential ring stress and the maximum allowable load was 6138 lb. At this maximum load, the six stresses had the following values:

Tangential Ring Stress	100,000 psi
Longitudinal Hub Stress	99,796 psi
Radial Ring Stress	8,559 psi
Tensile Stress in Nut Thread Section	31,918 psi
Thread Shear Stress	8,704 psi
Tensile Stress in Nut Hub	35,410 psi

In order to make the most efficient use of the nut material, it is desirable that the maximum nut load under operational conditions, i.e., the maximum operational load, be equal to the maximum allowable nut load. If the maximum operational load is different from the maximum allowable load, the nut, and hence the fitting, will be over- or under-designed, resulting in excessive weight or failure. Thus, in constructing the preload

58

diagram, or in considering the preload relationships, the maximum operational nut load and the maximum allowable nut load are considered to be synonymous. Figure 24 shows the location of the maximum allowable load on the preload diagram for the experimental fitting.

(6) Desired Nut Spring Constant

The desired spring constant for the selected nut (the inverse of the slope of KT_{RT}) can now be determined from the preload diagram. To determine the slope of KT_{RT}, it is necessary to locate at least two points on the line - one point can be located on the basis of the minimum seal load and KC_{cold}. The other can be located on the basis of the maximum allowable load and KC_{hot}. These two sets of conditions represent the extremes between which the fitting will operate.

To establish the first point, a vertical line which by scale is equal to the maximum expected structural load of 2762 lb (see page 49) is drawn from the intersection of the minimum seal load and KC_{cold}. The top of this line locates Point A, Figure 24. The second point is established by locating a vertical line also equal to the maximum structural load to fit between the maximum allowable load and KC_{hot}. This establishes the second point at B, Figure 24. The inverse slope of the line drawn through A and B is the desired spring constant. For the experimental nut, the value was 0.389×10^{-6} in-lb.

(7) Actual Spring Constant

The desired spring constant for the selected nut is based on the service requirements, while the actual spring constant is based on selected nut dimensions and is computed by means of the equations in Appendix VI. The spring constant consists of (1) the elongation of the nut hub under load, (2) the elongation of the nut thread section under load, and (3) the rotation of the nut flange. If the actual nut spring constant is less than the desired nut spring constant, the nut will be too stiff and it will not have sufficient thermal capability. If the actual nut spring constant is equal to or greater than the desired nut spring constant, the nut will function satisfactorily. Because many nut configurations may function satisfactorily, a final choice of the best nut from candidate nuts is made on the basis of lightweight and insensitivity to machining variations. For the optimum experimental nut, the spring constant was 0.393×10^{-6} in-lb.

Appendix V describes the experimental work done to verify the selected nut spring constant as predicted by the above design procedure.

These considerations emphasize the fact that "beefing up a nut" will not necessarily improve the fitting performance. The stress in the nut may be protected from overtorquing, but the spring constant may be decreased to the point where the nut will fail in service. Failure may occur from leakage due to a cold thermal transient, or from nut deformation caused by a hot thermal transient.

(8) Preload Limits

The intersection of the actual KT_{RT} with KC_{RT} determines the recommended preload for the selected nut, while the intersection of KT_{RT} with the abscissa determines the origin of the axial displacement axis. For the experimental fitting the recommended preload was 3785 lb. This was equal to a torque of 63.1 lb-ft as defined by Equation (20).

The preload diagram in Figure 24 is based on the maximum allowable stress equal to two-thirds the yield strength of the material. It is also important to know what values would result from a preload diagram based on 100 per cent of the yield strength. These values can then be used to determine the maximum permissible torque. Such a diagram is shown in Figure 25 by the lines designated by a single prime. In addition, Figure 25 shows what preload force would cause the axial seal load to fall to zero during the cold transient. This relationship is shown by the lines designated by a double prime. The preload diagram in Figure 25 is based on the following three assumptions.

(1) The lowest permissible preload is that preload which will result in a residual axial seal load of zero when the fitting is subject to a cold thermal gradient equal to the design gradient.

(2) The highest permissible preload is that preload which will result in the maximum nut load reaching a value such that the nut is stressed to the yield stress of the material when the fitting is subjected to a hot thermal gradient equal to the design gradient.

(3) A primary seal is obtained at a preload value less than the lowest permissible preload. If this is not so, the lowest permissible preload must be based on a load necessary to achieve an initial seal.
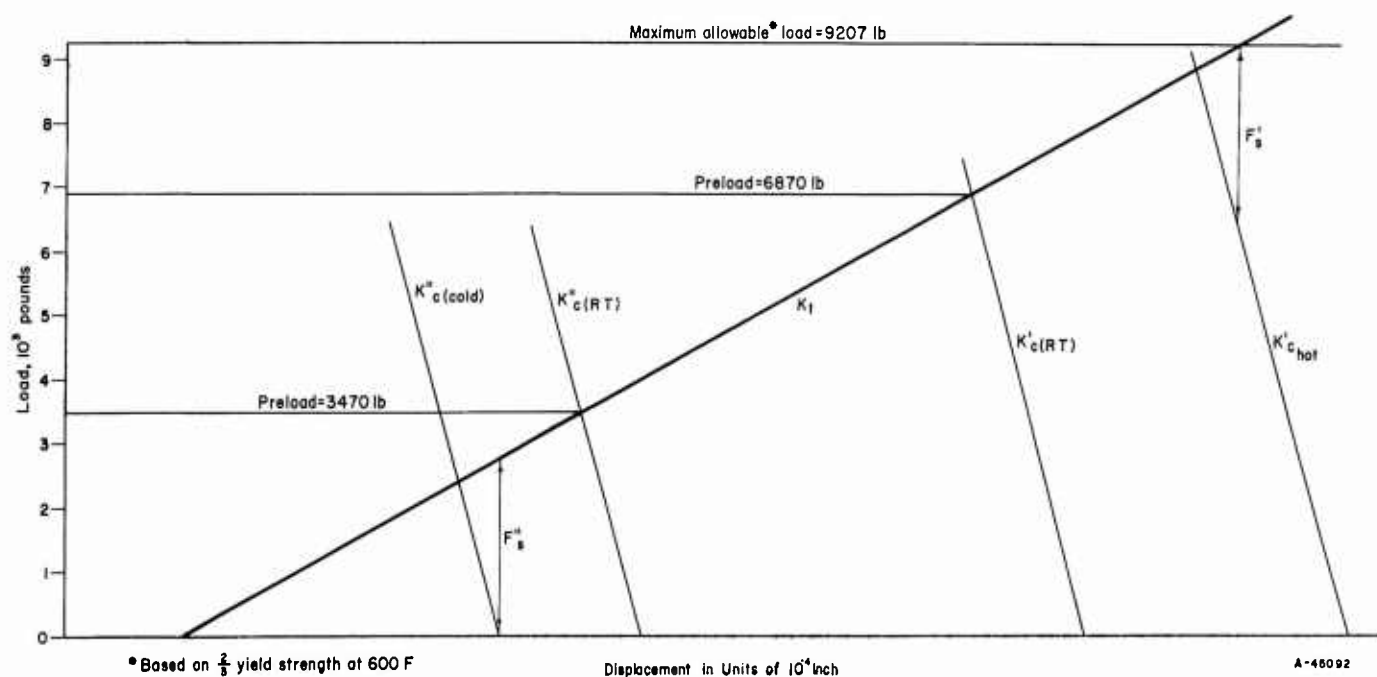
FIGURE 25. MODIFIED PRELOAD DIAGRAM BASED ON (A) 100 PER CENT OF YIELD STRENGTH AND (B) MINIMUM SEAL LOAD EQUAL ZERO

The actual preload of a fitting is difficult to predict. The initial value is subject to many variations, and operation of the fitting in service usually results in a significant reduction in preload. While it may be acceptable for the designer to establish a practical preload range within the preload limits established above, it is possible to design into the fitting a preload range which will still allow the fitting to accommodate the thermal gradient and maximum allowable stress requirements. This can be done by purposely selecting a nut which has an actual spring constant greater than desired spring constant.

As illustrated in Figure 26, the upper preload limit is determined by the maximum allowable load. A line equal in slope to the actual KT is drawn through Point B established in Figure 24. The upper preload limit, then, is determined at the intersection of this line with KC_{RT} (Point U). The lower preload limit is determined by the minimum sealing load in a similar manner. A line equal in slope to KT is drawn through Point A. The intersection of this line with KC_{RT} is then the lower preload limit (Point L). The upper and lower limits of preload then determine the preload range of the selected nut. If the range is not satisfactory, another nut can be evaluated.

For the experimental fitting, an installation preload range was established for the laboratory work by arbitrarily reducing the safety factor applied to the maximum allowable load. Torques of 65 lb-ft and 75 lb-ft were selected for specification, while an overtorque limit of 85 lb-ft was chosen. This overtorque capacity provided a safety factor of 28 per cent in respect to the maximum expected operational stress.

Computer Use for Nut Selection. The nut dimensions used in the example are the nut dimensions which were found to be optimum for the given service conditions. Normally the original choice of nut dimensions would not only not be optimum, but probably would not even be satisfactory. To obtain a satisfactory set of conditions alone may require many iterations. However, to be of optimum design, a fitting for use in missiles must not only be satisfactory, but must also be of minimum weight. If only the nut hub thickness and the nut flange thickness are varied, there are still a great number of nut designs which are possible. For every nut hub thickness there may be a nut flange thickness which will produce a satisfactory design. In order to choose an optimum design, then, a very large number of calculations are necessary.

A digital computer program was prepared to perform the iterations necessary for the choice of an optimum nut for the experimental fitting. The Threaded Fitting Design computer program is listed in Appendix VI, along with an input data sheet, and a typical output from the computer.

Basically, a digital computer does the same operations as a desk calculator. The advantage of a computer lies in its speed and accuracy. For example, in designing the experimental nut, the digital computer performed approximately 840 iterations in 2 centihours. It would have taken one man working approximately 3 years to perform the same number of calculations and there would have been no guarantee of accuracy.

The inputs into the computer program consist of two sets of information. One set includes fitting dimensions and material properties that are constant. The second set includes dimensional variables. The computer is programmed to perform iterations in which all variables but one are held constant, while the single variable is changed in increments. The output of the computer consists of a listing of the maximum allowable load, the recommended preload, the critical stresses, the desired spring constant of the nut, the actual spring constant of the nut, and the corresponding volume for each set of conditions. The final choice of the optimum nut design based on minimum weight, is then done by a manual comparison.

The iterations of the Threaded Fitting Design computer program are performed in the following manner: A nut hub thickness is chosen and the flange thickness is incremented, with an output being obtained for each flange thickness; a new nut hub thickness is then chosen and the process repeated until the nut hub thickness variation limits which
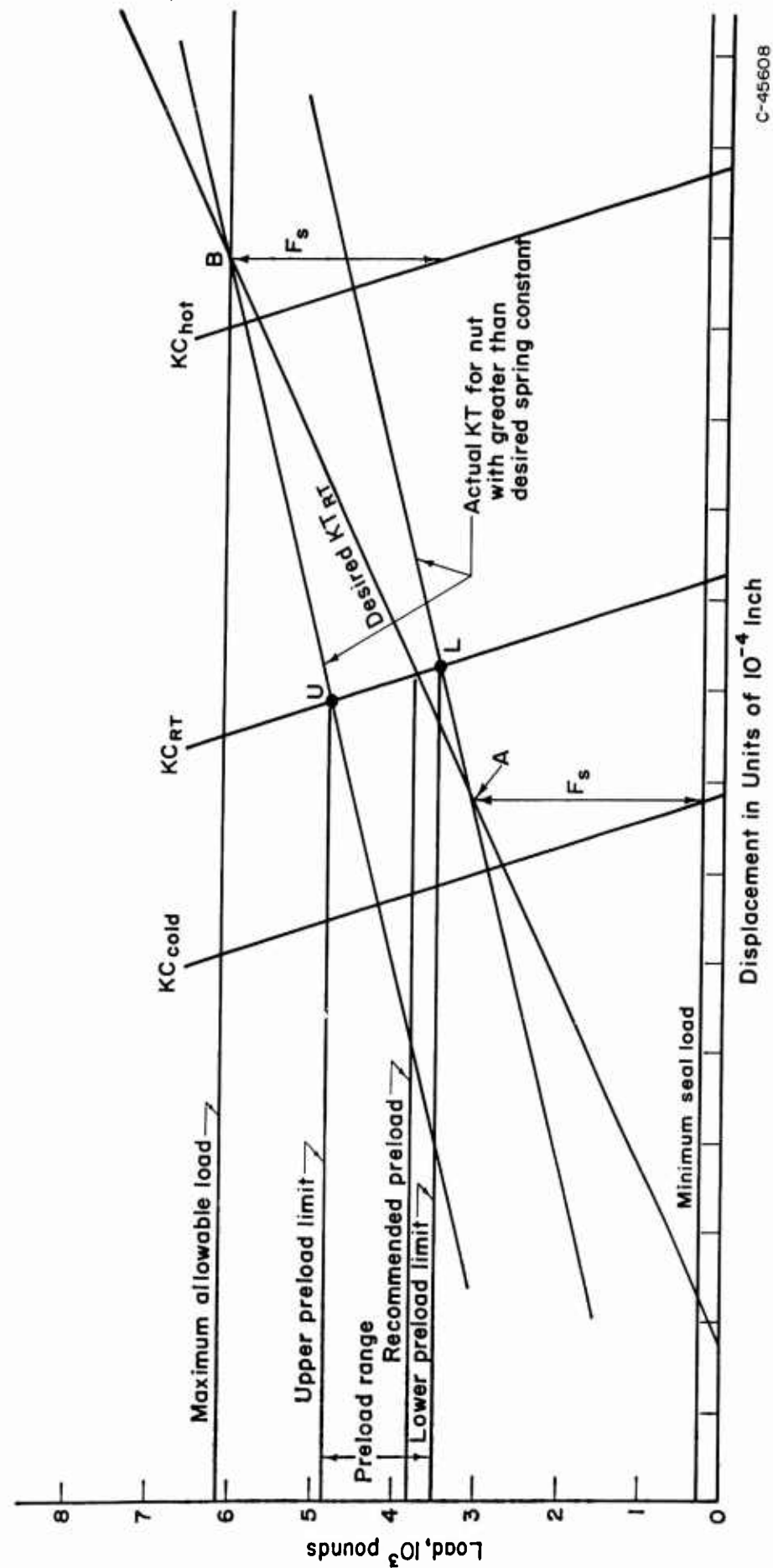
FIGURE 26. PRELOAD DIAGRAM FOR ESTABLISHING A RECOMMENDED PRELOAD RANGE

C-45608

62

are built into the program are reached. For the experimental nut, this required compu-
tations for the twelve values of the nut hub thickness shown in Table 10. Each combina-
tion of the nut hub thickness and flange thickness shown in Table 10 represents an opti-
mum combination as determined by comparing the desired spring constant for the nut
with the actual spring constant in the computer output (see Appendix VI) and picking the
combination of dimensions which gives the minimum volume for which the actual spring
constant of the nut is greater than the desired spring constant of the nut.

TABLE 10. POSSIBLE NUT CHOICES
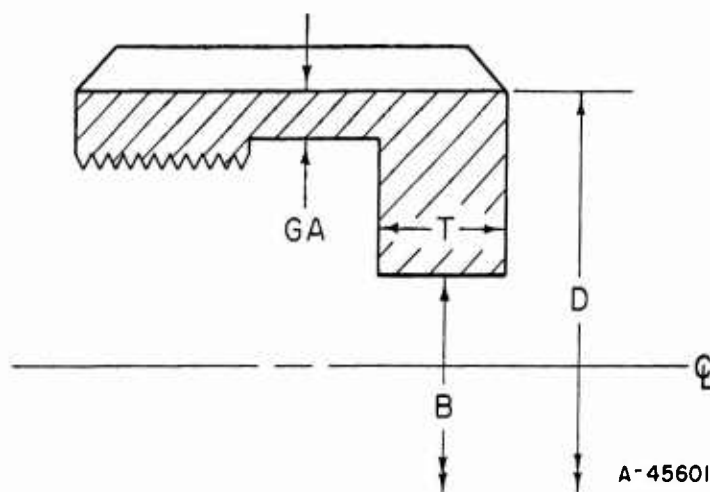
Item	T, in.	GA, in.	W_{max}, lb	$W_{preload}$, lb	V, in.^{3}
1	0.249	0.0313	6409	3840	0.2993
2	0.249	0.0283	6366	3881	0.2968
3	0.246	0.0253	6138	3785	0.2923
4	0.252	0.0223	6176	3798	0.2941
5	0.255	0.0193	6116	3763	0.2939
6	0.261	0.0163	6192	3810	0.2957
7	0.264	0.0133	6163	3804	0.2954
8	0.267	0.0103	6148	3810	0.2951
9	0.267	0.0073	6021	3755	0.2926
10	0.267	0.0043	5905	3710	0.2900
11	0.270	0.0013	5923	3755	0.2897
12	0.270	-0.0017	5827	3736	0.2871

The final choice was made by comparing the twelve possible designs on the basis
of volume and nut hub thickness. Item 3 was the design chosen. Although Items 10, 11,
and 12 would have resulted in a lighter nut, the spring constant and load capacity char-
acteristics would have been more sensitive to machining tolerances because of the
smaller hub thicknesses. The minus value shown for GA in Item (12) indicates that al-
though the nut is theoretically adequate, it is not a practical choice because the ligament
between the threaded portion and the nut flange exists only in the six corner projections
of the hex.

During the Phase II effort it became desirable to be able to determine the capabili-
ties of a fitting when the dimensions were known. By a slight modification of the
Threaded Fitting Design computer program, a Threaded Fitting Capabilities computer
program was prepared. This program is listed in Appendix VI. The output of this pro-
gram consists of spring constants for both tensile and compression members, the maxi-
mum allowable nut load, and the thermal-gradient capabilities.

63

Design Procedure for Flanged Connections

Flanged connections are usually designed for specific systems. This is possible because considerably fewer flanged connections are used in aerospace vehicles, and because it is much more difficult to standardize on flanged connection designs without imposing a severe weight penalty on many installations. This section contains a detailed discussion of the important design parameters. In addition, an example is presented to illustrate a recommended design procedure, brief comments are given concerning the problems of manufacture and assembly, and specific designs are presented for selected fitting classes and sizes. Two basic types of connections are considered: those containing integral flanges and those containing separate flanges.

Definition of Symbols

The design of aerospace flanged connections requires the use of a large number of design parameters. The symbols used in the discussion are defined in Figure 27 and Table 11 below.

Integral Flange — Type I   Separate Flange — Type II

A-45610
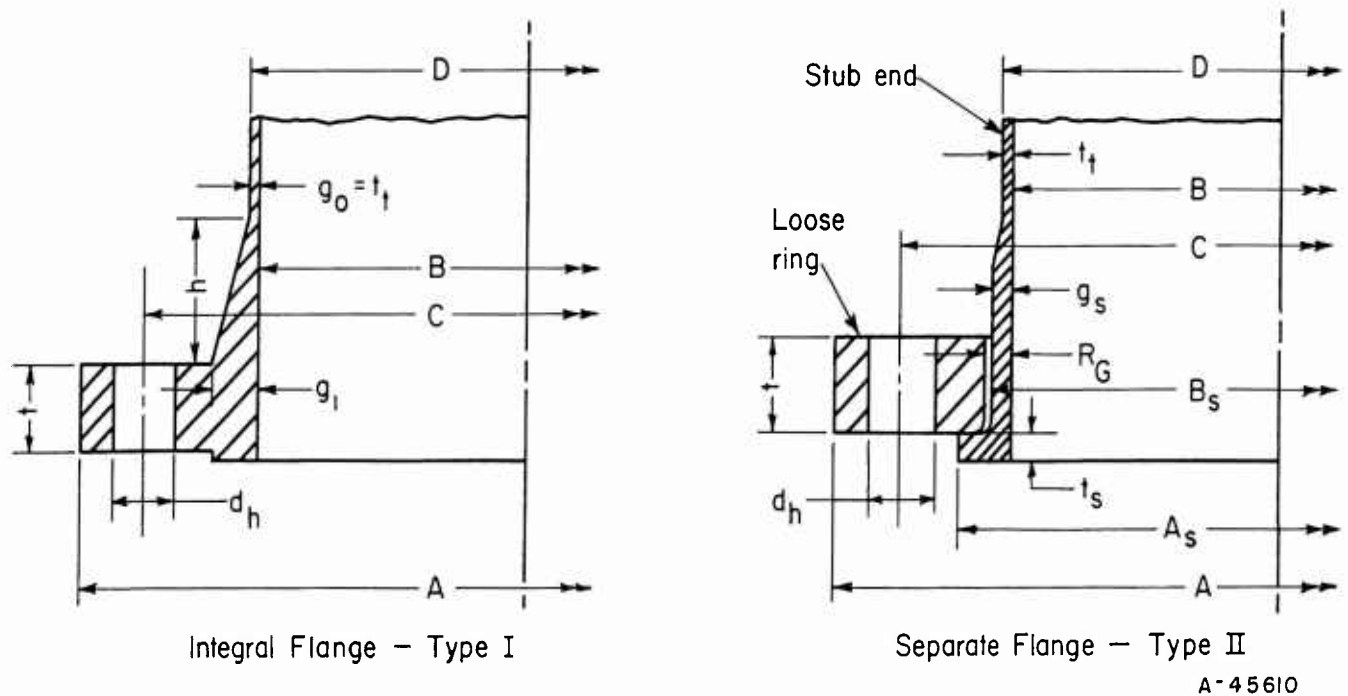
FIGURE 27. ILLUSTRATION OF DIMENSIONAL SYMBOLS

TABLE 11. DEFINITION OF FLANGE-DESIGN SYMBOLS

A	Outside diameter of flange
A_B	Total thread root area of bolts
A_{BG}	Required bolt area for seating gasket
A_{BS}	Required bolt area for operating conditions
A_{BT}	Required bolt area for test conditions
A_{B1}	Thread root area of one bolt
A_G	Gasket seating area
A_S	Outside diameter of stub end
a_1, a_2, etc.	Stress calculation parameters
B	Inside diameter of flange
B_S	Inside diameter of stub end
C	Bolt circle diameter
D	Outside diameter of tube attached to flange or stub end
d_h	Bolt hole diameter
E_f	Modulus of elasticity of flange material
F	Flange stress calculation parameter
f	Stress correction factor
G	Average diameter of annular ring gasket
g_0	Thickness of hub at small end
g_s	Thickness of hub of stub end
g_1	Thickness of hub at back of flange
h	Hub length
h_D	Load moment arm
h_G	Load moment arm .
K	Dimensional ratio: A/B
L	Flange displacement calculation parameter: $L = a_6$
M_e	External bending moment
M_G	Total flange moment, gasket seating conditions
M_S	Total flange moment, operating conditions

TABLE 11. (Continued)

M_T	Total flange moment, test conditions
m	Residual gasket stress factor
N	Number of bolts
n	Approximation factor in estimate of flange thickness
P	Maximum operating pressure
P_B	Internal pressure equivalent to external bending moment
P_E	Sum of P_B and P_e
P_e	Design internal pressure
P_T	Maximum test pressure (at atmospheric temperature)
R_G	Radial clearance between flange and stub end (Figure 27)
R_R	Minimum radial clearance
R_S	Minimum space between bolts
$\sigma_1, \sigma_2, \sigma_3$	Calculated flange stresses per unit load moment
σ_c	Controlling flange stress per unit load moment
S_{ba}	Allowable stress, bolt material at atmospheric temperature
S_{bt}	Allowable stress, bolt material at maximum operating temperature
S_{bys}	Yield stress, bolt material at atmospheric temperature
S_{fa}	Allowable stress, flange material at atmospheric temperature
S_{ft}	Allowable stress, flange material at maximum operating temperature
S_{fys}	Yield stress, flange material at atmospheric temperature
S_G	Gasket seating stress
S_{te}	Fatigue endurance strength of tubing material
S_{sys}	Yield stress, stub end material at atmospheric temperature

TABLE 11.   (Continued)

T	Flange stress calculation parameter
T_e	External torsional moment
t	Flange thickness
t_{AG}	Flange thickness, Type II flanges, gasket seating conditions
t_{AS}	Flange thickness, Type II flanges, operating conditions
t_{AT}	Flange thickness, Type II flanges, test conditions
t_{EG}	Estimated flange thickness, Type I flanges, gasket seating conditions
t_{ES}	Estimated flange thickness, Type I flanges, operating conditions
t_{ET}	Estimated flange thickness, Type I flanges, test conditions
t_s	Thickness of lap on stub end
t_t	Wall thickness of tube attached to flange
U	Flange stress calculation parameter
U.T.S.	Ultimate tensile strength of a material
V	Flange stress calculation parameter
W_s	Load due to internal pressure plus external bending moment
w	Width of annular ring gasket
X	Average diameter of contact area between loose flange and stub end
Y	Flange stress calculation parameter
Z_t	Section modulus of tube attached to flange
Z	Flange stress calculation parameter

Design Considerations

Service Requirements: Before the detailed design of a bolted-flanged connection can be started, the following service requirements must be known:

(1) Tube diameter, wall thickness, and material

(2) Maximum and minimum operating pressure

(3) Maximum and minimum operating temperature

(4) Material compatibility requirements

(5) Required service life

(6) Thermal gradients

(7) External loads

(8) Contained fluid and maximum permissible leak rate.

Items (1) through (4) will normally have been established in the design of the tubing system; Item (4) will direct the flange designer in the choice of materials for the flange and the gaskets. The required service life, Item (5), is a major factor where service temperatures are sufficiently high so that metal creep becomes significant. The required service life, in conjunction with the rate of load application, will also determine the number of cycles of loads that can be applied.

Thermal gradients, Item (6), refer to conditions where a rapid temperature change occurs, e.g., liquid oxygen or a hot gas or fluid is admitted at a high flow rate into a pipeline. Thermal transient conditions are quite often the severest loading that occurs on a bolted-flanged connection.

External loads, Item (7), are defined as those loads applied to the connection through the attached tubing, other than the axial force created by internal pressure. In many cases these loads are difficult to predict qualitatively. In such cases, it may be possible to design the connection for the maximum loads that can be carried by the tubing and other equipment.

Item (8) of the list of service conditions calls attention to the fact that "zero leakage" in a bolted-flanged connection is difficult, if not impossible, to obtain with light gases such as hydrogen or helium. Where leakage must be restricted to a very low value, this should be taken into consideration when (1) selecting the gasket, (2) specifying the gasket seating surfaces, and (3) calculating the load required to "seat" the gasket.

Type of Flanged Connection. The design procedure is directly applicable to two basic types of connections as shown in Figure 27. While there are many types of bolted-flanged connections[*], these two appear to be best suited to aerospace application. For the same flange material, Type I connections will generally be lighter than a corresponding Type II connection. However, alignment of bolt holes is easier with Type II

[*] See, for example, Figure UA-48 of Reference (8).

connections. In some cases, it may be possible to select a higher strength material for the flange of the Type II connection, since it need not be compatible with the fluid in the system nor need it be weldable or brazeable to the tubing material.

In many cases it will be desirable to attach a flange directly to a piece of equipment which itself is subjected to high stresses due to internal pressure. Care should be taken that the flange hub does not act as a reinforcement for the opening; such reinforcement should be added independently of the flange hub.

Tube-to-Flange Joint. Details of the tube-to-flange joint may affect the bolted-flanged connection in two ways:

(1) In Type I flanges the hub contributes to the flange strength. Details at the juncture may be involved in the flange strength computation.

(2) The process of joining the tube to the flange may cause distortion of the gasket seating surfaces.

Where the tube material and wall thickness are suitable for butt welding, a butt-welded joint as shown in Figures 28a and 28b provides an excellent means of joining the tube to the flange. When the tube material or wall thickness is not suitable for butt welding, a fillet-welded, seam-welded, or brazed joint may be used. For manually butt-welded joints, a hub length, h, equal to or greater than $1.5\sqrt{Bg_0}$ (see Figure 28) has generally proven adequate, from the standpoint of avoiding seating surface distortion, provided the hub was a taper angle, α, (see Figure 28) of about 20 degrees or less.

a. Butt-Welded
Type I Flange

b. Butt-Welded
Type II-Stub-End

c. Internal Socket
Fillet Welded
or Brazed

d. External Socket
Fillet Welded, Brazed,
or Seam-Welded

*If socket length $\geqq \sqrt{Bg_0}$, g_0 may be taken as $t_t + t_s$; otherwise, $g_0 = t_t$.

A-45611
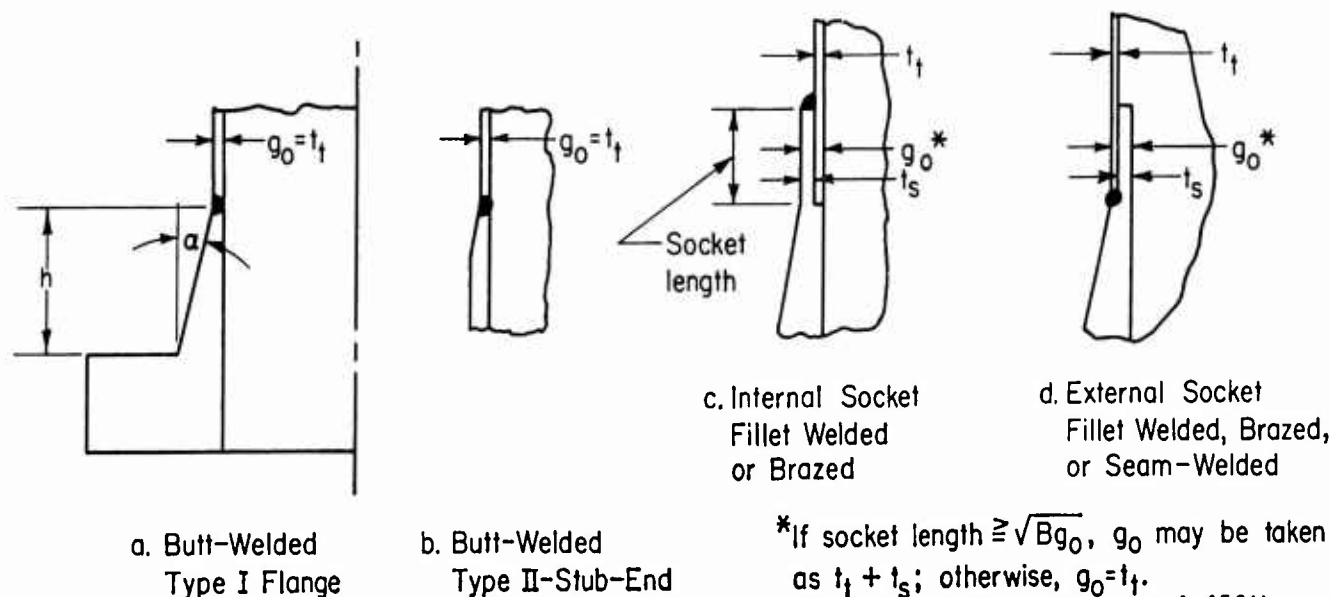
FIGURE 28. FLANGE OR STUB END-TO-TUBE JOINING METHODS

For socket-welded or brazed types, g_0 may be taken as the socket-plus-tube thickness, provided the length of the socket is at least $\sqrt{Bg_0}$. Where the socket length is less than $\sqrt{Bg_0}$, g_0 should be taken as equal to t_t.

69

Materials and Allowable Stresses. Aerospace applications, with emphasis on minimum weight, have made substantial use of the aluminum alloys, or where elevated temperatures are involved, austenitic stainless steels. The advent of missiles and space exploration has put additional emphasis on minimum weight with the introduction of materials with improved strength-to-weight ratios; e.g., titanium alloys, precipitation-hardenable stainless steels, René 41, etc. Use of AM-350 stainless steel in tubing, for example, enables a significant reduction in tubing weight. Similarly, AM-355 or René 41 may serve to reduce the weight of mechanical connections.

In many cases it will be found desirable to make the flange, in Type I joints, or the stub end, in Type II joints, of either the same material as the tube, or very similar material, since this will reduce problems at the tube-to-flange joints.

Material properties which should be considered in making a selection are

(1) Short-time yield strength

(2) Tensile test elongation

(3) Charpy V-Notch or similar indication of toughness

(4) Modulus of elasticity

(5) Coefficient of thermal expansion

(6) Creep or relaxation data

(7) Stress-to-rupture data.

These properties should be available for the complete service-temperature range.

The short-time yield strength of the material, where creep is not significant, is the primary factor in flange design from a strength standpoint. The ultimate strength of the material is only of indirect significance. The ductility or toughness may be significant. Existing flange-design methods are based on evaluation of an approximate maximum stress; there may be local areas of stress concentration which require a certain degree of ductility in the material. The tensile test elongation, Charpy V-notch or similar tests give some indication of this desired material property. However, in the present state of the art, it is not possible to assign a limiting value to these properties. Possibly a tensile elongation of 5 to 10 per cent indicates adequate ductility for most flange applications. Variation of elongation and toughness properties with temperature should also be considered; at liquid-oxygen temperatures or lower, many materials become excessively brittle, even though they have adequate ductility at room temperature.

The modulus of elasticity and coefficient of thermal expansion are important properties in designing flanged joints where significant thermal gradients occur. Creep or relaxation data plus stress-to-rupture data must be considered when temperatures are sufficiently high to cause active creep.

In order to establish dimensions for flanged joints, it is necessary to establish allowable stresses for the selected materials. Allowable stresses, in relationship to material properties, involve a complex interaction between the accuracy of the stress

calculation methods, the precision with which loads are known, and a balance between reliability and minimum weight. Although the following suggestions should be useful, allowable stresses must be established in light of the specific design problem, reliability requirement, experience, etc.

In flange design where creep is not a factor, allowable stresses may be related to the short-time yield strength of the material. A suggested criteria for establishing allowable stresses is

Flanges, stub ends

$$S_{fa} = 2/3 \quad Y_a$$

$$S_{ft} = 2/3 \quad Y_t$$

Bolts

$$S_{ba} = 1/2 \quad Y_a$$

$$S_{bt} = 1/2 \quad Y_t \ ,$$

where:

Y_a is the minimum yield strength at room temperature

Y_t is the minimum yield strength at service temperature, but not greater than Y_a.

An allowable stress for flange material equal to two-thirds of the material yield strength conforms to general pressure-vessel-design practice. (The ASME Code[8] uses 62.5 per cent for ferrous materials, two-thirds for nonferrous materials.) Because in flanged joints, the criterion of failure involves excessive deformation rather than rupture, the material ultimate tensile strength is not directly considered; however, the preceding remarks on minimum ductility requirements should not be neglected. An allowable stress of two-thirds of the yield strength implies that at a test pressure of 1.5 times the operating pressure, the stress may reach the yield strength of the material. While for pressure vessels in general, this limit is reasonable, in the case of flanged joints which are quite deformation sensitive, the design procedure described later establishes an additional check which limits calculated flange stresses to 90 per cent of the yield strength of the flange material under test conditions.

The allowable stress for bolting is set lower than for the flanges for a number of reasons:

(1) Bolts are loaded in tension, with no ability to transfer load to some other part of the structure in case of overload.

(2) The only bolt stress calculated is that due to the axial forces whereas, in service, the bolts will have some bending stresses due to rotation of the flanges.

(3) The threads on the bolts form notches with accompanying stress intensifications.

(4) In service, the bolts are loaded in initial bolt make-up by tightening with a wrench, which introduces shear stresses and a reduction in axial yield strength.

For these reasons, allowable bolt stresses no higher than 50 per cent of the material yield strength are suggested. For a test pressure of 1.5 times the operating pressure, it will be necessary to tighten the bolts to 75 to 90 per cent of their yield strength. The design procedure described later limits the calculated bolt stress at test conditions to 75 per cent of the bolt material yield stress under test conditions.

A few typical values resulting from the application of the above criteria are shown in Table 12. It should be noted that these allowable stresses, particularly for materials with high yield strength-to-ultimate strength ratios, are substantially higher than established in the ASME Unfired Pressure Vessels Code[8], or would be established following the basis for establishing allowable stresses, Appendixes P and Q, of that Code.

Materials which obtain their high strength by heat treatment may be altered in welding or brazing flanges or stub ends to the tube. If the joining process is such as to limit the heat-affected zone to a small volume of material at the end of the hub, design of the bolted-flanged connection may be based on the heat-treated properties of the material.

Gasket and Facing Details. This part describes several factors related to the determination of gasket and facing details.

(1) Annular Ring Gaskets

The most widely used gasket for bolted-flanged connections is an annular ring as shown in Figure 29. A basic design criterion in such gaskets is the "seating stress", i.e., the average stress which must be exerted on the gasket face to force it into any scratches on the gasket seating surfaces of the flanges and to compensate for any waviness of the flange faces. Suggested design values for "seating stresses" are shown in Table 13. While seating stresses are tabulated as a function of gasket material, these stresses are also dependent upon the flange seating surfaces, the type of fluid and its pressure, and the tolerable leakage rate. The suggested design seating stresses are

Gasket area, $A_G = \pi G w$

A-45612
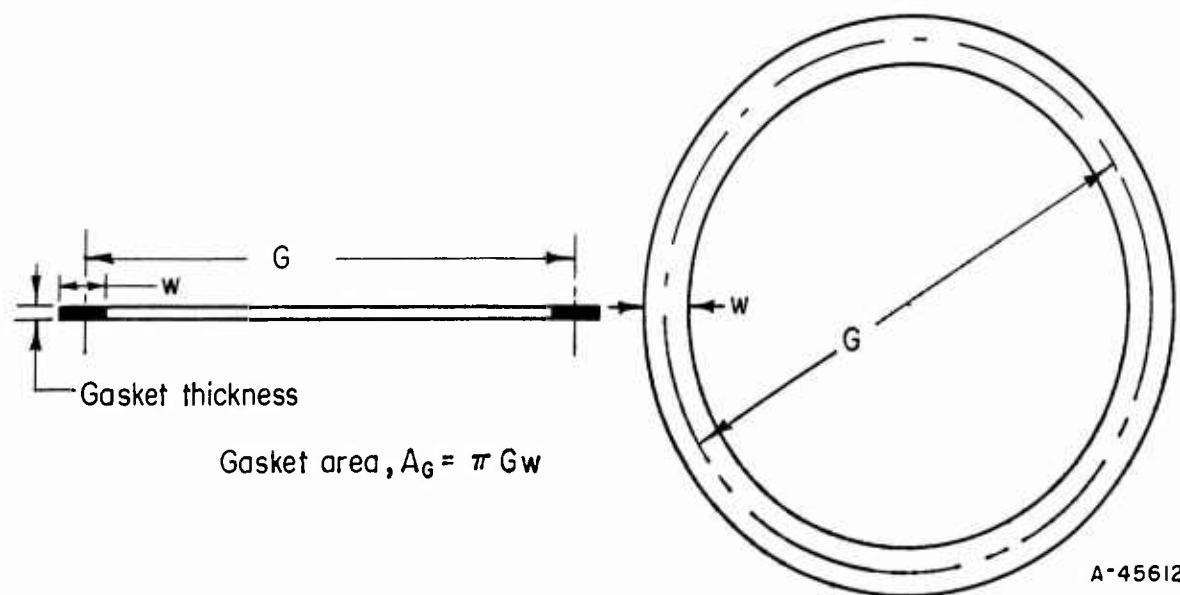
FIGURE 29. ANNULAR RING GASKET NOMENCLATURE

72

TABLE 12. TYPICAL ALLOWABLE STRESS VALUES USING CRITERIA: ALLOWABLE STRESS
FOR FLANGES ≈ 2/3 YIELD STRENGTH; ALLOWABLE STRESS
FOR BOLTS ≈ 1/2 YIELD STRENGTH

Material[a]	Allowable Stress, psi, for Indicated Temperature			
	Up to 100 F	150 F	200 F	250 F
Aluminum alloy, 6061-T6 35,000-psi yield strength 38,000-psi ultimate tensile strength				
Flanges	23,300	23,000	22,700	21,900
Bolts	17,500	17,200	17,000	16,400
Aluminum alloy, 2014-T6 55,000-psi yield strength 65,000-psi ultimate tensile strength				
Flanges	36,700	35,800	34,500	31,200
Bolts	27,500	26,800	25,700	23,400
	Up to 100 F	300 F	500 F	700 F
Type 347, annealed stainless steel 35,000-psi yield strength 75,000-psi ultimate tensile strength				
Flanges	23,300	20,000	18,900	18,900
Bolts	17,500	15,100	14,200	14,200
Type 301, cold-rolled stainless steel 90,000-psi yield strength 115,000-psi ultimate tensile strength				
Bolts	45,000	40,000	38,000	36,000
	Up to 100 F	300 F	500 F	600 F
AM 355, precipitation hardened 150,000-psi yield strength 200,000-psi ultimate tensile strength				
Flange	100,000	85,000	79,000	73,000
Bolts	75,000	63,000	59,000	54,000
	Up to 100 F	400 F	600 F	800 F
René 41, nickel-base alloy 130,000-psi yield strength 170,000-psi ultimate tensile strength				
Flanges	86,000	84,000	82,000	80,000
Bolts	65,000	63,000	61,000	60,000

(a) Yield strengths are specified minimums.

73

based on the use of flanges with carefully machined seating surfaces and with no distortion of those surfaces in the process of joining the flange to the tube. In the case of metal gaskets, it is further assumed that the gaskets and seating surfaces have a surface finish of the order of 14 rms.[10] This is approximately equivalent to an AA value of 12.6. With good surface finish, in combination with the relatively high seating stresses shown in Table 13, the leakage rates should be quite low, even for high-pressure helium. For heavier gases or liquids, or where high leakage rates can be tolerated, these gasket-seating-surface requirements can be relaxed.

TABLE 13. GASKET SEATING STRESSES AND "m-FACTORS"

Material	S_G, psi	"m"
Rubber, 1/16 inch thick	2,000	2
Asbestos composition		
1/16 inch thick	4,000	2
1/32 inch thick	6,000	2
Teflon, 1/16 inch thick	8,000	3
Aluminum, max yield strength = 8,000 psi	16,000	3
Copper or brass, max yield strength ≈ 10,000 psi	20,000	3
Nickel, max yield strength ≈ 20,000 psi	40,000	3
Stainless steel, max yield strength = 35,000 psi	70,000	4
Metal plated[a] with tin, copper, silver, or gold	30,000	3

(a) Plating should be of sufficient thickness to readily fill surface imperfections on the flange seating surfaces, normally 3 to 7 mils.

A second design criterion in connection with gaskets is the residual stress required on the gasket to maintain a low-order leakage rate. Suggested design values are shown in Table 13 as a factor, "m", which is multiplied by the pressure to establish a minimum residual gasket stress. It may be shown[11] that for perfectly compliant gaskets, the "m-factor" approaches a lower limit of unity. Actual gaskets, however, may not exhibit this perfect compliance and a residual stress is required. As in the case of the "seating stress", the "m-factor" depends not only upon the gasket material, but also upon the applied seating stress, the flange seating surfaces, the type of fluid, and the tolerable leakage rate.

The preceding criteria give minimum required gasket stresses; however, a maximum gasket stress may also be needed to limit the plastic deformation subsequent to initial tightening of the bolts. With metal gaskets, or narrow asbestos gaskets, plastic deformation may also occur in the gasket seating surfaces on the flanges, particularly at elevated service temperatures. Such plastic flow can substantially reduce the available bolt load. It is suggested that maximum gasket stresses be limited so that with a load equal to W_s, the maximum stress for metal gaskets is not over two times S_G, and for nonmetallic gaskets, not over four times S_G. These limits are indicated by the equations for gasket width w_2 shown on Figure 30.
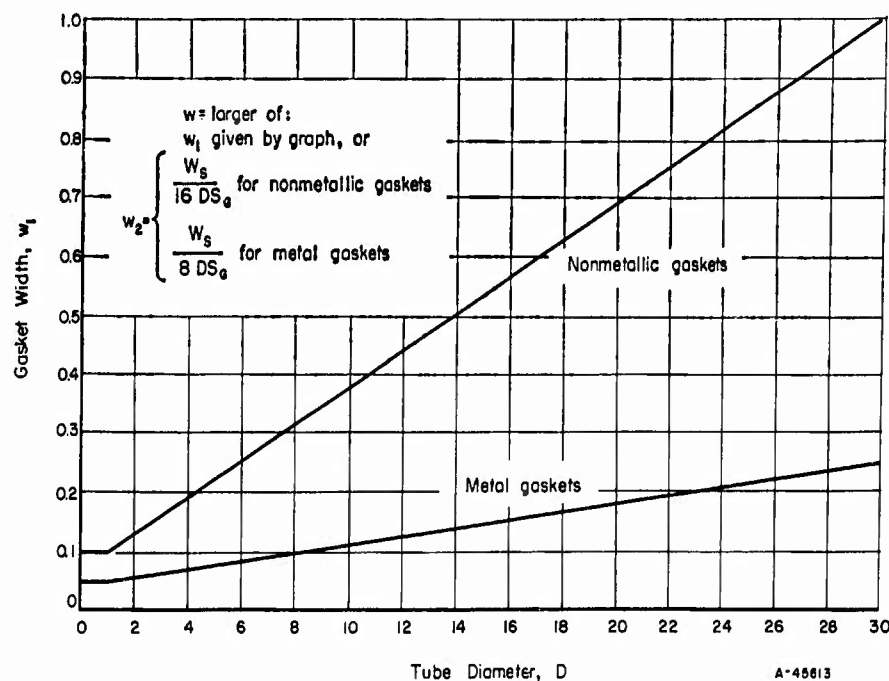
FIGURE 30. SUGGESTED GASKET WIDTH, w, FOR ANNULAR GASKETS

(2) Materials for Annular Ring Gaskets

Most gasket materials in industrial use are made of nonmetallic materials — rubber, cork, paper, asbestos with rubber binder, etc. These materials have the ability to deform readily, and hence are capable of flowing into scratches on the flange seating surfaces and to compensate for waviness of the seating surfaces. The ability to flow readily must be balanced against the need for stability under high stresses over a period of time corresponding to the service life. This stability must be maintained over the temperature range encountered in service.

In addition to the above considerations, aerospace applications may require gasket stability under high radiation or in a hard vacuum. In applications requiring very small leakage rates, porosity of the gasket may become a significant factor.

The "conformability" of an annular ring gasket generally increases with the thickness, e.g., a 1/8-inch-thick asbestos composition gasket can more readily fill surface scratches and compensate for sealing surface waviness than a 1/32-inch-thick gasket. Thicker gaskets, however, are less stable and more apt to "blow-out" when residual gasket surface stresses are low and the internal pressure is high.

A variety of metals are used for gaskets, ranging from lead, which in compliance and stability is similar to some nonmetallic materials, to austenitic stainless steels with poor compliance but excellent stability under a wide range of temperature and environmental conditions. Finally, there are composite materials such as metal jacketed asbestos and spirally wound metal strips with asbestos interlayers.

75

(3) Facing Details

Annular ring gaskets are often used with raised face flanges as shown in Figure 31. The purpose of the raised face is to

(1) Limit the gasket contact area. If a full-face gasket is used (which may be done just to help in centering of the gasket in make-up), the effective gasket contact area is still limited to the raised face area.

(2) Insure that the flanges will not contact each other along their outer periphery, even with a very thin gasket.

With regard to the second point, the deflection of flanges can be computed by the Equations[6]

For Type I flanges

$$\delta = \frac{0.91 \text{ V M}\lambda}{L\sqrt{Bg_o}\ g_o^2 E_f} \tag{22}$$

For Type II flanges

$$\delta = \frac{0.829 \text{ M}\lambda}{t^3 E_f \log_{10}K} \quad . \tag{23}$$

The axial displacement, δ, and rotation radius, λ, are defined by Figure 31. The moment, M, to be used in Equations (22) and (23) should be largest of M_G, M_S, or M_T, calculated as indicated in Figures 35 or 36. The remainder of the symbols used in Equations (22) and (23) are defined later.

The raised face plus the gasket thickness (fully compressed) should exceed the axial displacements in order to prevent the outer edges of the flanges from contacting.

It is often desirable to use a tongue-and-groove or male-female facings as shown by Figure 31. These facings aid in locating and holding the gasket during assembly and reduce the possibility of gasket blowout. Further, at least one of the faces is partially protected against damage during handling and assembly of the joints. With metal gaskets and where low-leakage rates with gases are desired, protecting the flange seating surface during shipment, storage, fabrication, assembly, and possibly re-assemblies, becomes very important. The double-groove facing, shown in Figure 31 used with plated metal gaskets, may be useful in this situation.

Where the joints will be subjected to high temperatures in service, followed by the need for disassembly and re-assembly, the possibility of partial welding of metal gaskets to the flange faces should not be overlooked. Use of dissimilar metals will help, and in some cases a graphite lubricant film on the seating surfaces may aid in disassembly. Nonmetallic gaskets will generally harden after long periods of high-temperature service. The raised face configuration has some advantage in this respect since the old gasket can be removed more easily than with the tongue and groove or male-female facings.
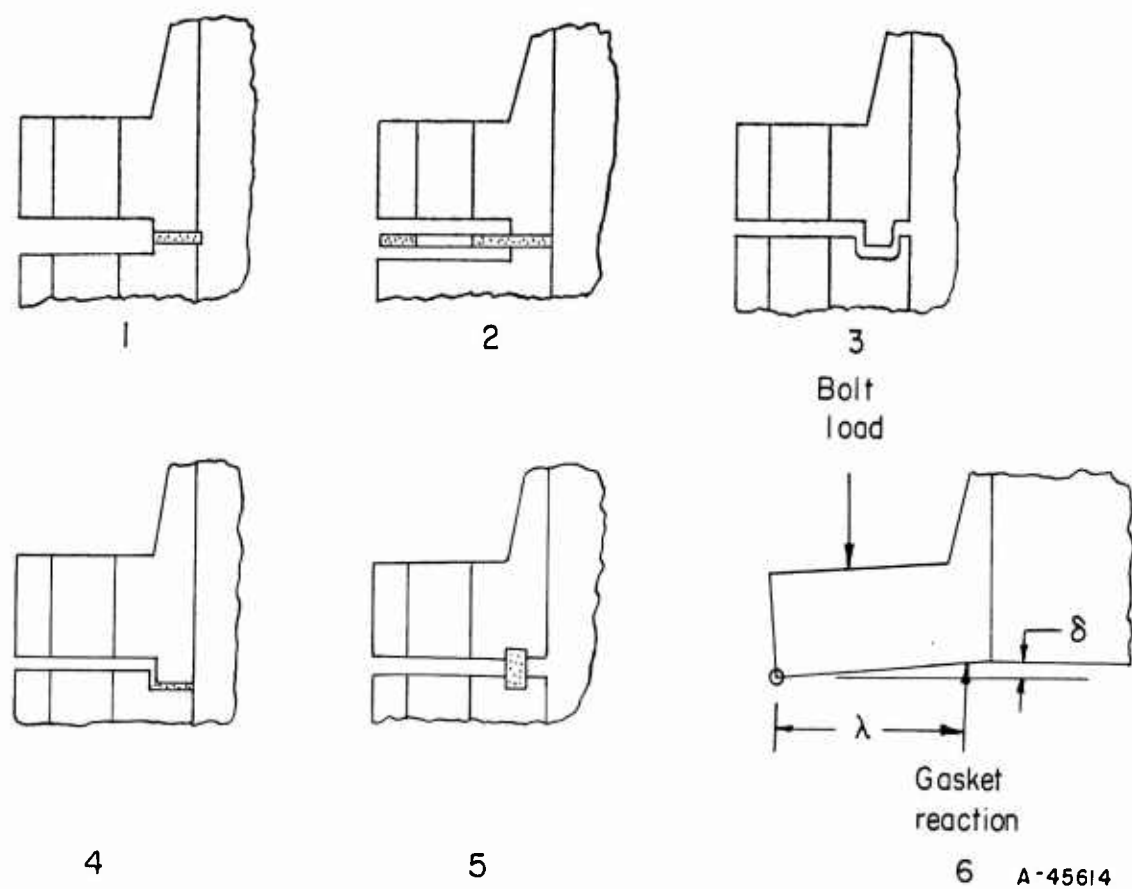
1. Raised face, gasket on facing only
2. Raised face, gasket extending to flange OD for ease in centering
3. Tongue and groove facing
4. Male-female facing
5. Double-groove facing, with plated metal gasket
6. Deflected flange under load. Facing plus gasket thickness must be sufficient to prevent contact of flanges with each other. See p 76 for equations for calculating displacement, δ.

FIGURE 31. TYPICAL FACINGS

(4) Pressure-Energized Gaskets

A pressure-energized gasket is defined here as a gasket with sealing action aided by internal pressure; several typical pressure-energized gaskets are shown in Figure 32. Perhaps the most widely used pressure-energized gasket is the elastomeric O-ring, both for static and either rotating or reciprocating seals. The use of elastomeric O-rings in pipeline flanges, however, has been quite limited. In pipeline flanges the standard octagonal ring is quite widely used and has some pressure-energization properties. The lens ring is occasionally used for high pressures. The bellows-type gasket has also been used to a limited extent.

While pressure-energized gaskets have major advantages in many applications, their advantages in a mechanical connection in a tubing system may be marginal. This arises, in part, because of the independence of internal pressure and the external loads acting on a joint in a tube or piping system. Where pressure energization of a metal gasket occurs, vibration of the piping system due to cyclic application of an external bending moment may lead to abrasion of the seating surfaces or fatigue failure of the metal seal.

In addition, resistance to external torsional moments in a joint with a pressure-energized gasket may be low. While rotation is limited to bolt-hole clearances, this may be enough to cause abrasion of the seating surfaces if the torsional moment is cyclic.

Accordingly, while pressure-energized gaskets may provide a desirable safety margin against leakage for internal pressure loading, where external loads may occur the flanges, bolts, and initial bolt load should be designed independent of the pressure-energization capability of the gasket.

(5) Full-Face Gaskets

A bolted-flange connection with a full-face gasket, as illustrated in Figure 33, is often used. Despite many years of use, a generally accepted design method for flanged connections with full-face gaskets has not been achieved; part of the problem lies in the statically indeterminate ratio of gasket loading inside the bolt circle to loading outside the bolt circle. The design with full-face gasket has the advantage that stresses are lower than for the corresponding flange with an "inside gasket". The disadvantages are that a flanged connection with full-face gasket has less tolerance against thermal gradients and there is a much greater tendency for the load on the gasket to be concentrated at the bolt holes and on the portion of the gasket outside the bolt circle. (The inner part of the gasket must be adequately loaded to prevent leakage through the bolt holes.) For this reason, flanged connections using full-face gaskets generally require higher bolt loads than comparable connections using inside gaskets. In commercial pipeline practice, connections with full-face gaskets are widely used for mild service conditions (e.g., water- or gas-distribution lines at or near atmospheric temperature) but seldom used for severe service conditions involving either high (above 450 F) or low (cryogenic) temperatures or high (above 300 psi) pressures.

Bolting Dimensional Details. Table 14 gives pertinent details on bolting suitable for bolted-flanged connections designed for minimum weight. It is desirable to locate the bolts as close to the tube wall as possible, consistent with required flexibility for

Flange Bore
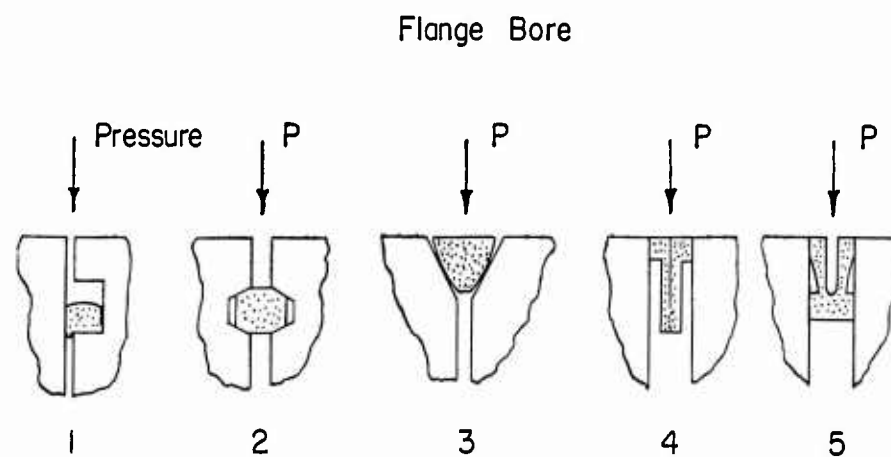
1. Elastomeric O-ring
2. Octagonal ring joint (ASA B16.5)
3. Lens ring
4. Bellows gasket
5. Aerospace-type bellows gasket

FIGURE 32. EXAMPLES OF PRESSURE-ENERGIZED GASKETS

A-45615
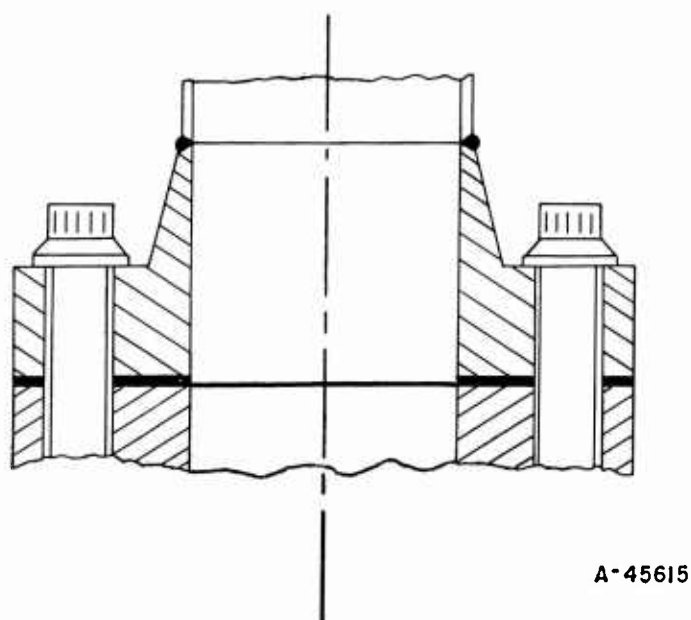
FIGURE 33. BOLTED-FLANGED CONNECTION WITH FULL-FACE GASKET

handling thermal gradients. The bolting listed in Table 14 requires a minimum of radial clearance between bolts and flange hub or stub-end wall. Socket-head cap screws are suggested in small sizes, NAS 624 through 636 external wrenching bolts in larger sizes. NAS-type bolts are suggested for the larger sizes since standard socket-head cap screws may have inadequate bearing areas for these sizes. The radial and between-bolts minimum clearances shown in Table 14 are based on allowances for fillets, use of standard socket wrenches, and for minimum space between bolts the rule of thumb that the ligament between bolt holes should be at least equal to the bolt-hole diameter.

TABLE 14. BOLTING DIMENSIONS

Nominal Size(a)	Threads per Inch	Root Area, A_{B1}, in.^{2}	Radial Clearance, R_R, in.	Minimum Space, R_S, in.	Hole Size, d_h, in.	Maximum Head Diameter, in.
No. 5	44	0.00716	0.132	0.396	0.141	0.200
No. 6	40	0.00874	0.143	0.429	0.152	0.221
No. 8	36	0.01285	0.165	0.495	0.180	0.265
No. 10	32	0.0175	0.186	0.558	0.209	0.306
No. 12	28	0.0226	0.202	0.606	0.240	0.337
1/4"	28	0.0326	0.259	0.657	0.281	0.438
5/16"	24	0.0524	0.306	0.796	0.344	0.531
3/8"	24	0.0809	0.365	0.974	0.406	0.649
7/16"	20	0.109	0.415	1.125	0.469	0.750
1/2"	20	0.149	0.464	1.242	0.532	0.828
9/16"	18	0.189	0.519	1.407	0.594	0.938
5/8"	18	0.240	0.575	1.575	0.687	1.050
3/4"	16	0.351	0.665	1.845	0.812	1.230
7/8"	14	0.480	0.779	2.157	0.937	1.438
1"	12	0.625	0.870	2.437	1.062	1.620

Outside of hub
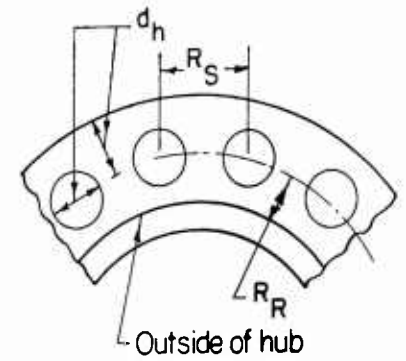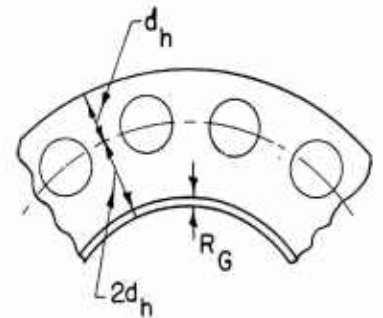
Type I

Type II

A-45602

(a) Sizes No. 5 through No. 12, American Standard Socket Head Capscrews, ASA B18.3-1954

$$R_R = \frac{\text{Maximum head diameter}}{2} + 0.030"$$

$$R_S = 3 R_R$$

Sizes 1/4" through 1": dimensionally to Material Aircraft Standards NAS 624 through 636

R_R = 1/2(maximum head diameter) + 0.040"   1/4" through 7/16"
    1/2(maximum head diameter) + 0.050"   1/2" through 3/4"
    1/2(maximum head diameter) + 0.060"   7/8" and 1"
R_S = 1.5 x maximum head diameter.

A maximum spacing between bolts equal to $2(d_h + t)$ is suggested, where d_h is the bolt-hole diameter, t is the flange thickness. If bolts are too far apart, the gasket load will be concentrated at the bolt holes with possible leakage midway between bolts. The maximum bolt spacing is also a function of gasket characteristics. Reinforcement of the flange ring by the hub, in Type I flanges, or distribution of the load by the stub end, in Type II flanges, are also factors. However, present knowledge of flange behavior is not sufficient to accurately predict these effects.

80

Bolting shown in Table 14 may either be used with nuts or the bolts may be studded into tapped holes in a mating flange. The studded design is advantageous from the standpoint of assembly and provides a slight weight reduction; use of bolts and nuts provides for longer bolt bodies and, hence, is safer against loss of preload and permits easier replacement in case of damaged or seized threads. This is a particularly important consideration if disassembly and reassembly are required after service at high temperature or under a hard vacuum, since thread seizing is a strong possibility.

Designing for Thermal Gradients. Data on temperature gradients in bolted-flanged connections are quite scarce. References (12) and (13) give some experimental data on thermal gradients in flanged connections during start-up conditions in steam lines. References (14) and (15) discuss methods of calculating thermal gradients in flanged connections. Another potential thermal gradient effect, in which the pipe attached to the flange is at a different average temperature than the flange rings, is by Dudley[16] who gives theoretical methods of calculating the influence of this gradient on flanged-connection performance. In general, where service conditions are such that the maximum temperature differences between parts of the flanged-joint connection do not exceed about 100 F, the design procedure given later will have sufficient reserve margin to compensate for such thermal gradients. When maximum thermal gradients may be higher than 100 F, additional checks on the bolted-flanged-connection performance using methods such as those suggested in Appendix I and Reference 17, pp 62-63, may be advisable.

Designing When Creep is Significant. Since bolted-flanged connections are highly strain sensitive, plastic flow as a function of time (i.e., creep or relaxation) becomes a dominant factor in design at elevated temperatures. Where the temperature, for a given material, is sufficiently high so that plastic strain due to creep in the required service lifetime exceeds about 10 per cent of the elastic strain, special design procedures[*] should be used to include the effect of plastic flow as a function of time.

Analysis of a bolted-flanged connection under creep or relaxation conditions presents formidable difficulties and no generally accepted design method under such conditions is available. The problem of the relaxation of a bolt in a rigid flange has been considered by several investigators[18,22]. A suggested design method for bolted-flanged connections is given in Appendix II and Reference 17, pp 64-69.

Bolted-flanged connections for high-temperature service involving creep may be designed in conformance with the ASME Unfired Pressure Vessels Code (8) using allowable stresses based on the lower of

(1) The stress to produce a creep rate of 0.01 per cent per 1000 hours

(2) The stress to produce rupture at the end of 100,000 hours.

Application of these criteria gives fairly low design stresses, e.g., 4000 psi for 6061-T6 aluminum alloy at 400 F; 750, 1000, and 1500 psi for Types 304, 347, and 316 stainless steels, respectively, at 1500 F. As applied to pressure-vessel shells, these allowable stress levels are intended to insure service life of 100,000 hours. When applied to bolted-flanged connections, however, the service life (without retightening of bolts) becomes more difficult to define since a small plastic strain (e.g., 0.01 per cent),

---
[*]See, for example, References (17) through (22).

81

while insignificant with respect to a pressure-vessel shell, may be sufficient to reduce the bolt load in a bolted-flanged connection by a substantial amount.

In many aerospace applications, relatively short service life is required, perhaps 1/2 hour being ample. In such applications, direct use of the ASME Code design method may result in unnecessarily heavy bolted-flanged connections, hence a design based on one of the referenced methods is advisable.

Design Procedure

The design procedure given herein is essentially a procedure for

(1) Calculating the required bolt load and bolt area for a bolted-flanged connection

(2) Calculating the stresses produced on a dimensionally established flange when loaded by the bolt load and a given internal pressure.

After estimating the required bolt load, the next step is to calculate the stresses in a dimensionally established flange; flange dimensions may then be changed (if necessary) until (1) a flange of adequate strength is obtained, as indicated by calculated stresses being less than allowable stresses, and (2) a flange of minimum weight is obtained, as indicated by calculated stresses being close to the allowable stresses.

A method is presented for calculating the required bolt load and bolt area, and for making a preliminary estimate of flange dimensions. In addition, a step-by-step procedure is given for making detailed stress calculations of the flanges established in the preliminary estimate. The design procedure is summarized in Tables 15 and 16, which are discussed in the following sections.

Type I Flanges. As an example, assume that a bolted-flanged connection is to be designed for a 2.00-in.-OD tube with a wall thickness of 0.020 in. The tube material is to be AM-350 with 150,000-psi yield strength, 200,000-psi ultimate tensile strength. The endurance strength of the tube material is to be taken as 90,000 psi. Maximum operating pressure is to be 2000 psi at 600 F maximum operating temperature. Test pressure is to be 3000 psi. The external loads are not known.

A Type I bolted-flanged connection is to be used, with both flanges and bolting made of AM-355 material. The gasket is to be silver-plated stainless steel, using a double-groove facing as shown in Figure 31. An internal socket-type brazed joint is to be used between the flange and the tube. Using the suggested allowable stresses from Table 13 and the gasket parameters from Table 13, the "Initial Data" section of Table 15 can be filled in. Note that g_o is the combined socket-plus-tube thickness (see Figure 28).

(1) Calculation of Equivalent Internal Pressure, P_B

Where the external moment is known, a value of the equivalent internal pressure, P_B, can be calculated such that it produces an axial stress in the tubing equal to the

TABLE 15. BOLTING AND PRELIMINARY DIMENSIONAL ESTIMATE SHEET – TYPE I FLANGE

Initial Data

Tube

Outside diameter	$= D$ 2.000 in.	
Wall thickness	$= t_t$ 0.020 in.	
Section modules	$= z_t$ 0.0610 in.[3]	
Material:	AM-350	
Endurance strength $= S_{te}$ 90,000 psi		

S_{fys} = 150,000 psi

Gasket material   Silver-Plated St. St

Flange material   AM-355

Bolt material   AM-355

S_{sys} = 150,000 psi

S_{bys} = 150,000 psi

Max operating pressure P = 2000 psi

Max operating temp   600 F

Test pressure P_T = 3000 psi

$g_o g_o$ = 0.060 in. B = 1.960 in.

R_G = -- in. B_S = -- in.

M_e _____ in-lb (if known)

S_G = 30,000 psi m = 3

S_{fa} = 100,000 psi S_{ft} = 73,000 psi

S_{ba} = 75,000 psi S_{bt} = 54,000 psi

(1) Calculation of P_B

(a) External moment known:

$$P_B = \frac{4 M_e \, t_t}{z_t \, D} = \text{-- psi}$$

(b) External moment unknown:

$$P_{B1} = \frac{4 S_{te} \, t_t}{3D} = 1200^{(a)} \text{ psi}$$

P_B = smaller of P_{B1} or P_{B2}

$$P_{B2} = \frac{240 (D+3)^3 \, t_t}{z_t \, D} = 4918 \text{ psi}$$

(2) Calculation of W_s

Type I: $W_s = B^2 \, P_E$ = 12,293 psi $P_E = P + P_B$ = 3200 psi

Type II: $W_s = B_S^2 \, P_E$ =   --   psi

(3) Calculation of A_B

$$A_{BG} = \frac{A_G \, S_G}{S_{ba}} = \quad 0.145 \text{ in.}^2$$

w = 0.0538 in.

G = 2.141 in.

$A_G = \pi w G = 0.362$ in.^{2}

$$A_{BS} = \frac{W_s + m \, P \, A_G}{S_{bt}} = 0.268^{(a)} \text{ in.}^2$$

$$A_{BT} = \frac{W_s \left(\dfrac{P_T + P_B}{P_E} \right) + m \, P_T \, A_G}{0.75 \, S_{bys}} = 0.172 \text{ in.}^2$$

A_B = largest of A_{BG}, A_{BS}, or A_{BT}

TABLE 15. (Continued)

(4) Tentatively Select Bolting

From Table 7, select number N and size of bolts so that $(N)(A_{B1})$ is equal to or larger than A_B

Size, in.	A_{B1}, in.^{2}	$N^{(b)} = A_B/A_{B1}$	d_h, in.	R_R, in.	R_S, in.	$\leqq \pi C^{(c)}/N$, in.
1/4	0.0326	8.2 ~ 9	0.281	0.259	0.657	1.0325

(5) Calculation of C and A

Type I: $C_1 = B + 2(g_1 + R_R) = 2.958^{(a)}$ in.

$C_2 = G + w + d_h = 2.550$ in.

Type II: $C_1 = B_S + 2(g_s + R_G + d_h) = $ -- in.

$C_2 = G + w + d_h = $ -- in.

$C = $ larger of C_1 or C_2

$A = C + 2d_h = 3.520$ in.

$g_1 = $ smaller of:

$4g_o = 0.240^{(a)}$ in.

or

$\frac{2}{3}\sqrt{Bg_o} + g_o = 0.289$ in.

(6) Estimate of t

$$t_{EG} = \frac{2}{3}\left(\frac{A_{BG}\ Y\ h_G\ S_{ba}}{B\ S_{fa}}\right)^{1/2} = 0.187 \text{ in.}$$

$h_G = \frac{C - G}{2} = 0.409$ in.

$$t_{ES} = \frac{2}{3}\left(\frac{A_{BS}\ Y\ h_G\ S_{bt}}{B\ S_{ft}}\right)^{1/2} = 0.253^{(a)} \text{ in.}$$

$K = \frac{A}{B} = 1.796$

$Y = 3.487$ from Figure 34

$$t_{ET} = \frac{2}{3}\left(\frac{A_{BT}\ Y\ h_G\ S_{bt}}{0.9B\ S_{fys}}\right)^{1/2} = -0.149 \text{ in.}$$

$t = $ largest of t_{EG}, t_{ES}, t_{ET}

(7) Check Maximum Space Between Bolts

$\frac{\pi C}{N} \leqq 2(d_h + t)$

If space between bolts is satisfactory, proceed to stress calculations, if not:

$1.0325 \leqq 1.068$

return to Step (4) and reselect number and size of bolts

(8) Estimate Hub Length (Type I Flanges)

$h = 1.5\sqrt{Bg_o} = 0.514$ in.

(a) Lower value is controlling factor.

(b) Guide: N = about 2 or 3D (inches) but not less than 4.

(c) Check after C is obtained.

TABLE 16. STRESS-CALCULATION SHEET – TYPE I FLANGES

Type I Flanges

A-45603

$F/\sqrt{Bg_o} = \alpha_1$	1.706	
$Ug_o{}^2\sqrt{Bg_o}/V = \alpha_2$	0.118	
t	0.253	0.258
$t\,\alpha_1 + 1 = \alpha_3$	1.432	1.440
$\alpha_3/T = \alpha_4$	0.903	0.908
$t^3/\alpha_2 = \alpha_5$	0.137	0.145
$\alpha_4 + \alpha_5 = \alpha_6$	1.040	1.053
$f/\alpha_6 g_1{}^2 B = \sigma_1$	8.518	8.407
$4/3\, t\,\alpha_1 + 1 = \alpha_7$	1.575	1.587
$\alpha_7/\alpha_6 t^2 B = \sigma_2$	12.087	11.534
$Y/t^2 B = \alpha_8$	27.807	26.700
$\alpha_8 - z\sigma_2 = \sigma_3$	4.854	4.800

P	2,000	P_T 3,000
P_B	1,200	P_E 3,200
S_G	30,000	m 3 A_G 0.362
S_{fa}	100,000	S_{ft} 73,000
S_{fys}	150,000	

σ_c 12.087 11.534

(σ_c = largest of: σ_2, σ_3, $2/3\,\sigma_1$, $\dfrac{\sigma_1 + \sigma_2}{2}$, $\dfrac{\sigma_1 + \sigma_3}{2}$

Unit Stress Calculations:

A	3.520	
B	1.960	
A/B = K	1.796	
U	3.832	from
Y	3.487	Figure 13
Z	1.899	For K
T	1.586	
g_o	0.060	
g_1	0.240	
g_1/g_o	4.000	
h	0.514	
$\sqrt{Bg_o}$	0.343	
$h/\sqrt{Bg_o}$	1.500	
F	0.585	from
V	0.040	Figures 14
f	1.000	and 15

Moment Calculations:

C	2.958	
G	2.141	
$(C - G)/2 = h_G$	0.409	
$(C - B - g_o)/2 = h_D$	0.469	
$A_G S_6 h_G = M_G$	4442	
$0.785\,G^2 P_E h_o = \alpha_9$	5400	
$mP A_G h_G = \alpha_{10}$	888	
$\alpha_9 + \alpha_{10} = M_s$	6288	
$\alpha_9(P_T + P_B)/P_E = \alpha_4$	7088	
$\alpha_{10} P_T / P = \alpha_{12}$	1332	
$\alpha_{11} + \alpha_{12} = M_T$	8420	

Stress Calculations:

$\sigma_c M_G\ (\leqq S_{fa})$	53,690	51,234
$\sigma_c M_G\ (\leqq S_{ft})$	76,003	72,525
$\sigma_c M_T\ (\leqq g S_{fys})$	101,772	97,116

85

maximum axial stress produced in the tubing by the bending moment. This is a conservative approach, since the maximum tensile stress produced by bending occurs at only one point.

When the external moment is not known an estimate of its value, in terms of P_B, is obtained by the equations for P_{B1} and P_{B2}. P_{B1} is an upper limit based on the fatigue strength of the attached tubing while P_{B2} is an upper limit based on pipeline practice and represents, to some extent, an upper limit that can be withstood by typical equipment attached to the piping (e.g., pumps, compressors, valves, pressure vessels).

In the example, P_{B1} is the controlling value and P_B is calculated to be 1200 psi.

(2) Calculation of Total Load, W_s

The external moment and the internal pressure both give forces tending to separate the connection components, the total of which is W_s. The pressure will act on an area approximately equal to $\frac{\pi}{4} G^2$; however, since G is unknown it is taken as 1.125 B, and $W_s = \frac{\pi}{4} (1.125 \text{ B})^2 P_E = B^2 P_E$.

In the example, the equivalent design pressure, P_E, is 3200 psi and the corresponding W_s is 12,293 lb.

(3) Calculation of Bolt Area, A_B

The value of W_s is used in establishing a minimum required bolt area. The bolt area must be sufficient for the most severe of these design conditions:

(a) The bolts must be sufficient to seat the gasket, i.e., to force the flange seating surfaces into intimate contact with the gasket seating surfaces. This process is accomplished in initial tightening of the bolts, assumed to be done at atmospheric temperature, hence the load is divided by the allowable stress of the bolt material at atmospheric temperature.

(b) The bolts must be sufficient to withstand the end force represented by W_s, plus an additional margin represented by the quantity mPA_G. These loads occur at the operating temperature; hence, the load is divided by the allowable stress of the bolt material at maximum operating temperature.

(c) The bolts must be sufficient to withstand the loads imposed under test conditions, assumed to be carried out at atmospheric temperature. This design condition may control if the test pressure is greater than 1.5 P.

The three design conditions are represented by the bolt areas A_{BG}, A_{BS}, and A_{BT}, respectively. The largest of these areas must be used in the design.

In order to calculate the bolt areas, it is necessary to select a gasket width, w, and mean gasket diameter, G. A guide to selection of gasket width is given by Figure 30; this width, in combination with desired facing details, gives Dimension G.

In the example, the gasket width from Figure 30 is 0.0538 in. A facing detail sketch is shown on Figure 37, from which G = 2.141 in. The controlling bolt area, A_{BS}, is 0.268 in.[2].

(4) Tentative Bolting Selection

Having computed the required bolt area, a combination of size and number of bolts may be selected from Table 14 so that the required bolt area is obtained. Within the range of bolt spacing suggested herein, in general, there will be considerable latitude in bolt selection. That is, either a large number of small bolts or a small number of large bolts can be used. Use of small bolts will result in a lighter flange, because of reduction in radial dimensions of the flange; however, this should be balanced against the longer assembly time required for installation and the resulting higher cost. The general trend in aerospace application is to use a rather large number of small bolts; this has an added advantage of greater reliability since failure of one bolt will be of less significance.

The bolting selected must meet these criteria:

(a) Area must be equal to or greater than A_B.

(b) Spacing must be sufficient to permit wrench application.

(c) Spacing must be small enough to prevent excessive bowing of the flange between bolts.

Criterion 1 is satisfied directly as shown in Table 15. Criteria (b) and (c) are checked as the bolt circle and flange thickness are developed in subsequent steps. In the example, nine 1/4-in. bolts are tentatively selected. Spacing will be checked after obtaining the bolt-circle diameter, C, and the flange-thickness estimate, t.

(5) Calculation of Bolt Circle, C, and Flange OD, A

The bolt circle, C_1, for Type I flanges is such as to provide sufficient clearance between bolts and flange or stub end hub. For Type II flanges, C_1 is established to provide a ligament inside the bolt holes equal to the hole diameter. The bolt circle, C_2, is such as to insure that the bolts do not intrude on the gasket.

The flange outside diameter, A, is established to provide a ligament outside the bolt holes equal to one-half the hole diameter. In the example, the bolt circle, C_1, is controlling. Having a value of C, the minimum bolt spacing check can be made and is satisfied since R_s is less than $\pi C/N$.

87

(6) Estimate of Flange Thickness, t

For Type I flanges, an estimate of flange thickness is necessary. As in establishing bolt areas, three design conditions are considered, resulting in thicknesses t_{EG}, t_{ES}, and t_{ET}, the largest of these being taken as the estimated flange thickness. The estimate is based on an approximation that the thickness of a Type I flange will be about 2/3 of the computed thickness of a Type II flange. The thickness of a Type II flange can be computed directly from the equation

$$t = \sqrt{\frac{Y M}{B S_f}} \quad,$$

where

Y is a factor obtained from Figure 34

M is the applied moment

B is the flange inside diameter

S_f is the flange material allowable stress.

In the example, the largest flange thickness is $t_{ES} = 0.253$ in.

(7) Check of Maximum Bolt Spacing

Having obtained a value of t, it is possible to check the maximum spacing. The equation given is a generally conservative rule of thumb for a very complex problem in which other factors such as gasket characteristics and hub stiffness are involved.

In the example, the selection of bolting meets the criterion since $2(d_h + t)$ is larger than $\pi C/N$.

(8) Estimate of Hub Length

In the preceding steps, values for all flange dimensions have been estimated, except for the hub length, h. In the example, a hub length of 0.514 in. is obtained.

(9) Stress Calculation

Having calculated the required bolting and obtained estimates of all dimensions in the preceding steps, the values so obtained may now be used in the stress-calculation sheet, Table 16. The equations used for stress calculations are based upon an elastic stress-analysis method developed by Waters, et al.[9] Stresses, per unit applied

moment, σ_1, σ_2, and σ_3, at three critical locations in the flange are computed. The stress σ_1 is a bending stress in the flange hub and is allowed to be 1.5 times the flange material allowable stress, provided σ_2 and σ_3 are such that $\dfrac{\sigma_1 + \sigma_2}{2}$ and $\dfrac{\sigma_1 + \sigma_3}{2}$ are both less than the flange material allowable stress.

The stress-calculation parameters* T, U, Y, and Z are given by Figure 34. Parameters F, V, and f are given by Figures 35 and 36. These parameters were developed by Waters, et al.[9]

The moment calculations are quire similar to the moment calculations given by the ASME Code.[8] Three moments are calculated corresponding to the three design conditions discussed above, i.e., (1) M_G for seating the gasket at initial bolt-up, (2) M_S for operating conditions, and (3) M_T for test conditions.

The stresses are obtained by multiplying the controlling flange unit stress, σ_c, by the moments M_G, M_S, and M_T. The stresses are then compared with the appropriate allowable stress, S_{fa} for $\sigma_c M_G$, S_{ft} for $\sigma_c M_S$ and 90 per cent of S_{fys} for $\sigma_c M_T$.

If the computed flange stress is greater than the allowable stress, a change in dimensions is required. Unfortunately, explicit relations between the dimensional variables and the stresses do not exist. Generally, a slight increase in flange thickness will adequately reduce the stresses; however, in some designs, it may be better to change hub dimensions. If the computed stress is below the allowable stress, flange dimensions may be reduced to obtain minimum weight.

In the example, the estimated thickness resulted in a stress, $\sigma_c M_S$, greater than the allowable stress, S_{ft}. By increasing the flange thickness, t, to 0.258 inch, the calculated stresses are reduced to acceptable values. The resulting flange is shown in Figure 37.

Type II Flanges. The design procedure for Type II flanges is much simpler than for Type I flanges, since the controlling flange stress is given explicitly by equation

$$\sigma = \frac{Y}{t^2 B} \ .$$

The gasket, bolting, and flange OD can be established using the same procedure as discussed above for Type I flanges. The inside diameter of the flange ring is larger than the base of the stub end, i.e.,

$$B = B_S + 2\,(g_s + R_G) \ .$$

The radial clearance, R_G, between the flange and stub end can be estimated by $R_G = 0.020 + 0.0025\,D$.

The outside diameter of the stub end, A_S, must be large enough to provide sufficient flange/stub end bearing area, i.e.,

$$A_S \geq \sqrt{\frac{4A_B}{\pi} + B_S{}^2} \ .$$

---

* These parameters do not represent physical dimensions. Rather they are dimensionless design variables
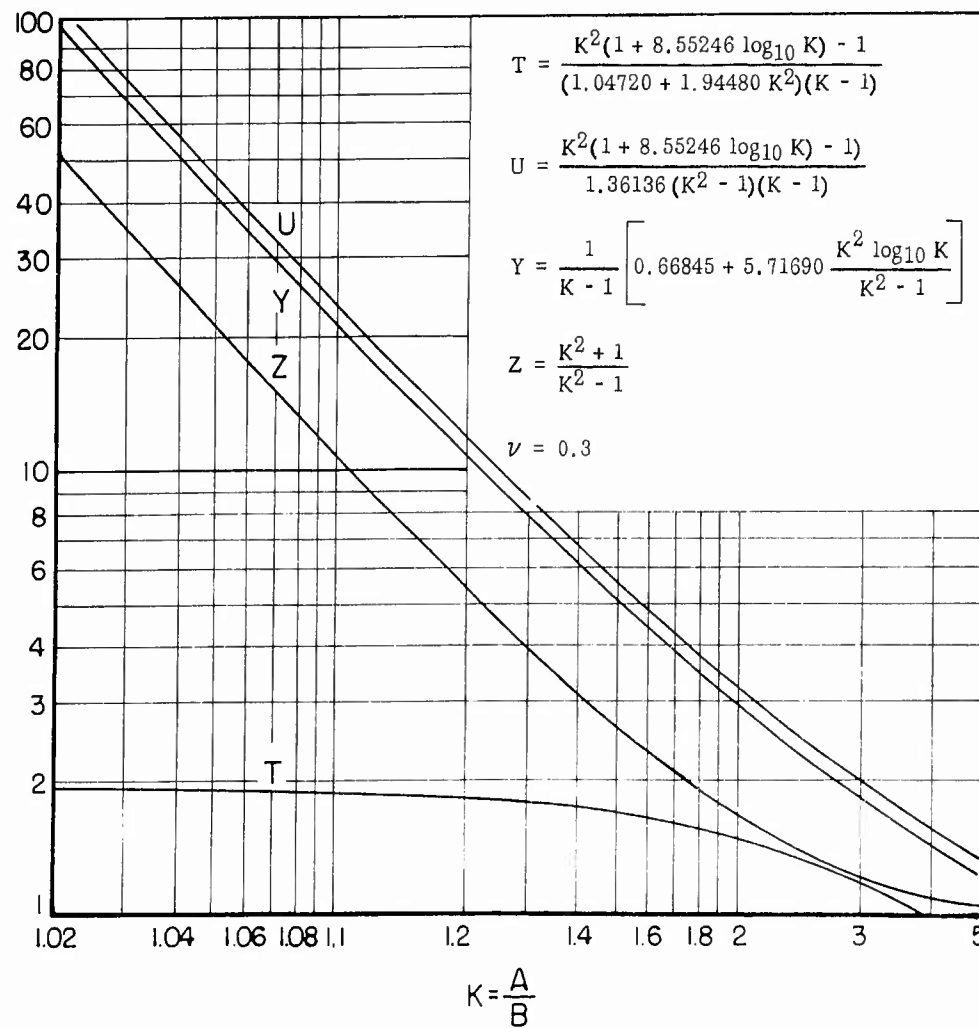
FIGURE 34. VALUES OF T, U, Y, AND Z WHEN f = 0. 3

From Reference (9).

90
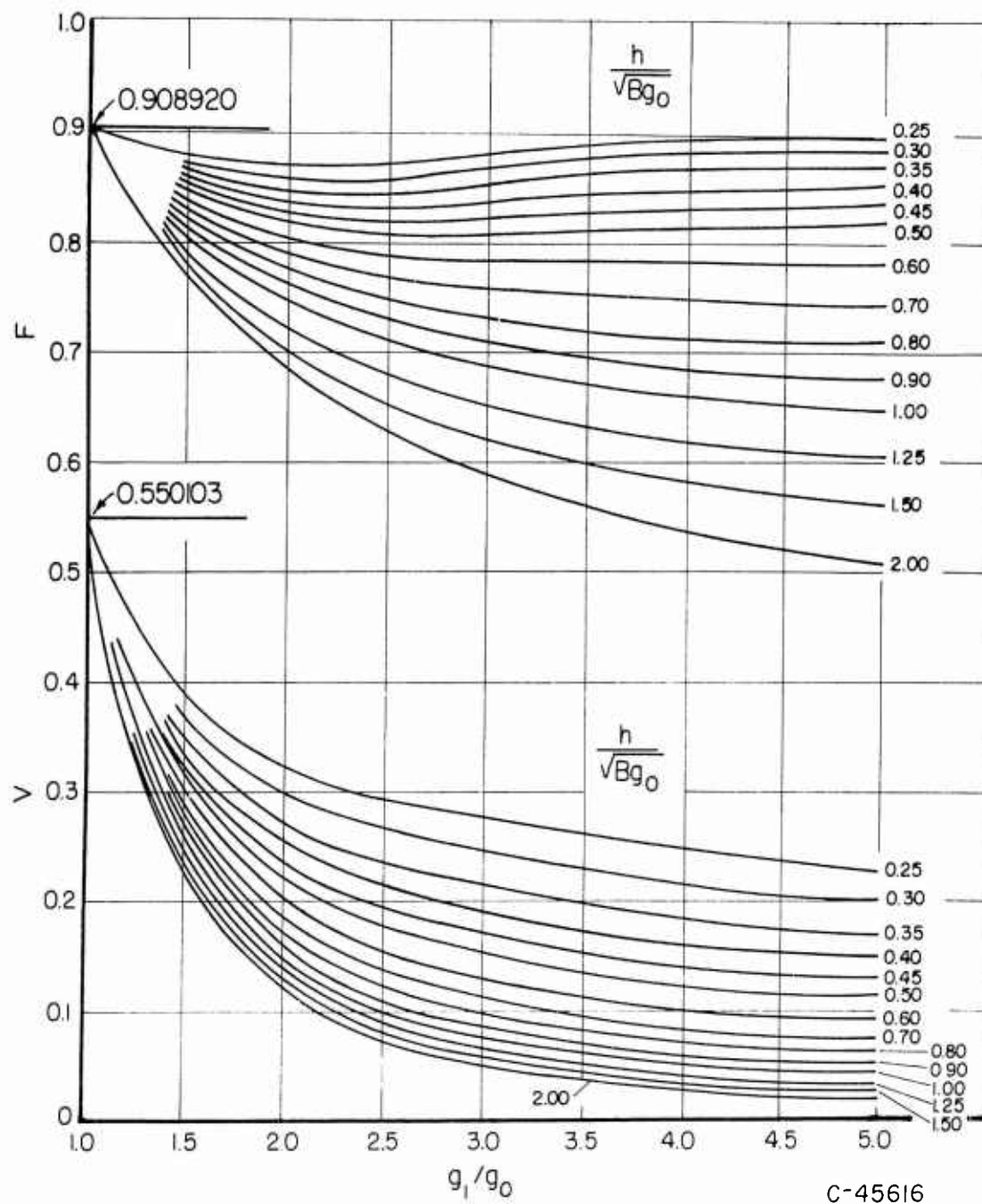
FIGURE 35.   VALUES OF F AND V FOR AN INTEGRAL FLANGE

From Reference (9).
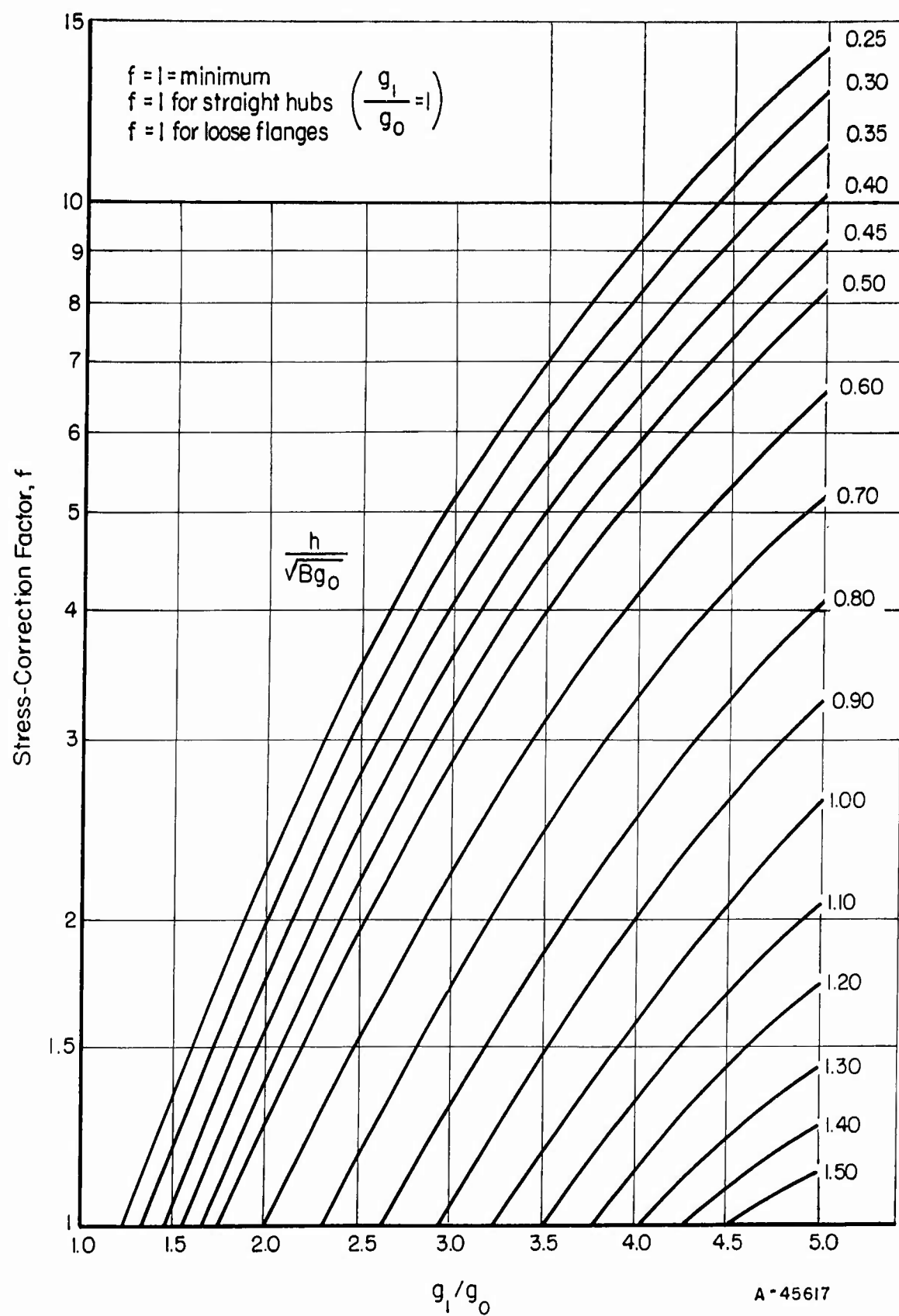
FIGURE 36. VALUES OF STRESS-CORRECTION FACTOR

From Reference (9).
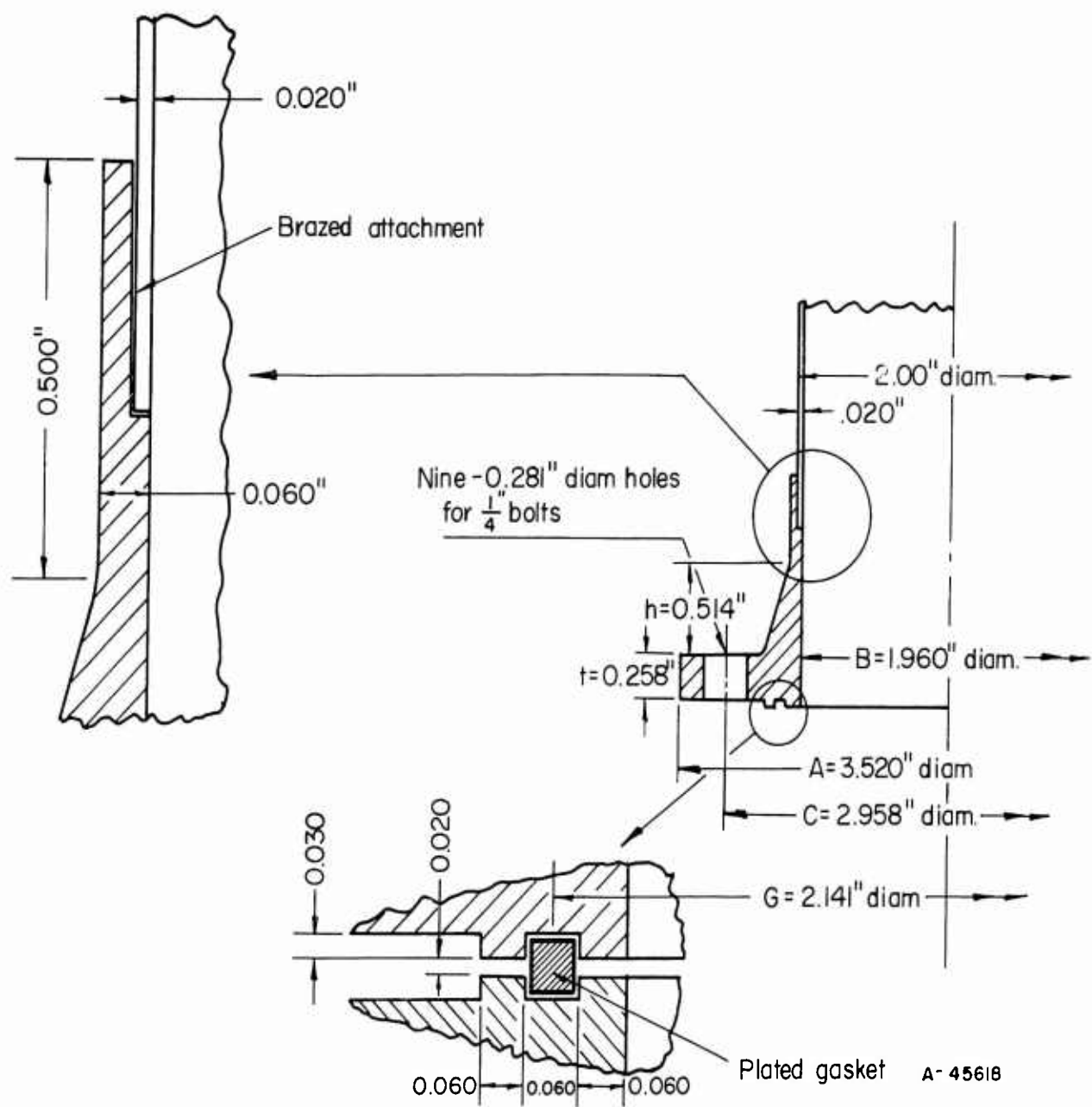
FIGURE 37. TYPE I FLANGE DESIGNED IN EXAMPLE

92

Figure 38 indicates the moment calculations and thickness calculations for Type II flanges. The moment calculations are to be completed first, after which the required flange thickness can be computed. The maximum bolt spacing (Table 17) can be made after obtaining the required flange thickness from the computations shown in Figure 38.

Stub ends of the type shown in Figure 39a do not require a detailed stress check since the gasket prevents the lap from rotating and the dimensions are such as to provide ample shear and bearing area. The required gasket seating stress and/or the stress obtained by multiplying the gasket factor, m, by the operating pressure, P, usually must be less than the allowable bolt stress in order to use a stub end with gasket over the entire face (Figure 39a) and at the same time meet the requirement that the bearing area between stub end and ring flange be equal to the bolt area. Where the gasket material-bolt material combination is such that a full-face gasket cannot be used, a local gasket can be used as shown in Figure 39b. Where used with a localized gasket, permitting the stub-end lap to rotate, the stub end should be designed as a Type I flange, as indicated by Figure 39b.

Manufacturing and Assembly Comments. Upon completion of the design of a bolted-flanged connection, there remains the task of insuring that the component parts are properly manufactured, handled, and assembled in accordance with the design assumptions. Several aspects of these problems are discussed in the following paragraphs.

(1) Manufacturing Specifications

Materials for the various components, and their heat treatment, should be carefully specified to insure that the materials actually used have at least the physical properties assumed in the design. It should be noted that some flange sections may become relatively thick; physical properties obtained on thin sheets may not adequately represent the properties of the material as used in flanges. Materials should be of high quality, free of cracks, flaws, or inclusions.

For most dimensions, tolerances can be quite liberal. Exceptions are

(1) Bolt-hole spacing — where bolt-hole clearance is small, bolt holes must be spaced within close tolerances.

(2) Flange-facing surface for metal gaskets — surfaces should be carefully machined to obtain the desired surface finish and also so that the facing lies in a single plane. The later is seldom a problem, except in light flanges where lathe chucking with excessive forces may distort the flanges.

(3) Metal-gasket thickness — while the average thickness is not too important, variation in thickness in a given gasket should be small. For example, a metal-gasket thickness might be specified as 0.020 ± 0.002 inch, provided the thickness in any one gasket does not vary by more than ±0.0001 inch.
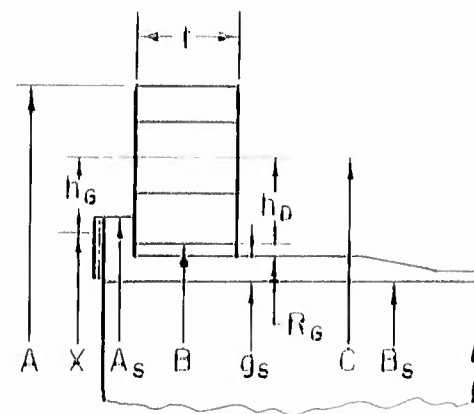
Type II Flanges

Moment Calculations

$$A_S$$
$$B$$
$$(A_S + B)/2 = X$$
$$(C - X)/2 = h_G$$
$$(C - B)/2 = h_D$$
$$A_G S_G h_G = M_G$$
$$0.785\, G^2 P_E h_D = a_1$$
$$m P A_G h_G = a_2$$
$$a_1 + a_2 = M_S$$
$$a_1 (P_T + P_B)/P_E = a_3$$
$$a_2 P_T/P = a_4$$
$$a_3 + a_4 = M_T$$

Flange Thickness Calculations

$$A$$
$$A/B$$
$$Y \,(\text{Figure 34})$$
$$t_{AG} = \sqrt{\dfrac{M_G Y}{S_{fa} B}}$$
$$t_{AS} = \sqrt{\dfrac{M_S Y}{S_{ft} B}}$$
$$t_{AT} = \sqrt{\dfrac{M_T Y}{0.9 S_{fys} B}}$$

t = largest of t_{AG}, t_{AS}, or t_{AT}

A 45619

FIGURE 38.   MOMENT AND THICKNESS CALCULATION — TYPE II FLANGES

For stub end material equal to or stronger than tube material. If stub end material is weaker than tube material, adjust dimensions upward proportionately.
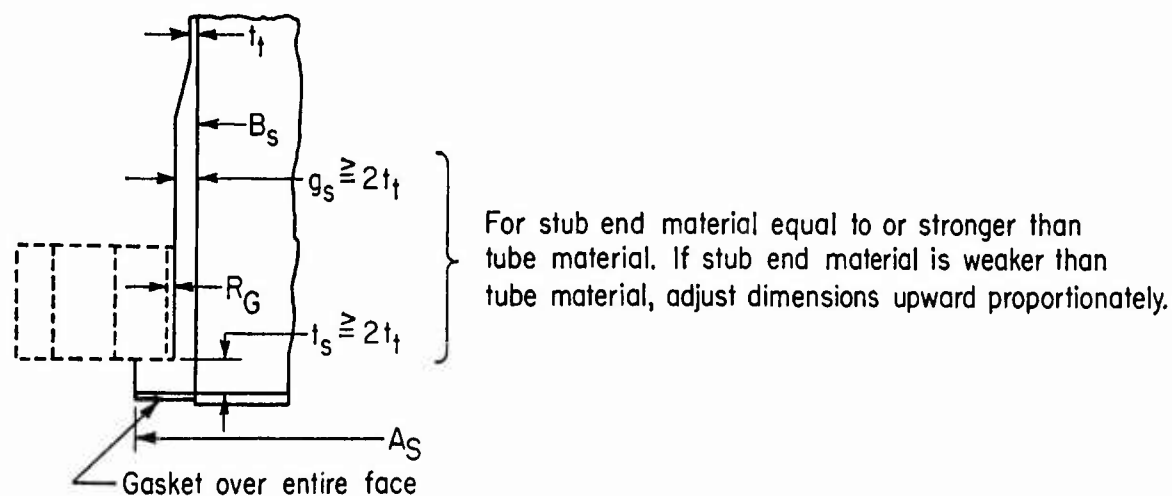
A_S should be such that bearing area is equal to or larger than the total bolt area, A_B; adjusted proportionately upward if bolt material is stronger than stub end or flange material.

a. Stub End Not Requiring Stress Check
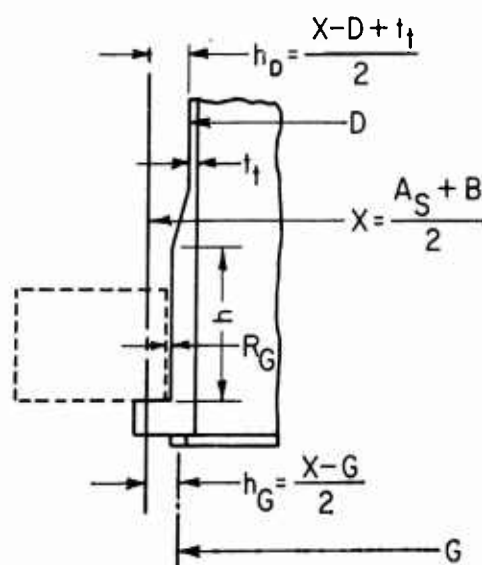
Use Stress Calculation Sheet, Table 17, with $g_1 = g_0 = g_S$ if $h \geq \sqrt{Bg_S}$, otherwise design as tapered hub flange.

Moment arms h_G and h_D as shown.

A-45620

b. Moment Arm and Hub Definitions for Checking Stresses in Stub Ends Using Table 17 Stress-Calculation Sheet

FIGURE 39. CONDITIONS FOR DESIGNING STUB END TYPE II FLANGES

95

(4) Threading on bolting — a high-quality threading specification is desirable for bolts, nuts, and tapped holes, in part for strength assurance but also to obtain consistent torque-axial load relations

(5) Attachment of flanges or stub end to tube — close diameter tolerances may be required for butt welding thin-wall tubing or for a brazed joint.

Where both flanges of a joint are Type I, it is necessary to carefully specify bolt-hole position, particularly if tubing subassemblies are used. Pipeline flange practice is based on bolt holes in multiples of four, with bolt holes straddling center lines of equipment. Similar practice can be considered in special flange design, provided weight penalty is not excessive. Use of a Type II flange for one of the two mating flanges eliminates this problem.

Gasket seating surfaces, particularly for metal gaskets, should be protected during handling and shipment. A wood or fiber-board disk, covering the flange faces and wired to the bolt holes, is often used for this purpose. For thin-walled hubs, where tolerances for tube attachment must be maintained, a temporary plug or cap on the hub end may be desirable. Bolting and gaskets should be well packed to prevent damage in handling.

(2) Assembly Precautions

Flange facing should be perpendicular to the axis of the pipe. In some types of joints this requires that the end of the tube be cut square with the tube axis. The joining method (welding, brazing, etc.) should not cause distortion of the flange seating surface. In case of doubt, the facing should be checked with a face plate after the joint is completed.

For flanged connections it is desirable that the bolt load be controlled by use of a torque wrench in tightening the bolts. Considerable data is available[24-26] on relationship between torque and axial load in bolts. Since these relationships depend upon bolting material, thread class, surface finishes, and lubricant, in some cases it may be desirable to check this relationship with the particular combination of bolting, surfaces, and lubricant to be used in the flange assembly.

To facilitate proper assembly, whether with a nut and bolt or a stud and nut arrangement, it is necessary to clean the threads and to be sure that the nuts do not bind when assembled. Flange seating surfaces and gasket should be checked for cleanliness. The gasket should be carefully placed in position, all bolts inserted and tightened finger-tight. Bolts should then be sequence tightened as indicated in Figure 40. It is desirable to recheck the bolt torque after a period of 24 to 48 hours and, if possible, after a short period of operation under service conditions. For bolted-flanged connections designed in accordance with the design procedure described above, bolts should be tightened to produce a stress equal to 85 per cent of the yield strength of the bolt material.

Misalignment of the tubing system may be apparent during assembly of a tie-in flanged connection*. It is not practical to put any general dimensional limits on

---

*Fabricators may ease the problem of making up to the joint by loosening clamps at anchors. This, of course, does not necessarily reduce the misalignment in the system after the clamps are retightened. However, in some cases, anchor clamps may be adjusted to reduce misalignment.
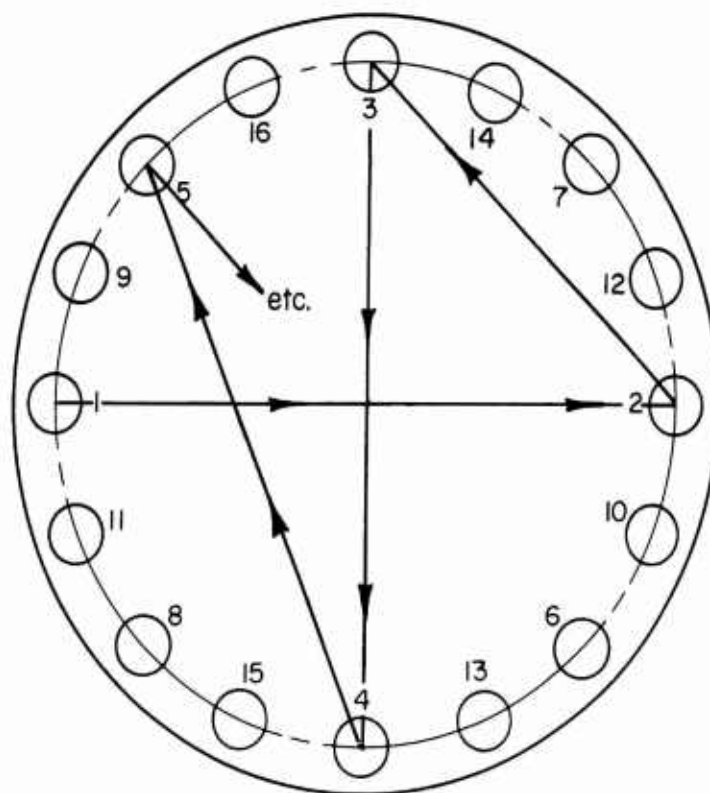
Tightening sequence – tighten bolts approximately diametrically across from each other

First round – about $\frac{1}{4}$ of final torque
Second round – about $\frac{1}{2}$ of final torque
Third round – about $\frac{3}{4}$ of final torque
Fourth and subsequent rounds – final torque

Continue until all bolts have final torque on recheck   A-45621

FIGURE 40.   EXAMPLE OF BOLT-TIGHTENING SEQUENCE

97

misalignment since the effect of misalignment on the flanged connection depends greatly on the flexibility of the tubing system. If, however, a substantial part of the total bolt load is required just to bring the flange faces into alignment, the design basis should be examined to see if adequate allowance was made for external bending moments.

Computer Use for Design Optimization

The design procedure for bolted fittings as discussed in the above sections was incorporated into a digital computer program. An input data sheet, source card listing, and typical output sheets are given in Appendix VI. On the basis of tube (or pipe) diameter and wall thickness, material properties, and known operational requirements, the Flanged Connector Design computer program can (1) select the number of bolts, (2) check bolt spacing and stresses, and (3) optimize the flange thickness according to stress levels. The program is capable of designing either integral or ring-type flanges with metallic or nonmetallic gaskets for various types of flange facings.

As discussed in "Proposed Threaded-Fitting Design", the major advantage of a computer lies in its speed and accuracy. It is, therefore, pertinent to consider the time required to design bolted fittings in the absence of a high-speed digital computer and an appropriate computer program. For a specific example, assume that the designer is to establish the dimensions for a bolted fitting of the type shown in Figure 41. He will be furnished the following design conditions:

(1) Maximum and minimum operating temperature and pressure

(2) Matching tube diameter, wall thickness, and material

(3) Thermal gradients

(4) External loadings (bending, axial, and torsional)

(5) Contained fluid or fluids .
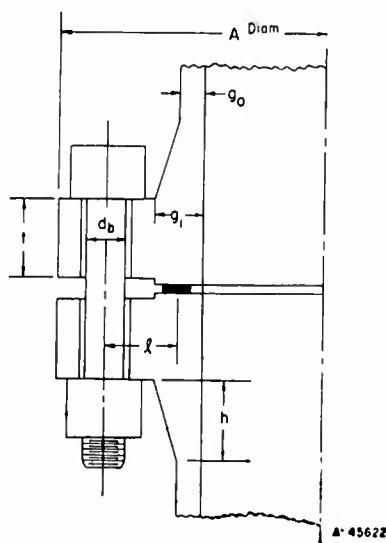
FIGURE 41. ILLUSTRATION OF INDEPENDENT DIMENSIONAL VARIABLES
IN A BOLTED FITTING

98

From the above, the designer may select suitable materials for flanges, bolts, and the seal based on suitability for the operating temperatures, compatibility with the fluids, and possibly from the standpoint of weldability or brazeability to the matching tube. Having selected materials, the designer may choose suitable allowable stresses for the flanges and bolts. This step requires the selection of seven independent variables. In other words, on Figure 41 the dimensions t, g_1, g_o, h, l, A, and d_b. Having selected these dimensions, the designer then makes four types of calculations. The times required to complete these calculations, using a desk calculator or a slide rule, are approximately as shown:

Stress calculations	1 hour
Displacement calculations	2 hours
Preload calculations	2 hours
Creep design calculations	3 hours

After completing from 5 to 8 hours' work (depending upon whether creep is involved) the designer will know whether the dimensions he has selected will provide a satisfactory fitting. This will be shown if the maximum calculated stresses are less than the pre-established allowable stresses, or, in the case of creep design, if the calculated service life is adequate. If the fitting meets the design criteria (and after some experience, most designers can readily select dimensions so that the criteria are met) the question arises whether the fitting is of minimum weight. That is, is there some other combination of the variables t, g_1, g_o, h, l, A, and d_b which would also meet the design criteria and would be of less weight. Unfortunately there are no established analytical relationships between the seven independent variables, the design parameters, and the fitting weight. In order to answer the question, it is necessary to vary each of the seven variables while holding the other six constant. Even for a very limited investigation of the variable ranges, it is apparent that hundreds of calculations are involved, each of which requires some 5 to 8 hours' design time. (For example, if only two steps are used for each variable, 128 calculations are needed.)

The value of the digital computer program is obvious since the computation time involved could be reduced from hundreds or thousands of hours to a few hours. With the computer program as now written, over 800 flanges were designed in an actual computer run time of 6.6 minutes. On the basis of the above time estimates, this would require approximately 4000 hours using a desk calculator or slide rule.

The Flanged Connector Design Computer Program as now written is based on the design procedure given in Tables 15 and 16 (and Figure 38) which does not include the creep design calculations, and on the basis of flat annular gaskets.

Several degrees of sophistication in a computer program could have been used. At one extreme, a program which would be an extension of the present program would entail feeding into the computer only the design parameters of tube size, design pressure and temperature, external loads, thermal gradients, and material properties. The program would then automatically perform a series of iterations with various step values of the independent variables, would compute and compare weights, would print out the values of the independent dimensional variables for a fitting of minimum weight, and would give the fitting weight. While technically feasible, preparation of such a program would have required more time than was available during this project.

99

The present program, which is much simpler, was developed as a logical first step. Future additions to the present program can be easily made due to the flexibility of the FORTRAN programming language. The output of the present computer program consists of dimensions and volumes based on a particular set of input variables. Independent dimensional variables can be varied in incremental steps by the designer, each step reintroduced into the computer, and successive steps varied as indicated by the results of the previous computations. This program, through repeated application, gives general indications of the relationships between the independent dimensional variables, the design parameters, fitting volume, and the optimum flange thickness for a given fitting design.

For 3- and 6-inch pipe flanges, general relationships between bolt size and bolt circle diameter, flange thickness and pressure for various bolt sizes, and flange volume and pressure for various bolt sizes, are given in Figures 42, 43, and 44, respectively.

In the flange-connector design procedure there are several conditions controlling the bolt size and number of bolts required for a particular-type flange, for a particular pressure requirement. One of the most interesting results from the computer program is that for a particular bolt size the number of bolts required as the pressure requirement is increased may be reduced. This is shown in Table 17. For example, notice that for a 1/2-inch bolt at 250 psi 10 bolts are required. As the pressure is increased to 2000 psi, the number of bolts decreased to 8, and then increases again to 9 at 5000 psi. This is due to the interrelationship between the controlling conditions and the fact that an integer number of bolts must be specified.

TABLE 17. NUMBER OF BOLTS REQUIRED FOR 3-INCH FLANGE

Bolt Size	Number of Bolts Required at Indicated Pressure						
	250 psi	500 psi	1,000 psi	1,500 psi	2,000 psi	5,000 psi	10,000 psi
No. 8	19	23	--	--	--	--	--
No. 12	14	13	18	--	--	--	--
1/4 in.	13	12	12	15	18	--	--
1/2 in.	10	9	9	9	8	9	--
3/4 in.	8	8	7	7	7	7	9
1 in.	6	6	6	6	6	6	5

Selected Designs

Dimensions for 3- and 6-inch bolted fittings for 500, 1000, and 1500 psi are shown in Figures 45 through 50. These designs were determined by means of the computer program and are based on a 150,000-psi yield strength for AM-355 at 200 F, with a gasket material of silver-plated stainless steel. The designs utilize the minimum acceptable bolt size on a bolt circle determined by wrench clearances.
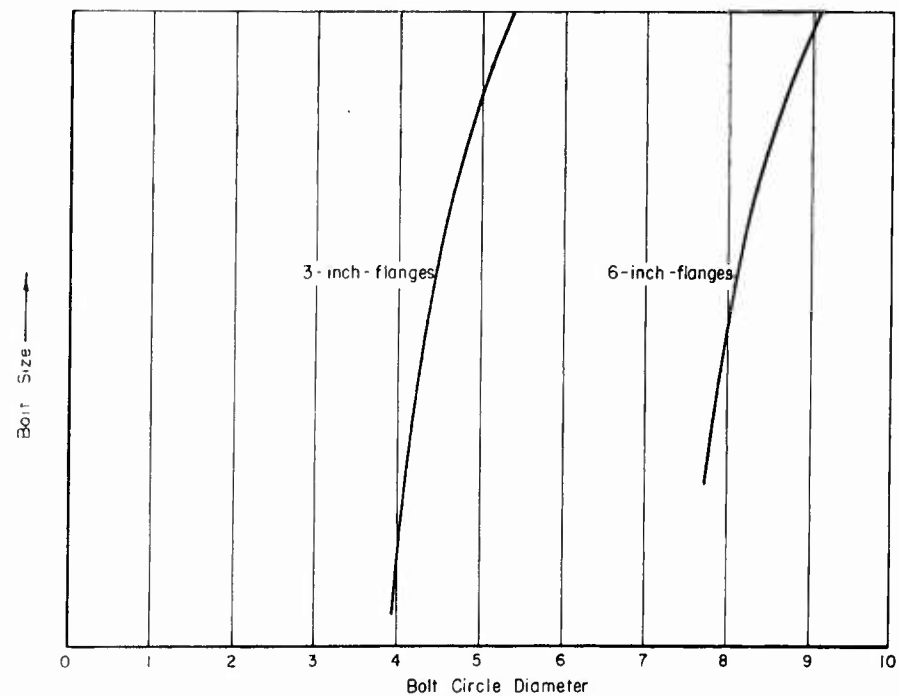
FIGURE 42. RELATIONSHIP BETWEEN BOLT SIZE AND BOLT
CIRCLE DIAMETER
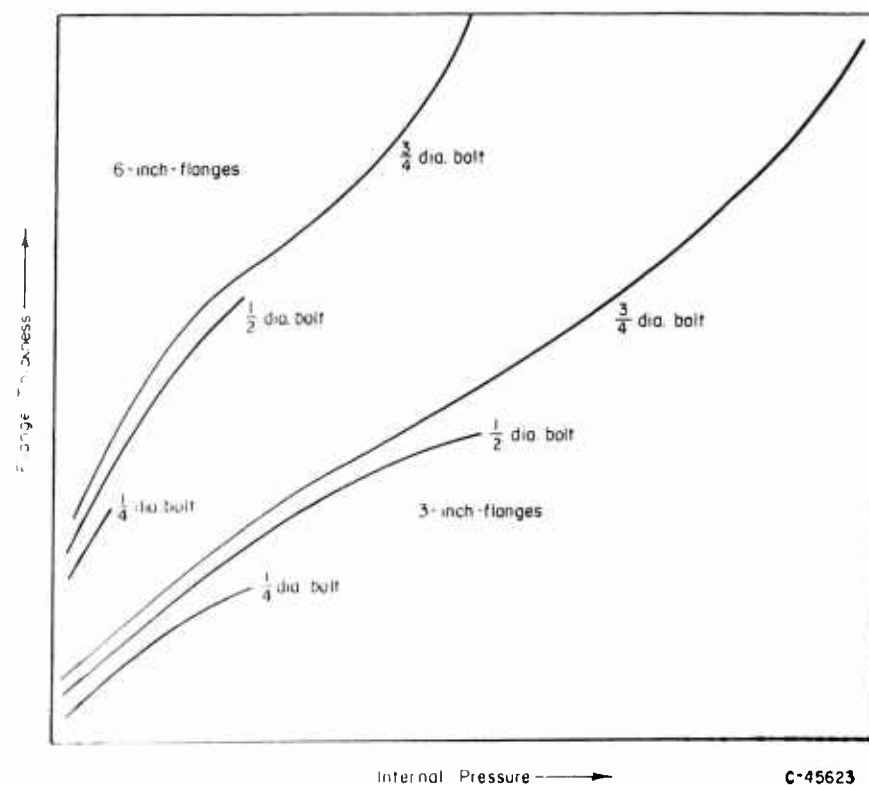
RELATIONSHIP BETWEEN FLANGE THICKNESS AND
INTERNAL PRESSURE FOR VARIOUS BOLT SIZES
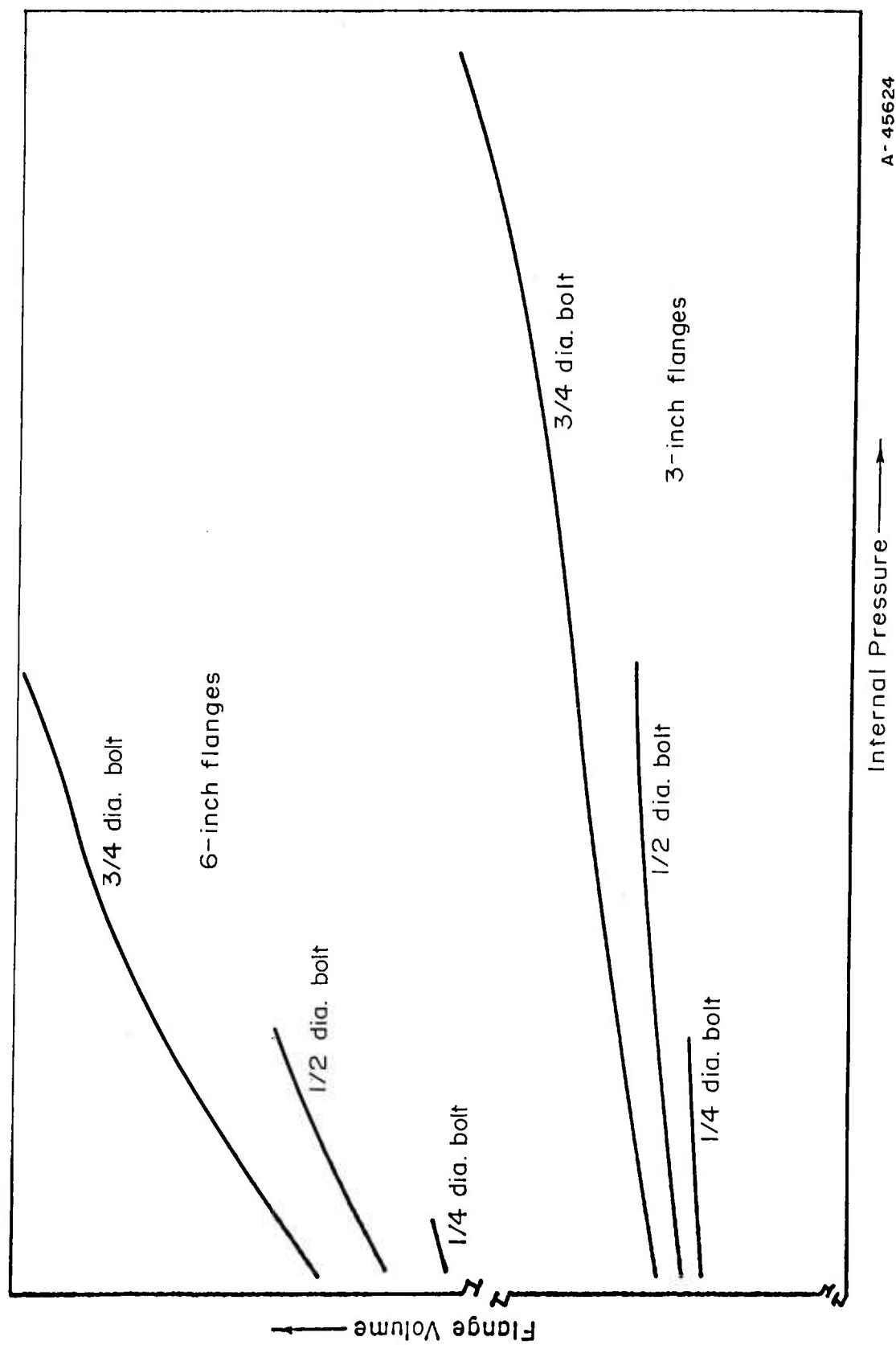
FIGURE 44. RELATIONSHIP FLANGE VOLUME AND INTERNAL PRESSURE FOR VARIOUS BOLT SIZES

A-45624

102
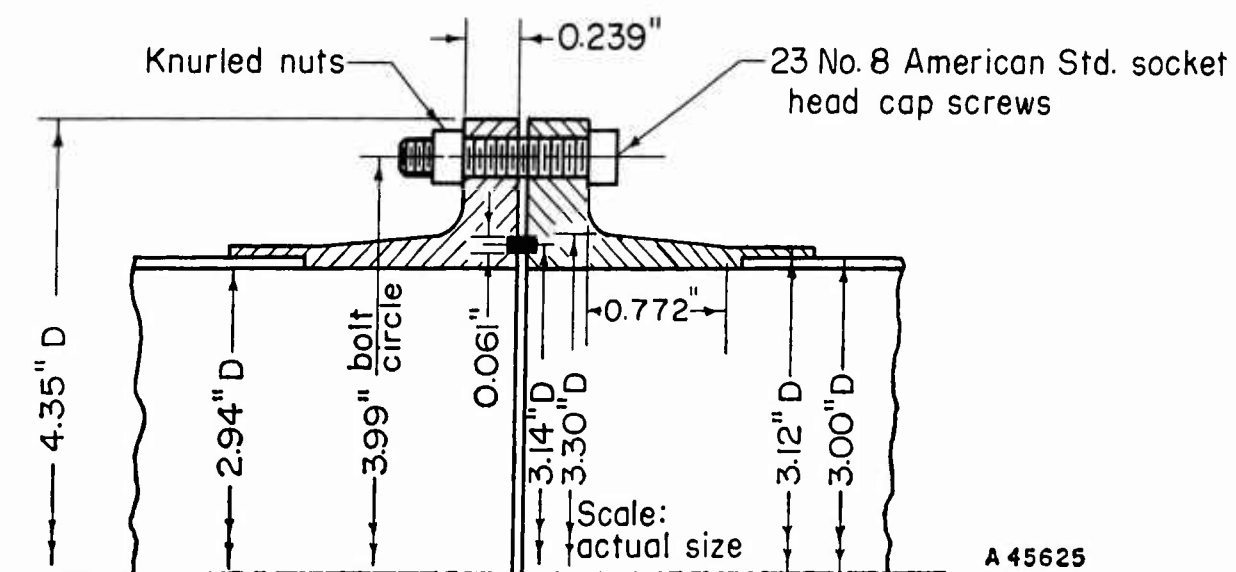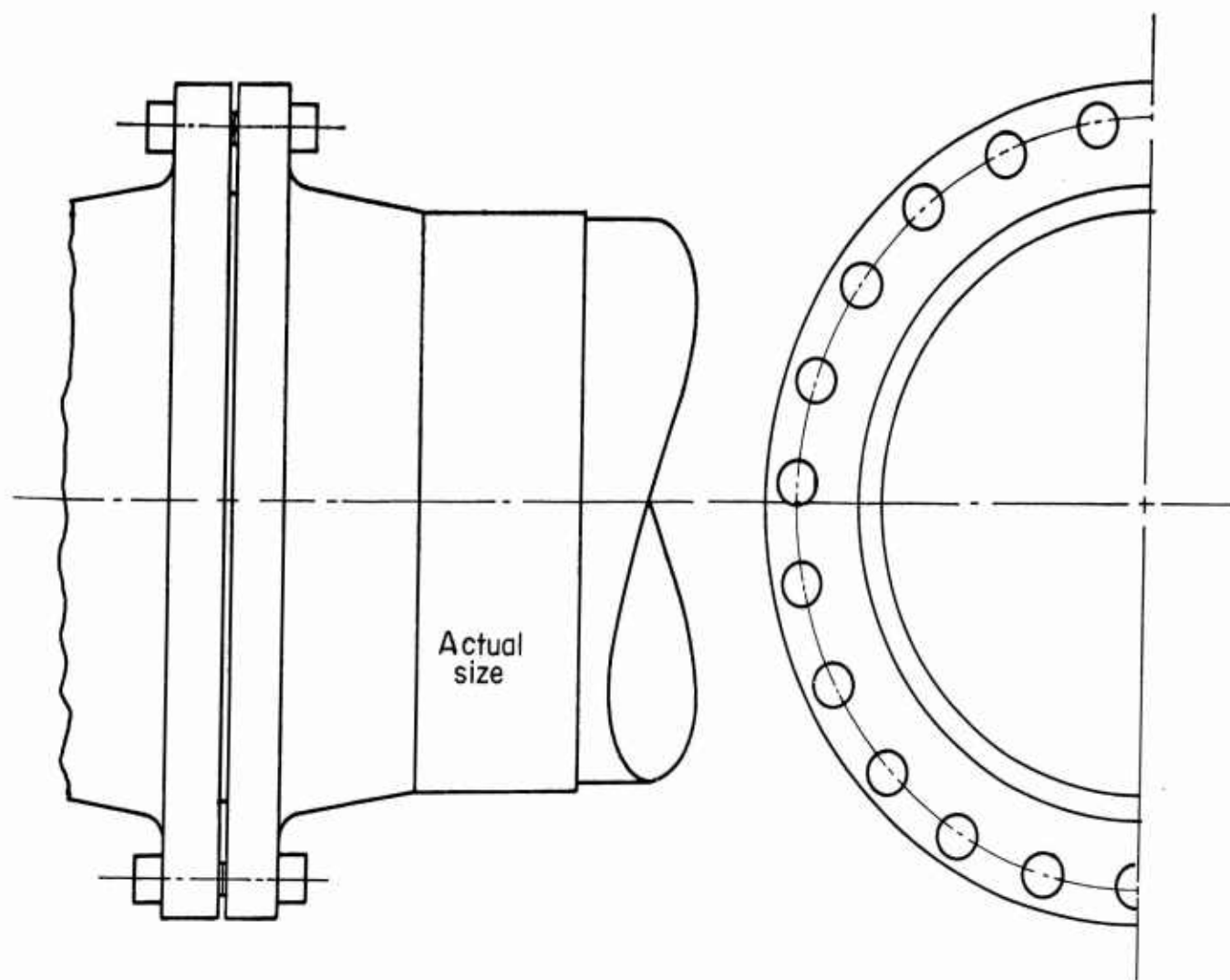
FIGURE 45. 3-IN. BOLTED FITTING, 500 PSI, 200 F, AM-355

Actual
size

Knurled nuts

←0.285"

18-No. 12 American Std. socket
head cap screws

4.54" D

2.94" D

4.06" bolt
circle

0.061"

3.14" D

3.30" D

←0.772"→

3.12" D

3.00" D

Scale:
actual size

A 45626
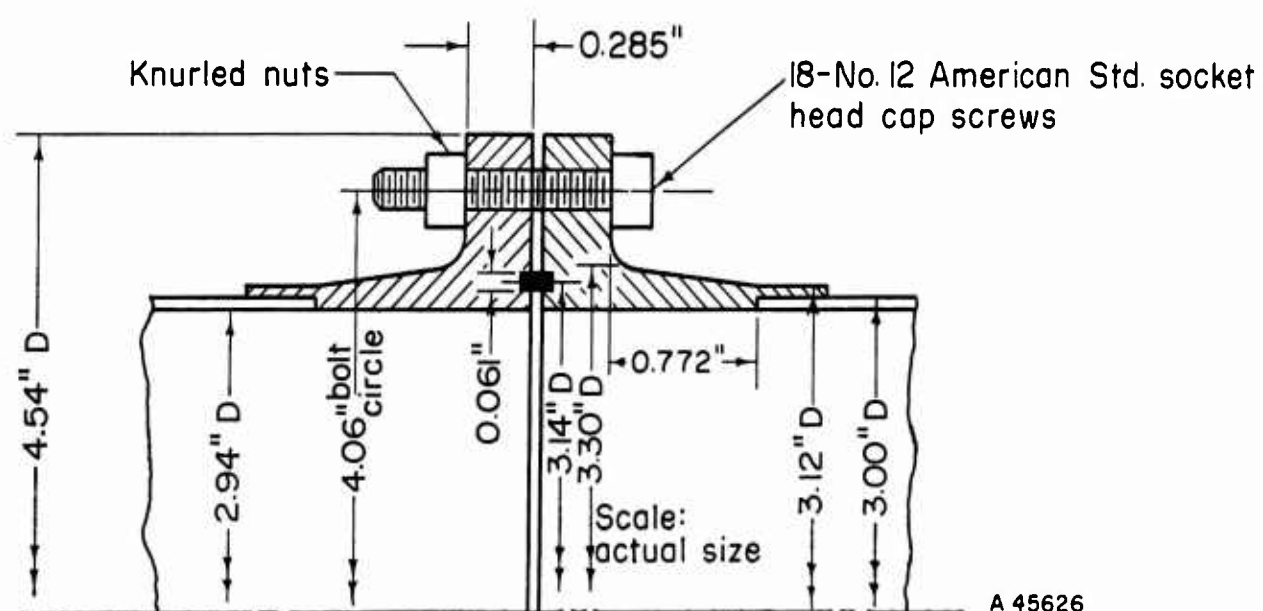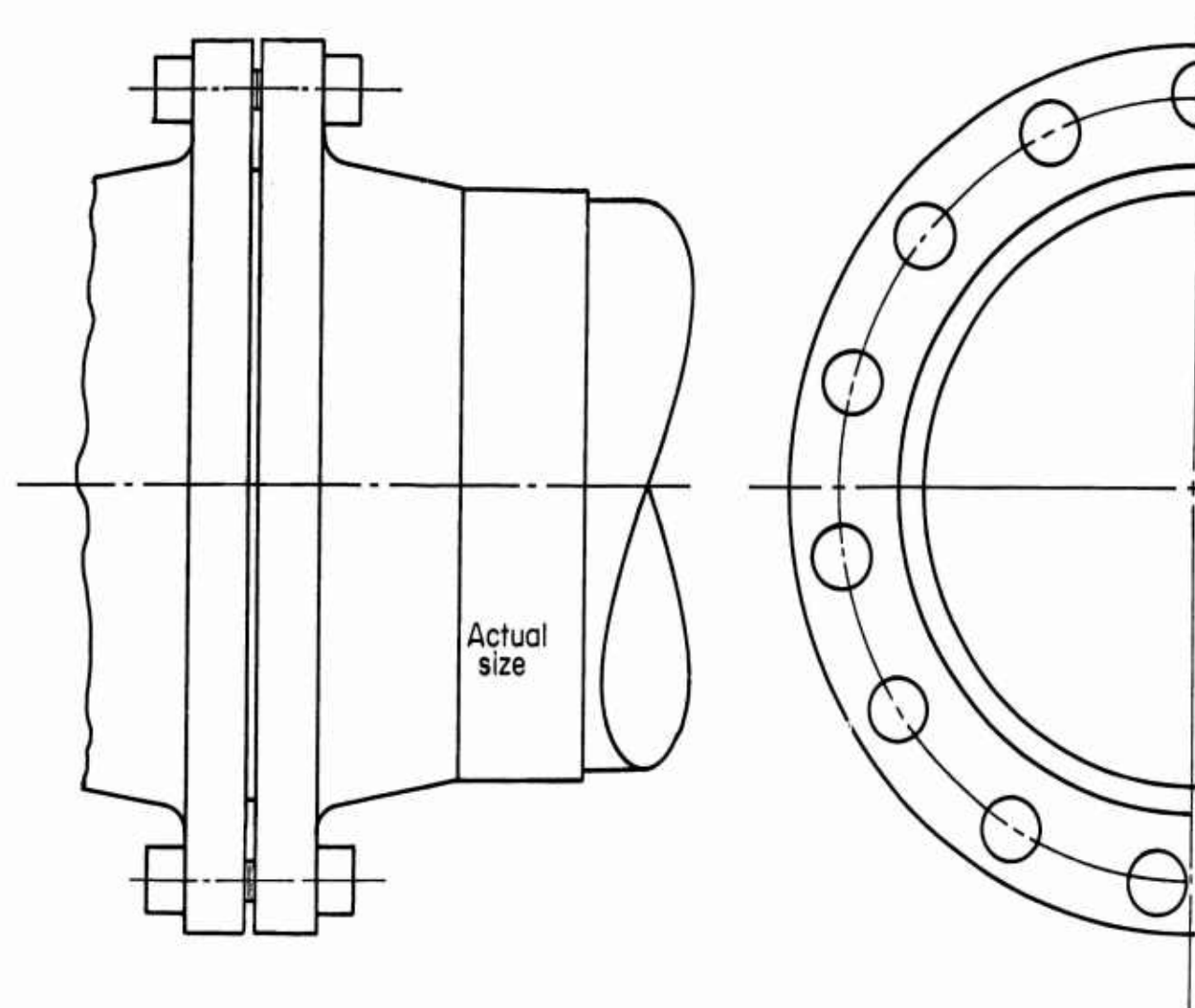
FIGURE 46. 3-IN. BOLTED FITTING, 1000 PSI, 200 F, AM-355

Actual
size

Knurled nuts
0.331"
(15) $\frac{1}{4}$-inch 28 NAS

4.74" D

2.94" D

4.18" bolt circle

0.061"

3.14" D
3.30" D

0.772"

Scale:
actual size

3.12" D

3.00" D

A 45627
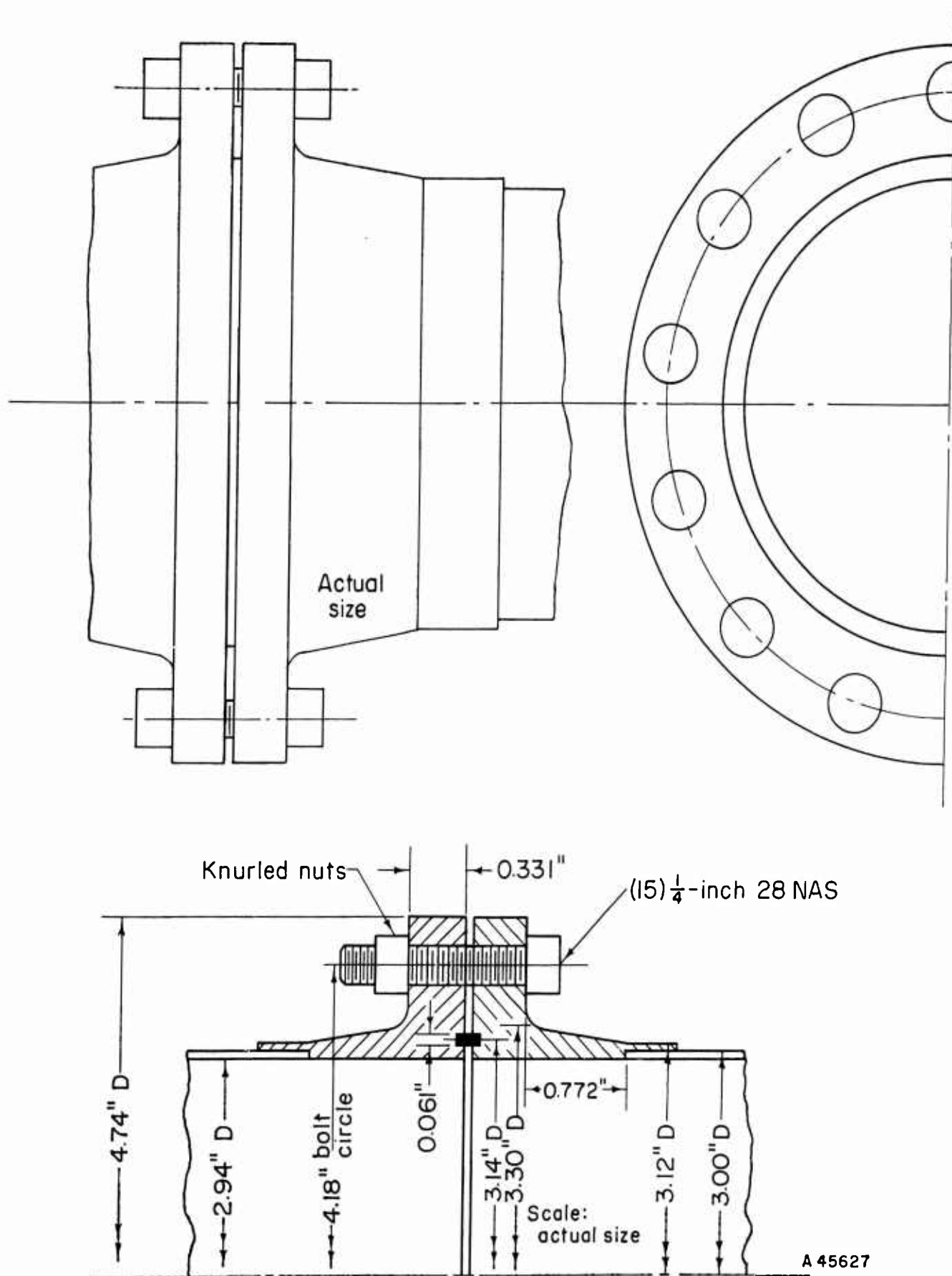
FIGURE 47.   3-IN. BOLTED FITTING, 1500 PSI, 200 F, AM-355

Half
size

Knurled nuts

0.432"

(33)$\frac{1}{4}$-inch 28 NAS

8.40" D

5.88" D

7.84" bolt circle

0.082"

6.14" D

6.60" D

1.54"

6.24" D

6.00" D

Scale:
half size

A 45628
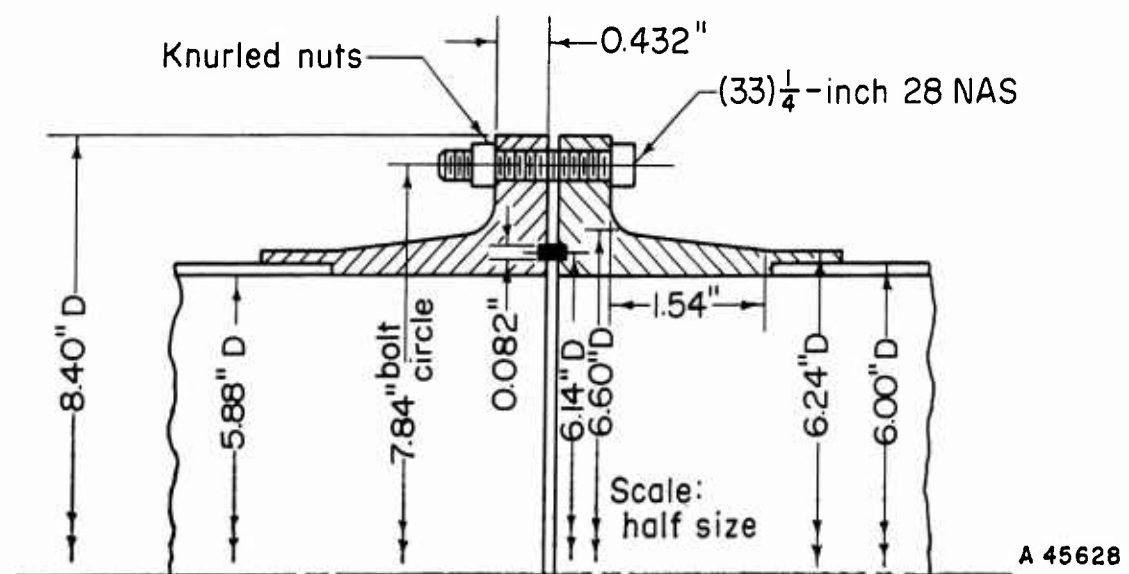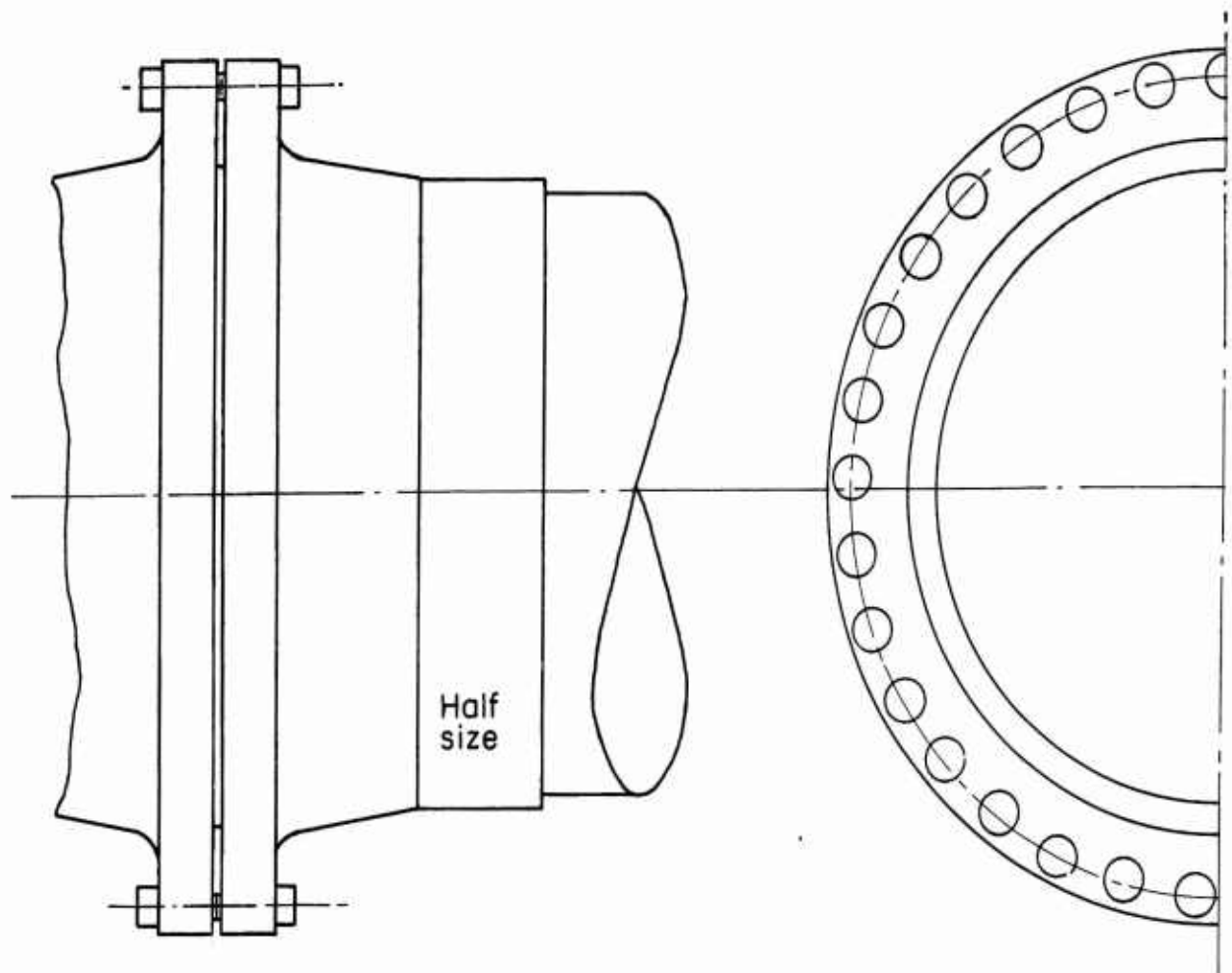
FIGURE 48.   6-IN. BOLTED FITTING, 500 PSI, 200 F, AM-355

106

Half
size

Knurled nuts

0.511"

(27) $\frac{5}{16}$-inch 24 NAS

8.62" D

5.88" D

7.93" bolt
circle

0.082"

6.14" D
6.60" D

1.54"

6.24" D

6.00" D

Scale:
half size

A-45629
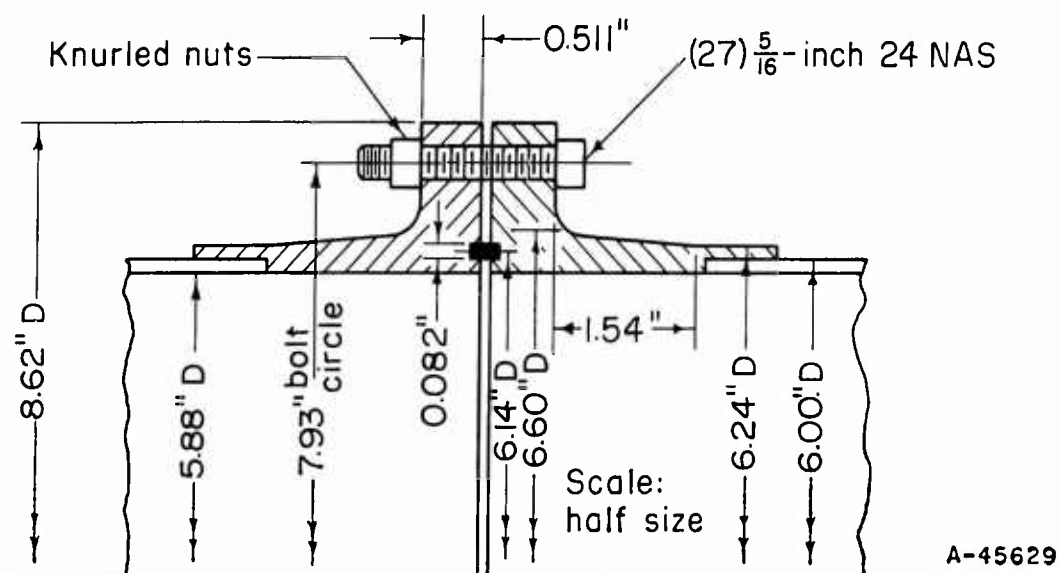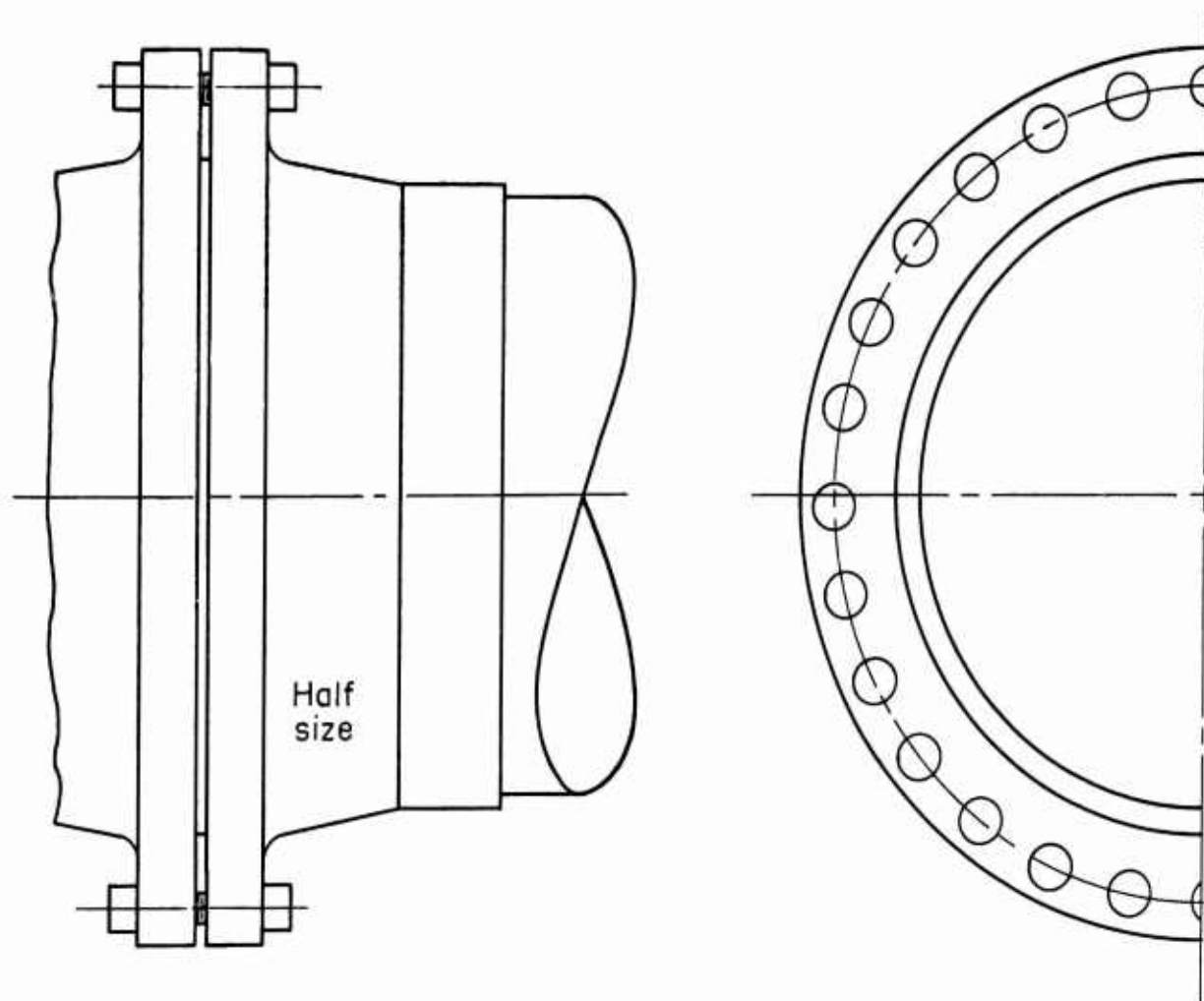
FIGURE 49.   6-IN. BOLTED FITTING, 1000 PSI, 200 F, AM-355

107

Half
size

Knurled nuts

←0.586"

(22) $\frac{3}{8}$-inch-24 NAS

8.86" D

5.88" D

8.05 bolt circle

0.082"

6.14" D
6.60" D

1.54"

Scale:
half size

6.24" D

6.00"D

A 45630
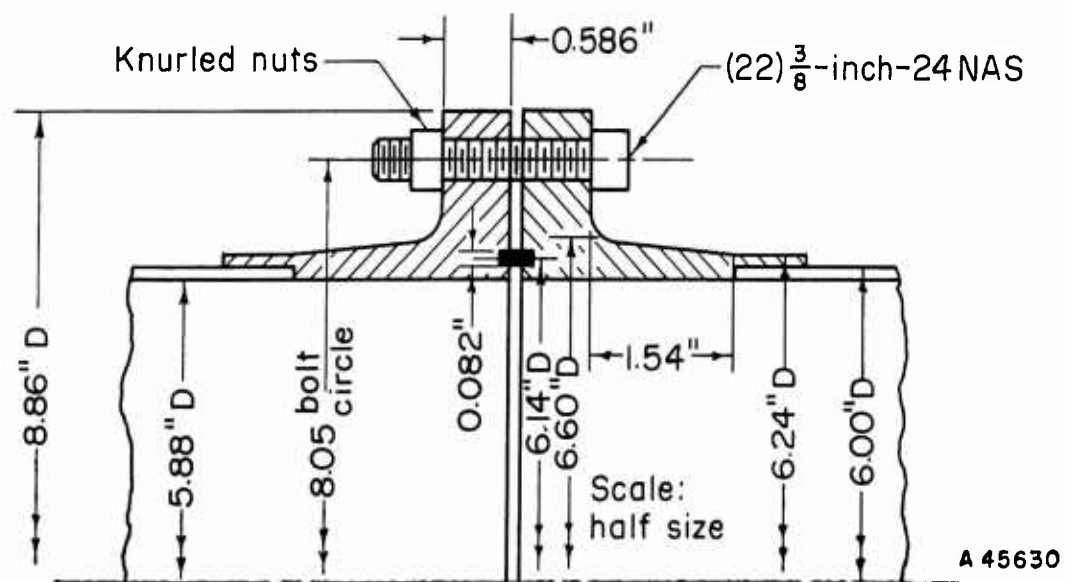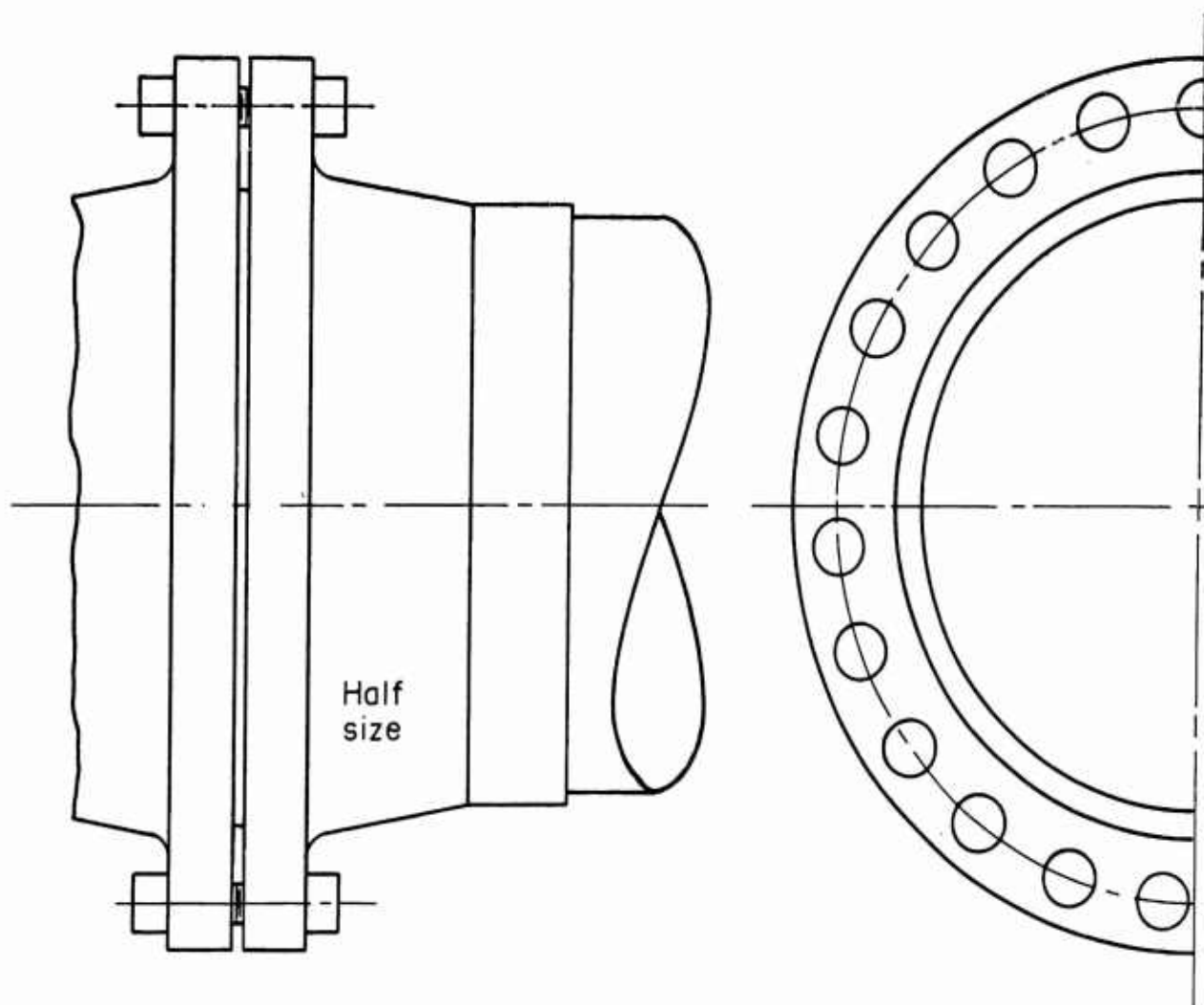
FIGURE 50.   6-IN. BOLTED FITTING, 1500 PSI, 200 F, AM-355

The volumes for each pair of flanges corresponding to Figures 45 through 50 are 5.07, 6.41, 8.05, 31.24, 37.89 and 45.68 cu in., respectively. When compared to standard carbon steel welding neck ASA flanges rated for equivalent pressures the weight ratios* corresponding to Figures 45 through 50 are 20.8, 25.6, 28.6, 9.5, 15.2, and 16.9, respectively. This major reduction in size and weight is achieved by (1) use of high-strength materials for both flanges and bolts; (2) use of the proper number and size of bolts as required for specific design conditions; (3) use of socket-head or similar bolts to eliminate or reduce wrench clearance between nut and flange hub.

Although the selected designs represent a departure from standard pipeline practices in many ways, other elements of the design are quite similar to conventional flange designs, i.e., raised faces and tapered hubs. Raised faces partially convert the flange rings into springs which can compensate for temperature gradients; the tapered hub provides maximum reinforcement, per unit weight, to the flange ring. In addition, the tapered hub provides a gradual transition in thickness between the flange rings and the attached tube for optimum fatigue resistance to cyclic bending loads.

References

(1) "Strength of Aircraft Elements", Military Handbook 5 (March, 1961).

(2) "Air Weapons Materials Application Handbook, Metals and Alloys", ARDC TR 59-66 (December, 1959).

(3) "Fittings, Flareless, Fluid Connection", Military Specification MIL-F-18280A (A56) (April 24, 1956).

(4) "Mechanical-Drive Steam Turbines", National Electrical Manufacturers Association (NEMA) Standards Publication No. SM20-1958 (revised November, 1959).

(5) Rossheim, D. B., and Markl, A.R.C., "The Significance of and Suggested Limits for the Stress in Pipe Lines Due to the Combined Effects of Pressure and Expansion", ASME Trans. (July, 1940).

(6) Wesstrom, D. B., and Bergh, S. E., "Effect of Internal Pressure on Stresses and Strains in Bolted-Flanged Connections", ASME Trans. (July, 1951).

(7) Rodabaugh, E. C., Discussion of Reference (6), ASME Trans. (July, 1951).

(8) American Society of Mechanical Engineers Boiler and Pressure Vessel Code Section VIII, Rules for Construction of Unfired Pressure Vessels, 1959 Edition.

(9) Waters, E. O., Wesstrom, D. B., Rossheim, D. B., and Williams, F.S.G., "Formulas for Stresses in Bolted-Flanged-Connections", ASME Trans. (1937).

(10) "Development of Analytical Techniques for the Design of Static, Sliding and Rotating Seals for Use in Rocket Engine Systems", Armour Research Foundation of Illinois Institute of Technology, Report No. 86017-13 covering period from February 1, 1963 to February 28, 1963, Contract No. AF 04(611)-8020.

(11) Roberts, Irving, "Gaskets and Bolted Joints", J. Appl. Mech. (1950).

* Weight ratio equals $\dfrac{\text{weight of standard ASA flange}}{\text{weight of proposed flange}}$.

(12) Shannon, W. B., Discussion of: "First Report of the Pipe Flanges Research Committee", Proc. Inst. Mech. Engrs., 132, 279 (1936).

(13) Begg, G. A. J., Discussion of "Second Report of the Pipe Flanges Research Committee", Proc. Inst. Mech. Engrs., 141, 461 (1939).

(14) "Design Criteria for Zero-Leakage Connections for Launch Vehicles", Quarterly Progress Report No. 2, October 11, 1962, Contract NAS-8-4012, General Electric Company, Schenectady, New York.

(15) "Design Criteria for Zero-Leakage Connections for Launch Vehicles", Quarterly Progress Report No. 3, January 11, 1963, Contract NAS-8-4012, General Electric Company, Schenectady, New York.

(16) Dudley, W. M., "Deflection of Heat Exchanger Flanged Joints as Affected by Barreling and Warping", Trans. ASME (November, 1961).

(17) "Development of Mechanical Fittings, Phase I", Technical Documentary Rept. No. RTD-TDR-63-14, February, 1963, Air Force Flight Test Center, Rocket Propulsion Laboratories, Edwards Air Force Base, California.

(18) Marin, Joseph, Engineering Materials, Prentice-Hall, Inc., New York (1952).

(19) Finnie, Iain, and Heller, W. R., Creep of Engineering Materials, McGraw-Hill Book Company, New York (1959).

(20) Popov, E. P., "Correlation of Tension Creep Tests with Relaxation Tests", J. Appl. Mech. (June, 1947).

(21) Robinson, E. L., "Steam-Piping Designs to Minimize Creep Concentrations", ASME Trans. (1955).

(22) Waters, E. O., "Analysis of Bolted Joints at High Temperature", ASME Trans. (1938).

(23) American Standards Association, Standards ASA B16.1, ASA B16.2, ASA B16.5, published by the American Society of Mechanical Engineers, 345 East 47th Street, New York 17, New York.

(24) Torque Manual, Third Edition (1962), P. A. Sturtevant Company, Addison, Illinois.

(25) Lensen, K. H., "Strength and Clamping Force of Bolts", Prod. Eng. (December, 1947).

(26) Scott, A. M., "Effect of Plating, Coating, and Lubrication on Tightening Torque for Bolts", Assembly and Fastener Engineering (June, 1962).

TUBE–TO–FITTING DESIGN

Design Parameters

Brazing and Welding

High-Energy-Rate Welding

References

TUBE-TO-FITTING DESIGN

The tube-to-fitting connection must satisfy two major requirements: it must contain the fluid with no leakage, and it must maintain structural integrity throughout the design life of the system. The structural loads which the tube-to-fitting connection must withstand are similar to many loads discussed in the section on fitting-to-fitting connections and hence will not be discussed here in detail. The other design parameters will be described.

Design Parameters

Reliability

Reliability of the tube-to-fitting connection is of such prime importance that the method chosen by which this connection is made must assure repeatable joint integrity within close limits. Ideally, reproducibility as established by statistical evaluation should be adequate to preclude preliminary tests. However, some provision for visual inspection is desirable to guarantee that all parts are assembled in their correct position.

Weight

A permanent connection would be the most reliable type of joint and would result in a mechanical fitting of least weight. This is especially true when the effects of the connection on the tubing wall thickness are considered. Because the tubing may constitute as much as 90 per cent of the total system weight, it is essential that its wall thickness be kept as low as possible. If the tube-to-fitting connection is not a permanent connection, as is the case with the flareless fitting, additional tubing strength must be provided at the point of connection because of the stresses caused by the clamping of the tubing wall. Practically speaking, this can be done only by increasing the wall thickness, with a resulting over-all weight increase.

Assembly

The tube-to-fitting connection must be simple to enhance its reliability and it must also be easily assembled. The method of making the connection must therefore be relatively independent of tubing tolerances, surface finishes, surface cleanliness, and operator skill. If this is not possible, a suitable technique or piece of equipment must be developed which will satisfactorily reduce these to minor considerations.

Misalignment of the tubing within the system must be compensated for. The program objectives were to provide a fitting which would tolerate 4° included angle misalignment for fitting sizes up to and including 4 in.; 1-1/2° for size up to and including 6 in.; and 1/2° for sizes up to and including 16 in. An axial misalignment capability 1/4 in. from center line was desired for all fitting sizes greater than 1 in.

One approach was to use a ball-and-socket joint at the fitting-to-fitting connection. Any such joint conceived, however, was excessively heavy. Within the fitting structure the tube-to-fitting connection is the only other choice for misalignment compensation. The misalignment of the tubes to be joined might be measured and compensated for in the process of joining the tube to the fitting. Because the system will probably be fabricated from a high-strength heat-treated material, not easily deformed or modified, it is possible that misalignment can best be compensated for by means of adjustable tubing supports. In any case the tube-to-fitting connection must be designed to withstand these imposed loads.

Material

Recent advances in metallurgy have provided alloys with very good strength-to-density ratios. In the future, even better materials probably will be available. The assembly method, therefore, should be such that new materials can be used with a minimum of development work. Furthermore, the assembly method should not cause degradation of the mechanical properties of the tube or fitting materials. Many of the newer alloys, including the three selected for the improved fittings, attain their high strength-to-density ratios because of heat treatment. This strength advantage is minimized when excessive temperatures are applied to local areas. The thickness and hence the weight of the fitting must then be increased in proportion to the reduction in material strength.

Candidate Joining Methods

Two kinds of joints were considered, namely, "hot" and "cold". Hot joints are those which require an external source of heat, e.g., soldering, brazing, and the many types of welding. Cold joints are those which require only mechanical energy, e.g., swaging, roll bonding, friction welding, and high-energy welding.

Of the many types of joints considered, three are recommended for the tube-to-fitting connection: brazed, hot welded, and explosive welded. However, unlike the fitting-to-fitting connection, a configuration for the tube-to-fitting connection cannot be derived readily by analytical methods within the present state of the art. Experimentation is necessary to define the critical parameters. Therefore in the following discussion instead of presenting preliminary designs, the recommended methods for making the tube-to-fitting connection will be described and the effect of these methods on the final configuration will be discussed.

Brazing and Welding

Considerable work has been done by North American Aviation* on welded and brazed joints for tubing for aerospace applications. The results of this work have been reviewed in detail and have been found to be directly applicable to the problem of making a satisfactory tube-to-fitting connection for improved missile mechanical fittings. Many of the NAA procedures are illustrated in a paper by G. R. Barton, et al.,[1]** and a full description will soon appear in an official report. The possible application of these concepts to a mechanical fitting is discussed below.

Choice of Materials

Materials that are compatible with the welding and brazing operations must be chosen. North American Aviation has reported that the materials recommended by Battelle for separable fittings have been successfully brazed and welded by NAA as part of their joint development effort. Therefore, no difficulties should arise because of the materials selected.

Source of Heat

Heat sources selected by NAA include a modification of the standard induction heating system for the brazed joint and the tungsten, inert-gas (TIG) process for the fusion-welded joint. Although other heat sources may be used, the ones chosen offer the advantages of being clean, neat, versatile, and, most important, easily controlled. Very close control is necessary when heat-treated materials such as AM-350 are used, to prevent the heat-affected zone from extending outside the fitting envelope.

Joint Fit-Up

Because OD tolerances of purchased tubing are too liberal, the tubing must be sized before joining to insure correct braze capillary action and proper weld penetration and heat transfer, and to insure the proper fit of the tube and fitting to withstand external bending loads. Typically, total diametrical tolerances of 0.002 to 0.005 in. are required.

Filler Material

In the NAA brazed joint, illustrated in the Barton paper[1], brazing alloy reservoirs are provided to obtain optimum capillary flow during brazing. The brazing alloy must be selected for structural strength, service temperature, and corrosion resistance to the contained fluid. Nominally, its melting temperature should be at least 300 to 500 F above the expected service temperature[2]. Fluid compatibility is minimized in fusion welding because there is no alien filler material present[1].

Cleanliness

To insure highly reliable joints, whether brazed or welded, all components must be specially cleaned. It is also necessary to purge with a specially prepared inert gas before, during, and after the application of heat because of the detrimental effect of surface oxides.

Conclusions

In spite of some apparent drawbacks associated with North American Aviation's hot-joining techniques, the probability of successfully satisfying the stringent requirements of joint integrity are much better for the immediate present with these methods than with other methods or concepts suggested or studied. The need for sizing the tube

for joint fit-up will necessitate a quality-control program. Special handling and assembling procedures are also serious limitations. However, it is believed that such limitations can be sufficiently overcome to make the brazed or welded joint a practical tube-to-fitting connection. Furthermore, extensive field experience and experimentation should lead to further refinements and simplifications.

High-Energy-Rate Welding

High-energy-rate welding is a process which utilizes high pressures for extremely short periods of time to obtain a metallurgical union between two metallic parts. High-energy-rate welding differs from high-energy-rate forming only in the magnitudes and time-variant characteristics of the applied forces.

Two basic energy sources presently being utilized for high-energy-rate forming are (1) the electrical energy stored in a bank of high-voltage capacitors, and (2) chemical explosives. No data have been found on the use of capacitor discharge for welding metal, although the operation is theoretically possible. On the other hand, considerable work has been done by several companies on the use of chemical explosives to weld different metal shapes. Much of this work appears pertinent to the problem of making satisfactory tube-to-fitting connections.

Chemical Explosives

Chemical explosives are classified into two general categories: low explosives and high explosives. Low explosives, such as smokeless powder and black powder, have a burning rate or deflagration velocity ranging from a few inches to a few feet per second and can produce pressures in the order of 30,000 to 300,000 psi, depending on the degree of confinement. High explosives, such as TNT, PETN, and dynamite have a detonation velocity in the order of 6000 to 28,000 ft/sec and can produce pressures up to about 4-million psi. Low explosives are normally used in enclosed systems where the containment helps increase the impulse imparted to the workpiece. High explosives are normally fired as bare charges in open systems because the peak pressure is relatively independent of the degree of confinement[3]. Some characteristics of high explosives are given in Tables 18, 19, and 20. From Table 19 the total energy available from 1 lb of PETN is approximately 1.74-million ft-lb ($4.35 \times 10^5 \times 4$). With a typical conversion time of 2 μ sec, this is equivalent to approximately 1.57-billion hp.

The total impulse imparted to the workpiece is represented by

$$I = \int_{t_o}^{t_f} Pdt, \qquad (24)$$

where

I = impulse, lb-sec/in.^{2}
P = pressure, psi
t = time, sec.

TABLE 18. CHARACTERISTICS OF HIGH AND LOW EXPLOSIVES[4]

Property	High Explosives	Low Explosives
Method of initiation	Primary high explosives-- ignition, spark, flame, or impact	Ignition
	Secondary high explosives-- detonator, or detonator and booster combination	
Conversion time	Microseconds	Milliseconds
Conversion rate	6,000 to 28,000 ft/sec	A few inches to a few feet per second
Pressures	Up to about 4,000,000 psi	Up to about 40,000 psi

TABLE 19. CHARACTERISTICS OF HIGH EXPLOSIVES[4]

Explosive	Specific Gravity	Detonation Velocity, 1-1/4-In. Diameter, ft/sec	Energy[a], 10^5 ft-lb/lb	Maximum Pressure[b], 10^6 psi
RDX (cyclotrimethylene trinitramine)	1.7	27,500	4.25	3.4
PETN (pentaerythritol tetranitrate)	1.6	26,500	4.35	3.2
Pentolite (50 PETN/50 TNT)	1.6	25,000	3.17	2.8
TNT (trinitrotoluene)	1.6	23,000	2.62	2.4

(a) Based on ballistic-mortar comparisons. Total energy would be four times these figures.

(b) At 1-1/4-in. diameter. Based primarily on the calculations by the methods of Cook. By Taylor's methods, this pressure will be 10 to 20 per cent lower.

TABLE 20. PROPERTIES OF EXPLOSIVES[3]

Explosive	Specific Gravity	Detonation Temperature, C	Detonation Pressure, 10^6 psi
RDX	1.6	5450	375
PETN	1.6	5400	330
Tetryl	1.6	4400	290
Picric acid	1.6	3900	265
TNT	1.6	3900	225

For a given impulse, which is proportional to the energy imparted to the workpiece, the pressure-time relationship can take many forms. In explosive welding both the total impulse and the pressure-time relationship are important. For example, if the high-pressure loads are released too fast, the tensile stresses induced by the over-recovery of the material may tend to distort or fracture the piece[3]. Typical pressure-time curves for low and high explosives are shown in Figure 51. The conversion time, i.e., the time required to convert a working amount of explosive into gaseous products, is measured in microseconds for high explosives and milliseconds for low explosives[3]. To date, only high explosives have been shown to be applicable to welding operations[5].

Explosive-Welding Variables

The variables that must be controlled in explosive welding are primarily those affecting the velocity of the interface closure. If the developed interface angle and the closure velocity are correct, welding occurs. In the case of tubular or concentric components, interface angle and closure velocity can be varied by changing wall thickness, charge density (amount of explosive per unit of surface area being welded), or the initial clearance or separation at the interface. It is not necessary that all of these be variables if one or more can be changed to bring the system into proper balance[5].

Two explosive-welding techniques are possible[3]. In one method the parts are placed in contact and are then subjected to a load applied normal to the surface to be welded in an underwater standoff operation. This method is applicable mainly to flat plates. In the second method, which is applicable to flat plates and tubular components, the parts are not initially in contact. This is the method discussed below.

When an explosive detonates, there is a finite time during which the detonation travels symmetrically outward from the initiation point. For a line charge set off at one end, the detonation progression is, of course, along the length of the line. For example, Figure 52 shows a linear charge, consisting of a stick of dynamite, detonating under water. The V-shaped shock wave produced is essentially a conical front around the explosive[6]. The effect of the shock wave is apparent in the displacement of the suspended wire.

The principles of explosive welding can be illustrated by the system of plates shown in Figure 53. As the detonation progresses along the sheet of explosive, a shock wave and gas cloud are produced. For high explosives not in contact with the workpiece, the major portion of the usable energy is provided by the shock wave, whereas for low explosives the gas-cloud pressure provides a major portion of the usable energy. The velocity of the shock wave in the direction perpendicular to the plate is essentially the velocity of sound in the transfer medium between the explosive and plate. In the space immediately adjacent to the explosive the velocity will be much greater due to the rapid expansion of the gaseous products. With contact charges the gaseous expansion also adds to the usable energy transfered to the workpiece.

Figure 54 depicts the manner in which the peak pressure at the workpiece may be varied as a function of charge size and standoff distance. An explosive with a detonation velocity of 25,000 ft/sec was used in constructing these curves on the basis of the following equations[4]:

116
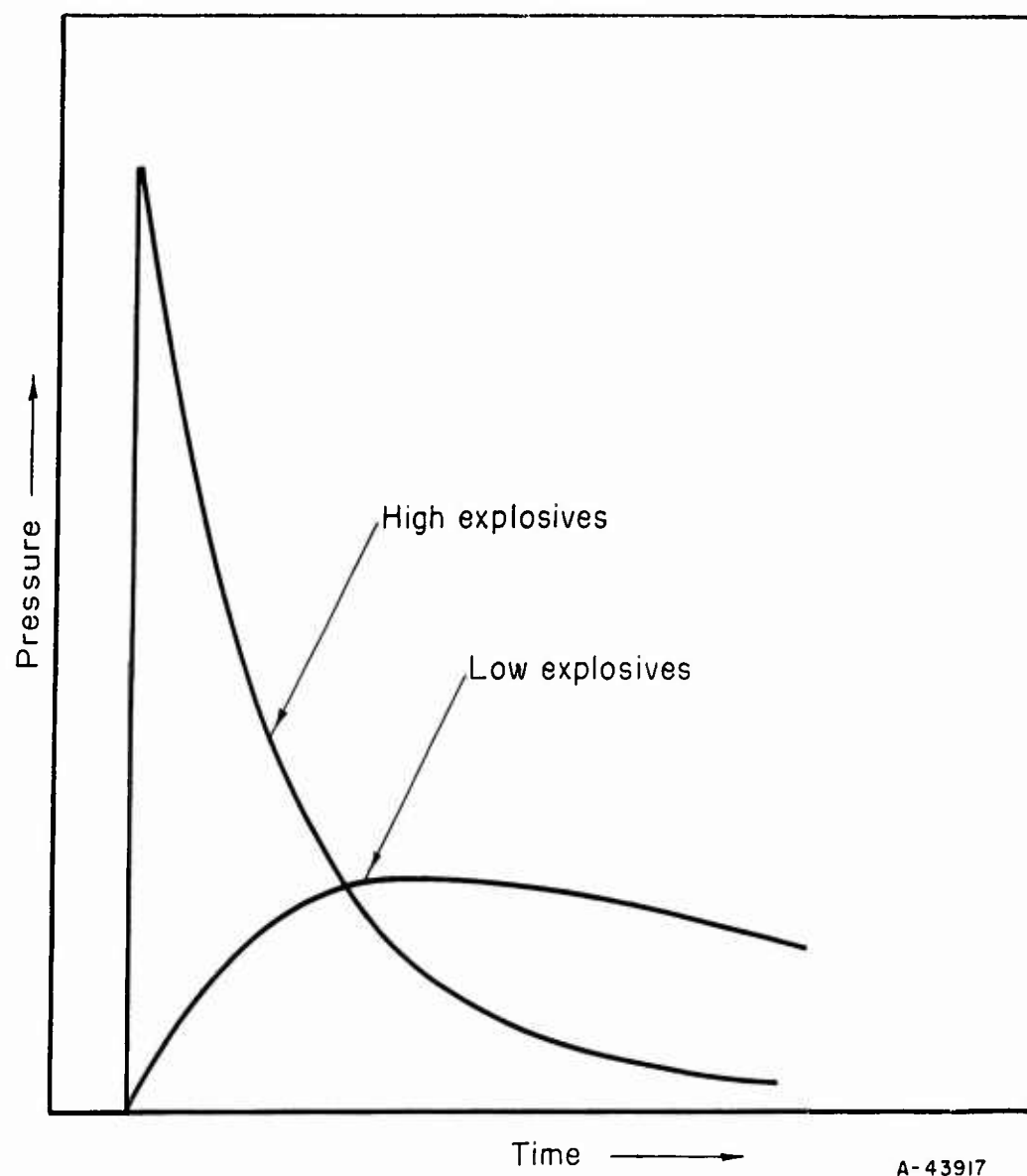
FIGURE 51.   TYPICAL TIME-PRESSURE PROFILES FOR LOW AND HIGH
EXPLOSIVES[4]

Gas Cloud

Shock Wave
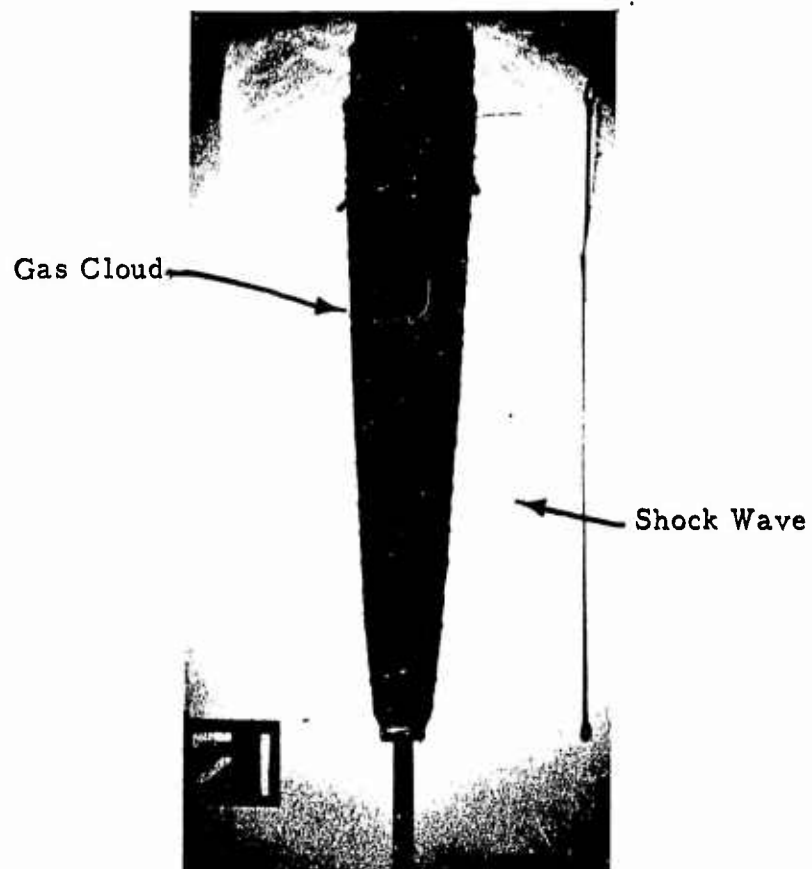
FIGURE 52. LINE CHARGE DETONATING IN WATER[6]
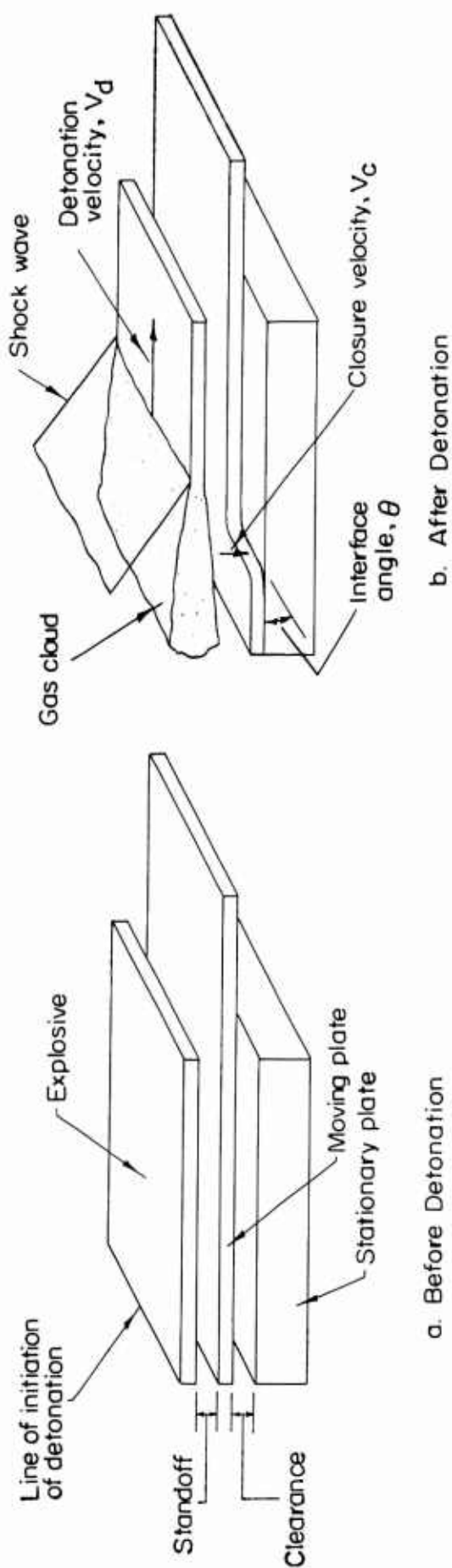
FIGURE 53. EXPLOSIVE WELDING OF FLAT PLATES

Shock wave

Detonation velocity, V_d

Gas cloud

Closure velocity, V_c

Interface angle, θ

b. After Detonation

A-43931

Explosive

Line of initiation of detonation

Standoff

Clearance

Moving plate

Stationary plate

a. Before Detonation

119
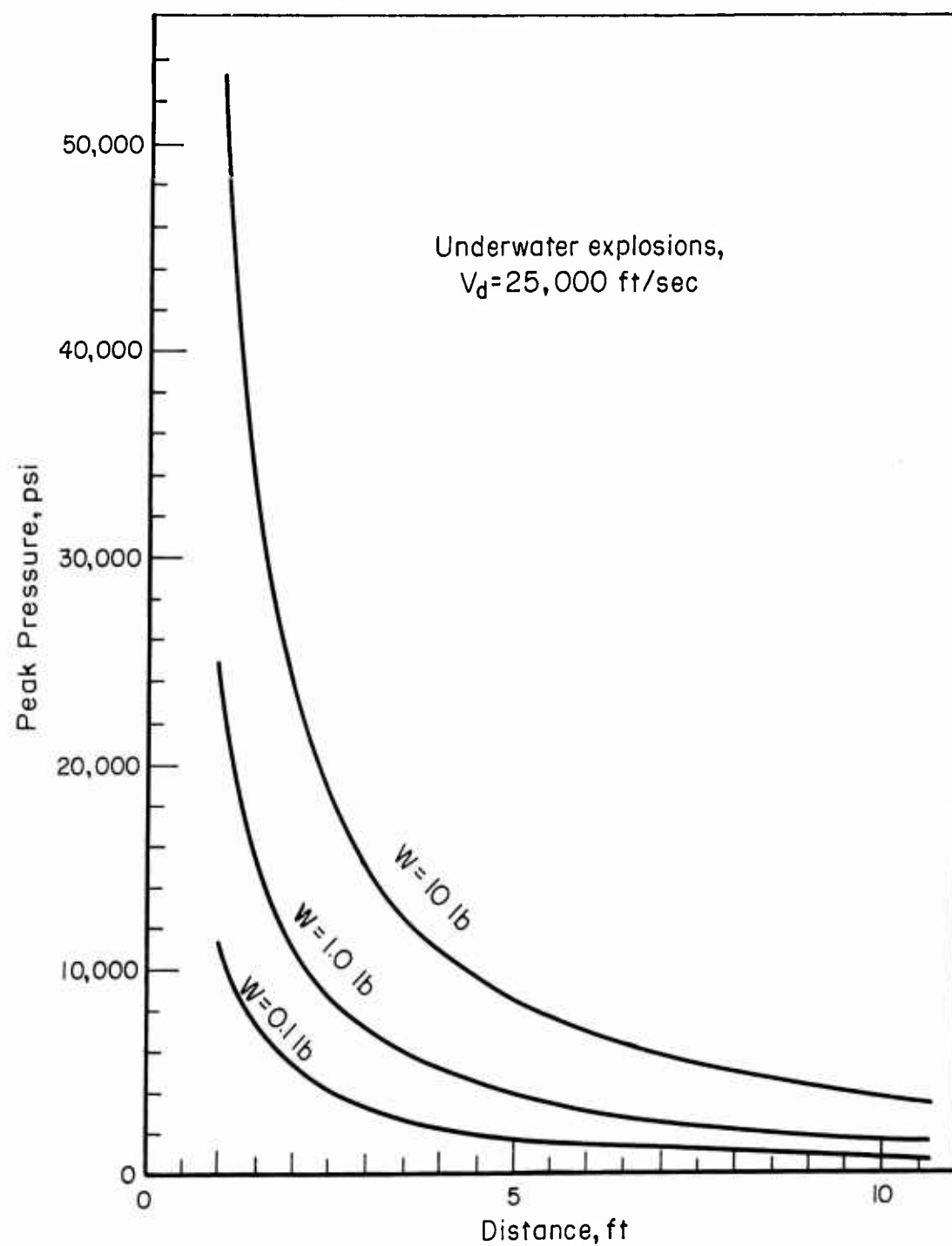
FIGURE 54. EFFECT OF CHARGE SIZE AND STANDOFF DISTANCE ON PEAK PRESSURE[4]

$$P = K_1 \left(\frac{W^{1/3}}{R} \right)^{\alpha} \tag{25}$$

and

$$P = 155 \left(\frac{W^{1/3}}{R^{1.15}} \right) \sqrt{V_d}, \tag{26}$$

where

   P = peak pressure, psi
   W = weight of explosive, lb
   R = distance from explosive, ft
   K_1 = constant which varies with the explosive
   α = constant which is generally equal to 1.15
   V_d = detonation velocity of explosive, ft/sec

It is not necessary to perform the welding operation in water. However, the constants in Equations (25) and (26) must be modified where air is the transfer medium. The peak pressure with air as the transfer medium will be approximately 30 per cent of the peak pressure with water as the transfer medium.

Figure 55 shows the effect of the transfer medium and the standoff distance on the peak pressure at the workpiece. If a charge were detonated at the end of a tube, the peak pressure would diminish along the length of the tube as shown. Therefore, a piece of equipment 3 ft from an explosive charge equal to 4 lb of TNT would be subjected to a pressure of only 500 psi in air.

The shock wave, as it progresses (Figure 53b), imparts an impulse load to the plate. The velocity of closure, V_c, is much smaller than the velocity of detonation, V_d, and hence the plate, as it deforms, forms the interface angle, θ, between the stationary plate and the moving plate.

The developed interface angle, θ, will depend on the relative magnitudes of V_c and V_d and the initial clearance between the two plates. As the initial clearance between the plates is increased, θ becomes larger. For a given type of explosive, the detonation of velocity, V_d, is a constant. The closure velocity, V_c, which is a function of the total energy delivered to the upper plate, can be varied over a wide range by changing the charge density, the upper plate thickness, and the charge standoff distance. The closure velocity also depends on the density and dynamic yield strength of the upper-plate material. Variations in the charge density and standoff distance change the peak pressure and hence also change the total amount of energy delivered to the workpiece.

The total energy delivered to the workpiece is expended in three ways. Part of the energy is used to overcome the material inertia, part causes deformation of the upper plate, and the remainder causes the plate to accelerate. The final closure velocity is a function of the acceleration of the plate. Any parametric change that affects the percentage of total energy left for acceleration of the plate will also cause a change in the closure velocity. Hence, an increase in plate thickness, material density, or dynamic yield strength will diminish the closure velocity.
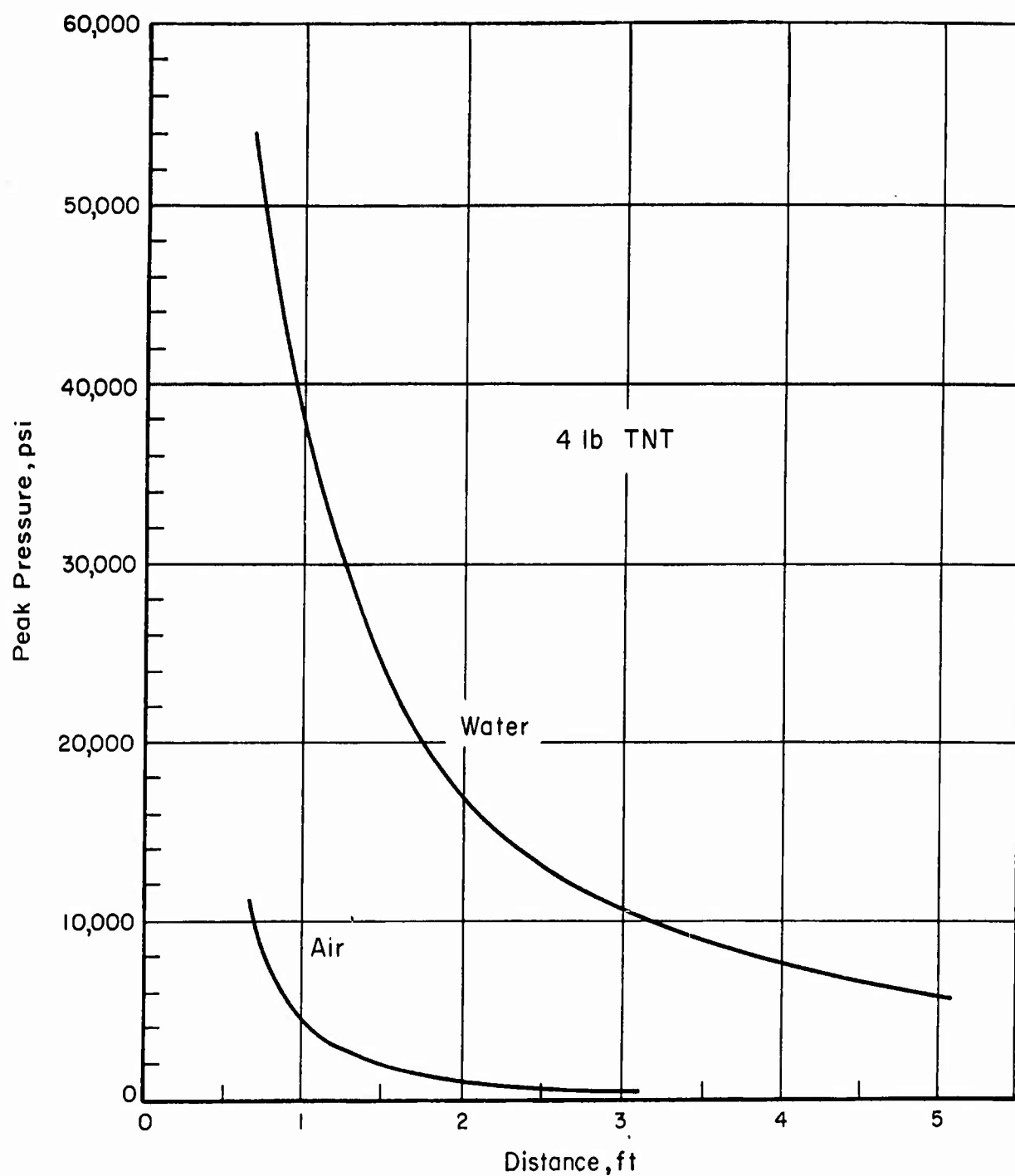
FIGURE 55.   EFFECT OF TRANSFER MEDIUM AND STANDOFF DISTANCE ON
PEAK PRESSURE[4]

In much of the past work on explosive welding, the interface between the two plates has been evacuated. However, it has been shown that evacuation is not necessary to obtain welding. The principal advantage to be gained from evacuation is the reduced compound formation when dissimilar materials are being welded. However, even in cases in which dissimilar metals are joined, the small amount of compound formation usually has little effect on the strength and integrity of the joint.

Experience has shown that the explosive welding process is not sensitive to surface cleanliness or roughness. Degreasing and wire brushing are usually the most stringent surface preparations necessary. Welds have been obtained even without the wire brushing, and it has been reported that degreasing is unnecessary[6,7]. A series of experimental runs at Battelle on the explosive welding of Zircaloy-2 tubing to Type 410 stainless steel tubing indicated that changes in the surface finish in the range of 300 μin. rms to 1500 μin. rms had no effect on the accomplishment of a weld[8]. A Type 304 stainless steel sleeve with a 100-μin. rms finish was successfully welded to the inside of a Type 304 stainless steel ring with a surface finish of 30 μin. rms.

Characteristics of Explosively Welded Connections

Among the principal advantages of explosive techniques are the absence of heat-affected zones, the absence of excessive compound formation in cases in which the welded elements are dissimilar metals, the lack of effect on the mechanical characteristics of most materials, the ability to treat large areas and geometries which present difficulties with other processes, and the relatively small and simple equipment required[4,5].

Separable connections which utilize a replaceable seal are particularly susceptible to the effects of heat applied near the seal surface because of the tendency for the seal surface to warp under nonuniform heating. A rule of thumb states that a fusion weld should be a distance of $2\sqrt{Dt}$ from the sealing surface, where D is the tube diameter and t is the tube-wall thickness. The temperature necessary to fusion weld or braze may also affect the strength of the material, as previously discussed. An explosive weld, because of the low amount of heat generated, and because of the symmetrical nature of the forming process, would minimize the warping problem.

When dissimilar metals are fusion welded the relatively large melted zone causes considerable compound formation. Again, because there is no melted zone with explosive welding, this problem is minimized.

Figure 56 shows five possible arrangements of tube, fitting, and explosive. Figure 56a shows the working explosive charge in contact with the inside of the tube. The working charge is set off by means of the detonating cap attached to an explosive leader, which is tented so that the detonation progression of the working explosive is symmetrical with the tube axis. Figure 56b shows a line charge placed on the axis of the tube. A modification of Figures 56a and 56b is shown in Figure 56c, in which the working explosive is wrapped on a mandrel centered in the tube. Variations in mandrel diameter would vary the charge standoff distance. With a given total explosive charge, the peak pressure at the tube would be a maximum in Figure 56a, and a minimum in Figure 56b. Any pressure between the maximum and minimum could be obtained by means of the configuration in Figure 56c. An externally placed explosive charge is shown in Figure 56d. Again, a tenting arrangement is provided to obtain the proper detonation progression.

In each of the configurations in Figure 56 it would be possible to make the explosive into a package that could be inserted and set off by semiskilled personnel. The only other equipment needed for all fittings would be a battery detonator no larger than a lunch pail and a length of wire to lead from the detonator to the detonating cap. For some fittings, depending on the tube wall thickness, the size of explosive charge, and the configuration, it might be necessary to provide internal or external backup dies to prevent excessive deformation of the tube and/or fitting.

Because of the possibility of developing a "package" for a particular size fitting, an explosively welded joint should be extremely reliable.

Conclusions

Although adaptation of the North American brazed or welded joint appears to be the best method of achieving a reliable tube-to-fitting connection in the next year or two, it is believed that an explosively welded joint might be a significant improvement for introduction at a later date. For this reason it is recommended that further research be pursued to determine the general problems of explosively welding AM-355, 17-4PH, and René 41, which are the materials selected for use in improved fittings. It is difficult to estimate the proper size range that future development should be concerned with because economic and logistic considerations are as important as the safety of the operation and the technical feasibility. At Battelle, a 3-in.-diameter Zircaloy tube with a wall thickness of 0.045 in. was successfully welded to a stainless steel header with a 45-gram charge of PETN. This appears to be a reasonable estimate of the conditions that might be encountered in making a 3-inch welded tube-to-fitting connection, and this size of charge probably represents the maximum that could be readily handled.

References

(1) Barton, G. R., et al., "Tubular Joining by Induction Brazing and Fusion Welding Methods", SAE Aerospace Manufacturing Forum, The Ambassador Hotel, Los Angeles, California, October 8, 1962.

(2) Personal communications with Robert M. Evans of Metals Joining Division, Battelle Memorial Institute.

(3) Pearson, John, "The Explosive Working of Metals", Navord Report 7033 (1960).

(4) Simons, Charles C., "Explosive Metalworking", DMIC Memorandum 71, OTS PB 161221 (November 3, 1960).

(5) Personal communication with Ronald J. Carlson and Charles C. Simons of the Department of Metallurgy and Physics, Battelle Memorial Institute.

(6) Douglass, John J., "Forming Practices With High Explosives", Du Pont Technical Bulletin (May 26, 1960).

(7) Yernow, Dr. Louis, "Explosive Welding", Paper presented at New Bonding Methods Symposium of Annual ASM Metals Show, New York, New York, October 30, 1962.

(8) Paprocki, Stan J., Porembka, Stanley W., et al., "Joining Zircaloy-Stainless Steel and SAP Alloys by Friction, Rolling, and Explosive Techniques", report BMI-1594 to the AEC (September 4, 1962).
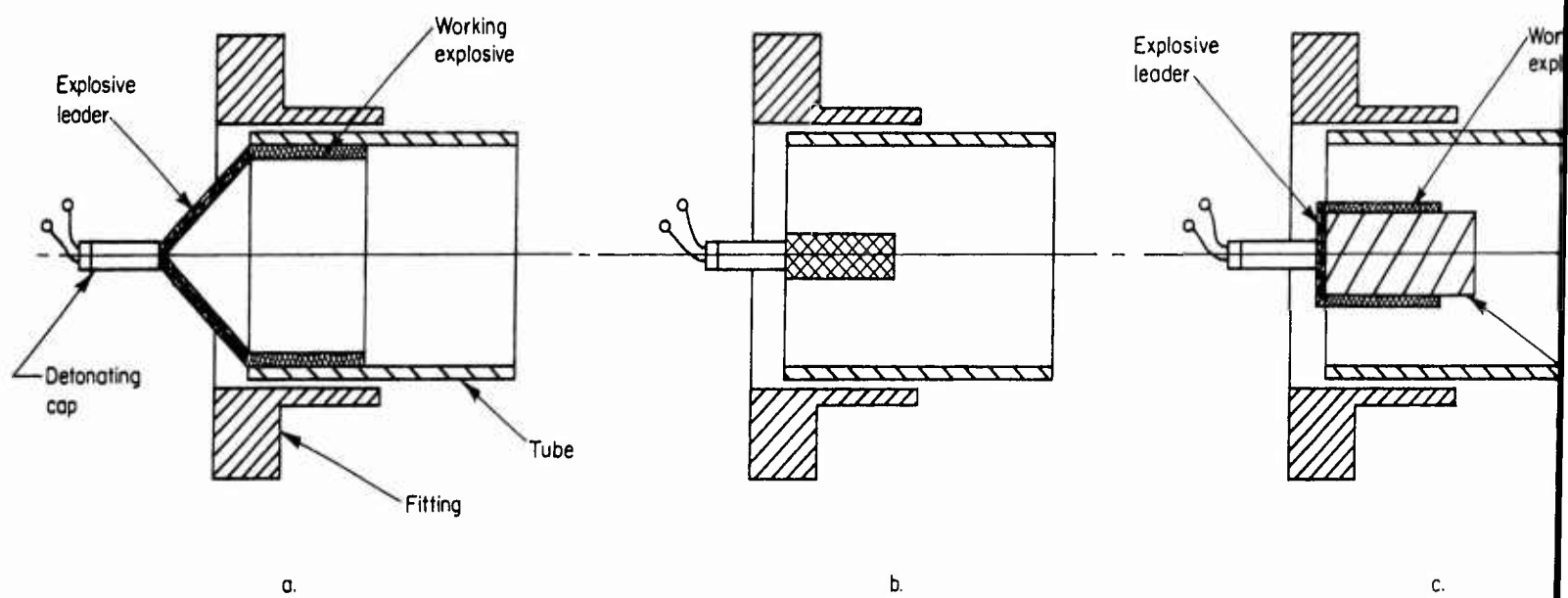
FIGURE 56. EXPLOSIVE-WELDING ARRANGEMENTS
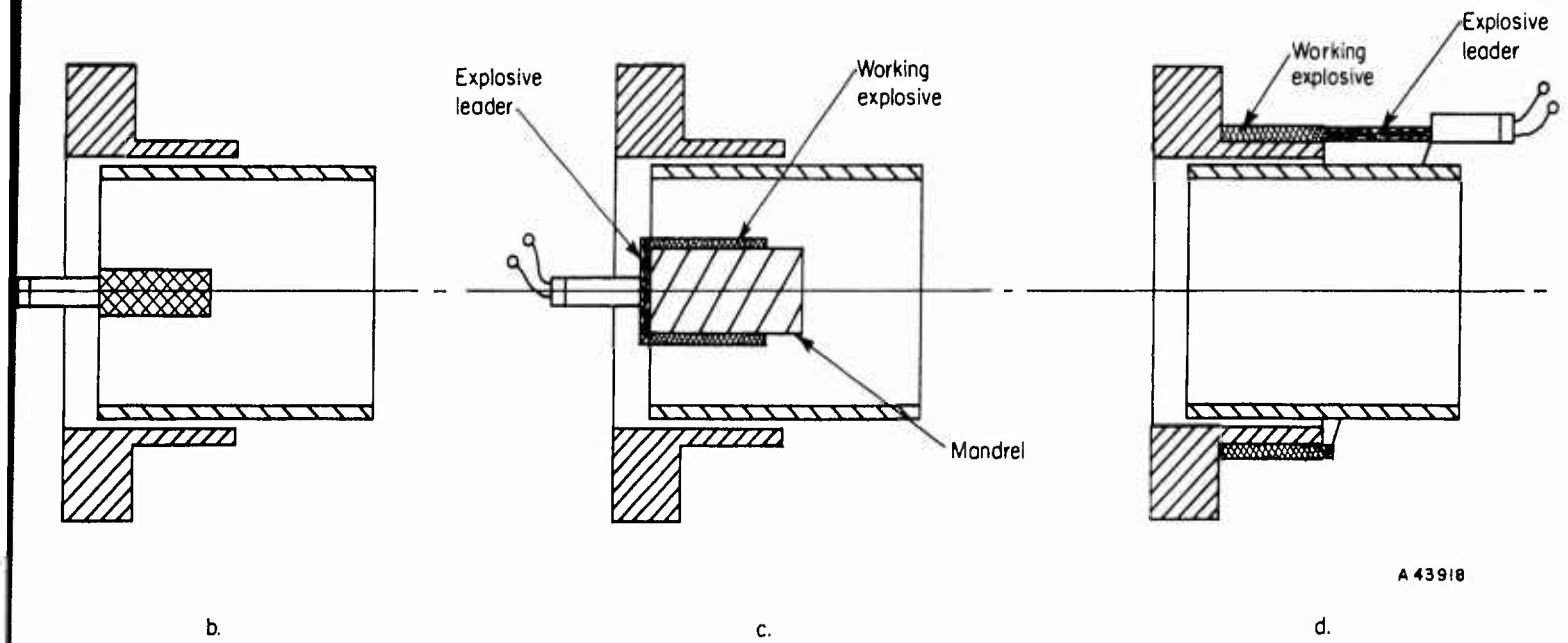
2

b.

c.

d.

G ARRANGEMENTS

A 43918

SEAL DESIGN

SEAL DESIGN

Throughout Phases I and II, the seal posed the most difficult design problem. The required service-temperature ranges preclude the use of a nonmetallic seal, and experience has not resulted in a clearly defined understanding or agreement among designers on the optimum mode of sealing for metal seals. Fortunately, both General Electric[1]* and Armour Research Foundation[2] have developed important guidelines as a result of their studies of interface phenomena and sealing contact stresses. However, analytical studies do not provide all the data needed to design a satisfactory seal, and past laboratory evaluations of commercial seals have been inconclusive because of the predisposition of the evaluators or because of the small sample size tested.

As described in a previous section of the report, it is believed that satisfactory seals can be selected and applied to flanged fittings if the known design principles are properly applied. For the threaded fittings, however, the problem is much more complex. In the following sections, the problems of adequately sealing separable flanged and threaded connections are discussed, two interesting seal concepts are described, and the development and evaluation of a recommended radial seal for threaded fittings is detailed.

Design Parameters

An understanding of the problems involved in attaining a helium tight seal is dependent on the analysis of certain factors known to affect leakage when the seal is initially established as well as after the seal is established. These factors include (1) the geometry of the leakage path and the nature of the leakage flow, (2) the magnitude of the seating loads needed to produce an initial seal, (3) the plastic flow of the seal material, (4) the interaction of sealing members, and (5) the effects of temperature. Also in this section, brief discussions are given of the design thinking in relation to pressure-energized seals, and of the effect of seal configuration on preloading.

Leakage Analysis

The flow of a viscous fluid through the seal interface can be analyzed on the basis of laminar flow if the mean free path of the fluid's molecules is less than the height of the smallest passage along the leak path. If the mean free path is the same order of magnitude as the passage height, molecular flow results, and a correction for slip flow along the wall must be applied to the laminar-flow analysis. A more detailed analysis is presented in Appendix VII. In general, the flow may be considered laminar if

$$\frac{\lambda}{h} < 1.0 \quad , \tag{27}$$

*References are listed on page 164.

127

where

$\dfrac{\lambda}{h}$ = Knudsen number

λ = mean free path of molecule

h = passage height.

If the Knudsen number approaches 1.0 it is still possible to analyze the flow on the basis of laminar flow by use of a correction factor which is a function of the Knudsen number.
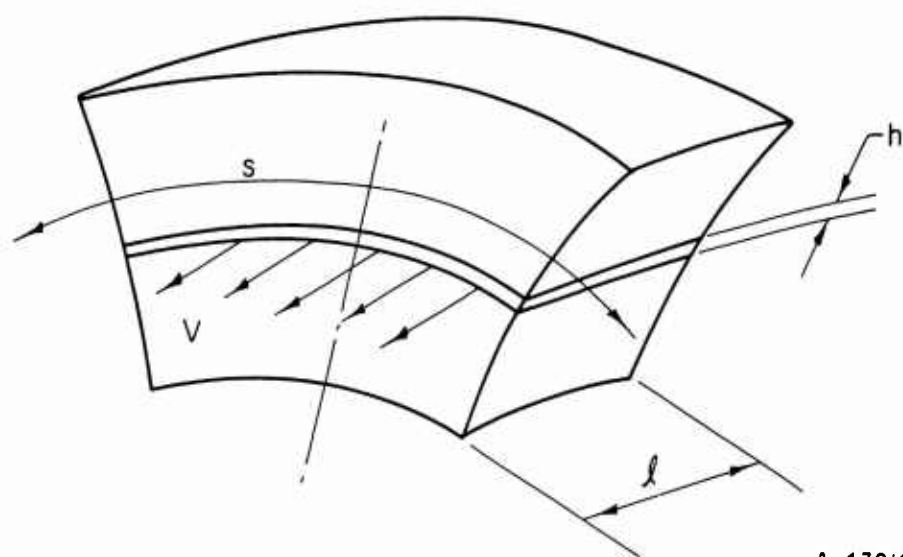
A-43919

FIGURE 57. MODEL OF TYPICAL LEAKAGE PATH

The narrow slot in Figure 57 represents a typical flow passage. Flow takes place at velocity V in the direction of the length, ℓ. The width, s, corresponds to the periphery of a circular seal and h is the passage height. For the case where flow is laminar, the mass-flow equation in terms of the discharge pressure is

$$M_L = \frac{sh^3 \left[\left(\dfrac{P_1}{P_2} \right)^2 - 1 \right] P_2 \rho_2}{24\,\eta\,\ell} \quad , \tag{28}$$

where

M_L = mass rate of flow

P_1 = inlet pressure

P_2 = discharge pressure

ρ_2 = discharge-gas density

η = viscosity.

128

For molecular flow, the mass-flow equation is

$$M_m = \frac{16sh^2(P_1 - P_2)P_{avg}\lambda}{9\pi\eta RT} \quad , \tag{29}$$

or more simply,

$$M_m = 6.8 \frac{\lambda}{h} M_L \quad . \tag{30}$$

When the flow is neither laminar nor molecular, i.e., for Knudsen's number close to 1.0, the flow equation of state is defined as

$$M_T = M_L + EM_m \quad , \tag{31}$$

where E is a constant found experimentally to be approximately 0.9 for single gases and 0.66 for gaseous mixtures[3]. The total flow, by substitution of Equation (30) and the value of 0.9 for E, is

$$M_T = M_L (1 + 6.1 \frac{\lambda}{h}) \quad . \tag{32}$$

This expression holds when the mean free path is evaluated at the average pressure in the passage.

The above expressions indicate the important effect the length and height of the leakage path have on flow rate. For both the laminar and molecular flow conditions, the rate of flow is inversely proportional to passage length. Therefore, one conclusion is that the seal passage should be of considerable length. However, increasing the length of the seal passage is a severe handicap from the viewpoint of seating loads and minimum assembly torque, especially for annular face seals.

The effect of the second parameter, height, makes it obvious that the degree of surface conformity is extremely critical. In the case of laminar flow, mass rate of flow is dependent on the cube of the passage height, whereas in molecular flow it is dependent on the square of the passage height.

Because of the random variations in surface profile, the best measure of required average passage height for seals capable of sealing gases would be in microinches or angstroms, where one angstrom equals 3.937×10^{-3} μin. Extrapolation of leakage-rate charts[4] indicates that a passage height ranging between 3 and 25 A is required to seal helium gas at 2,000 psi, with a leakage rate no greater than 7.7×10^{-7} atm-cc/sec.

Seating Loads

A basic problem in designing a metal-to-metal fluid seal is the determination of the "seating load", i.e., the load required to produce intimate contact between the sealing surfaces initially. The problem is essentially the same whether the seal is pressure energized or not and is independent of operating pressures or external loads.

Below are some of the factors that must be considered in determining seating loads:

(1) Seal Design. The seal width largely determines the magnitude of the seating load, since seating load is a function of sealing area.

(2) Metal Properties. The hardness, compressive yield strength, and strain-hardening characteristics of the seal material will determine the unit stress necessary to effect a seal.

(3) Surface Properties. The surface finish determines the total amount of yielding necessary to close all leak passages. Gross distortion such as waviness and warping is ordinarily a minor problem but can become serious when processes which cause distortion, such as welding, brazing, and swaging, are used to effect the tube-to-fitting connection.

(4) Contained Fluid. The viscosity, density, surface tension, and state of the contained fluid determine the maximum size of leak path which can be tolerated.

(5) Pressure. The pressure, which affects the rate of flow through a passage, also determines the maximum size of leak path acceptable.

(6) Allowable Leakage Rate. Obviously, as the allowable leakage rate is lowered, higher seating loads may be required to reduce the size of the leak paths.

A widely used set of gasket seating-stress constants are those given in the ASME Code for Unfired Pressure Vessels.

Material	Seating Stress[a], psi
Soft aluminum	4,400
Soft copper or brass	6,500
Iron or soft steel	9,000
Monel or 4 to 6 per cent chromium	10,900
Stainless steels	13,000

(a) Gaskets not over 1/2 in. wide.

These gasket constants are based on experience and rather limited test data and are justified[5] principally on the observation that flanged joints when designed on the basis of these constants almost always work satisfactorily.

In addition, it should be noted that the gasket stresses are interrelated with a comparatively low bolt design stress so that, in actual installations, considerably higher stresses can be and probably generally are applied.
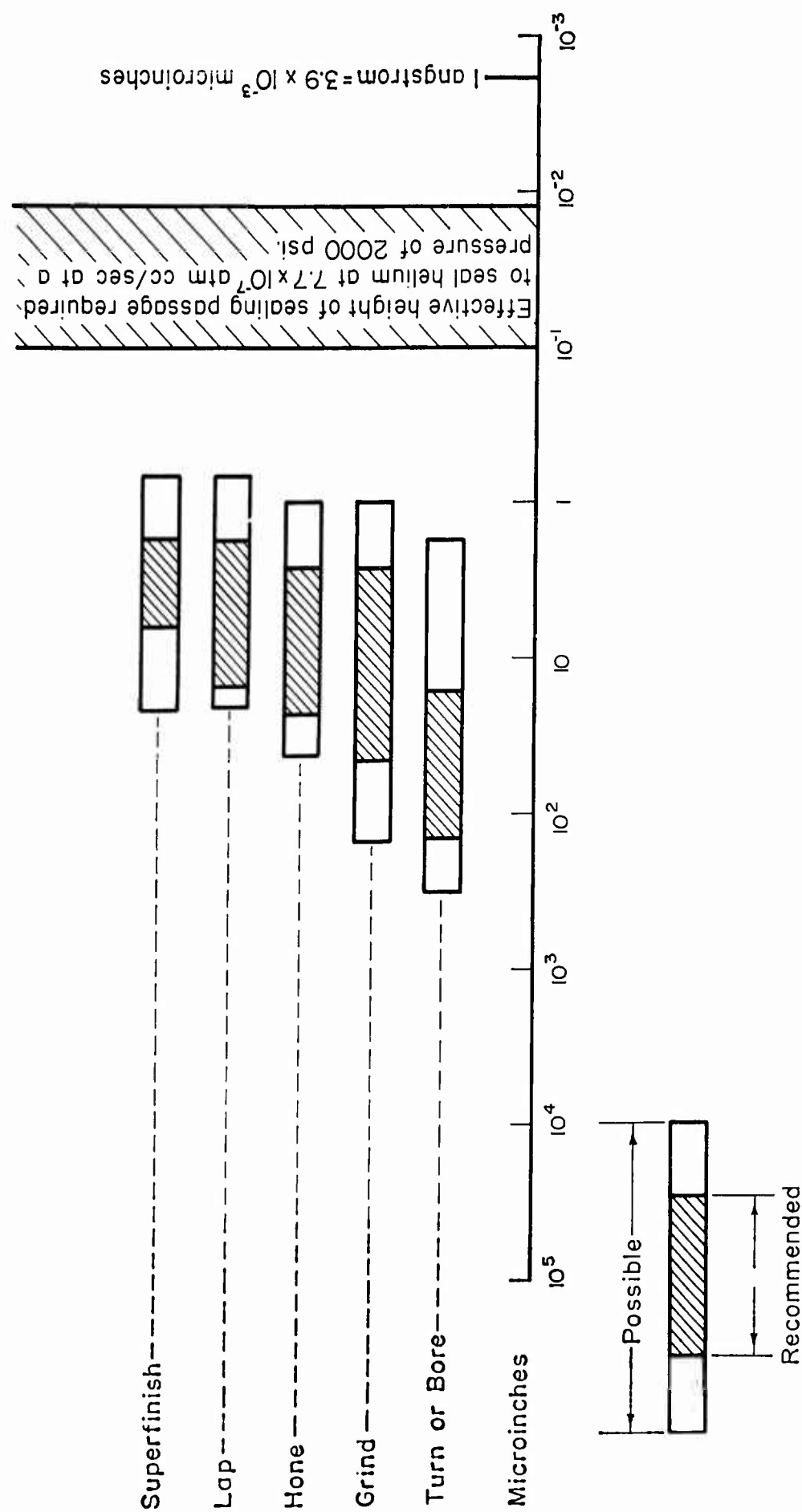
FIGURE 58. TYPICAL SURFACE ROUGHNESS FROM COMMON PROCESSING TECHNIQUES IN COMPARISON TO REQUIRED HEIGHT OF SEALING PASSAGE

131

The previous discussion of seating loads was based on gross effects and on data gathered from experience. Another approach to the problem is a consideration of microscopic effects at the seal surface. Figure 58 shows the average surface finishes achievable by different machining processes. It also includes the range of sealing passage heights considered necessary to achieve a helium seal. It is apparent that the required leak-path height is at least one order of magnitude smaller than that achievable with two superfinished surfaces properly mated.

This chart shows dramatically that one of the materials involved in the seal must yield plastically to achieve a surface contact which will limit the leakage of helium to the order of 1×10^{-7} atm-cc/sec.

The work at Armour and General Electric on the characteristics of such seals has given good data on the forces needed for common seal materials. The work at the two facilities shows that contact stresses ranging from 3 to 5 times the apparent yield strength of the softer material are needed.

Because metallic seals are needed for most of the required applications and because such seals cannot satisfactorily be made to yield more than a few times to the extent required, it has been concluded that a separable connection must employ a gasket. For adequate reliability, this gasket must be replaced at each disassembly and reassembly of the connection.

Although this conclusion is far-reaching in its effect on determining candidate design configurations, the methods of achieving and maintaining adequate seal loading remain as formidable barriers to a successful connection.

Temperature Effects

Two temperature effects of particular importance are the steady-state effect at the temperature extremes and the transient effect during temperature changes. Dimensional changes due to temperature occur axially, radially, or both, depending on the configuration of the seal. Typical configurations are shown in Figure 59. Seals may contain variations or even combinations of these basic seal configurations.

a. Axial Seal   b. Radial Seal
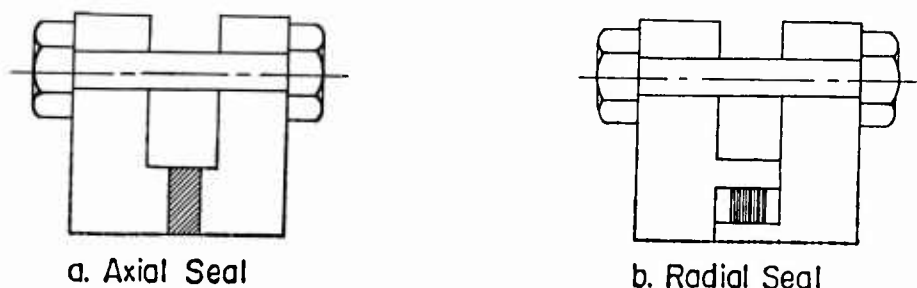
A-43920

FIGURE 59. AXIAL AND RADIAL SEALING CAVITIES

At a temperature extreme, if the seal and the flanges are made of dissimilar materials, the sealing pressure may increase or decrease due to relative expansion or contraction of the seal and the structural components of the fitting. The actual changes

depend on the location of the parts and their thermal coefficients of expansion. At elevated temperatures the effects of creep must be considered. The magnitude of the initial axial preload must be sufficient to compensate for these effects. Axial preload is a minor consideration in a radial seal, but the seal must be elastically deflected initially and must be able to follow up when dimensional changes occur.

Large thermal gradients, caused by transient thermal states, aggravate the problems described above. In addition, thermal gradients are more likely to cause a momentary shifting of the sealing surfaces, and this may destroy the surface mating which was achieved when the fitting was originally assembled and one material yielded against the other.

Pressure Energization

The concept of a pressure-energized metal seal has become increasingly popular. Many new seals and fittings have been designed which incorporate this principle. Basically, it is postulated that by elastically deflecting "cantilevered" legs a sufficient amount when the fitting is initially assembled, the seal can breathe with the system as the sealing load relaxes. Relaxation could be caused by pressure end loads, vibration or reverse bending, creep, thermal gradients, or torque relaxation. Further, as the system pressure increases, more force is applied to the deflectable leg by the pressurized fluid, thereby causing additional sealing force.

The major problems that would be encountered if a pressure-energized seal were used are related to the temperature range required, the fluids handled, and the low leakage requirement. Until more suitable nonmetallic materials are developed, it is believed that such a seal must be metal. Further, because of temperature problems and fluid-compatibility problems, it appears that the softer metals such as aluminum, copper, and gold may not be suitable. Thus, any candidate seal material, such as nickel, has a fairly high yield stress. As explained previously, the contact stress needed to seal helium is estimated to be up to five times the apparent yield stress of the softer material.

The strength necessary in a cantilever leg to seal helium can be provided with present materials only by designing a stiff leg with low deflection. In a commercially available seal using several such legs to increase the deflection, the total deflection is of the order of 0.005 in. Manufacturing tolerances and thermal gradients make this low movement difficult to design for. The use of this and similar seals has resulted in difficulties for temperature ranges similar to Class I. For temperatures ranging from -425 to 1500 F it is believed that it will be exceedingly difficult, if not impossible, to apply a cantilever seal satisfactorily with acceptable manufacturing and assembly tolerances.

A further complication of the cantilever seal is its normal tendency to move slightly. For many applications this movement is not harmful. For sealing helium, a very slight movement of one surface relative to the other probably will destroy the intimate surface conformity obtained by yielding one material against the other. It is believed that a satisfactory seal must be designed to be stationary and firmly clamped in place.

Preloading as Affected by Seal Configuration

The importance of fitting preload has been discussed in several previous report sections. Three aspects of preloading are affected by the seal configuration, (1) the magnitude of the preload, (2) the fatigue of the tension members, and (3) the variation in seal load. These aspects are critical to the weight and proper functioning of the fitting.

Preload Magnitude. High seating forces are required for metal seals to seal helium. As discussed on p 35, the seal seating force of the smaller fittings can establish the force required of the nut, and hence the size and weight of the nut. If a seal is selected whose sealing surface is at an angle with the axis of the fitting, it is possible to magnify the axial force for sealing. Thus by selecting a radial (see Figure 59) or partially radial seal for some threaded-fitting sizes, it is possible to lower the preload to that required by the structural load. This results in a more lightweight fitting than would be possible with an axial seal of the same material and seal width.

Tension Member Fatigue. One of the critical aspects of proper preloading is the reduction in fatigue of the tension members. By making the spring rate of the compression members at least three times greater (stiffer) than that of the tension members, the magnitude of the change in load in the tension members is greatly reduced for the application of a given structural load. This is illustrated in Figure 60.

To accommodate material and manufacturing variations, most seal materials are relatively soft. This is true even for metallic seals. When the seal is in series with the compression members, as shown in Figure 60, the tendency is to decrease the spring rate of the compression members and to increase the change in tension load and hence the fatigue of the tension member. This must be compensated for by increasing the strength and hence the weight of the tension member. If a seal is selected which is in parallel with the compression members, as shown in Figure 60, the spring rate of the compression members is the same as that of the stiff flange members, unless the flanges separate. Thus a parallel seal is preferred over a series seal. A 100 per cent radial seal is a special case in which the seal load is completely independent of the compression load on the fitting structure.

Seal Load Variation. A comparison of the series and the parallel seal configurations from the standpoint of seal load variation also shows that the parallel seal is to be preferred. Unless the fitting compression members separate, the seal load of the parallel seal and the radial seal does not fluctuate with changes in structural load. The contact stress of the series seal, however, fluctuates in response to every change in load. While this fact does not automatically mean the series seal will leak, the minute surface contact needed to seal helium emphasizes the potential leakage problem of a seal in series with the compression members.

Conclusions

Of all the parameters discussed, the one which influences and predetermines the seal and fitting design most is that concerning plastic yielding at the sealing surface. Once it is concluded that plastic yielding is essential for sealing helium, the choices
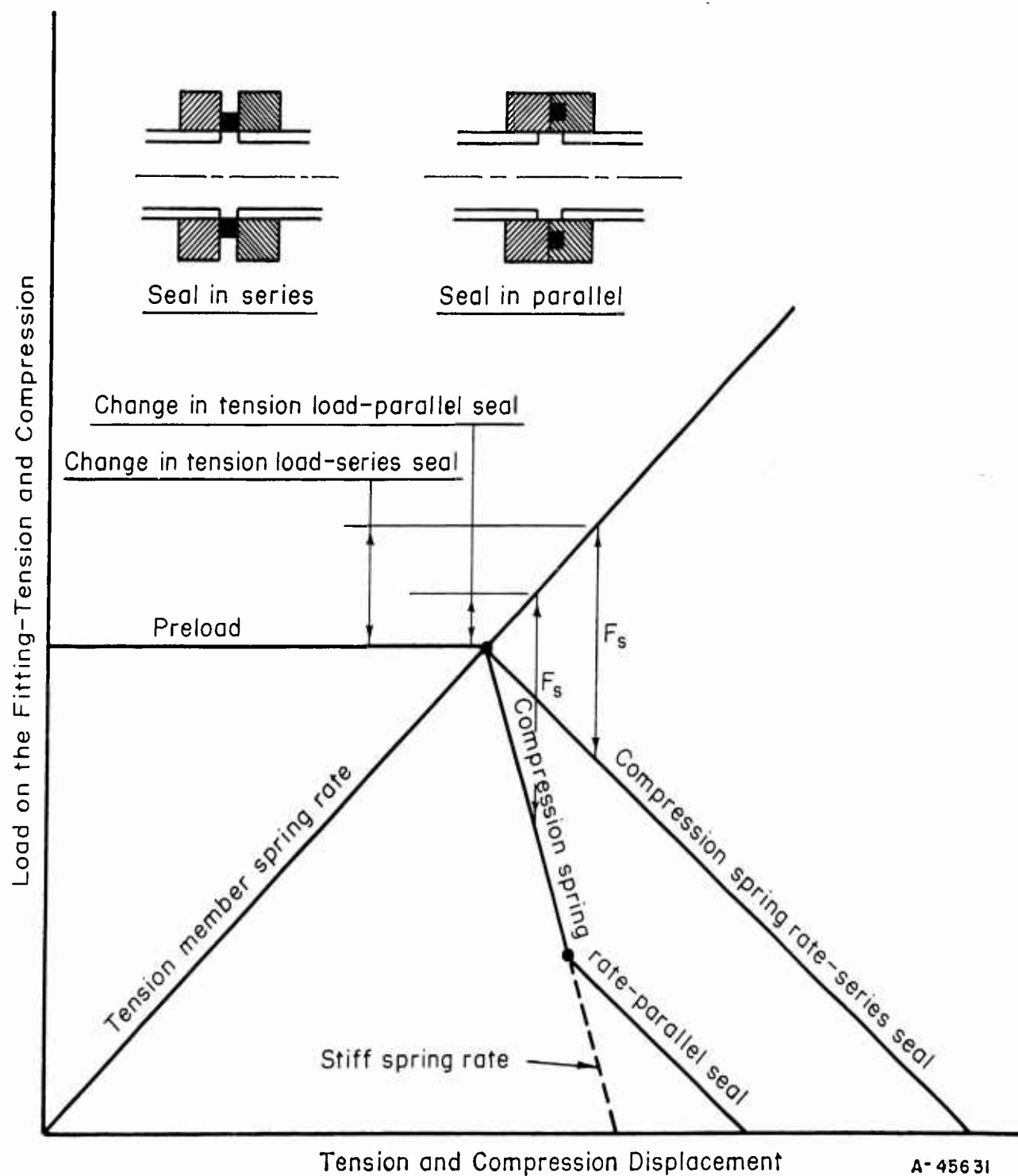
FIGURE 60. EFFECT OF SEAL CONFIGURATION ON CHANGE IN LOAD
OF THE TENSION MEMBER

135

available as to the size of the sealing area, the amount of preload, and the choice of materials become limited. The conclusions drawn can be summarized as follows:

(1) The effective height of the sealing passage must be of the order of 3 to 25 A. This surface contact can be achieved only by plastic yielding of one or both surfaces. To effectively reduce the seating load, a relatively low-yield-strength metal such as nickel might be used as a surface coating on the seal.

(2) An initial seating stress possibly as high as five times the apparent yield stress of the gasket material is necessary to achieve the desired degree of yielding.

(3) A pressure-energized seal may not be necessary, or even desirable.

(4) The axial force of a mechanical seal should be magnified to produce the sealing force.

(5) The seal load should either be independent of or in parallel with the fitting compression load.

Pressurized Metallic O-Rings

Present Theory

The sealing force generated between the walls of a standard metallic O-ring and the walls of the flange is a function of the spring constant of the toroidal configuration of the O-ring and the properties of the material of the ring. The presently accepted theory defining this operation is that upon flange closure, the contacting surface of the O-ring is plastically deformed into the seal cavity. The combination of the spring-back resiliency of the ring and the action of the fluid pressure on the exposed surface of the ring (see Figure 61a) tend to further force this deformed surface against the flange walls. This produces a significant contact stress between these two surfaces which, being greater than the fluid pressure, acts as an efficient seal.

The spring-back resilience of this configuration can be increased by using the pressurized metallic O-ring (Figure 61b) or the self-energized metallic O-ring (Figure 61c). In both, pressure inside the O-ring increases the ring's spring constant and its spring-back resiliency after plastic deformation has taken place. The self-energized O-ring has the further feature of allowing an increase in pressure inside the ring as the pressure of the fluid to be sealed increases.

a. Standard Metallic O-Ring b. Pressurized Metallic O-Ring c. Self-Energized Metallic
O-Ring
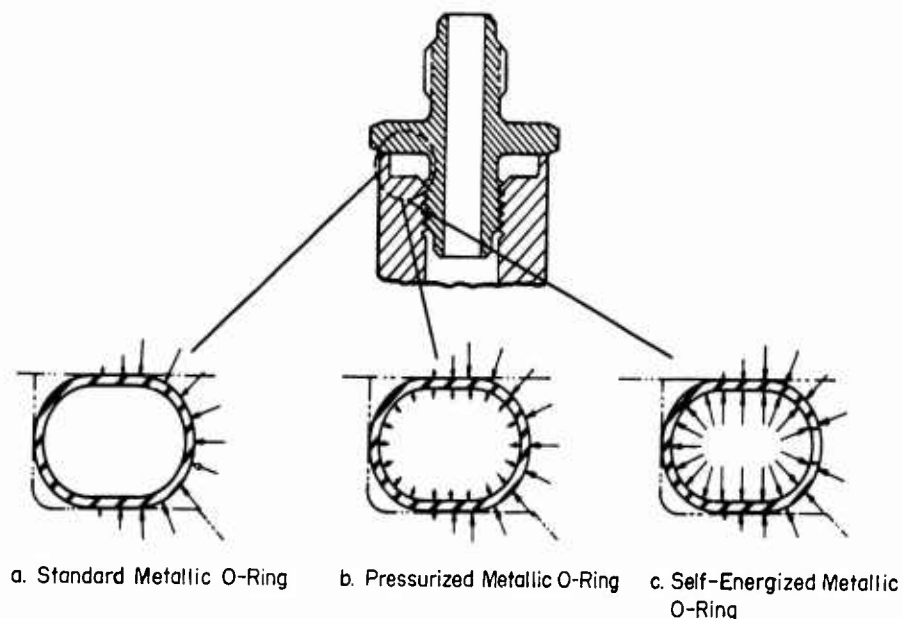
FIGURE 61. PRESSURE FORCES ACTING ON VARIOUS
TYPES OF METALLIC O-RINGS

These sealing methods have been shown to be successful for many applications. However, where high temperatures or severe induced vibrations or bending loads are encountered, leakage will almost invariably occur. It would appear that in the case of elevated-temperature operation the change in material properties of the O-ring material becomes a definite parameter. As the temperature is raised, both the yield stress and the elastic modulus of the material are lowered. These changes have the effect of decreasing the spring constant and the spring-back resiliency of the ring. Such decreases will result in a reduction in the contact stresses found at the interface of the sealing surface and so reduce the sealing capabilities.

New Design Principle

With this in mind, a seal design is postulated which could operate successfully in the elevated-temperature range. This concept, which might be called a plastic-state O-ring (illustrated in Figure 62), utilizes to advantage the change in material properties of the ring at elevated temperature.

137

A-42465
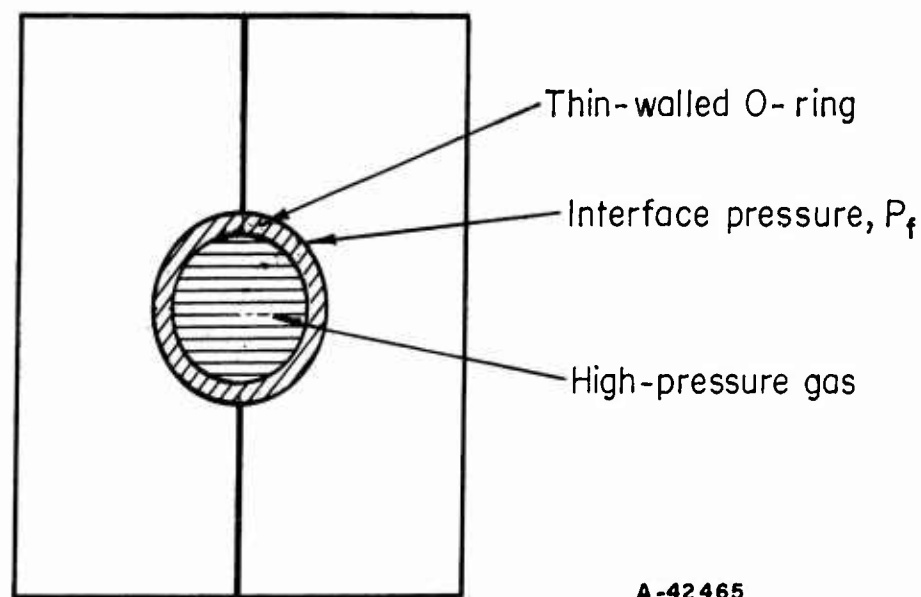
FIGURE 62. INTERNALLY PRESSURIZED O-RING

When assembled, the O-ring is fitted into a cavity which supports the torus in all directions. In order to compensate for tolerances it may be advisable to make the cavity and the torus dissimilar in cross section. When the flanges are assembled and the tightening preload is applied, the torus will be deformed to conform to the cavity geometry, and metal-to-metal contact will be obtained. Included inside the O-ring torus is a gas-emitting crystal or a low-energy pyrotechnic. The gas-producing reaction would be initiated after the fitting is completely assembled and torqued.

Since the gas in the ring is completely sealed in a fixed volume, the change in pressure of this gas would be a simple function of the operating temperature of the fitting (see Equation 34); a rise in temperature would induce a rise in pressure.

The material of the O-ring should be so chosen that when the operating temperature of the fitting is increased, its elastic-stress capability is drastically decreased. If the O-ring material and the type and volume of gas in the O-ring are carefully selected, a point somewhere below the normal operating temperature of the fitting will be reached where the O-ring is in a fully plastic state. This can be clearly seen if we consider the O-ring — flange configuration as a cylindrical pressure vessel with an infinite outside diameter and an inside diameter equal to that of the O-ring. In this consideration, of course, the curvature of the ring as well as the large but finite thickness of the flange wall as compared with the O-ring inside diameter are neglected. However, for a close approximation this assumption serves adequately. The point at which the inner fibers of the wall become plastic will be reached when the internal pressure equals $0.577\,\sigma_y$ (yield stress at any given temperature of the material as determined from a simple uniaxial tensile test). This criterion is derived from the maximum-distortion-energy-criterion of failure for material, sometimes called the Hencky-von Mises criterion.

Noting that the wall of the O-ring is very thin, we can further assume that the tube will be fully plastic when the pressure is slightly greater than $0.577\,\sigma_y$.

138

The action is qualitatively illustrated in **Figure 63.**
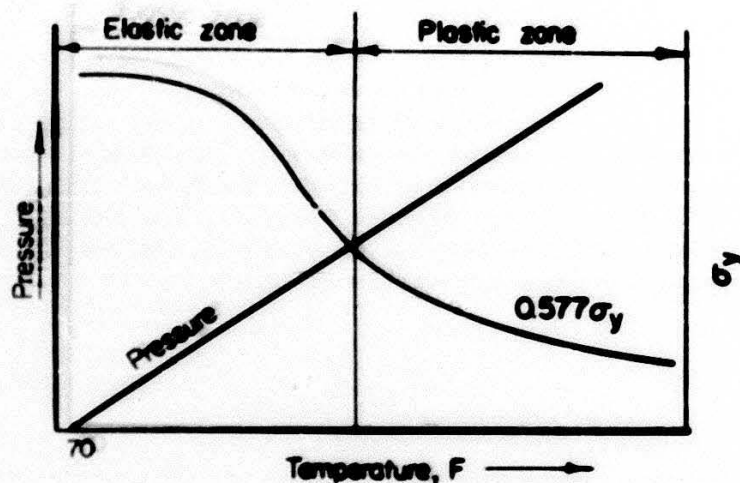
FIGURE 63. PRESSURE-TEMPERATURE-YIELD STRESS RELATIONSHIP FOR O-RING SEAL

The internal pressure, P, is defined as

$$P = \rho \, ZRT ,$$

(33)

where

ρ = gas density

Z = compressibility factor

R = universal gas constant

T = absolute temperature.

Assuming that the internal volume is essentially unchanged and discounting the compressibility factor,

$$\frac{P_1}{P_2} = C \frac{T_1}{T_2} ,$$

(34)

where C includes the ρ, Z, and R terms. Therefore the internal pressure increases linearly with the change in temperature ratio.

In this situation the high internal pressure is contained in a fully plastic O-ring which is in turn fully contained by the walls of the seal cavity of the flange. As long as there is no separation of the flange faces the tube cannot blow out, since there is no place for the tube material to go. In fact, as long as the flange faces stay in contact the

internal pressure in the ring could still be raised significantly (as would occur with a further increase in temperature).

The advantages of this concept are: (1), that in the fully plastic state the O-ring material, under the action of the high internal pressure, will flow into the small surface discontinuities of the seal-cavity walls, thereby forming a seal that should be effective in stopping even molecular leakages, and (2) with the advent of the relaxation of the flange prestress, which is encountered at elevated temperatures, the high contact stress required to maintain this close interface fit is achieved by the action of the internal pressure. A serious disadvantage would be encountered if this type of seal were to be exposed to conditions where the temperature variation would be cyclic, resulting in a condition where the O-ring would vary between the plastic and the elastic state. Such a condition could adversely affect the physical properties of the ring material, resulting in a low-cycle fatigue phenomenom and early ring failure.

Conclusions

As presently conceived, the O-ring would not become plastic until some elevated temperature was reached. The primary reason for this requirement is to prevent rupture at room temperature and to permit safe handling at assembly and disassembly of the pressurized O-ring. Therefore, the seal could be primarily of use for high temperatures and might be considered only in the role of a secondary seal. In the plastic zone there would be no significant time lag, as the seal breathes with the strain fluctuations and essentially a steady state condition would exist. Probably the most advantageous application would be in sealing hot gases for Class V fittings where temperatures range from 1000 to 3000 F. Development of an O-ring seal that could operate in this temperature range will require utilization of metals with very high melting points. Tantalum seems to be a possible choice. In the lower temperature range, 600 to 1500 F, nickel or copper could be used.

Aside from the temperature ranges, one other limitation must be emphasized. As previously indicated, when the O-ring is in the plastic zone the flange separation must be kept below a few thousandths of an inch to prevent rupture or blowout.

High-Energy-Rate Formed Seal

Considerable experimental evidence has been developed concerning the conformity of one metallic surface with another when caused by high-energy rate forming. As discussed in the section "Tube-to-Fitting Design", explosive energy has been used to achieve a good mechanical bond, equivalent to a weld, between several kinds of metals either flat or tubular in configuration. On the basis of an analysis of this work, it was believed that the surface conformity needed to seal helium could be easily provided by high-energy-rate forming.

Two basic configurations were envisoned as a means of applying explosive energy to the formation of a seal in a fitting. The first was an internal formed seal in which the expanding explosive force would be used to seal a sleeve against the inside of the fitting parts. This configuration would make the best use of the available energy, but a problem existed in the contamination of the fluid system by the explosive. The second configuratioi

140

was an externally formed seal which would collapse radially or seal against the flange faces. Because it was difficult to postulate the energy needed to achieve adequate conformity for the possible configurations, preliminary laboratory experiments were made to obtain a general idea of the effect of different amounts of explosive on basic seal shapes.

Experiments Performed

Seal formation by means of an internal explosive charge was investigated with the configuration shown in Figure 64. The ferrules, representing the stub-end portion of the fitting attached to the tubing, were separated by a spacer ring which would be used to facilitate disassembly. The seal ring was expanded by means of an explosive charge to form a seal between the ferrules. The mandrel diameter upon which the explosive charge was mounted was changed in successive experiments to provide variations in the standoff distance.

Use of an external explosive for formation of the seal was investigated by means of the configuration shown in Figure 65. The explosive was contained in a groove machined on the outside diameter of the seal ring. The walls between the flanges and explosive were approximately 0.010 in. thick, and it was hoped that these walls would be sealed against the flanges.

Description of Results

For the internal explosive charge, five experiments were made with various size mandrels. The mandrel size determined both the total charge and the standoff distance. In all cases the seal ring was displaced slightly in the direction of the detonation progression, that is, from right to left as shown in Figure 64. Figure 66 is a photomicrograph of Area B in Figure 64, polished and etched. Excellent conformity was achieved between the seal ring and the spacer ring and ferrule. Figure 67 is a photomicrograph of Area C polished but not etched.

Eight experiments were made with the external explosive-charge configuration. The original attempt was to form a seal at, Point A in Figure 68. However the best bond occurred at Point B. Evaluation will show that this is a reasonable result, since Poisson's effect is most pronounced at Point B when the seal ring is under a high external load, as shown in Figure 69. The thin seal flanges shrouding the explosive were too flexible and probably sprang back after the explosive pressure was dissipated.

However, when the force, w, is high, as in the case of an explosive charge, the actual strain, ϵ_2, is much greater than the elastic strain and a considerable seating load is applied from the seal to the flange face.

Possible Externally, Explosively Formed Seal

The design concept shown in Figure 70, although preliminary in nature, illustrates the basic premises on which an external high-energy seal might be based.

Ferrules

A

Explosive

Mandrel

Detonating cap

Seal ring

B C

Spacer ring
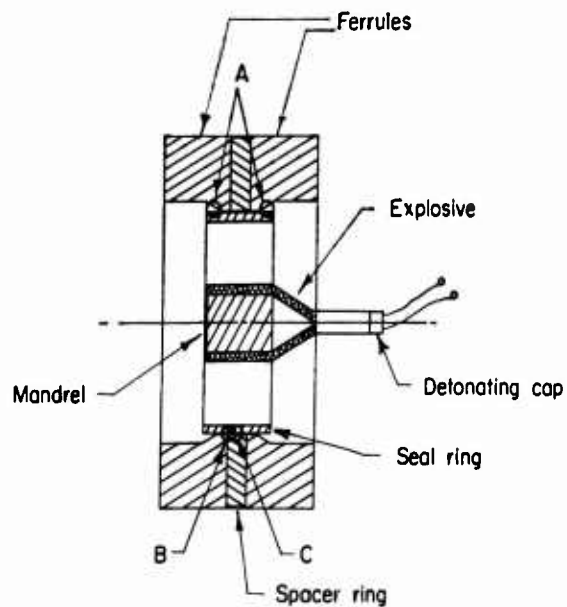
FIGURE 64. CONFIGURATION FOR INTERNAL-CHARGE SEAL EXPERIMENT

Detonating cap

Primacord leader

Explosive

Seal ring

Flanges
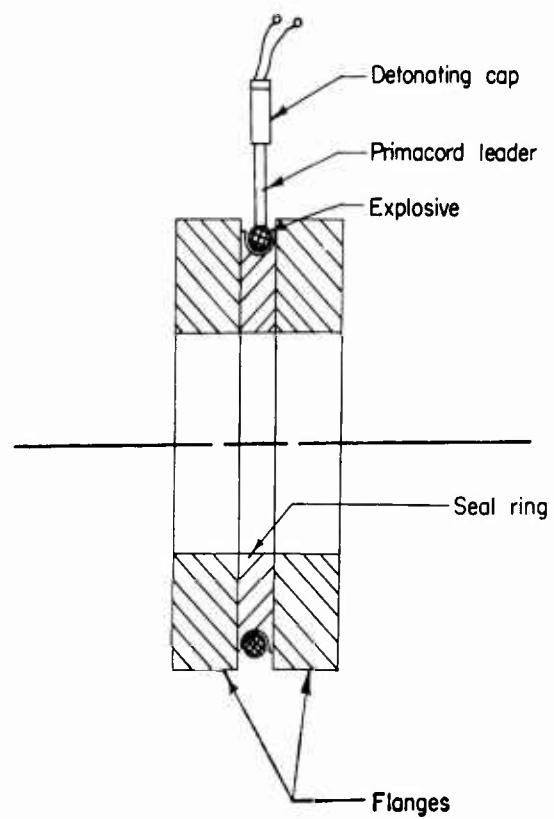
B-43923

FIGURE 65. CONFIGURATION FOR EXTERNAL-CHARGE SEAL EXPERIMENT

Seal ring

Spacer ring

Ferrule

100X   Etched   RM22186
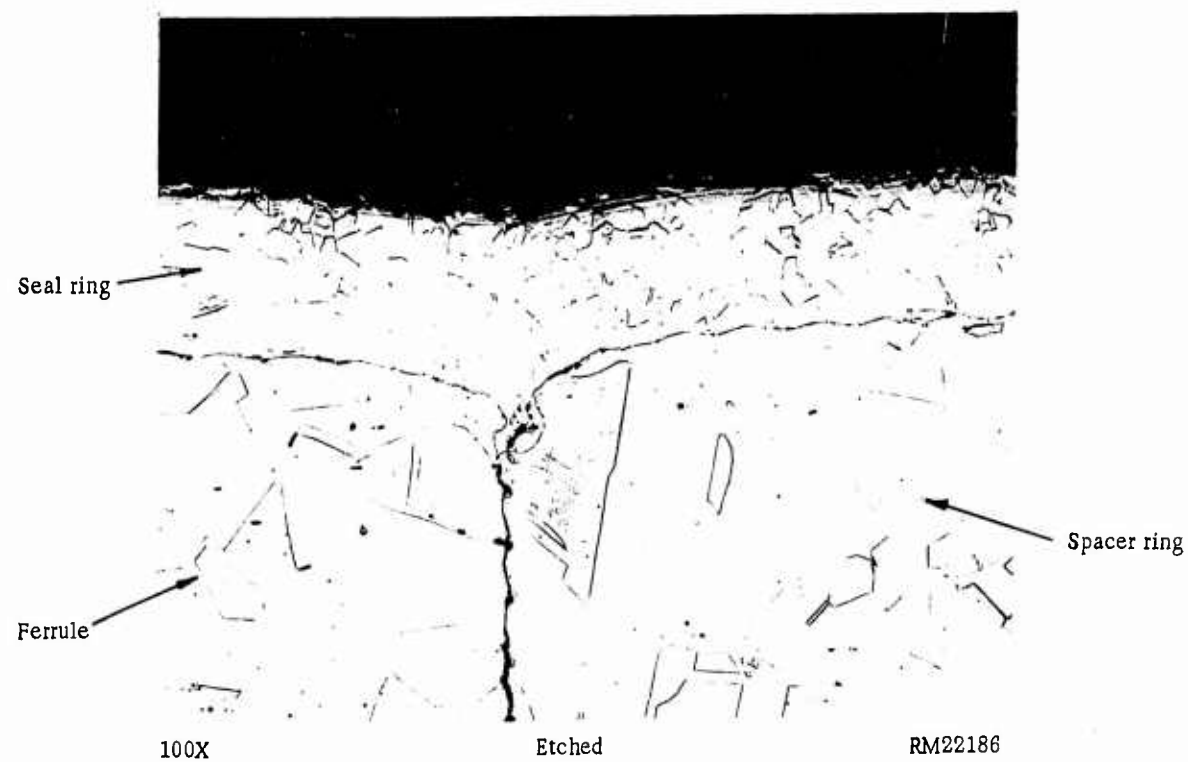
FIGURE 66. AREA B OF FIGURE 64

Interface →

Seal ring

Interface

Spacer ring

1000 X   Unetched   RM22256
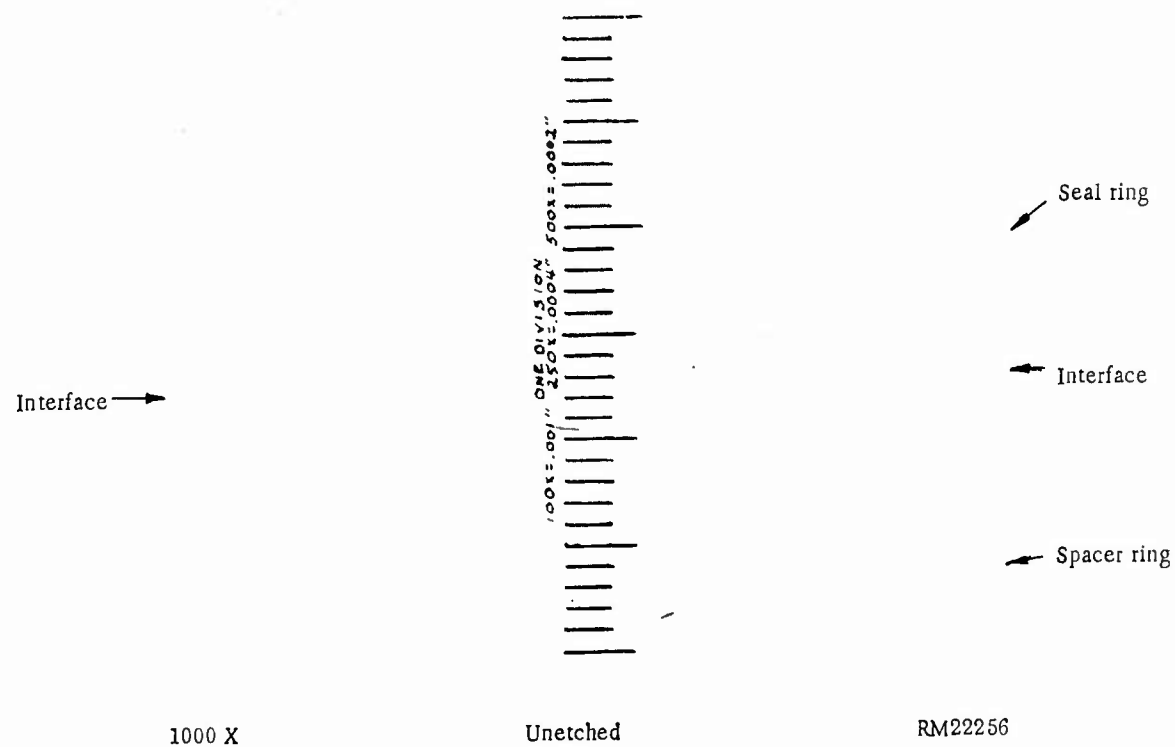
FIGURE 67. AREA C OF FIGURE 64

143
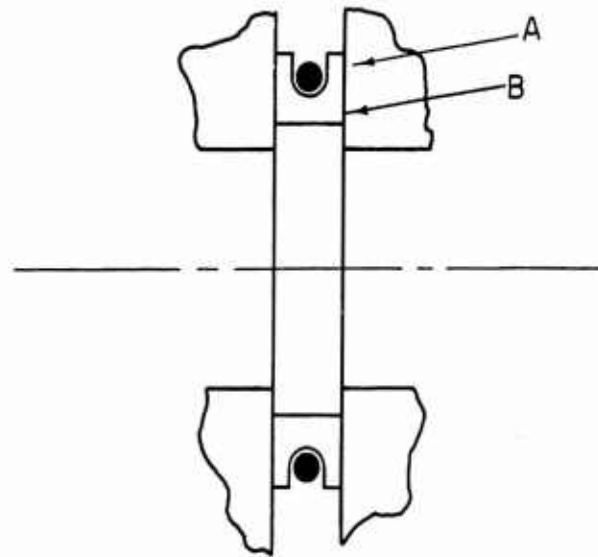
FIGURE 68. EXTERNAL-EXPLOSIVE SEAL
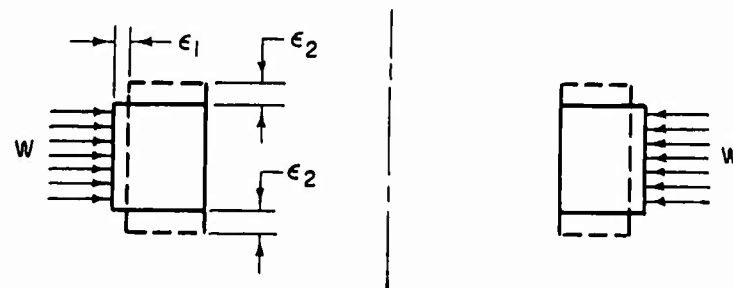
FIGURE 69. POISSON'S EFFECT ON SEAL RING

144
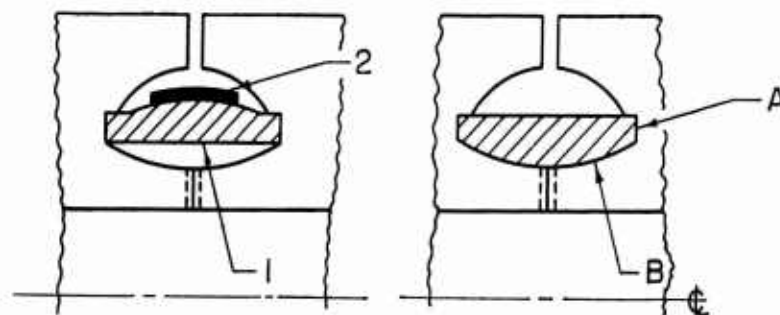
A-43926

FIGURE 70.   EXTERNAL EXPLOSIVE SEAL

A major consideration is the blowout effect of the internal pressure. The seal ring must be thick enough to withstand the developed hoop stress. Also, the initial strain on the seal interface must be sufficiently greater than the pressure-induced hoop expansion to maintain sufficient surface contact. The primary seal is developed at Point A because of the combined effects of initial preload, Poisson's ratio, and over-center tin canning. A secondary seal can be developed along Surface B. This secondary seal is highly desirable to reduce the force of the fluid acting on the seal and tending to blow it out. The overhanging lips at A also add structural support to the seal ring to prevent blowout.

Initially the seal ring is clamped between the flanges, which bottom out as in Figure 70. The ring can be made to bow under this clamping force to compensate for manufacturing tolerances and discrepancies. In the example illustrated a contact explosive charge, Point 2, is used.

The assembly preload is predicated on the eventual structural load requirements, since the effective seating load will result from the high-energy discharge. The seal ring is deformed by the high-energy discharge and is pushed over center. The insertion of a transfer buffer at Point 2 may be necesary. A support die might have to be assembled onto the fitting to prevent stretch and expansion of critical sections and subsequent distortions and strain relaxations.

Other energy sources such as capacitor discharge or magnetic pulse might be used as a means of applying more than one sealing impulse. With this arrangement, a leaking seal could be tightened without disassembling the fitting.

Conclusions

It would be possible to use an internal explosive charge to form a seal if a method could be found to initiate the detonation without the need for lead wires. An exceptionally intimate bond is possible along the seal-retainer interface when a reasonable amount of explosive is used. Moreover, the problem of personnel safety and possible damage to surrounding equipment can probably be overcome. However, a major problem for which no immediate solution appears likely is the degree of contamination of the internal surfaces caused by the explosive materials.

Although the use of external explosive charges to form a seal would eliminate the contamination problems and allow easy detonation, further experimentation is necessary on selected configurations before the feasibility can be shown.

145

Unlike the self-energized O-ring or the high-energy-rate-formed seal, which may be termed "exotic", a mechanical toggle seal is conventional in principle. Seals of this general type are commercially available and have attained some measure of success in missile systems; especially in low-pressure gas ducts. Partly on the basis of data resulting from studies by General Electric and by Armour Research Foundation, but largely on the basis of its own analytical and experimental work, Battelle has developed a function analysis for a greatly improved mechanical toggle seal. The Battelle Bobbin seal design for threaded fittings which resulted from this study has successfully functioned under extremely severe environmental conditions, and represents perhaps the most significant step to date in the development of a zero-leakage metallic seal for helium.

Preliminary Mechanical Toggle Seal Study

A mechanical toggle seal can have many forms, and the toggle action can be made to magnify the axial sealing force in various directions. A preliminary analysis indicated that a radial seal would be the preferable type of seal. A Belleville-type disk is an example of a mechanical radial seal. This type of seal is shown in Figure 71.

Seating Action. Figure 71a shows the toggle seal when the seating load is first applied. The position of the seal after assembly is shown in Figure 71b.

a. Before Assembly   b. After Assembly
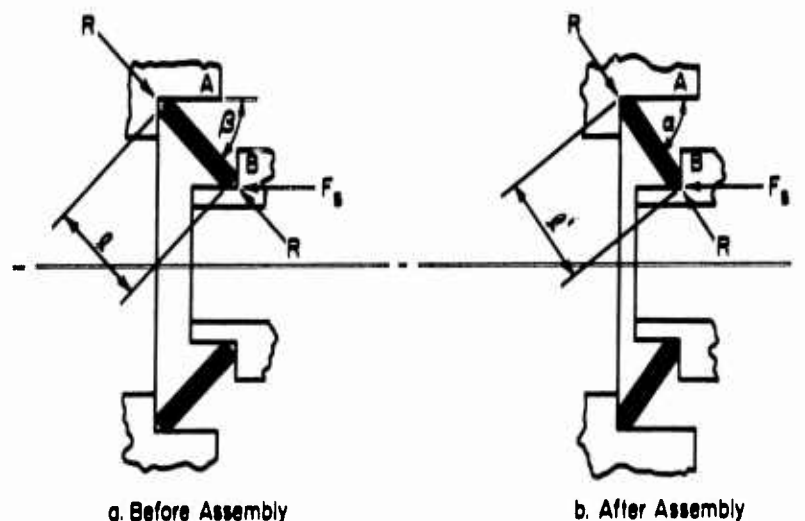
A-43927

FIGURE 71. SEATING ACTION OF MECHANICAL TOGGLE SEAL

As member B travels axially from right to left the resultant seating force, R, rotates through the angle $(\alpha-\beta)$. The axial seating force, F_s, increases as the seal is rotated, first to create elastic strain and then to cause plastic yielding. However, after plastic yielding commences, the force, F_s, is relatively constant. Because the seal is fully restrained at both the inside and outside diameters, there will be plastic yielding along the length, ℓ, if the seal does not buckle or bow.

146

The elastic limit may be reached when the seal has rotated through only a few degrees, depending on the configuration and support of the seal element. Plastic yielding then can occur during the major portion of the travel. This feature is a distinct advantage because dimensional discrepancies can be overcome more readily. When finally assembled, the angle α should be less than 90 degrees or removal of the seal will be difficult. The total angular rotation desired from the point of initial contact depends primarily on the manufacturing tolerances.

One problem encountered with this type of toggle seal is the rotation that occurs at the sealing surfaces. The area of contact shifts as the seal rotates. This means that the seal location is constantly changing as the rotation progresses, and the final contact area is determined only when the seal is seated in its final position. Moreover, the movement between the seal and the retainer is not pure rotation. Smearing of the sealing surfaces may occur because of sliding.

Force Magnification. The greatest advantage of the toggle seal for sealing helium is the effect of force magnification. In Figure 72 the force relationship on the toggle seal is compared to a flat metal washer. In the case of the flat washer, the force, F_2, needed to exceed the elastic limit must be greater than $(\sigma_y \cdot A_2)$. Assuming that the toggle seal is of the same material and that A_1 equals A_2, then R must approximately equal F_2 at all times. However, F_1, the axial force, is only equal to R sin θ.* The axial
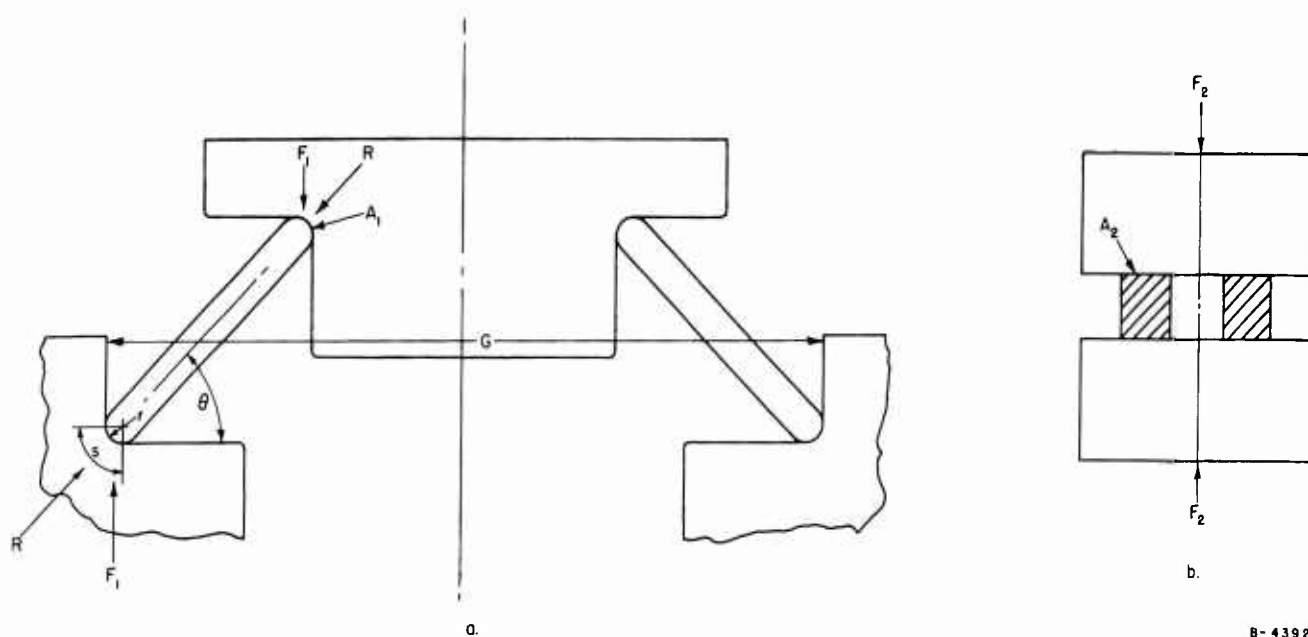
FIGURE 72. FORCE COMPARISON BETWEEN TOGGLE SEAL AND FLAT
METAL WASHER

*It is assumed that the strength of the toggle seal as a ring is negligible.

147

force needed to seat a toggle seal can be one-fifth the force needed with a flat washer and the input torque is correspondingly reduced. In itself, this feature is significant only where preload is determined by seal seating load rather than structural-load requirements. However, even when preload is predicated on structural loads, the additional axial force can be used effectively by increasing the seating area to its maximum limit. This can be beneficial since a longer seating surface will (1) improve the seal, according to leakage path analysis, and (2) minimize the effects of local, minute scratches and nicks on the sealing area.

Axial Backoff. Axial backoff due to torque relaxation, creep, or elastic deformations under load must be considered in determining the initial axial preload. The magnitude of the preload must assure that some residual strain is always present, even under the most severe set of conditions. However, the elastic recovery on the part of the seal must be at least equal to the amount of strain relaxation expected.

The amount of elastic recovery which may be possible with a toggle seal fabricated from a material with a yield stress of 150,000 psi is indicated in the ideal force-deflection curve in Figure 73. The stretch and rotation of the nut (Line adb) and the flange compression (Line cgd) are based on the analysis of a threaded connection with a flat metal gasket. However, if a toggle seal were used, the compression force-deflection plot would follow the discontinuous Line efgd. At Point g the seal would be completely seated, and additional torque would be translated to preload in the retaining members, Line cd. The negative slope of Line ef represents the elastic deflection of the seal alone. At Point f plastic yielding throughout the seal member commences, and the force, W, decreases at a low rate until Point g, at which time the axial load is nearly zero because all the force is transmitted in a radial direction.

The total elastic recovery is 0.0057 in. and is represented by Point h. However, not all of this recovery is available because the seal would be unsupported and would fail because of fluid pressure, vibration, or structural collapse. If an elastic recovery of only 0.002 inch, which is less than half of the total recovery possible, is considered, the equivalent load needed to cause this amount of backoff is 12,500 lb. This is far in excess of any expected operational load. A recovery of 0.002 inch is considered greater than that expected in actual practice.

Conoseal Evaluation. As discussed in the "Design Parameters" section, the theoretical analysis indicated that the seating action of the seal is a critical factor in obtaining a seal for helium. Because the Belleville-type seal appeared to contain possible undesirable seating action features, it was decided that the seating action of the Conoseal[*] should be investigated. The Conoseal is very similar to the Belleville-type radial seal initially analyzed. This evaluation was performed with Conoseals produced for three standard-size fittings, the -2, -8, and -16.

Fittings were assembled at various increments of axial force and then disassembled. The sealing elements were examined and measured. Other fittings were assembled in like manner, but the assembled fittings were encapsulated in epoxy and then sectioned and polished.

---

*Designed and produced by the Marman Division, Aeroquip Corporation.

148
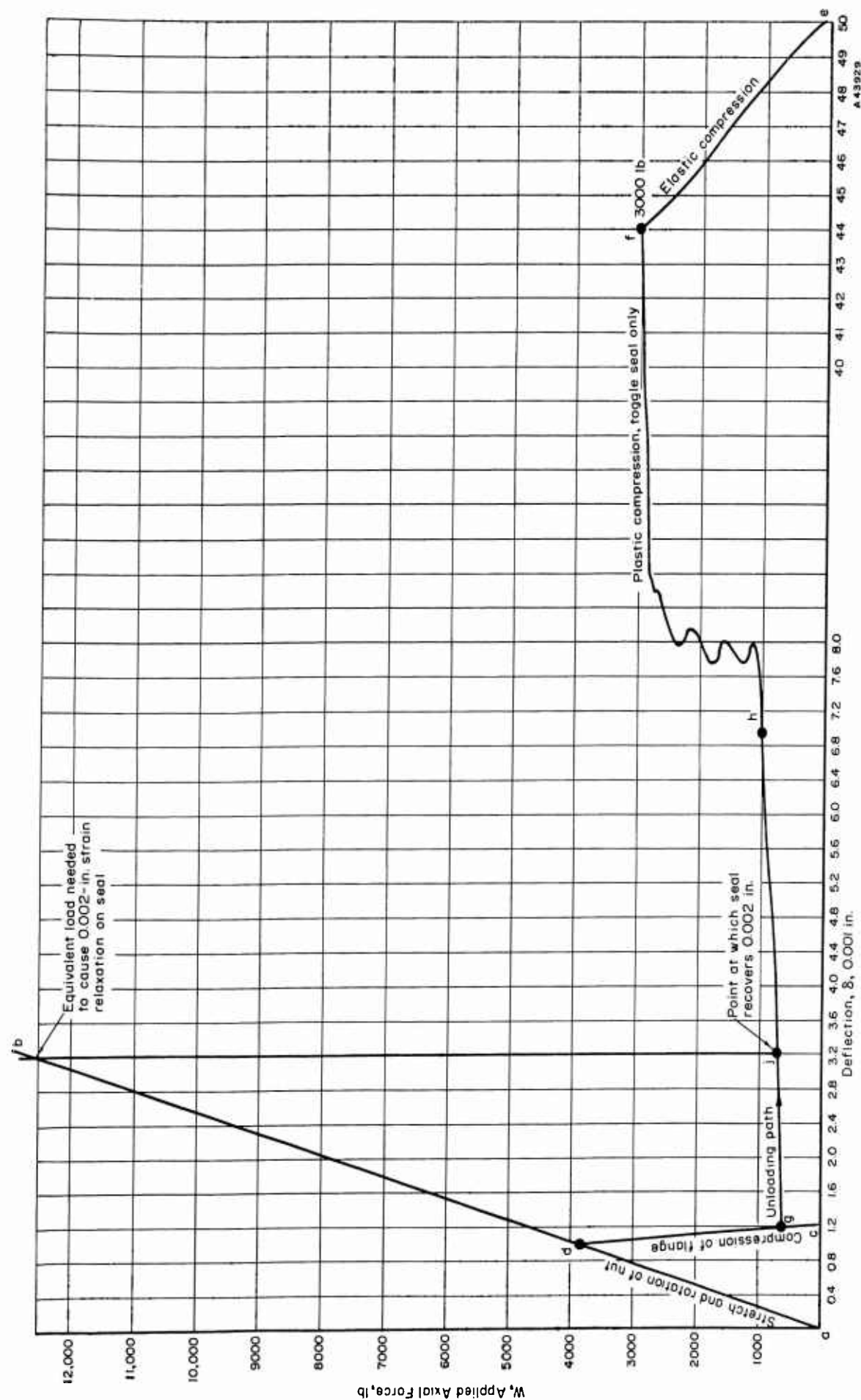
FIGURE 73. FORCE-DEFLECTION CURVE FOR TOGGLE SEAL

149

The force-deflection curves for all three sizes were similar in general form. However, considerable buckling occurred with both the -2 and -16 gasket.* This action was reflected in an irregular rise in force as the seal was seated. Although there were irregular sections in the force-deflection curve for the -8 gasket, the curve was considered to be very close to the force-deflection curve for an ideal seal. Microscopic examination showed that only a negligible amount of buckling or bowing had occurred in the -8 gasket.

The seating action was considered to be in need of considerable improvement. The seal element deflected in different ways for different tolerances and for different fitting sizes. This resulted not only in rotation of the sealing surfaces, but rotation in ways which would be difficult to predict and control. Such action was expected to result in unreliable sealing for helium.

Conclusions. It was concluded that the Belleville type seal more nearly approaches the ideal metallic seal for sealing helium than other types of mechanical seals. However, as a typical Belleville-type seal, the Conoseal did not incorporate certain features which our theoretical analysis indicated were desirable. First, the fitting was not preloaded independently of or in parallel with the seal. Second, the seal was created on two interacting diameters, thus requiring close machining tolerances of four different dimensions. Finally, the seating action varied greatly with changes in machining tolerances and with fitting size.

Based on these conclusions, it was decided that future design work should be devoted to the development of an improved type of mechanical toggle seal.

Preliminary Development of the Bobbin Seal

It is often difficult, if not impossible, to describe the conception of a unique configuration. With the understanding that many types of seals were considered for an improved mechanical toggle seal, this report section begins simply with the description of the seal concept which was the basis of the Bobbin seal, the design selected for laboratory evaluation. Outside and Inside Bobbin seal configurations are then discussed, and the aspects of contact stresses and nickel plating are described. This work led to the design of two Outside Bobbin seals for the experimental fitting.

Improved Seal Configuration. Figure 74 shows the seal concept which incorporated initially the greatest number of desired seal features. It was postulated that primary seals would be formed at the ID of the seal legs at A. These seals would be created as the legs were deflected through an appropriate angle until the ID of the legs contacted the OD of the inner hubs of the stub ends. With continued tightening of the nut, the toggle action of the seal legs would magnify the axial force to produce increased sealing forces. Elastic and plastic expansion of the seal tang would permit considerable tolerance variation in the diameters of the sealing surfaces and in the angles of the seal legs. Because the tendency of the legs to buckle would be resisted by the faces of the stub ends, it was postulated that secondary seals would be formed along the sides of the seal legs at B. The fitting would be preloaded through the inner hubs of the stub ends, thus creating a seal in parallel with the compression members.

---

*See Appendix VIII for detailed discussion of the Conoseal evaluation.

a. After Assembly | b. Before Assembly
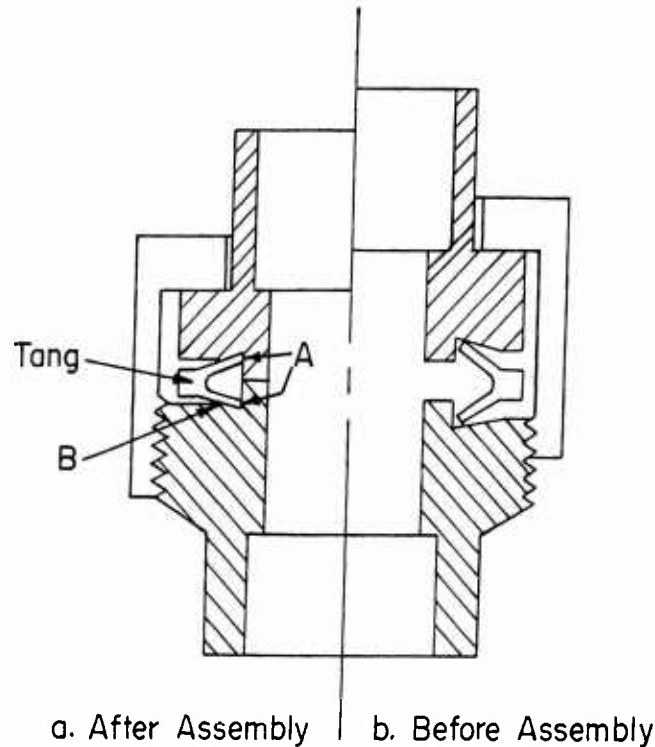
A-44071
FIGURE 74. INITIAL IMPROVED SEAL CONFIGURATION

This seal configuration had the following desirable features:

(1) Magnification of the axial force would be attained to produce the sealing forces.

(2) The sealing forces would be in parallel with the preload forces, thus assisting proper fitting preload, and minimizing seal load fluctuation.

(3) The effects of machining tolerances would be minimized because the action on one sealing surface would not directly affect the action of the other sealing surface.

(4) The expansion of the seal tang would accommodate machining and assembly variations by providing the plastic type of load-deflection curve illustrated in Figure 73.

(5) The rotation of the sealing surfaces would be more predictable and possibly minimized.

(6) By utilizing a base seal material having considerable strain-hardening ability, it would be possible through plastic yielding of the seal tang, to increase the elastic recovery of the seal over that available from an elastically deflected seal.

Various seals of this type were fabricated from stainless steel and assembled. Although the postulated action of the seal appeared to be approximated, two difficulties were encountered with the expansion of the tang. First, it appeared that insufficient

151

force was applied to the sealing surfaces. Second, it was realized that the clearance needed between the tang OD and the ID of the nut thread to prevent interference for all tolerance variations would result in the fitting being larger and heavier than would normally be required.

The best means of overcoming these two problems seemed to be the placement of the tang on the inside of the seal, as shown in Figure 75. By using part of the flow passage, if necessary, the tang could be made stronger and the variations in tang tolerances could be accommodated. Because of its resemblance to a bobbin, this seal was called the Bobbin seal. It was subsequently called the Outside Bobbin seal to distinguish it from the type of seal shown in Figure 74, which was called the Inside Bobbin seal.

When the tang was placed on the inside of the seal, it was also decided that the compression load of the fitting should be transmitted through the seal tang as shown in Figure 75. The sealing loads would still be in parallel with the compression load of the fitting, but the clamping of the seal tang might minimize any tendency of the seal to reduce the sealing loads at elevated temperatures.
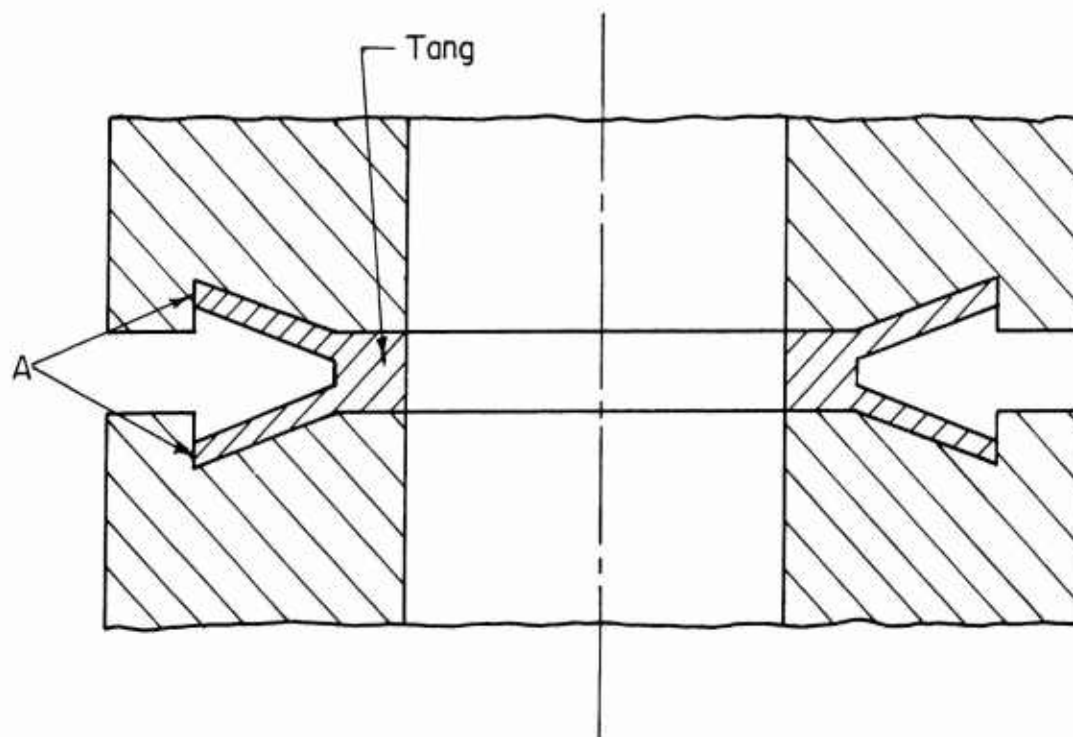
FIGURE 75. OUTSIDE BOBBIN SEAL AND MATING STUB ENDS

Outside Bobbin Seal. The major potential problem of the Outside Bobbin seal appeared to be the mating of the sealing surfaces. While relative movement of the sealing surfaces as the fitting was closed appeared to be reduced over that of the Belleville seal, there was still the possibility of some movement taking place. Because of the intimate surface contact needed to seal helium, such movement could be detrimental. Experiments were made to determine the effect of tolerance variations on the seating action of different sealing surface configurations.

Figure 76 shows the sealing surface geometries which were evaluated with various diametral clearances. In all cases the legs were machined at an angle of 30 degrees with

152
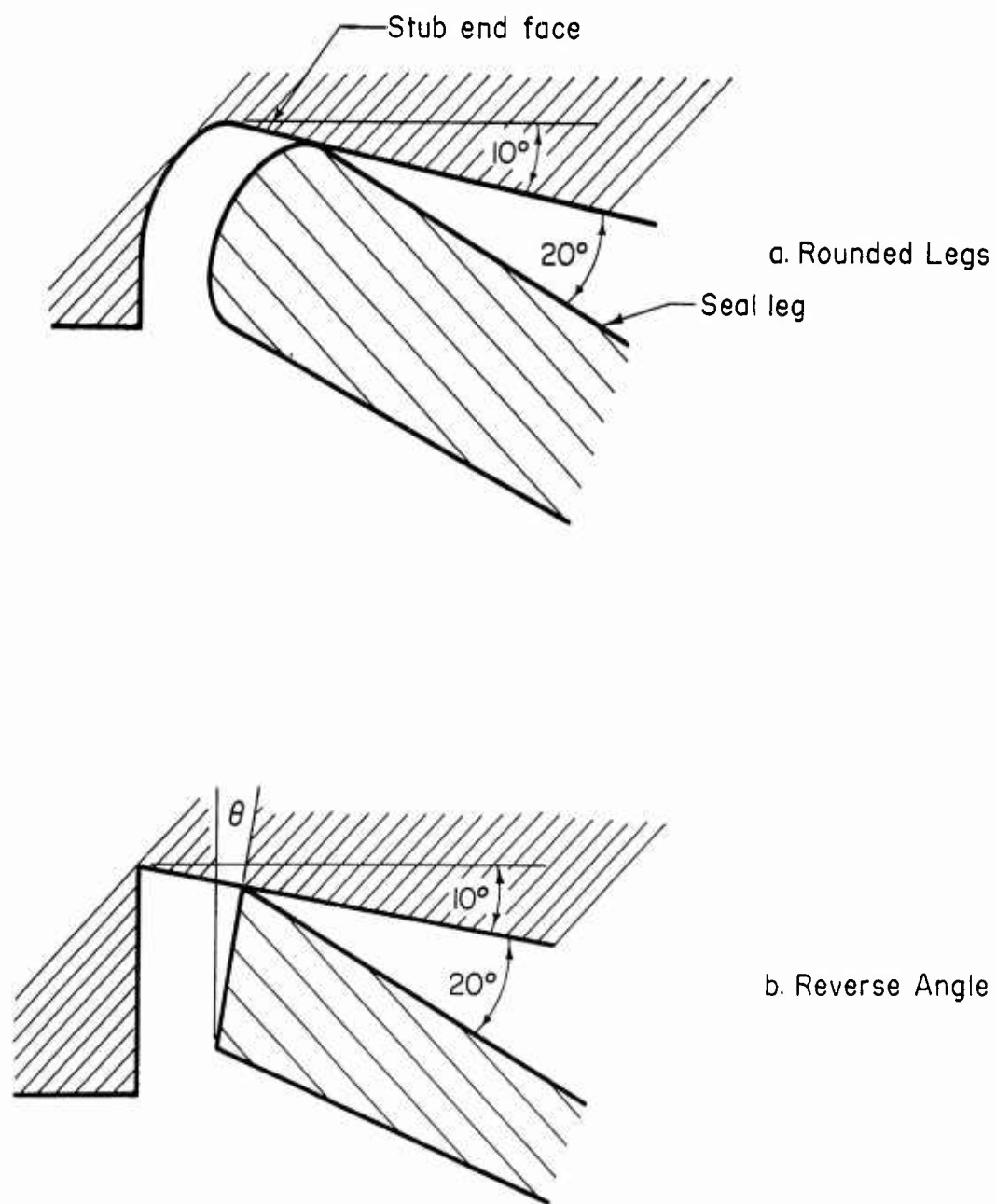
FIGURE 76. SEALING SURFACE GEOMETRIES INVESTIGATED
FOR THE OUTSIDE BOBBIN SEAL

153

Average length of
seal 0.020 in.

90X
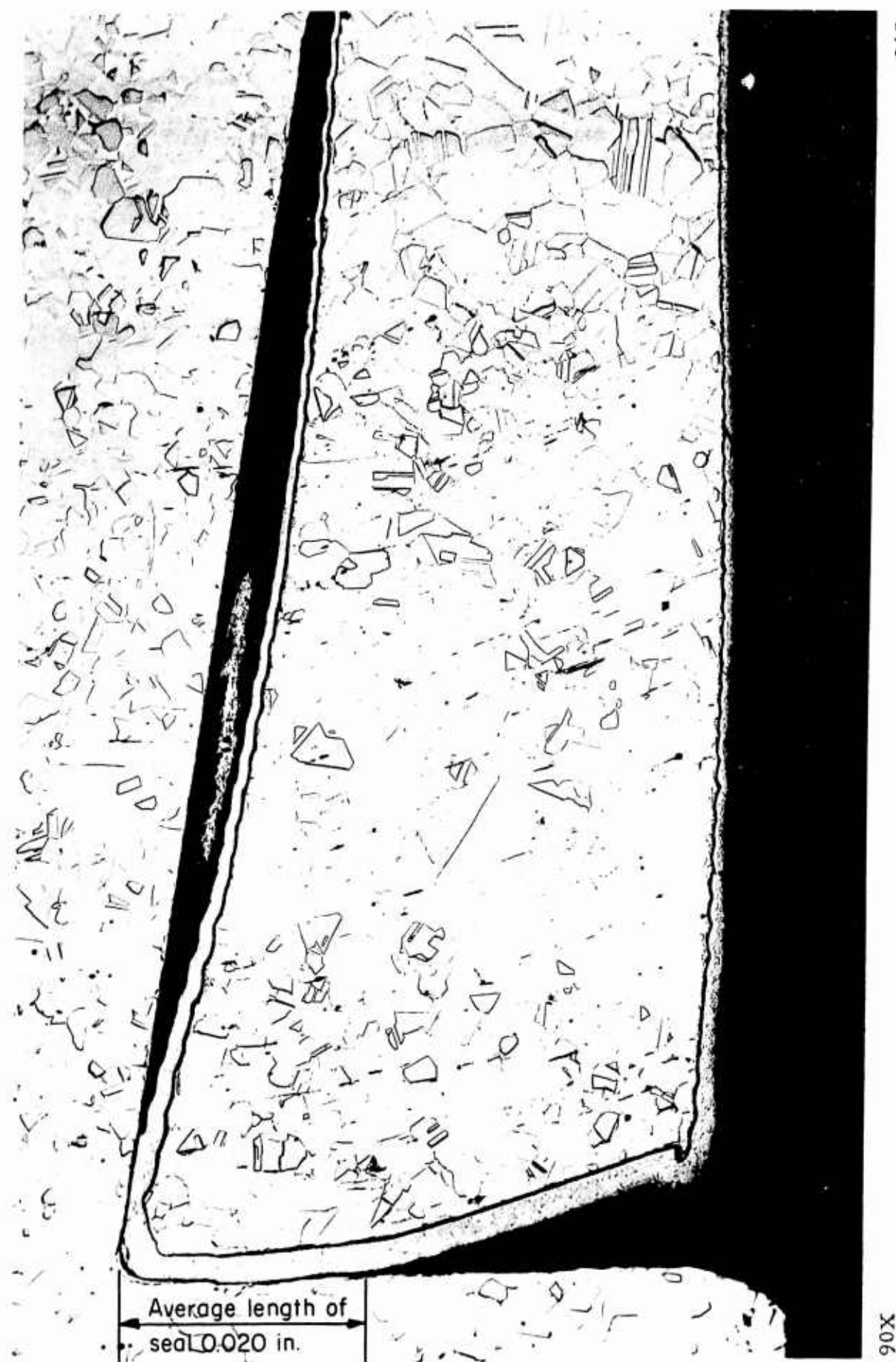
965

Polished and Etched

FIGURE 77. ASSEMBLED SEAL D-22: ORIGINAL DIAMETRAL CLEARANCE OF 0.007 INCH

154
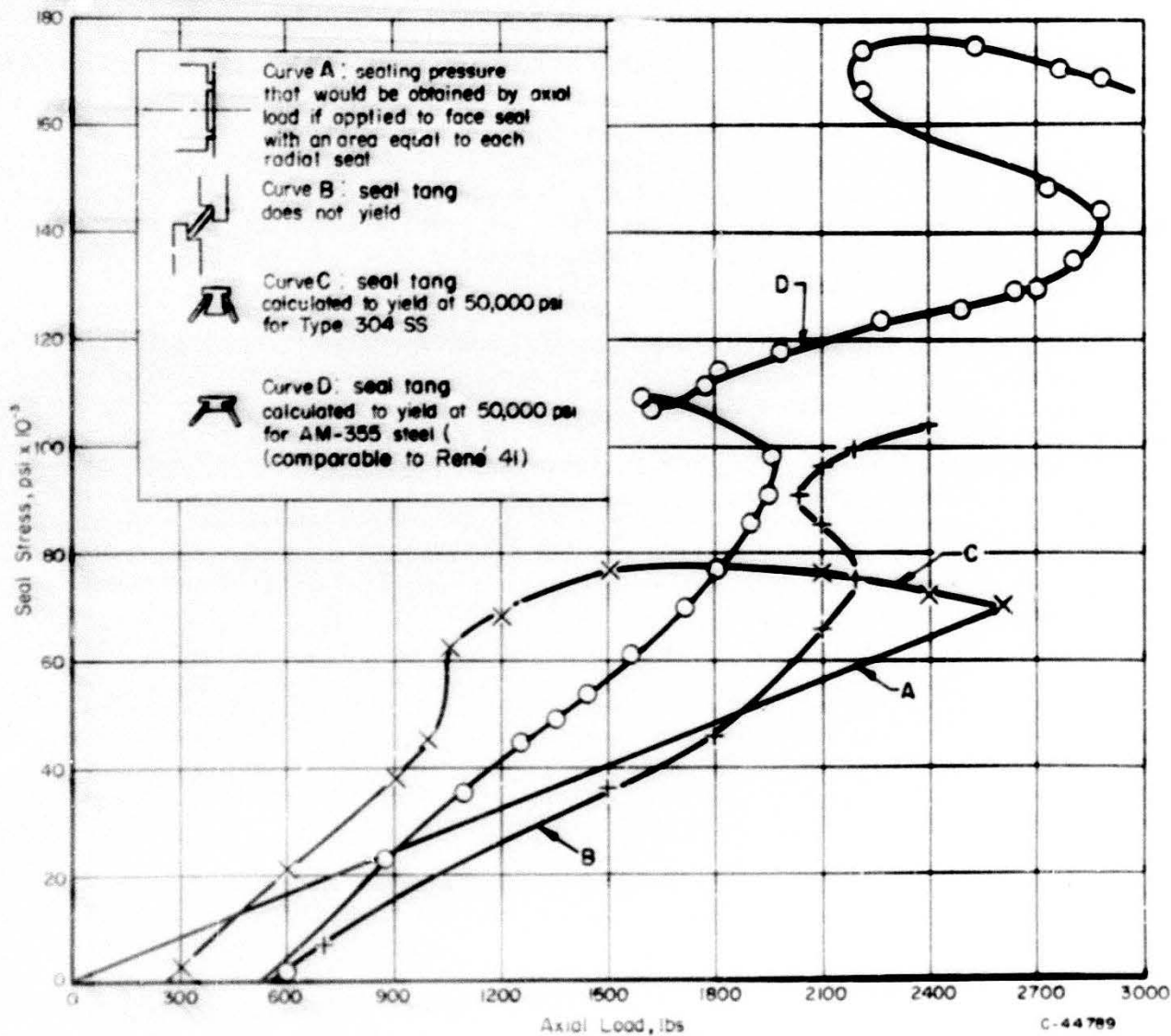
FIGURE 78. RADIAL SEAL STRESS VERSUS AXIAL LOAD

the seal tang face and deflected through an angle of 20 degrees during closure. Initial calculations indicated that this type of deflection would minimize the buckling of the seal legs, maximize the tolerance of machining variations, and prevent the seal from becoming locked in place. Specimens incorporating the variations were assembled, mounted, sectioned, polished, and examined microscopically.

Despite the apparent desirability of the seal with rounded legs, Figure 76a, the machining tolerances seemed to cause too much movement of the sealing surfaces. This, combined with the difficulty of machining the radii, resulted in the abandonment of the rounded-leg configuration.

Figure 76b shows the angle of the flat sealing surface on the seal leg which was varied (angles of 0, 10, and 20 degrees were evaluated) in an attempt to get the proper seating action. It seemed that seals with a 20-degree reverse angle did not have sufficient clearance tolerance. Seals with a 0- and a 10-degree reverse angle demonstrated little seating difference. In each case the deflection of the seal leg and the compression of the seal tang resulted in an interface contact length of approximately 0.020 inch. A typical plated specimen is shown in Figure 77.

Continued examination of the Outside Bobbin seal specimens showed that the seating action was good. After initial contact in the corner, the seal leg deflected until the seal contact lengthened to about 0.020 inch. No relative movement of the sealing surfaces could be detected during this action. When the seal was about 0.020 inch long the seal tang yielded plastically, thus maintaining both the seal length and the seal contact force. The seal tang continued to yield until the fitting was closed. The validity of this action for sealing helium was demonstrated subsequently when a satisfactory helium seal was obtained with only elastic deformation of the seal tang for maximum initial clearance, and with considerable plastic deformation (seal tang diameter reduced 0.006 inch) for mininum initial clearance.

Contact Stress Studies. Because of the combined elastic and plastic yielding which can take place in an Outside Bobbin seal, it was difficult to predict the actual stress obtained in the seal contact area. The importance of knowing this stress for sealing helium has been explained in previous report sections. It was decided that the sealing contact stress would have to be determined experimentally.

At the same time, another requirement arose. It became apparent that the Inside Bobbin seal configuration offered at least three possible advantages over the Outside Bobbin seal. First, the greater diameter of the seal tang of the Inside Bobbin seal offered greater dynamic stability for the fitting because the compression load would be on a larger diameter. Second, the sealing surface of the Inside Bobbin seal would be less susceptible to damage prior to and during assembly. Third, the circumference of the sealing surfaces, particularly for the smaller seal sizes, would be considerably shorter for the Inside Bobbin seal and thus the reliability of the seal might be significantly increased. However, there was still a question about the sealing contact stress possible with an Inside Bobbin seal. The decision was made to combine the study of contact stresses with further study of the Inside Bobbin seal. The similarity of the action of the Inside and Outside Bobbin seals was expected to permit much of the work to be extrapolated for the Outside Bobbin seal.

Primary interest of the experimental work was centered on three aspects: (1) the actual magnification of the axial force by the toggle action of the seal legs, (2) the abilit·

to predict the magnitude of the sealing force with a plastically yielded seal tang, and (3) the ability of the plastically yielding seal tang to maintain the force on the seal contact surfaces. Figure 78 shows the seal geometries investigated and the seal seating stresses for the different geometries. The seal legs were made 0.020 inch thick to limit the width of the sealing surface. The stresses were determined by the method shown in Figure 79. Part of the stub ends were replaced by a hardened support ring with the strain gages attached to the inside circumference. The assembled parts were placed in a press and the loads on the support rings were recorded as the stub ends were closed.
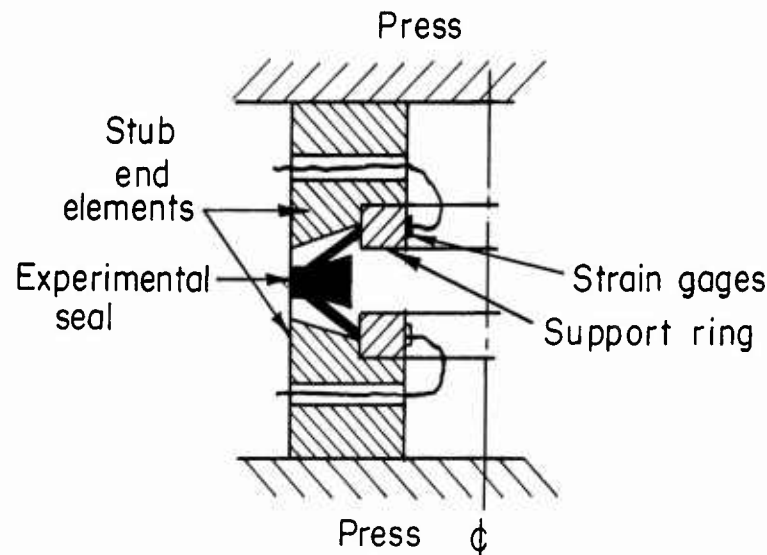
FIGURE 79. METHOD FOR MEASURING RADIAL SEALING FORCE
OF INSIDE BOBBIN SEAL

Curve A in Figure 78 was calculated by dividing the area of an arbitrarily selected axial seal by the axial load. The axial seal area was made equal to the area of the sealing surface on each seal leg of the Inside Bobbin seal. Thus the diameter of the radial sealing surface was made equal to the average diameter of an axial seal of the same seal width.

Curve B shows the sealing stress attained by a Belleville-type seal in which the restraining member or seal tang does not yield. This configuration was expected to give the highest sealing stress for a toggle seal. Curve C is to be compared with Curve B to understand the effect of the plastically yielding tang. Curve D is to be compared with Curve C because it represents the sealing stress that can be obtained by using a material with an increased rate of strain hardening.

The significant conclusions drawn from these studies were

(1) Considerable magnification of the axial force occurs in the Inside and Outside Bobbin seals.

(2) An adequate sealing stress can be obtained with Inside and Outside Bobbin seals having a soft nickel plate. Five times the yield strength of nickel is about 45,000 psi.

(3) A yielding seal tang maintains a relatively constant sealing stress.

157

(4) A seal tang with increased strain-hardening characteristics will produce a higher but less constant sealing stress.

(5) Yielding of the seal structure can be calculated with sufficient accuracy to accommodate machining and assembly tolerances while yet maintaining an adequate sealing stress.

Nickel Plating. Although the contact stress studies demonstrated the ability of the Inside and Outside Bobbin seals to magnify the axial force for sealing purposes, this magnification was not high enough that the seals could be used unplated. It has been shown that from three to five times the apparent yield strength of the soft material is needed to seal helium reliably. Figure 78 shows that, with a yield strength of Type 304 stainless steel of about 35,000 psi, and an annealed yield strength of AM-355 of about 56,000 psi, the maximum contact stress obtained experimentally was between two and three times the yield strength of the seal material. While it might have been possible to reduce the seal area to obtain a higher contact stress, it was believed that the seal should be at least 0.020 inch wide. Thus, it was decided that the Inside and Outside Bobbin seals should be plated with a softer material.

Nickel was chosen as the plating material for two reasons: (1) it had good compatibility with the anticipated fluids (the same as René 41), and (2) its high strength, in comparison to some of the softer materials such as silver, promised greater insensitivity to the vibration of the missile systems. As can be seen from the following properties of fully annealed pure nickel, five times the yield strength of the nickel could be expected with Bobbin seals whether the seal were made of 304 stainless steel, AM-355, or René 41:

Modulus of Elasticity	30×10^6 psi
Tensile Strength	46,000 psi
Yield Strength	8500 psi
Elongation	40 per cent

In cooperation with Battelle's Electrochemical Engineering Division, a nickel sulfamate plating bath was used to nickel plate the experimental seals. The plating thickness on the critical sealing surfaces was initially 0.002 inch and the hardness of the nickel as plated was approximately Rockwell C 23. The plating thickness was increased to 0.003 inch for the final test seals upon the advice of the International Nickel Corporation. The plated seals were subsequently annealed in a vacuum furnace at 1400 F for 30 minutes, after which the hardness of the nickel plating was approximately Rockwell B 53.

Protective Shroud. Although the sealing edges of the Outside Bobbin seal subsequently demonstrated a remarkable insensitivity to damage, a feature was designed, as shown in Figure 80, to reduce the vulnerability of the sealing edges. It was postulated that a thin metal or plastic protective shroud would be placed over the seal after plating. The shroud would remain on the seal throughout the entire assembly procedure. However, as the fitting was closed and tightened, the protruding lips on the shroud would abut the fitting stub ends and the shroud would be collapsed. This would expose the

sealing surfaces of the seal only <u>during</u> the assembly process. The necessity of such a device will depend on the experience gained with Outside Bobbin seals during experimental and developmental programs.
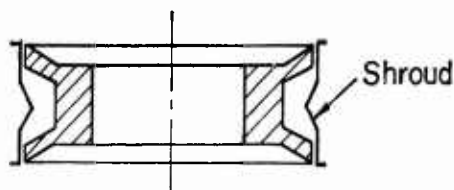
FIGURE 80.   OUTSIDE BOBBIN SEAL WITH SHROUD

Outside Bobbin Seals for the Experimental Fitting

Because of several advantages and disadvantages, it was not possible to determine whether the Outside or the Inside Bobbin seal configuration was better. With limited laboratory funds, it was decided that the Outside Bobbin seal would be designed for the experimental fitting. Many of the results would be applicable to the Inside Bobbin seal and the better configuration could be determined later. The best dimensions for the experimental Outside Bobbin seals were determined by a series of experiments.

Leakage Evaluation. By microscopic inspection (see p 156) it had been determined that seals with reverse angles of 0 and 10 degrees were preferable and that the seal legs should be deflected from an angle of 30 degrees to an angle of 10 degrees with the seal tang. However, leakage tests were conducted to verify these tentative conclusions and to determine what tolerance limits were needed on the sealing surfaces.

Two series of tests were made, as shown in Table 21. In the D series, the seal legs were deflected 20 and 30 degrees. Table 21 shows the stub ends for the D and E series tests and the variations in the seal dimensions. The microscopic examination work had shown that the seals could be assembled with a torque of about 600 lb-in. Torques generally in excess of this were selected to insure that insufficient axial load was not a cause of leakage.

The leak tests were performed under static conditions, at room temperature, and with a maximum internal pressure of 1500 to 1800 psi. The leakage rates achieved are shown in Table 21. Because of the sensitivity of the leak detector, it was necessary to denote many of the measurements as simply less than 0.04×10^{-7} atm cc/sec. After the leakage tests, representative fittings were mounted, sectioned, and polished.

The tentative conclusions concerning the reverse angles were substantiated for the D series seals. The seals with a 20-degree reverse angle did not seal adequately while those with 0- and 10-degree reverse angles sealed with a high degree of reliability. In fact, the ability of the seals to seal adequately with 0.012-inch diametral clearance was very surprising. Microscopic examination showed that the length of the seal was consistently about 0.020 inch. Three seals, D-21, D-22, and D-52, were deliberately scratched across the sealing surface with a tool bit prior to assembly. Each performed satisfactorily. Examination showed that in the assembly process some of the nickel plating had been forced into the scratch to form the necessary seal.

TABLE 21. DIMENSIONS AND LEAKAGE RATES FOR D AND E SERIES OUTSIDE BOBBIN SEAL

A 0.437 C E D 0.200 0.160 B

D-type stub end 10°

E-type stub end

A-45633
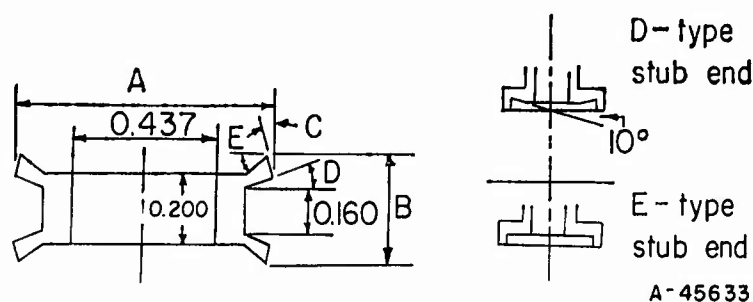
	Dimensions Before Nickel Plating					Nominal Diametral Clearance After	Assembly Torque,	Leakage, 10^{-7} atm cc/sec			
Seal	A	B	C	D	E	Plating, in.	lb-in.	200 PSI	500 PSI	1000 PSI	>1500 PSI
D-11	0.824	0.310	0	22	30	0.002	720	<0.04	<0.04	<0.04	<0.04
D-12	0.824	0.310	0	22	30	0.002	480	<0.04	<0.04	<0.04	<0.04
D-21[a]	0.819	0.310	0	22	30	0.007	960	0.25	0.18	0.03	0.42
D-22[b]	0.819	0.307	0	22	30	0.007	960		0.1	0.1	0.1
D-23[a]	0.819	0.307	0	22	30	0.007	960	0.25	0.25	0.25	
D-31	0.814	0.304	0	22	30	0.012	960	<0.04	<0.04	<0.04	<0.04
D-32	0.814	0.304	0	22	30	0.012	960	0.16	0.3	0.3	0.3
D-33	0.814	0.304	0	22	30	0.012	960	0.46	0.59	0.67	
D-41	0.824	0.303	10	20	30	0.002	720	<0.04	<0.04		<0.04
D-42	0.824	0.303	10	20	30	0.002	960	<0.04	<0.04	<0.04	<0.04
D-51	0.819	0.300	10	20	30	0.007	960	<0.04		0.34	0.6
D-52[a]	0.819	0.300	10	20	30	0.007	960	1.3	1.7	1.2	
D-61	0.814	0.296	20	20	30	0.012	960		Excessive leak		
D-71	0.824	0.296	20	18	30	0.002	1440			940	1200
D-72	0.824	0.296	20	18	30	0.002	1440	200	780	1340	
D-81	0.819	0.289	20	18	30	0.007	960		Excessive leak		
E-11	0.824	0.296	20	18	30	0.001	720	<0.04	<0.04	<0.04	
E-21	0.819	0.289	20	18	30	0.006	960	<0.04	120	Leaks excessively	
E-22	0.819	0.289	20	18	30	0.006	960	<0.04	<0.04	<0.04	<0.04
E-31	0.814	0.282	20	18	30	0.011	960	<0.04	0.07	0.07	0.07
E-41	0.824	0.283	10	18	20	Zero	960	<0.04	<0.04	0.045	0.045
E-42	0.824	0.283	10	18	20	0.001	960	<0.04	<0.04	<0.04	<0.04
E-52	0.819	0.280	10	18	20	0.004	840	<0.04	<0.04	<0.04	
E-61	0.814	0.277	10	18	20	0.011	960	0.05	3.4	1.3	76.0
E-62	0.814	0.277	10	18	20	0.011	960	<0.04	<0.04	4.2	
E-81	0.819	0.286	0	11	20	0.006	960	<0.04	<0.04	<0.04	1.3
E-82	0.819	0.286	0	11	20	0.006	960	0.42	0.6	0.55	0.5
E-91	0.814	0.283	0	11	20	0.011	960	0.17	0.13	0.08	0.08
E-92	0.814	0.283	0	11	20	0.011	960	<0.04	<0.04	<0.04	<0.04
E-101	0.824	0.332	10	22	30	0.003	960	<0.04	<0.04	<0.04	<0.04
E-102	0.824	0.332	10	22	30	0.003	960	<0.04	<0.04	<0.04	<0.04
E-121	0.814	0.325	10	22	30	0.007	960	<0.04	<0.04	<0.04	

(a) Sealing surface scratched.

(b) Pressurized at 1500 psi for 65 hours.

Although sealing was accomplished with practically all dimensional variations of the E series seals, microscopic examination showed that the seals were not properly seated in the fitting. Without exception, even with an assembly torque of 906 lb-in., the preload was not achieved at the tang as desired. Instead, the axial contact point between the flange and the seal was generally at the base of the seal leg, which was deformed as shown in Figure 81. According to our preload considerations, such an assembly presented possible fitting problems resulting from improper fitting preload.

A 45082
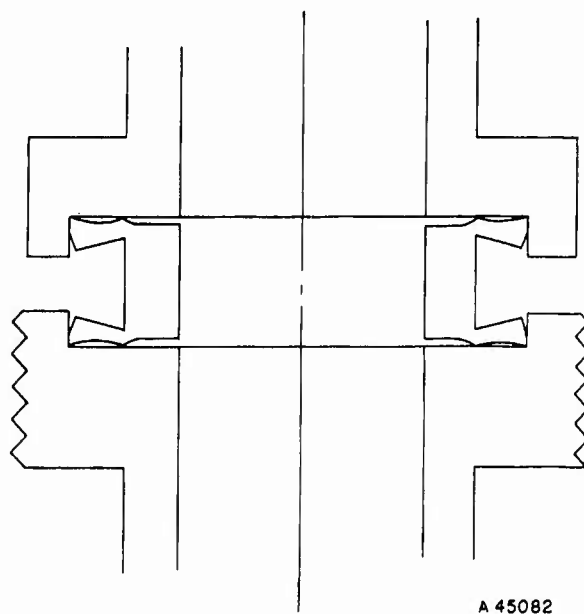
FIGURE 81. FINAL ASSEMBLED POSITION OF E SEALS

Experimental Stainless Steel Seal. Figure 82 shows the dimensions of the experimental stainless steel seal which were determined by the evaluations described above. The 0.437 ID allowed for 0.007 plastic compression of the seal tang to equal the 0.430 ID of the stainless steel tubing (see Table 7, p 48). Because the sealing effectiveness was the same for the 0- and 10-degree reverse angle specimens, and because the 0-degree reverse angle was easier to machine, this configuration was selected. The seal legs were machined at a 30-degree angle to permit a deflection of 20 degrees when mated with a D-type stub end. With 0.003-inch-thick plating, the diameter of the sealing surfaces could vary from 0.811 to 0.815 inch. This provided a maximum clearance of 0.009 and a minimum clearance of 0.003 inch when used with stub ends whose sealing surface diameters were $0.818^{+0.002}_{-0.000}$ inch.

Figure 83 shows the typical fluctuation of axial load as an experimental stainless steel seal is compressed between two stub ends. In almost every case one seal leg seats before the other because of a slight difference in strength between the two sides of the seal. The maximum axial seating force is usually about 1200 lb, although the force has been as high as 1320 lb. According to Figure 78, an axial load of 1200 lb may result in a stress on the seal contact surfaces of 70,000 psi. However, because the softness of the nickel plating might limit the seating stress, it was decided that a seating stress of 45,000 psi (about five times the yield strength of nickel) would be estimated until the value could be determined more accurately. With a seal width of 0.020 in., this means that the seal seating force is 900 lb/linear in.

161
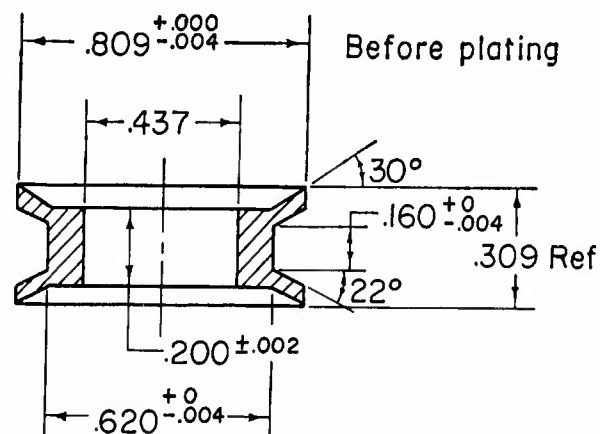
FIGURE 82. EXPERIMENTAL STAINLESS STEEL SEAL
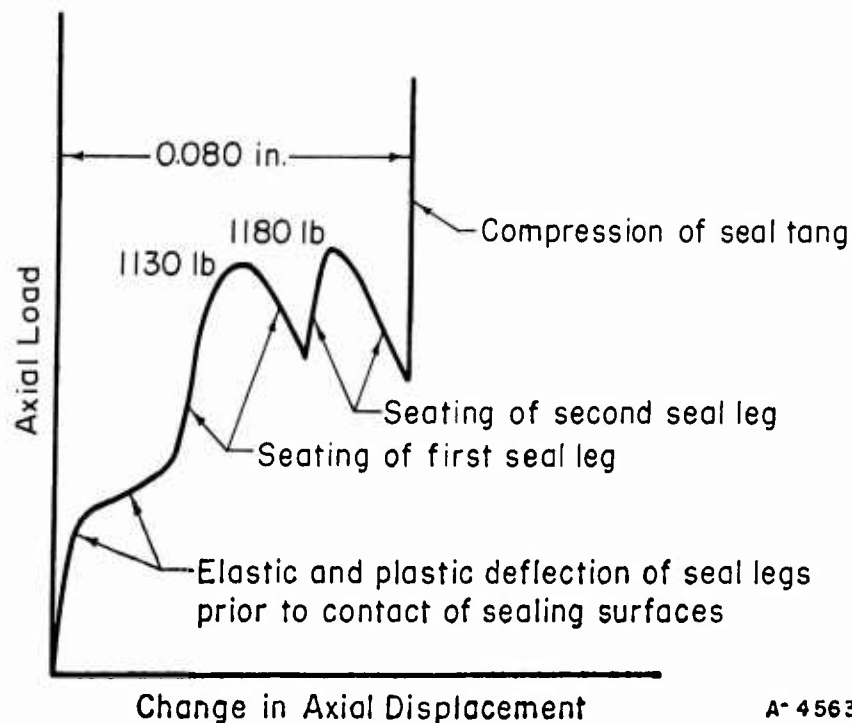
FIGURE 83. LOAD VERSUS AXIAL DISPLACEMENT CURVE FOR SEATING
OF TYPICAL EXPERIMENTAL STAINLESS STEEL SEAL
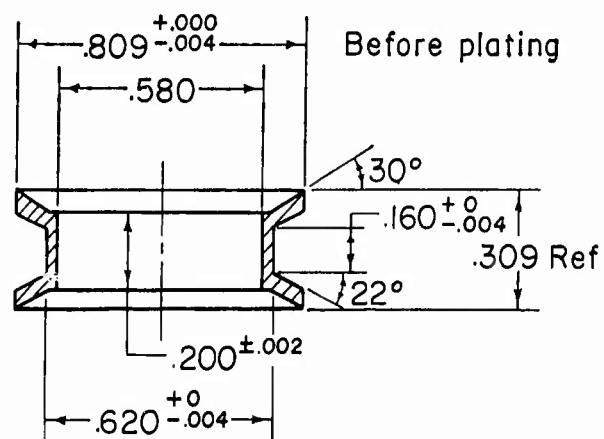
FIGURE 84. EXPERIMENTAL RENÉ 41 SEAL
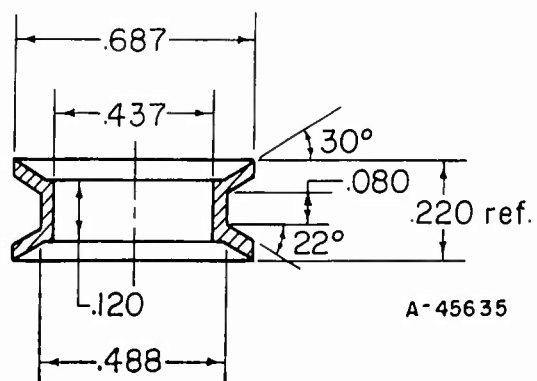
FIGURE 85. POSSIBLE LIGHTWEIGHT RENÉ 41 SEAL

According to Equation (20), p 41, a torque of 240 lb-in. is needed to supply an axial load of 1200 lb with a 1-inch thread. The work with the experimental fitting showed that the stainless steel seals could be seated with torques ranging between 360 and 600 lb-in. These variations were caused by more friction than allowed for in Equation (20) and by differences in the seal dimensions. Because it is difficult to estimate the axial force needed on the seal tang to maintain a seal once the seal has been seated, the minimum axial seal load was arbitrarily set at 10 per cent of the structural load of the fitting.

Experimental René Seal. Although there was mounting evidence that a nickel-plated stainless steel seal would work in the experimental fitting, there was one major potential source of failure. The experimental fitting was to be for Class II service and the fitting material for this service was to be René 41 (see p 19). It was possible that the the difference in the thermal coefficients of expansion for stainless steel and René 41 would cause leakage in the temperature range of -320 to 600 F. Although a seal made of annealed René 41 would be much more expensive than one of stainless steel because of the machining characteristics of René 41, experimental René 41 seals were made for evaluation in case the stainless steel seals demonstrated a temperature limitation.

Figure 84 shows the dimensions of the experimental René 41 seals. Except for an increase in the ID of the seal tang, all dimensions were the same as for the stainless steel seals. The use of similar dimensions allowed the René 41 seal to be evaluated in the same experimental fitting as was used for the stainless steel seal. The increase in the seal tang ID allowed the seating force to be adjusted for the higher yield strength of the René 41 material. Although the torques needed to seat the René 41 seals subsequently proved to be about 650 lb-in., the minimum fitting torque of 780 lb-in. (see p 61) was always more than enough to seat the René 41 seals.

Because of the high yield strength of annealed René 41, it is possible to get sufficient sealing force with less material than for a stainless steel seal. This is demonstrated by the thinner seal tang of the René 41 seal as compared with the stainless steel seal. If the ID of the René 41 seal tang is determined by the ID of the stainless steel tubing, the René 41 seal can be reduced considerably in size without reducing the sealing force. Figure 85 shows a smaller René 41 seal based on a stainless steel tubing system and the use of a 7/8-20 NEF thread on the nut. The fitting to use this seal was designed and a sample was fabricated, but no tests were conducted. The smaller fitting was 34 per cent lighter in weight than the fitting which was evaluated.

References

(1) "Design Criteria for Zero-Leakage Connectors for Launch Vehicles", General Electric NASA Contract NAS8-4012.

(2) "Development of Analytical Techniques for the Design of Static, Sliding and Rotating Seals for Use in Rocket Engine Systems", Armour Research Foundation, AF Contract AF 04(611)-8020.

(3) Loeb, L. B., The Kinetic Theory of Gases, Chapter 7, Dover Publications, Inc., New York (1961).

(4) "Design Criteria for Zero-Leakage Connectors for Launch Vehicles", General Electric Laboratories, Quarterly Progress Report No. 2, Contract NAS 8-4012 (October 11, 1962).

(5) Rossheim, D. B. , and Markl, A. R. C. , "Gasket Loading Constants", Mec. Eng. , 65, 647 (1943).

LABORATORY EVALUATION OF PROPOSED
ONE-HALF-INCH CLASS II FITTING DESIGN

Fitting Design

Experimental Procedure

Summary of Laboratory Results

Conclusions

LABORATORY EVALUATION OF PROPOSED ONE-HALF INCH
CLASS II FITTING DESIGN

During Phase I, design procedures and concepts were developed for improved threaded and flanged connections. Because Phase II funds were limited, and because a greater problem exists with threaded fittings than with flanged fittings on missiles, it was decided that the Phase II laboratory evaluation of the developed design procedures and concepts should be concerned with a representative threaded fitting. During a discussion with the project monitor at the end of Phase I, it was decided that a 1/2-inch Class II threaded fitting would be a representative fitting. The decision was based on the wide temperature range, -320 to 600 F, and on the general applicability of the fitting material — René 41.

The important dimensions of the 1/2-inch experimental fitting are discussed in detail in a previous report section entitled "Proposed Threaded Fitting Design". Figure 20 of that section shows the configuration of the proposed fitting as it would be installed in a tubing system. Because North American Aviation is still developing the tube-to-fitting connection, the Phase II laboratory work was concerned with the evaluation of the fitting principles not associated with the tube-to-fitting connection.

This report section is presented in three parts:

- Fitting Design

- Experimental Procedure

- Summary of Laboratory Results

The first part summarizes the experimental fitting by brief discussions of component pictures and drawings. Included in this part of the report are detail drawings of a promising reduced-size fitting which has yet to be evaluated.

The second report part describes the experimental procedure as defined by the contract and by discussion with the project monitor. The third part discusses the results of the laboratory evaluation.

Fitting Design

Experimental Fitting

Figure 86 shows the experimental fitting as it was designed for evaluation during temperature cycling. Figure 87 shows a section of the assembled fitting, while Figures 88, 89, 90, and 91 show the dimensions of the fitting components. The dimensions shown for the seal, the nut, and the flanges of the stub ends were the same as those for the proposed fitting. The dimensions of the hubs of the stub ends starting at the back of the stub-end flanges were dictated by the requirements of the temperature-cycling test equipment.

Knurl imprint   Seal   Knurl   Sealing surface

Stub end flange

Threaded flange

Sealing surface
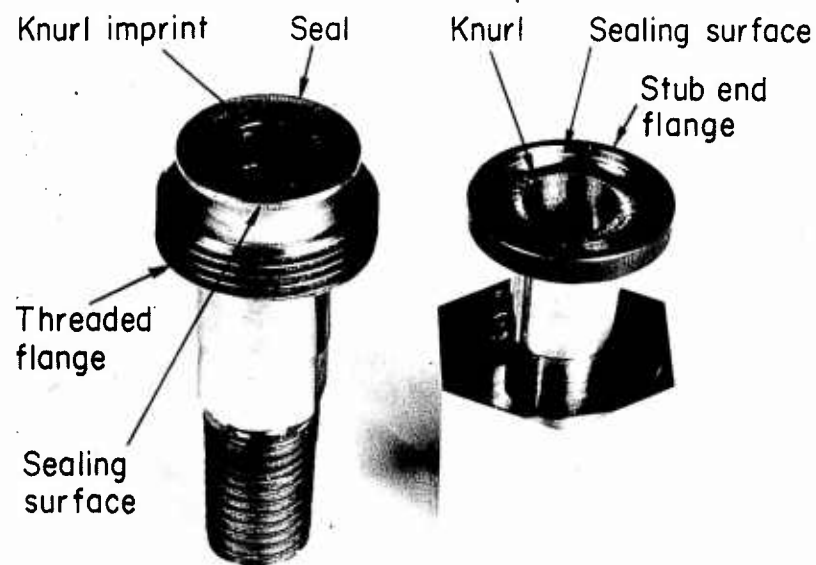
1843

a. Details of Flange Face and Seal
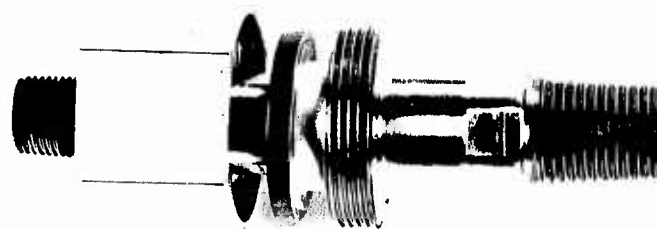
1842

b. Assembled Fitting With Nut Retracted

FIGURE 86. EXPERIMENTAL FITTING FOR
TEMPERATURE CYCLING
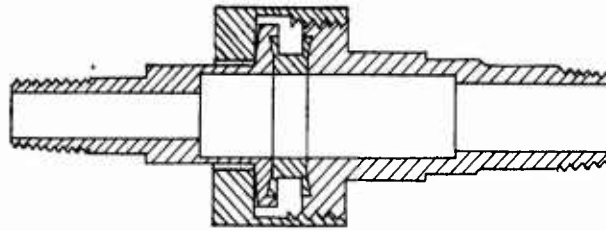
FIGURE 87. ASSEMBLED EXPERIMENTAL FITTING
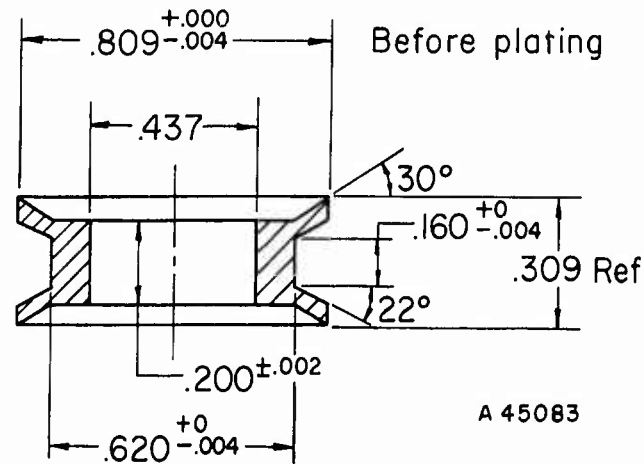
FIGURE 88. FINAL EXPERIMENTAL SEAL
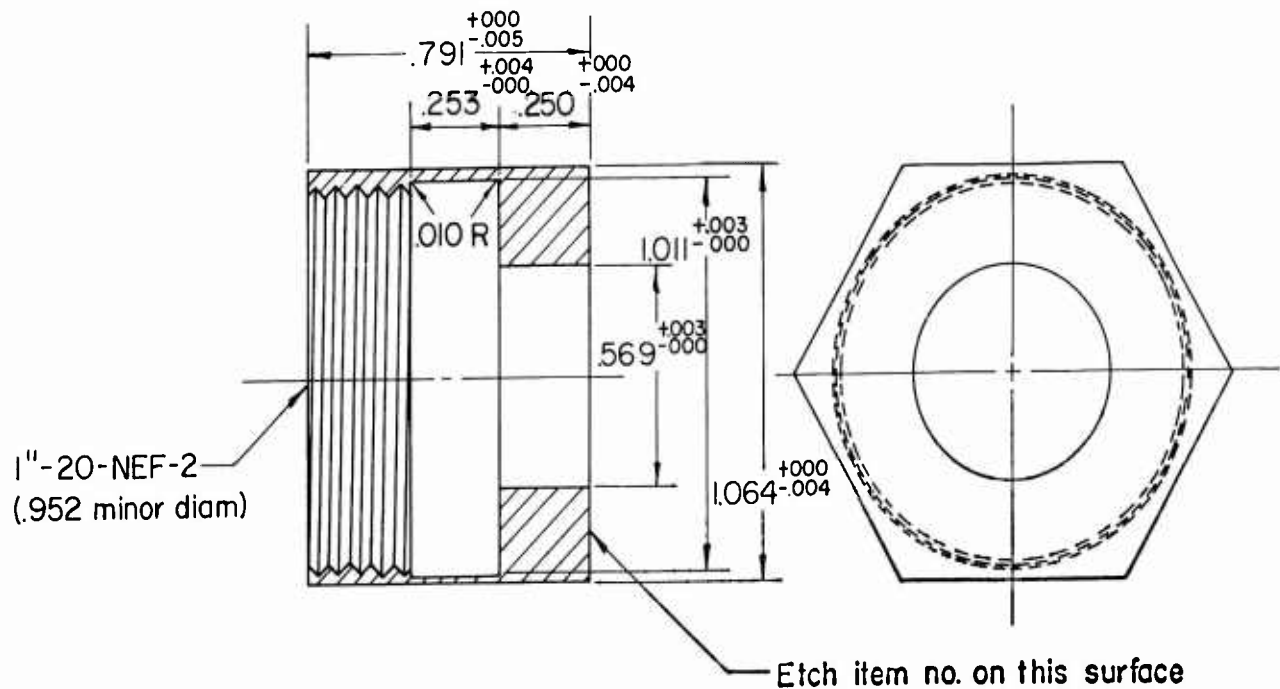
Break sharp corners approx. .010" R

FIGURE 89. EXPERIMENTAL NUT

169
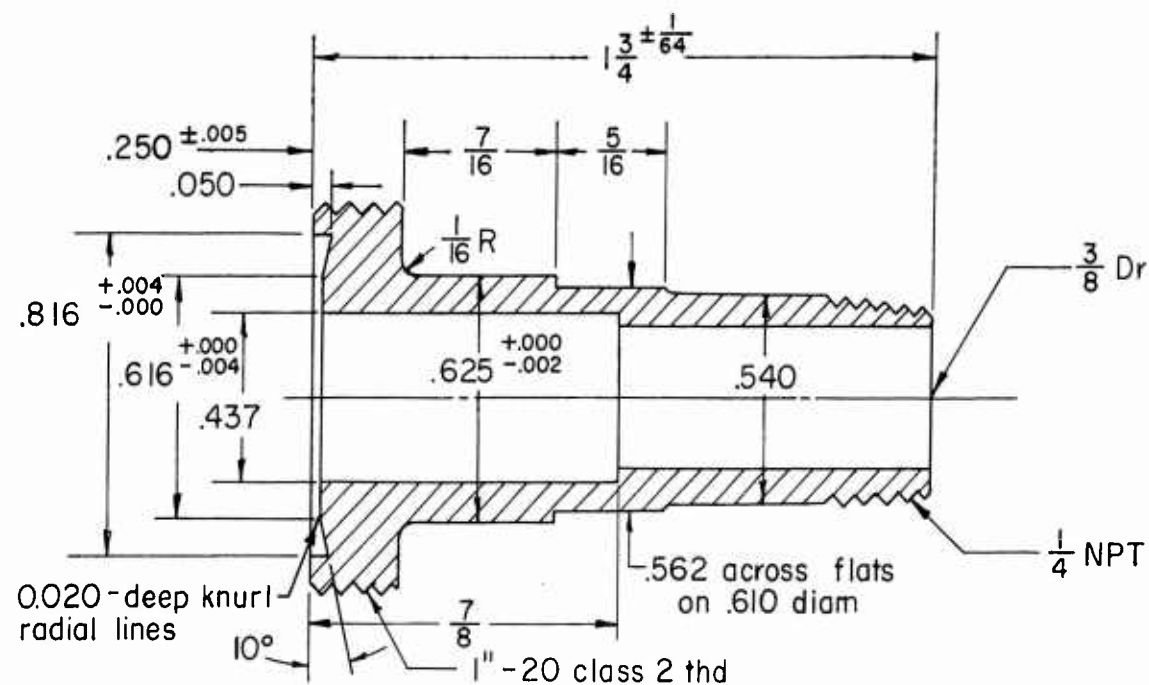
FIGURE 90.   EXPERIMENTAL THREADED STUB END
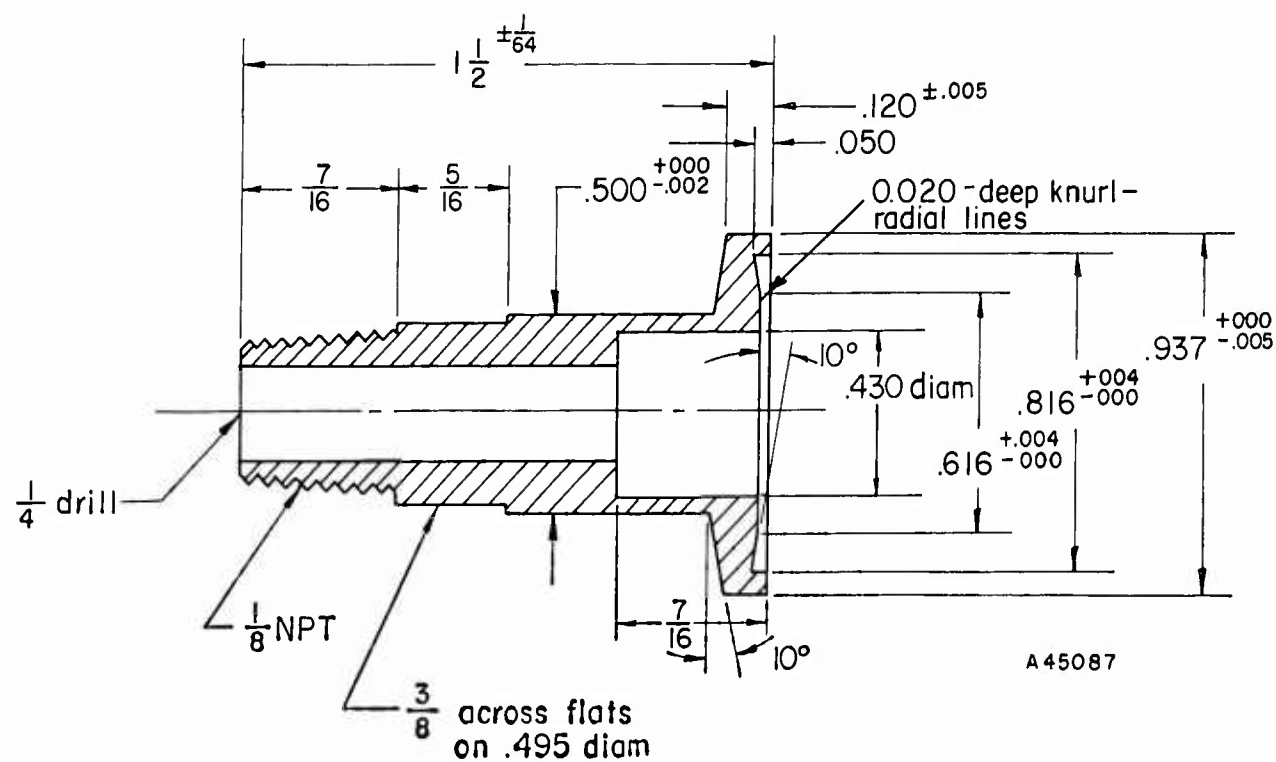
FIGURE 91.   EXPERIMENTAL PLAIN STUB END

170

Two important dimensions are shown which were not discussed in the "Proposed Threaded Fitting Design" section. First the plain stub end has a 10-degree angle on the back face of the flange to maintain the moment arm on the nut flange at a constant length. If this length changes, the effective spring rate of the nut changes and the proper preload relationship may be lost. Second, the face of each stub end which clamps the seal tang is knurled. These knurled surfaces prevent the friction of the nut flange from turning the plain stub end in relation to the seal or to the threaded stub end. Such movement can disturb the critical mating at the sealing surfaces.

Stub ends were also designed which permitted the fitting to be welded to stainless steel tubing for vibration and reverse bending evaluation. These stub ends were the same as the ones shown in Figures 90 and 91 except that the hubs were tubular with 0.505-inch OD and 0.430-inch ID. The hub on the threaded stub end also provided wrench flats.

Possible Lightweight Fitting

The experimental René 41 seal was designed to permit its evaluation in the same fitting used to evaluate the stainless steel seal. A fitting which would weigh 34 per cent less than the experimental fitting is possible if the René 41 seal is modified on the basis of an ID of 0.437, (see Figure 85) and if the wrench flats on the threaded flange are redesigned. The resulting lightweight fitting is shown in Figure 92. Details of the stub ends, nut, and seal are shown in Figures 93, 94, 95, and 96.

The tube-to-fitting connection would remain unchanged as would the stub-end flanges (except for reduction in flange OD). Reduction of the seal OD makes it possible to use a 7/8-20 thread instead of the larger 1-20 thread. Because of the reduced thread diameter, the distance across flats on the nut can also be reduced from 1-1/16 to 15/16 in. The redesigned nut is 30 per cent lighter than the standard nut.

A large weight saving would be realized if the wrench flats were replaced by a 3- or 5-spoke female spline machined in the hub of the threaded stub end, as shown in Figure 94. Of course, use of a spline will necessitate specification of a special wrench. However, such a tool could be simple, easily manufactured, and relatively inexpensive. If wrench flats were used instead of a spline, the total weight saving in the fitting assembly would be only about 24 per cent.

Experimental Procedure

As defined by the conditions of the contract and by detailed discussions with the project monitor, five types of experiments were performed during Phase II:

- Temperature Cycling

- Repeated Assembly

- Stress Reversal

- Vibration

- Operational Evaluation

171

Section A–A

A-45636
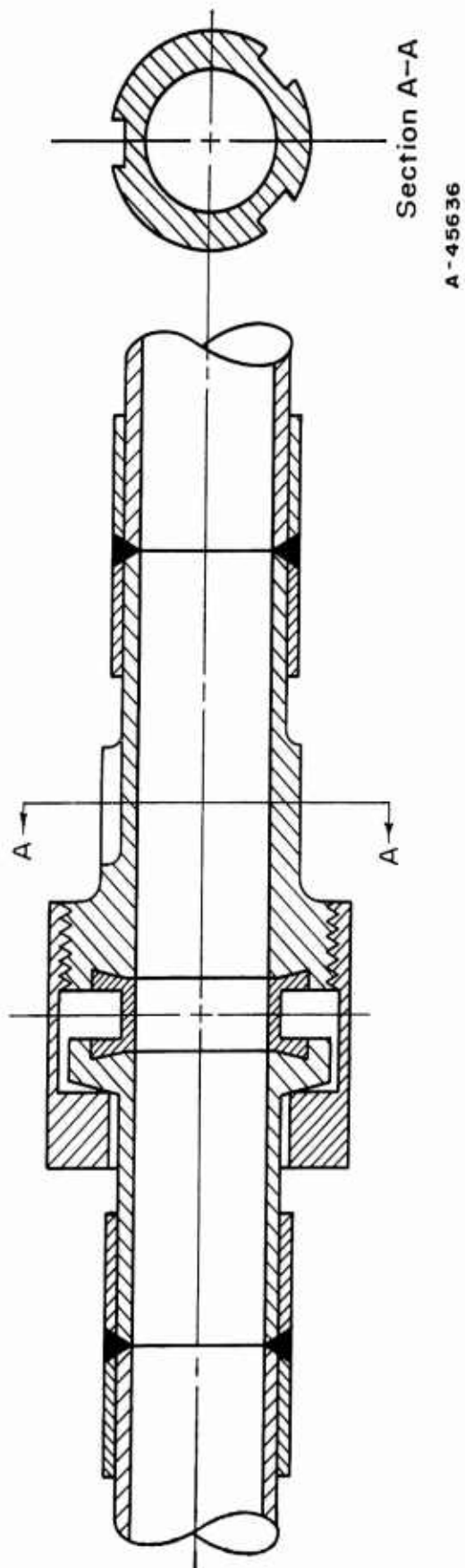
FIGURE 92. LIGHTWEIGHT 1/2-INCH CLASS II CONNECTION WITH RENÉ 41 SEAL
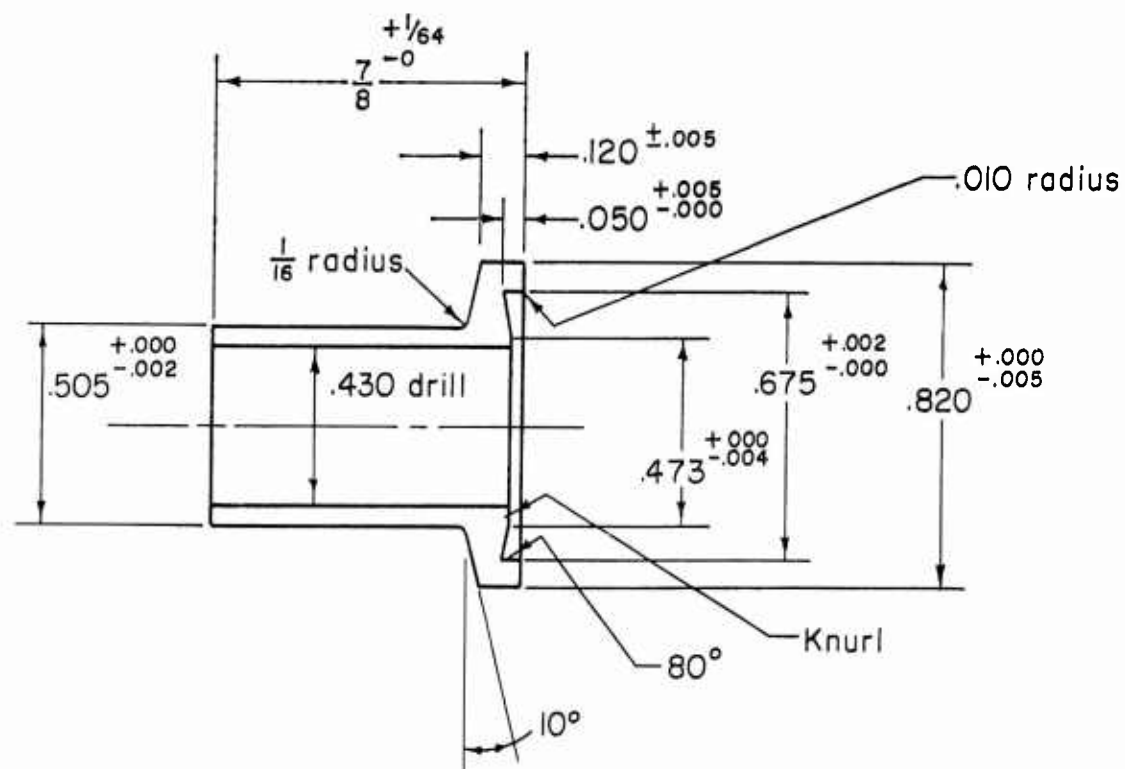
FIGURE 93. LIGHTWEIGHT PLAIN STUB END
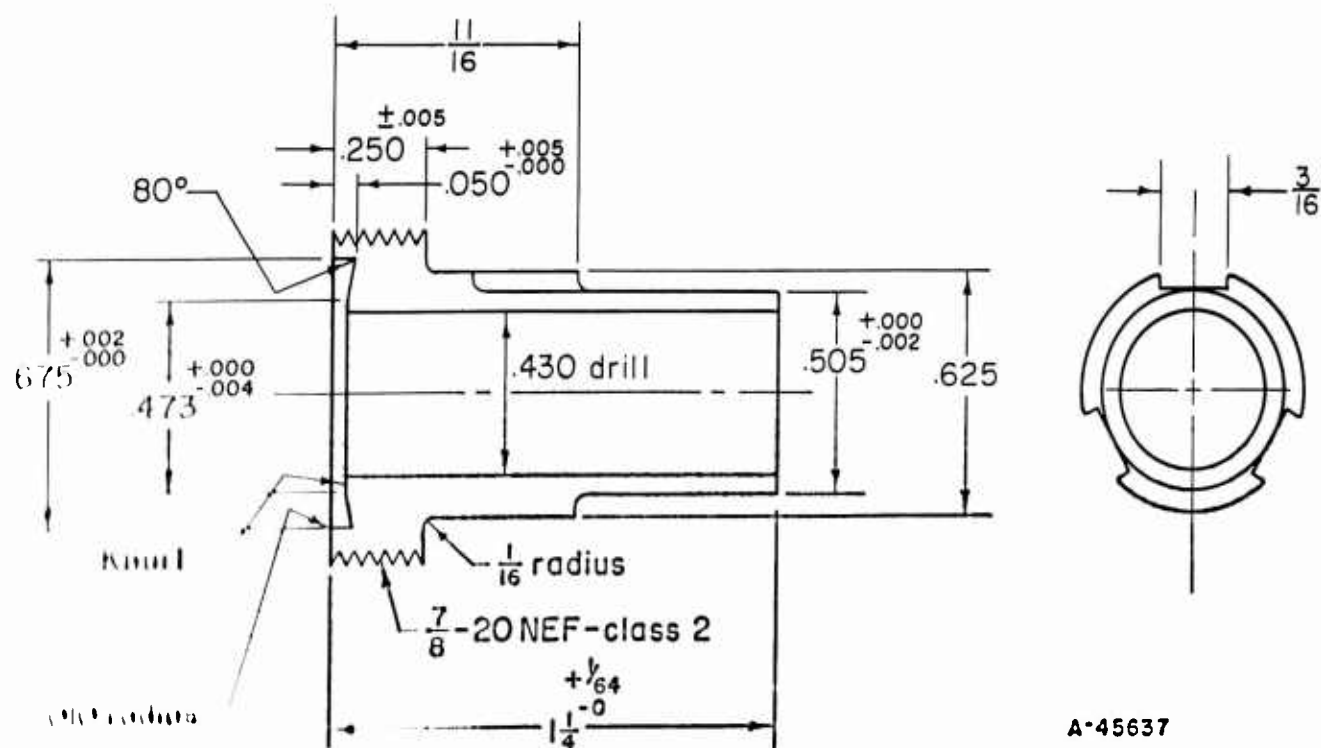
FIGURE 94. LIGHTWEIGHT THREADED STUB END

173
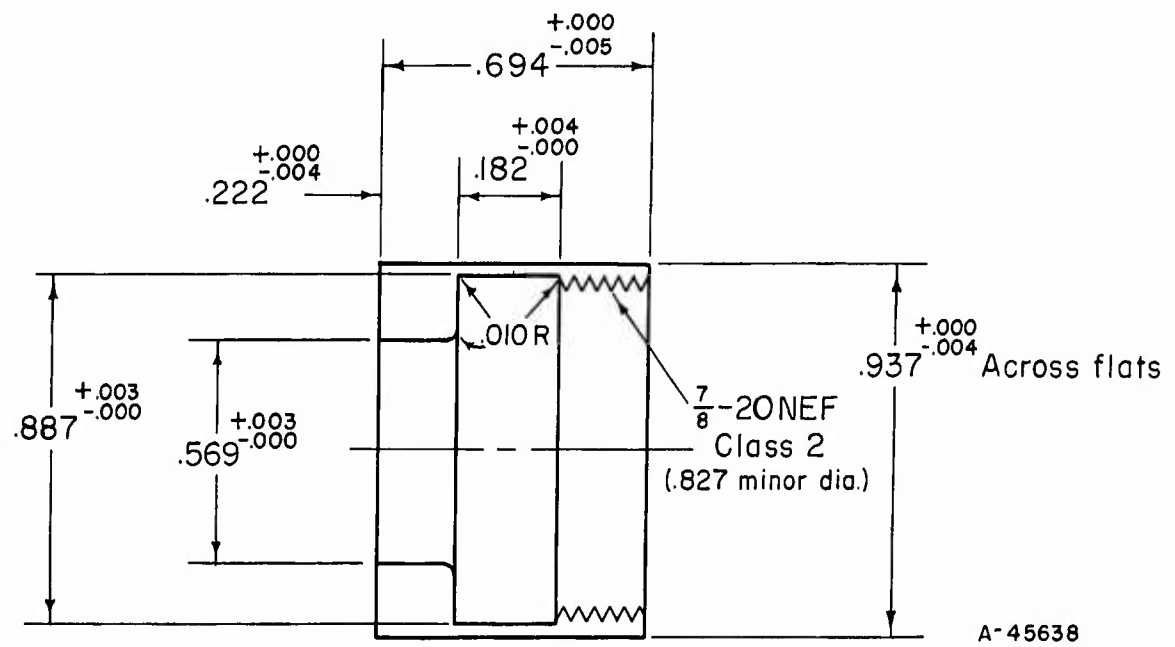
FIGURE 95.   LIGHTWEIGHT NUT
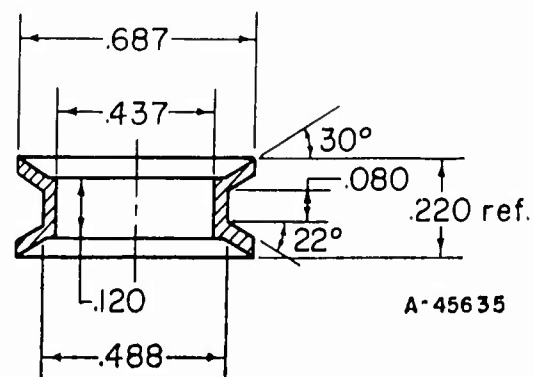
FIGURE 96.   LIGHTWEIGHT RENÉ 41 SEAL

174

Temperature Cycling

The effect of temperature variation was normally evaluated by three types of cycles: (1) between room temperature and -320 F, (2) between room temperature and 600 F, and (3) between 600 and -320 F. In addition, some extreme thermal cycles were performed between 1200 to 1500 F and -320 F.

The system used for these experiments is shown in Figure 97. A vacuum chamber was fabricated from 0.032-inch stainless steel and was welded directly to the fitting as shown. A thermocouple, which contacted the outer surface of the nut, was inserted into the vacuum chamber. Another thermocouple was inserted into the gas space in the fitting. The fitting was heated internally by an electric sheath heater and was cooled to -320 F by immersing the entire assembly in liquid nitrogen. The rate of heating was controlled by a Variac. Normally the fitting could be heated from -320 to 600 F in 5 to 7 minutes. Heating to 1200 F required 7 to 10 minutes. The fitting could be cooled from the highest temperatures to -320 F in about 5 minutes. An internal pressure of 1800 to 2200 psi was maintained by a pressure regulator with a built-in pressure-relief valve.
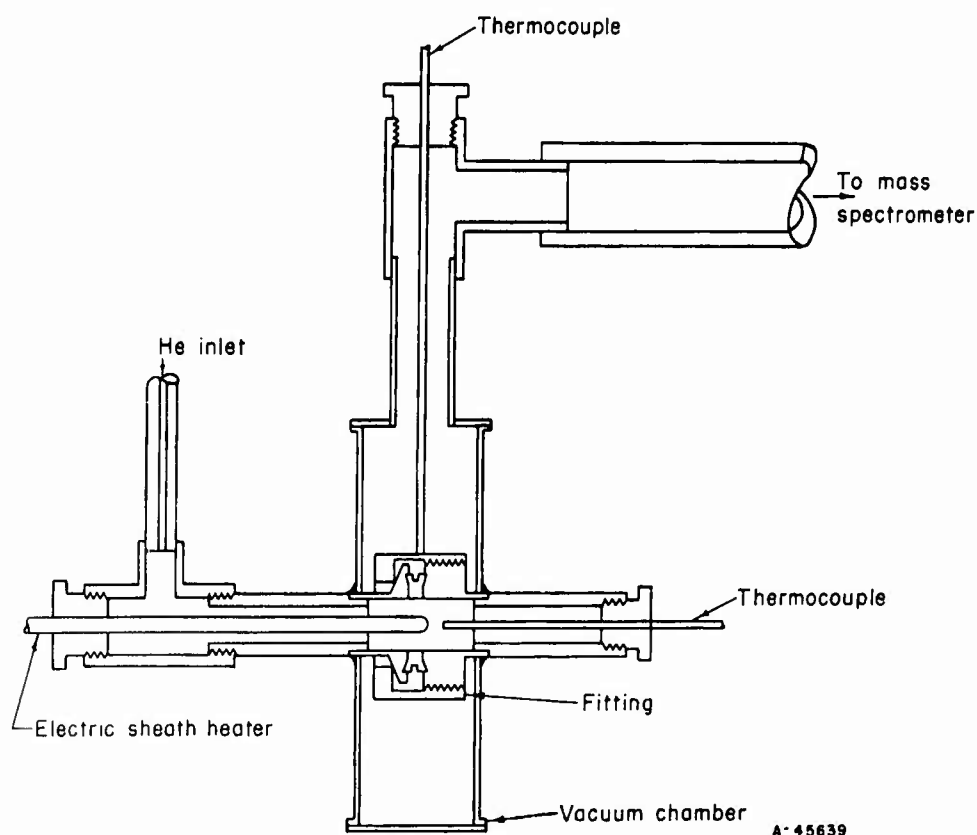
FIGURE 97. SYSTEM USED FOR GENERAL LEAK TESTING
AND FOR TEMPERATURE CYCLING

175

Repeated Assembly

The repeated assembly tests were performed with two different fittings and with stainless steel seals. The fittings were leak tested at room temperature and at 2200-psi pressure. Proof-pressure tests at 3000 psi were also performed. The lubricant used during these tests was FELPRO C5-A[*], a high-temperature antiseize colloidal, copper thread compound. After each assembly the threads were cleaned and fresh lubricant was applied.

Stress Reversal

Stress reversal conditions were simulated with the equipment shown in Figure 98a. Details of the fitting assembly location are shown in Figure 98b. The double eccentric cam on the motor shaft was first adjusted to a zero position; that is, no strain was registered by the strain gage as the motor shaft was rotated 360 degrees. The eccentric was then adjusted to register an amount of strain equivalent to a given stress level at Point A for an equivalent length of stainless steel tubing. Generally an equivalent stress of about 22,000 psi was imposed. The duration of the test was for 200,000 cycles at a rate of 1000 cpm.

Vibration

The vibration tests were performed on a standard Calidyne machine Model No. 174. The fitting and tubing assembly was clamped as shown in Figure 99 and vibrated at 35 g's as follows:

Frequency, cps	Time, minutes
Sweep, 40 to 2000	3
Sweep, 2000 to 40	3
Sweep, 40 to 2000	3
Sweep, 2000 to 40	3
142	24 (204,500 cycles)

A frequency of 142 cps was chosen because resonance of the entire assembly was induced. Essentially the fitting was in a stress-free state during the vibration test. It is presumed that if a fitting could successfully undergo the stress-reversal test, then it could also withstand whatever stresses would be imposed during a vibration test. Therefore, the purpose of the vibration test was to determine whether the vibration would cause any loosening or backoff of the nut irrespective of structural fatigue.

---

[*]Manufactured by Felt Products Manufacturing Company, Skokie, Illinois.

a. Fixture Assembly

b. Details of Fitting Assembly Location

A-45640
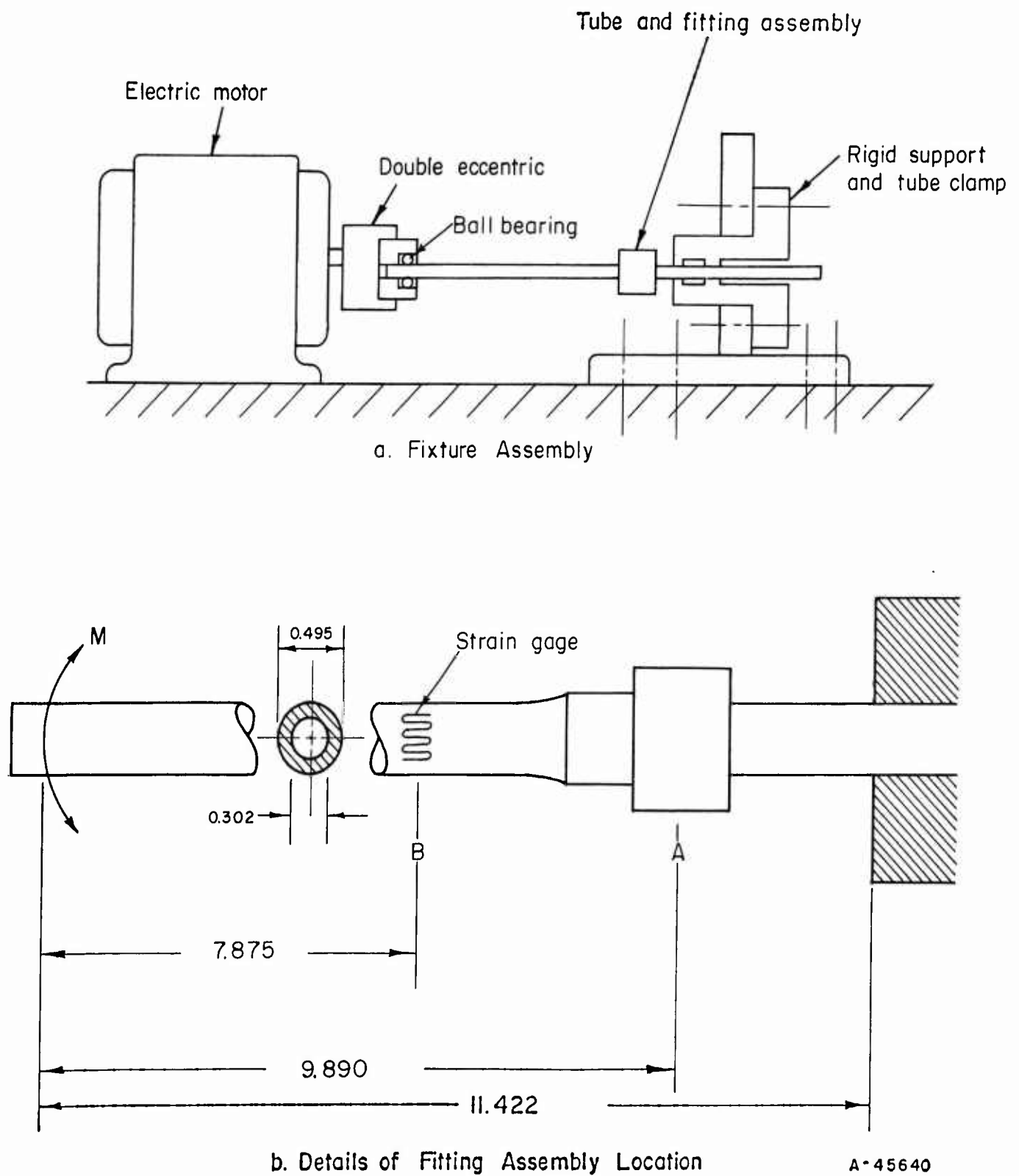
FIGURE 98. SYSTEM USED FOR STRESS-REVERSAL TESTS

177
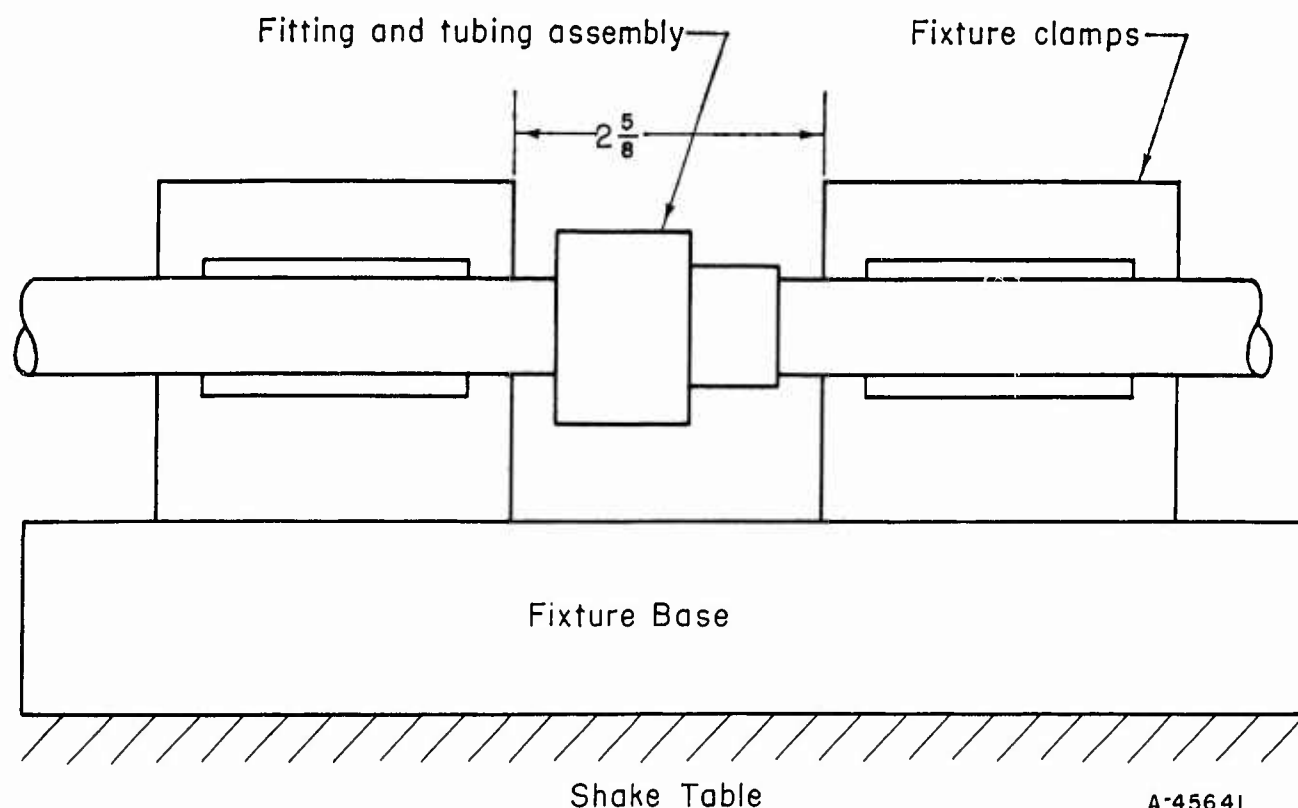
FIGURE 99.   FIXTURE USED FOR VIBRATION TESTS

Operational Evaluation

The operational service test specified in the contract included vibration and stress reversal at room temperature.   It was decided that a more realistic test would be made if the stress-reversal test was conducted with the fitting heated to 600 F.   For operational evaluation, each fitting assembly was subjected in turn to vibration, stress reversal at 600 F, three types of thermal cycling, and 3000-psi proof-pressure tests.   If leakage did not develop, the same fitting assembly was subjected to another complete set of tests.

Summary of Laboratory Results

Because some fittings were used in more than one type of experiment, the discussion includes the fitting number.   The fittings used for the different tests were:

Thermal Cycling	Fittings Nos. 3, 4, 6, and 9
Repeated Assembly	Fittings Nos. 7 and 12
Stress Reversal	Fittings Nos. 7 and 8
Operational – Vibration	Fittings Nos. 8, 9, 10, and 11

Thermal Cycling

Table 22 gives a summary of results for all the thermal cycling. The results are discussed briefly for each fitting.

Fitting No. 3. Initially this fitting was assembled with a stainless steel seal. Although the fitting did not leak on the first cycle from room temperature to 600 F and back, it did show an excessive leak on the second cycle.

A second stainless steel seal was assembled in the fitting. A total of 17 cycles were completed between room temperature and 600 F, and the fitting was under pressure for a total of 30-1/2 hours. No leakage was noted during the entire period.

Fitting No. 4. Assembled with a stainless steel seal, this fitting completed two cycles between room temperature and -320 F, two cycles between room temperature and 600 F, and one cycle between 600 and -320 F without leakage.

A second assembly with a stainless steel seal was cycled two times successfully between about room temperature and -320 F. On one cycle from room temperature to 600 F a small leak was indicated. On the first cycle from 600 F to -320 F an excessive leak occurred at about -200 F.

Fitting No. 6. The stainless steel seal which was first assembled in the fitting showed no leakage during 17 cycles from room temperature to -320 F. During the next seven cycles to -320 F a small leak was occasionally indicated. On the fourth cycle from room temperature to 600 F an excessive leak was indicated.

Because the stainless steel seals appeared to be having difficulty in sealing over the required temperature range, it was decided that tests should be initiated with seals made of René 41. If leakage was being caused by the difference in the coefficient of expansion between the stainless steel of the seal and the René 41 of the fitting stub ends, this problem would be greatly reduced by the use of a René 41 seal.

Fitting No. 6 was assembled with a René 41 seal. Although the leak detector was not free of helium at the start of the tests, it was decided that the thermal cycling should be initiated to get an indication of the performance of the René 41 seal. The fitting was subjected to 9 cycles between room temperature and 600 F and 3 cycles between -320 and 600 F. A steady decrease in indicated leak rate during the tests showed that the fitting was either not leaking or had only a very small leak.

Starting the next day, when the leak detector was functioning satisfactorily, 12 cycles were completed between -320 and 600 F and 8 cycles were completed between -320 and about 1200 F. No leakage was indicated in any of these tests. The entire 32 cycles extended over a 36-1/2-hour period.

Fitting No. 9. This fitting was assembled with a René 41 seal and used for the operational tests. The successful results of those tests are given in a later discussion. When the laboratory work of Phase II was essentially completed, it was decided that

179

TABLE 22. RESULTS OF LEAKAGE TESTS, FITTINGS NOS. 3, 4, 6, AND 9

Fitting No.	Seal No.	Assembly Torque, lb-in.	Cycle No.	Average Internal Pressure, psi	Average Temperature, F		Total Test Period, minutes	Maximum Recorded Leak Rate, 10^{-7} atm cc/sec
					Gas, Low/High	Nut, Low/High		
3	SS1	780	1	2000	RT/600		15	$0^{(a)}$
			2	2000	RT/600		15	1 (at 600)
			3	2000	RT		--	100
	SS2	720	1 and 2	2000	RT/600		5	0
			3	2000	RT		15 hours	0
			4-15	2000	RT/617		77	0
4	SS3	960	1-2	2000	RT/-320		40	0
			3-4	2000	RT/600		65	0
			5	2000	600/-320		5	0
	SS4	1020	1	1800	RT/-320		30	0
			2	1800	-320/150		15	0
			3	1800	150/-320		5	0
			4	1800	-320/130		10	0
			5	1800	130/600		15	0.8
			6	1800	600/90		10	0.8
			7	1800	90/600		10	0.8
			8	1800	600/-200			Excessive leak
			9	1800	RT		13 hours	1300
6	SS5	1020	1-17	1800	RT/-320		Hold at -320 for 15 minutes during each cycle	0
			18					34
			19					2.1
			20-23					0
			24					1.7
			25-26		RT/600		Hold at 600 for 15 minutes during each cycle	0
			27					0 at 600
			28		RT			1300
			28		600			1.7
			29		RT			1300
	R2	780	1	1600	355	200	35	$31^{(b)}$
			2	1600	435	255	30	$18.5^{(b)}$
			3	1600	555	365	30	$13.4^{(b)}$
			4	1600	575	295	30	$8.4^{(b)}$
			5	1500	630	410	30	$8.4^{(b)}$
			6	1400	605	410	35	$7.6^{(b)}$
			7	1400	600	465	40	$5.0^{(b)}$
			8	1400	610	480	30	$3.3^{(b)}$
			9	1300	605	405	20	$3.3^{(b)}$
			10	1200	-320/600	-170/430	60	$3.3^{(b)}$
			11	1200	-320/650	-130/425	45	$3.3^{(b)}$

TABLE 22. (Continued)

Fitting No.	Seal No.	Assembly Torque, lb-in.	Cycle No.	Average Internal Pressure, psi	Average Temperature, F Gas, Low/High	Nut, Low/High	Total Test Period, minutes	Maximum Recorded Leak Rate, 10^{-7} atm cc/sec
6	R2		12	1200	-320/620	-110/380	55	2.9[b]
			13-24	2200	-320/667	-137/390	50	0
			25-32	2000	-320/1225	928	70	0
9	R41	840	1	2000	-320/1444	-320/1210	50	0
			2	2000	-320/1530	-320/1270	50	0
			3	2000	-320/1400	-320/1040	50	0

(a) Because of machine sensitivity, the lowest leak rate recorded was .04 x 10^{-7} atm cc/sec. The actual leak rate was probably lower, and is designated by zero.

(b) Leak detector was flooded with helium and did not record properly.

extreme thermal cycling should be conducted in an effort to find the temperature limitations of the René 41 seal. Three cycles were completed between -320 and about 1450 F. No leakage was recorded.

Although this particular fitting structure cannot be specified for such extreme temperature service without reducing the allowable imposed loads and without specifying a service time, the ability of the fitting to withstand such a severe thermal shock shows that the basic fitting configuration can be designed for approximately 1500 F service.

Repeated Assembly

Fitting No. 7 was assembled 25 times with a torque of 840 lb-in. Seals Nos. 5, 10, 20, and 24 were leak tested at 2000 psi. Seal No. 25 was leak tested at 3000 psi, the proof-pressure rating. Seals Nos. 10 and 24 were not nickel plated, whereas the other three were. No leakage was recorded with any seal tested. The OD of the plain stub end flange was measured after each assembly. No measurable change occurred. Thread galling became noticeable on the 17th assembly but did not become severe until the 24th. However, even after the 25th assembly it was still possible to run the nut onto the threaded flange by hand.

Fitting No. 12 was assembled 21 times with a torque of 1020 lb-in. Seals Nos. 1, 9, 10, 20, and 21 were tested at the proof pressure of 3000 psi. Seals Nos. 9 and 20 were not plated. Again zero leakage was recorded in all tests and again the OD of the stub end flange was unchanged. However, thread galling became noticeable after only 11 assemblies, and after a few more assemblies it was not possible to run the nut onto the threaded flange by hand. The male threads on the threaded flange were chased with a thread file and this relieved the galling. However, because the nut threads had not been re-machined, thread galling increased until the final assemblies were again quite difficult.

Undoubtedly the difference in repeated-assembly results between the two fittings was caused by the difference in torque. Because the recommended torques are 780 lb-in. minimum and 900 lb-in. maximum, and because 1040 lb-in. represents the overtorque limit, the results reported above indicate that repeated assembly should not present a problem.

Stress Reversal

Fittings Nos. 7 and 8 were tested with René 41 seals in the preliminary stress-reversal experiments. These experiments were performed prior to the operational service experiments to evaluate the effects of nut orientation. Fitting No. 7 was oriented as in Figure 100a, and Fitting No. 8 was oriented as in Figure 100b. It was specified[*] that the fitting should be capable of withstanding a reverse stress equivalent to 75 per cent of the yield stress of the tubing material for 200,000 cycles at 1000 cpm. Although the fitting was fabricated from René 41, it is assumed that the tubing system will be stainless steel for the first installations. The yield stress of annealed stainless steel at 600 F is approximately 29,200 psi. The allowable stress level would, therefore, be 21,900 psi. The actual stresses imposed and the results of the leak tests, conducted at the end of each cycling period, are given in Table 23. Fitting No. 7 was originally cycled

---

[*]Paragraphs IIC3f and III2g of Contract AF 04(611)-8176.
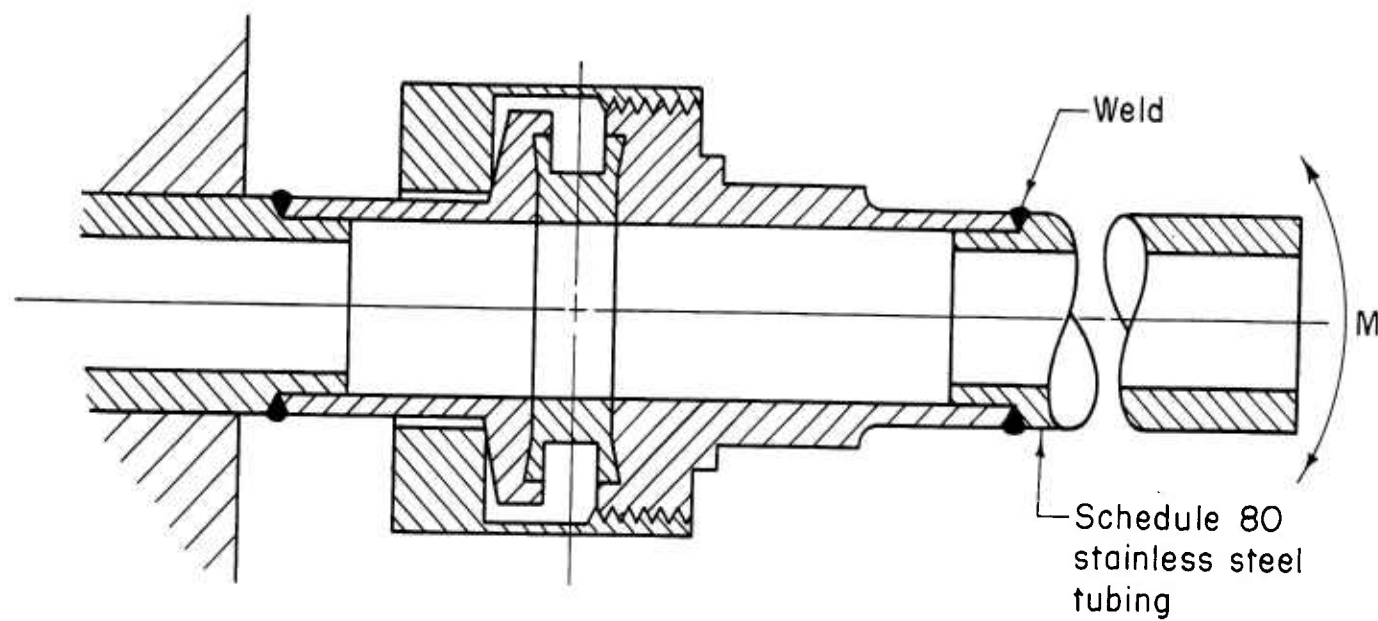
a. Fittings Nos. 7, 9, 11,
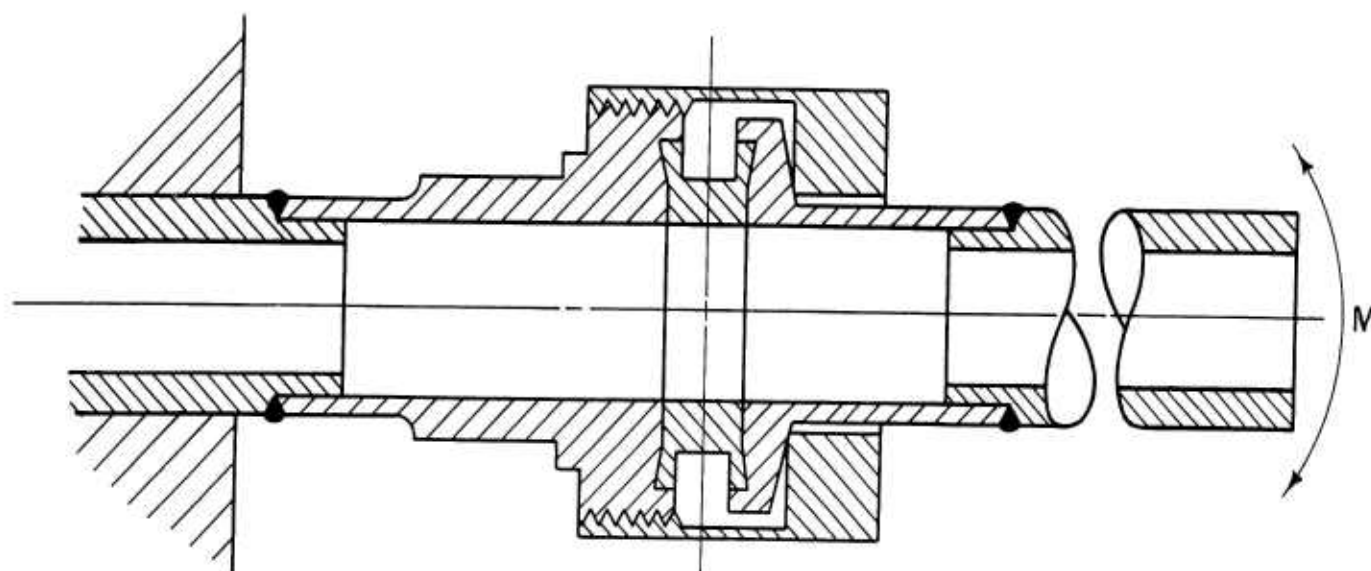
b. Fitting No. 8, 10,

A 45350

FIGURE 100. ORIENTATION OF NUT DURING STRESS-REVERSAL
AND OPERATIONAL TESTS

183

200,000 times at approximately half the allowable stress, to check out the equipment and the procedure. Three subsequent tests of 200,000-cycle duration were conducted at varying stress levels at room temperature. A fifth test of 200,000 cycles at 600 F was also successfully completed.

TABLE 23. CONDITIONS OF STRESS-REVERSAL TESTS AND LEAK-TEST RESULTS

Fitting No.	Assembly Torque, lb-in.	Nut Temp, F	Maximum Tensile[a] Stress, psi	Maximum Compressive[a] Stress, psi	Cycles	Gas Pressure, psi	Maximum Leak Rate, 10^{-7} atm cc/sec
7	840	RT	7,790	8,430	200,000	2000	0
		RT	20,320	18,820	200,000	2000	0
		RT	21,200	20,200	200,000	2000	0
		RT	29,200	26,000	200,000	2000	0
		600	20,320	20,200	200,000	2000	0
8	960	RT	25,300	22,600	200,000	2000	0
		RT	24,000	21,400	540,000	500	9
						1000	110
						2000	Excessive

(a) Based on .035 in.-wall stainless steel tubing.

Fitting No. 8 was assembled at a slightly higher torque and tested successfully for the required 200,000 cycles at room temperature at an average stress of 24,000 psi. A subsequent test for 540,000 cycles at room temperature and an average stress of 22,700 psi developed a leak. Although the fitting could almost seal adequately at 500 psi and the leakage at 1000 psi was only about 10^{-5} atm cc/sec, the leakage at 2000 psi was excessive. Because the leakage rate was not monitored during the stress-reversal tests, it is not known how many cycles caused the leakage to be measurable. During future test programs, a means of monitoring the leakage during the test should be devised. A possible method would be use of a bellows vacuum chamber which would deflect easily without adding to the rigidity of the tubing and fitting assembly.

Operational Evaluation

To provide an indication of operational capability, a fitting was put through four types of tests: 200,000 cycles of vibration at 35 g's, 200,000 cycles of reverse bending at 600 F, three types of thermal cycles (see Table 24), and 5 minutes at 3000-psi proof pressure. At the end of the reverse-bending tests, the fitting was tested for leakage with 2000-psi helium. During the thermal cycling and the proof-pressure tests, the leakage of the fitting was monitored constantly. For the thermal cycling, 2000-psi helium was used.

Fittings Nos. 9 and 10, assembled with René 41 seals, successfully completed two series of operational tests without leaking. This was equivalent to 1 hour of vibration at 35 g's, 400,000 cycles at an average stress of 24,000 psi at 600 F, approximately 14 thermal cycles, and 10 minutes at 3000-psi proof pressure.

184

TABLE 24. RESULTS OF OPERATIONAL TESTS

Fitting No.	Seal No.	Assembly Torque, lb-in.	Vibration[a]	Stress Reversal[b] (Nut Temperature)	Thermal Temperature, F		Leak Rate, 10^{-7} atm cc/sec
8	SS1	840	Test 1 Yes	Yes (600)		86	0
						-65	10
						-320	>300
						-155	150
						73	>300
9	D1	840	Test 1 Yes	Yes (RT)	Cycles 1-2	86/-320	0
					Cycles 3-5	86/600	0
					Cycles 6-11	600/-320	0
			Test 2 Yes	Yes (600)	Cycles 1-2	73/-320	0
					Cycles 3-4	86/600	0
					Cycles 5-6	600/-320	0
					3000 psi	86	0
10	R2	900	Test 1 Yes	Yes (600)	Cycles 1-2	86/670	0
					Cycles 3-5	80/-320	0
					Cycles 6-7	650/-320	0
					3000 psi	80	0
			Test 2 Yes	Yes (600)	Cycles 1-2	80/-320	0
					Cycles 3-4	80/600	0
					Cycles 6-7	600/-320	0
					3000 psi	77	0
11	SS2	840	Test 1 Yes	Yes (600)		86	0
						-320	>>300
						86	0
						-320	>>300
						86	84

(a) Sweep 10-3000 cps twice in 12 minutes, vibrate at 142 cps for 24 minutes.

(b) 200,000 cycles at $\sigma_t = 20,300$ and $\sigma_c = 22,600$.

Conclusions

In terms of the performance criteria established by the contract and by the Phase II work, the following tentative conclusions can be stated:

Initial Seal Reliability. The mechanical toggle seal has shown an initial seal reliability for sealing helium that is far beyond our expectations. Not only did the varied dimensions of the D and E series seals give

excellent initial sealing, but, of the 29 seals assembled for the tests described in this section, 26 showed no measurable leakage on a leak detector with a 10^{-9} sensitivity. One of the remaining seals (R2) was not measured accurately at the beginning because of the condition of the leak detector. Two plated stainless steel seals showed excessive leakage on initial assembly. The cause of these leaks has not been determined. However, the fact that four of the seals tested were unplated stainless steel emphasizes the high reliability of the plated mechanical toggle seal.

Tightening Allowance. With a seal-seating torque of 480-600 lb-in., with minimum and maximum recommended torques at 780 and 900 lb-in., respectively, and with an overtorque limit of 1040 lb-in., the fitting has an exceptionally wide tightening-allowance capability.

Repeated Assembly. The fitting can be assembled 25 times with no problem if the recommended torque values are used and if a new seal is used each time.

Proof Pressure. The fitting can adequately sustain a proof-pressure test of 3000 psi.

Temperature Performance. With a René 41 seal, the René 41 fitting is satisfactory between -320 and 600 F. There is substantial evidence that the fitting may be satisfactory between -320 F and 1500 F under conditions where fluid pressures and/or dynamic loads are reduced. The temperature range with a stainless steel seal has not been clearly established.

Operational Service. With René 41 seals, the general performance of the fitting during the operational tests was good. However, two aspects need further clarification. First, the method of loading the plain stub end by the nut flange may make the fitting too sensitive to reverse bending. If so, this will have to be corrected. Second, a more realistic series of operational tests must be made with the fitting, and leakage of selected fittings must be monitored constantly during all tests. However, in view of the little modification that has been done with the fitting design, there is every reason to expect that the fitting will be able to pass any realistic operational test satisfactorily.

SUMMARY OF RECOMMENDATIONS

As a result of the work, the basis for the development of an improved family of mechanical fittings has been established. Five primary recommendations have been formulated:

Fitting-to-Fitting Connection

The reconnectable union should be either threaded or flanged. Threaded fittings should be limited to those sizes and classes which can be assembled with 2000 lb-in. torque or less. In no case should a threaded connection be used for fittings on tubing greater than 1-inch diameter.

Tube-to-Fitting Connection

The connection between the tube and the fitting should be a permanent joint made independent of the seal mechanism or the reconnectable union. Furthermore, the brazed or welded joining method developed by North American Aviation should be adapted to expedite qualification of a mechanical fitting.

Seal

Seals for flanged connections should be selected on the basis of the flange-design procedure described in this report. Seals for threaded connections should be based on the mechanical toggle principle, employing either outside or inside sealing surfaces.

Fitting Classes

For the threaded fittings, four classes should be specified on the basis of temperature range and maximum pressure. Flanged fittings in general should be designed to satisfy specific service conditions by application of the design procedure illustrated.

Follow-On Development Program

Because the soundness of the threaded-fitting concept, developed during the program, was demonstrated by the laboratory studies, a follow-on developmental program should include the following studies:

(1) The comparative features of outside and inside seals should be investigated further, and the performance of the lightweight 1/2-inch fitting made of René 41 should be evaluated.

(2) A line of René 41 fittings — unions, tees, elbows, and crosses — should be designed, fabricated, and evaluated.

(3) One-half-inch-tube fittings of a low-strength material, probably Type 347 stainless steel, should be designed, fabricated, and evaluated.

(4) Typical fittings should be designed for two or three other materials and for a few combinations of likely materials.

(5) Selection criteria for threaded fittings should be established.

APPENDIXES

APPENDIX I

CALCULATION METHODS FOR STRESSES AND DISPLACEMENTS

Introduction

Most of the calculation methods described herein have been used for many years in the design of flanged connections for pipelines and pressure vessels. In particular, the stress calculation method for outwardly projecting flanges was developed by Waters, et al. [1]*, in 1937 and for several years has been a mandatory appendix to the American Society of Mechanical Engineers Boiler and Pressure Vessel Code, Section VIII, "Unfired Pressure Vessels"[2]. Displacement calculations, in commercial flange design, are used only for unusual designs or critical conditions since, in general, the incentive for minimum-weight design does not exist in piping and pressure-vessel applications to the same degree as in missile components. The calculation methods described herein have not been generally applied to the design of small (2-in. tube diameter and under) fittings, insofar as the authors are aware.

The calculation methods are based on the usual assumptions in engineering elastic theory, viz., the material is homogeneous and isotropic, stresses are proportional to strains, and displacements are small. In addition, in some of the calculation methods, it is assumed that the shells are thin walled and that radial dimensions of circular plates are large compared with the plate thickness and, in flange design, the flange radial width is small compared with the inside diameter**.

In addition to the general assumptions of elastic plate and shell theory, several additional assumptions are made in flange-calculation methods, e.g., the effect of bolt holes in the flange ring can be neglected, the localized bolt loads are uniformly distributed along the bolt circle, and the effect of the external moment on the flange depends only on the product of the bolt load and the lever arm.

As in many engineering elastic-stress-analysis methods, local stress concentrations are not calculated. For example, the design method computes the stress in a bolt as W/A_B, where W is the total load*** and A_B is the total root area of the bolts. Actually, as is well known, there may be higher stresses at the thread roots, depending on the root radius, and high local contact stresses will generally exist. Similarly, in the case of nuts on threaded fittings or flanges on bolted fittings, there may be "notches" (e.g., re-entrant corners) where high stresses may exist and, in general, there will be areas in which high local contact stresses occur.

Another approximation involved in the calculation method is the estimate of the lever arm in the calculation of moments. The lever arm is generally assumed to extend between midpoints of loaded surfaces; in the actual fitting the lever arms may be

---

*References for Appendix I are listed on page 200.

**In small-size standard pipe flanges this theoretical assumption is not justified, since the radial flange width may be several times the flange inside diameter. In the minimum-weight designs considered, however, the assumption is justified even for small-size flanges.

***W is used for load in this Appendix, rather than F as used in the text, to avoid conflict with the calculation parameter F used in this Appendix.

significantly changed by small construction tolerances. In addition, lever arms may be significantly altered by small elastic deformations; fortunately, these lever arm changes are such as to reduce the lever arm and hence make the calculation methods conservative.

It should be apparent from the above discussion that the calculation methods presented here are intended as a guide to the engineering design of fittings rather than methods of accurately calculating the stresses in a fitting. The use of the methods is justified, in part, by successful application to similar designs over a period of many years. It must be recognized, however, that the proposed application to minimum-weight design involving high-strength, low-ductility materials includes conditions where little experience is available. Accordingly, test verification of some of the fittings is recommended.

Outwardly Projecting Flanged Cylinders

Stress Calculations

Figure 101 applies to the flanged stub end of threaded fittings and to flanges of bolted-flanged fittings. The moment applied to the flange is $M_0 = Wh_G$, where W is the total load. The stress calculation method used for this shape was developed by Waters, et al.[1], and forms a part of the ASME Boiler and Pressure Vessel Code[2], Section VIII, Appendix II, "Rules for Bolted-Flanged Connections". The calculation method gives maximum stresses in the flange per unit moment applied by the loading. The method is applicable to either loose or integral flanges; integral flanges may have either a tapered hub or uniform-wall hub. The calculation method gives three values of S/M_0: the longitudinal bending stress in the hub, the radial bending stress at the inside of the ring, and the tangential stress at the inside of the ring. The maximum stress is taken as the largest of these three stresses. The maximum stress per unit moment is then multiplied by the applied moment to find the maximum stress. The stress equations for the integral flanges are:

Longitudinal Hub Stress

$$\frac{S_H}{M} = \frac{f}{Lg_1^2 B'} \tag{35}$$

Radial Ring Stress

$$\frac{S_R}{M_0} = \frac{(4/3\ te + 1)}{Lt^2 B'} \tag{36}$$

Tangential Ring Stress

$$\frac{S_T}{M_0} = \frac{Y}{t^2 B} - Z\ \frac{S_R}{M_0}. \tag{37}$$

190
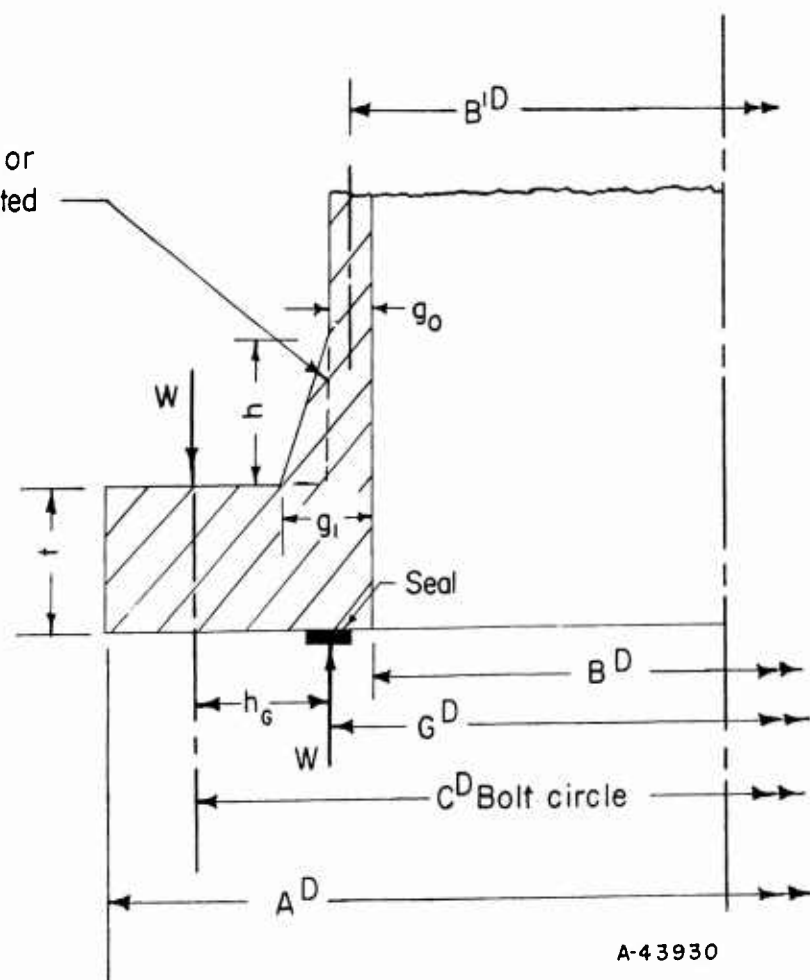
FIGURE 101.   DIMENSIONS OF AN OUTWARDLY PROJECTING FLANGE ATTACHED
             TO A CYLINDRICAL SHELL

For a loose ring flange, only one stress is calculated:

Tangential Ring Stress

$$\frac{S_T}{M_O} = \frac{Y}{t^2 B} \cdot \qquad (38)$$

The dimensional parameters A, B, B′, t, g_1, g_O and h are shown in Figure 101. Other parameters are: U, Y, Z, and T as functions of K = A/B as shown in Figure 102. F, V, and f are functions of g_1/g_O and $h/\sqrt{B′g_O}$, as shown in Figure 103 and Figure 104. Values of e, d, and L are obtained by the equations

$$e = \frac{F}{h_O} \qquad (39)$$

$$d = \frac{U}{V} h_O g_O^2 \qquad (40)$$

$$L = \left[\frac{te + 1}{T} + \frac{t^3}{d} \right], \qquad (41)$$

where $h_O = \sqrt{B′g_O}$.

Displacement Calculations

The rotation of the flange ring due to an applied moment, M_O, is given by Wesstrom and Bergh[3] as

$$\theta_m = \frac{0.91 \, V}{L h_O g_O^2 E} M_O , \qquad (42)$$

where V, L, h_O, g_O, and M_O are as defined in the preceding section on stress calculations and E is the modulus of elasticity of the flange material.

The axial displacement is $\theta_m h_G$, where h_G is the lever arm of the applied load as shown by Figure 101. The axial displacement of a bolted fitting with two identical flanges is $2\theta_m h_G$. Where the two flanges making up the joint are not identical, the total axial displacement is $(\theta_m + \theta_m′)h_G$ where θ_m and $\theta_m′$ are calculated by Equation (42) for the two flanges.

The rotation of the flange ring due to the radial component of the internal pressure is given by Rodabaugh[4] as

$$\theta_P = \frac{2.57 \times 10^{-8} B^2 \gamma}{t(t^2 + 1.82 \, g_e \gamma)} P , \qquad (43)$$
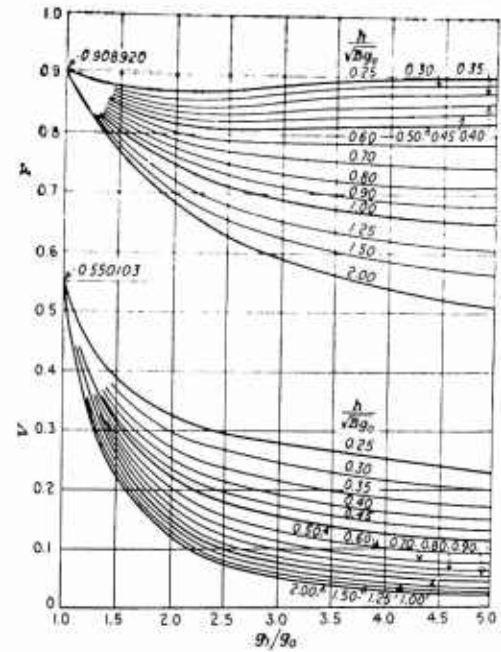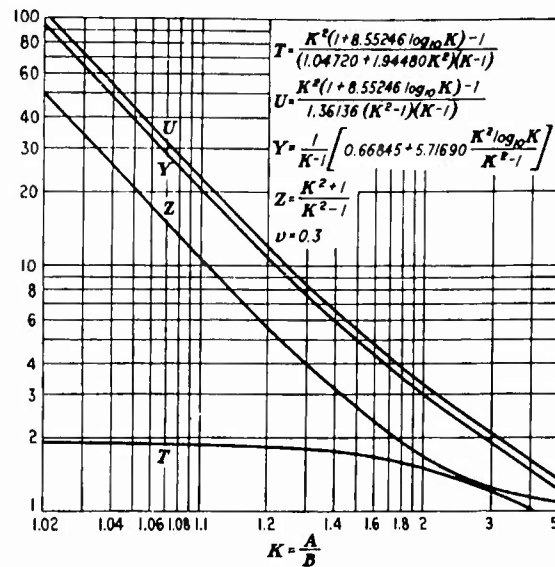
FIGURE 102.   VALUES OF T, U, Y, AND Z WHEN $\nu = 0.3$ FIGURE 103.   VALUES OF F AND V FOR AN INTEGRAL FLANGE
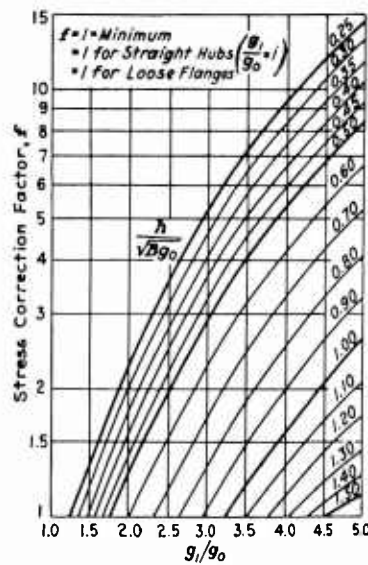
FIGURE 104.   VALUES OF STRESS-CORRECTION FACTOR

Figures 102, 103, and 104 are taken from Reference (1).

193

where

$$P = \text{internal pressure, psi}$$

$$\gamma = \frac{g_e(Z + 0.3)\left(1 + \dfrac{1.82\,t}{h_o{'}}\right)}{1 + \dfrac{Bg_e{}^3\,(Z + 0.3)}{h_o{'}t^3}\left(2 + \dfrac{1.82\,t}{h_o{'}}\right)}$$

(for $E = 3 \times 10^7$, $\mu = \text{Poisson's ratio} = 0.3$)

$$h{'}_o = \sqrt{Bg_e}$$

g_e = average hub thickness through a distance
from the back of the flange ring of

$$\sqrt{\frac{B(g_o + g_1)}{2}}\;.$$

Z, B, t, g_o and g_1 are defined in the preceding section on stress calculations.

The axial displacement in a bolted fitting with two identical flanges is $2\theta_p h_G$, where h_G is shown in Figure 101.

Under Equation (19) in the text of the report, in the definition of α, the term q_r is equal to θ_p/P. [Equation (19) is discussed in the last section of this Appendix.]

Inwardly Projecting Flanges

Figure 105 illustrates an idealized shape, consisting of a cylindrical shell with an inwardly projecting flange, which can be used in designing the nut on threaded fittings.

a.   b.

A-43931
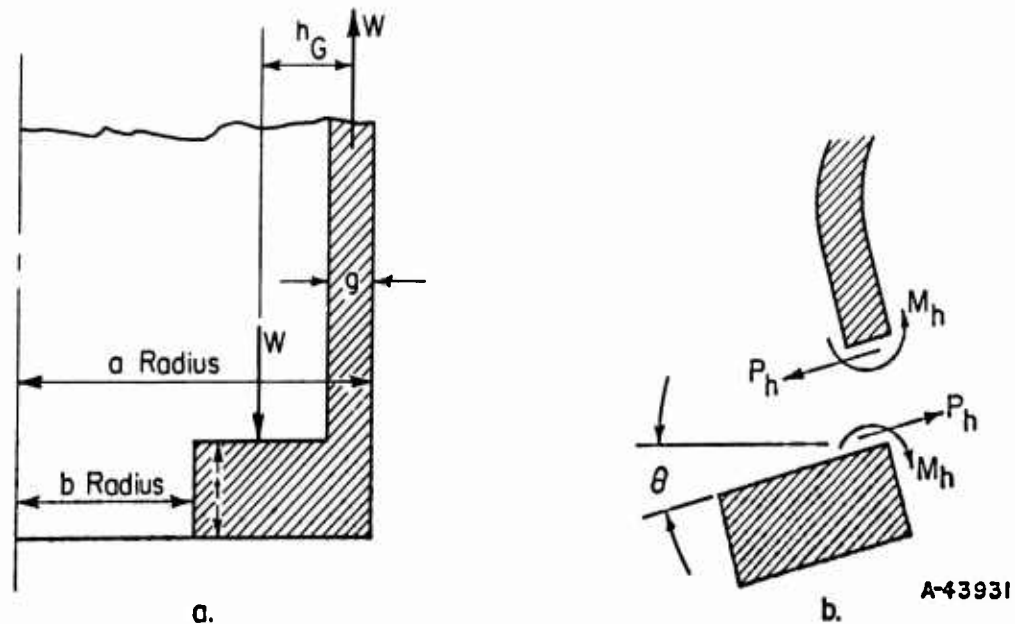
FIGURE 105.   INWARDLY PROJECTING FLANGED CYLINDER NOMENCLATURE

194

Stress Calculations

The moment applied to the flange ring in Figure 105a is $M_o = W \times h_G$ where W is the total load. Under the applied moment M_o, the flange will rotate as indicated in Figure 105b. There will be a moment M_h and a shear P_h acting at the juncture of the flange and the cylindrical shell; these are moments and forces per unit length.

The radial (outward) displacement w of the end of the cylindrical shell, loaded with end moment M_h and shear P_h, is given by Timoshenko[5] as

$$w = \frac{1}{2\beta^3 D} (P_h - \beta M_h) , \qquad (44)$$

where

$$\beta = \sqrt[4]{\frac{3(1 - \mu^2)}{a^2 g^2}}$$

$$D = \frac{E g^3}{12(1 - \mu^2)}$$

E = modulus of elasticity

μ = Poisson's ratio.

It is assumed that the relatively rigid flange does not undergo any radial displacement, hence

$$\frac{1}{2\beta^3 D} (P_h - \beta M_h) = 0 \qquad (45)$$

and

$$P_h = \beta M_h . \qquad (46)$$

The rotation of the end of a cylinder, loaded with an end moment M_h and shear P_h, is given by Timoshenko[5] as

$$\theta = - \frac{1}{2\beta^2 D} (P_h - 2\beta M_h) . \qquad (47)$$

The rotation of the flange ring is also given by Timoshenko[5] as

$$\theta = \frac{6 M_f (a + b)}{E t^3 \ln \frac{a}{b}} , \qquad (48)$$

where M_f, the moment applied to the ring per unit length of the ring center line, is

$$M_f = \frac{M_o}{\pi(a + b)} - M_h \frac{2a}{a + b} - P_h \frac{t}{2} \frac{2a}{a + b} . \qquad (49)$$

Since the rotation of the flange ring must be equal to the rotation of the end of the cylindrical shell, Equations (47) and (48) give

$$- \frac{1}{2\beta^2 D} (P_h - 2\beta M_h) = \frac{6 M_f (a + b)}{E t^3 \ln \frac{a}{b}} . \tag{50}$$

Substituting $P_h = \beta M_h$ from Equation (46) and M_f from Equation (49) in Equation (50):

$$\frac{M_h}{2\beta D} = \frac{6(a + b)}{E t^3 \ln \frac{a}{b}} \left[\frac{M_o}{\pi(a + b)} - M_h \left(\frac{2a}{a + b} \right) \left(1 + \frac{\beta t}{2} \right) \right] . \tag{51}$$

Solving Equation (51) for M_h:

$$M_h = \frac{M_o}{\pi \left[\dfrac{E t^3 \ln a/b}{12 \beta D} + 2a \left(1 + \dfrac{\beta t}{2} \right) \right]} . \tag{52}$$

Replacing D by its magnitude $E g^3 / 12 (1 - \mu^2)$,

$$M_h = \frac{M_o}{2\pi a \left[\dfrac{(1 - \mu^2)}{2\beta a} \left(\dfrac{t}{g} \right)^3 \ln \dfrac{a}{b} + 1 + \dfrac{\beta t}{2} \right]} . \tag{53}$$

Equation (53) gives M_h in terms of the loading ($M_o = W h_G$), the dimensions, and the material constant, μ. The maximum stress per unit applied moment are given by:

Longitudinal Hub Stress

$$\frac{S_H}{M_o} = \frac{3}{\pi a g^2 \left[\dfrac{(1 - \mu^2)}{2\beta a} \left(\dfrac{t}{g} \right)^3 \ln \dfrac{a}{b} + 1 + \dfrac{\beta t}{2} \right]} \tag{54}$$

Radial Ring Stress

$$\frac{S_R}{M_o} = \frac{3 \left(1 + \dfrac{\beta t}{2} \right)}{\pi a t^2 \left[\dfrac{(1 - \mu^2)}{2\beta a} \left(\dfrac{t}{g} \right)^3 \ln \dfrac{a}{b} + 1 + \dfrac{\beta t}{2} \right]} \tag{55}$$

Tangential Ring Stress

$$\frac{S_T}{M_o} = \frac{3(1 - \mu^2)t}{2\pi a b g^3 \beta \left[\dfrac{(1 - \mu^2)}{2\beta a} \left(\dfrac{t}{g} \right)^3 \ln \dfrac{a}{b} + 1 + \dfrac{\beta t}{2} \right]} . \tag{56}$$

196

Displacement Calculations

The rotation of the flange ring due to an applied moment, M_o, is given by Equation (47) and using $P_h = \beta M_h$ from Equation (46):

$$\theta = \frac{M_h}{2\beta D} \ .$$

(57)

The magnitude of M_h is given in terms of M_o by Equation (53). θ in terms of M_o is then

$$\theta_m = \frac{3(1 - \mu^2) \, M_o}{\pi a \beta g^3 E \left[\frac{(1 - \mu^2)}{2\beta a} \left(\frac{t}{g} \right)^3 \ln \frac{a}{b} + 1 + \frac{\beta t}{2} \right]} \ .$$

(58)

The axial displacement is $\theta_m h_G$.

Parts in Tension or Compression

Parts which are considered to be loaded in tension or compression are:

Bolts of bolted fittings (tension)

Cylindrical shell portion of nut in threaded fittings (tension)

Flanges of bolted fittings (compression)

Threaded stub end of threaded fittings (compression)

Flange of flanged stub end of threaded fittings (compression)

Seals (compression).

Stress Calculations

The general expression for stress in parts subjected to tension or compression is

$$S = \frac{W}{A} \ ,$$

(59)

where
W = total load, lb

A = cross-sectional area perpendicular to load, in.^{2}

For bolts:

$$A = A_b = A_{bl} \times n$$

where

A_{bl} = cross-sectional area at root of threads for one bolt, in.^{2}

n = number of bolts

. A_b = total bolt area.

Displacement Calculations

The general expression for displacement in parts subjected to tension or compression is

$$\delta = \frac{W\ell}{AE} \; , \tag{60}$$

where

W = total load, lb

ℓ = axial length, in.

E = modulus of elasticity of material, psi

A = cross-sectional area perpendicular to load, in.^{2}

Threads in Threaded Fittings

The nominal shear stress on the threads, S_T, is

$$S_T = \frac{W}{A_T} \; , \tag{61}$$

where

A_T = 0.80 $\ell\pi$D, in., where the 0.80 is an approximate factor to account for thread clearances of the buttress or NF threads used in the threaded fittings.

ℓ = thread length, in.

D_p = thread pitch diameter, in.

Bending stresses and local contact stresses in the threads will, of course, be substantially higher than the nominal shear stress. The thread length should be ample to keep these local stresses at a tolerable level.

General Displacement Equation for Bolted Fittings, Equation (19) of Text

Equation (19) of the text (with F changed to W for nomenclature of this Appendix) is

$$W_2 = W_1 + \alpha P ,$$

where

P = internal pressure, psi

$$\alpha = \frac{\pi h_G}{4Q} \left\{ \left[\frac{q_G}{h_G} - 2q_F (h_T - h_G) \right] G^2 - 2q_F B^2 (h_D - h_T) - \frac{8}{\pi} q_r \right\}$$

$$Q = q_B + q_G + 2q_F h_G^2$$

$$q_B = \frac{\ell_o}{A_B E_B}$$

$$q_G = \frac{V_o}{A_G E_G}$$

$$q_F = \frac{0.91 \, V}{L h_o g_o^2 E_F} \text{ (integral flanges) or } \frac{0.829}{t^3 E_F \log \frac{A}{B}} \text{ (loose ring flanges)}$$

$$q_r = \frac{\theta_P}{P} \text{ where } \theta_P \text{ is defined by Equation (43)}$$

ℓ_o = bolt length, in.

V_o = seal thickness (in axial direction), in.

A_B = total bolt area, sq in.

A_G = total gasket area, sq in.

E_B, E_G, E_F = modulus of elasticity of bolt, seal, and flange material, respectively.

$h_G = 1/2 \, (C-G)$

$h_D = 1/2 \, (C-B)$

$h_T = 1/2 \, (h_D + h_G)$

Dimensions A, B, C, G, t, and g_o are shown in Figure 101. L, V, and h_o are defined in the first section of the Appendix under "Outwardly Projecting Flanged Cylinders".

References

(1) Waters, E. O., Wesstrom, D. B., Rossheim, D. B., and Williams, F.S.G., "Formulas for Stresses in Bolted Flanged Connections", ASME Transactions (1937).

(2) American Society of Mechanical Engineers Boiler and Pressure Vessel Code, Section VIII, "Unfired Pressure Vessels", American Society of Mechanical Engineers, 345 East 47th Street, New York 17, N. Y. (1959).

(3) Wesstrom, D. B., and Bergh, S. E., "Effects of Internal Pressure on Stresses and Strains in Bolted-Flanged Connections", ASME Transactions (1951).

(4) Rodabaugh, E. C., discussion of Reference (3).

(5) Timoshenko, S., Strength of Materials, Part II, D. Van Nostrand Co., 250 Fourth Avenue, New York 3, N. Y.

APPENDIX II

DISCUSSION OF DESIGN FOR CREEP OR RELAXATION

Since mechanical tube connections of the types discussed are highly strain sensitive at higher temperatures, plastic flow as a function of time, i.e., creep or relaxation, becomes a dominant factor in design. The basic problem of the relaxation of a bolt in a rigid flange has been considered by several investigators[1-4]*. The method proposed here has been selected because of its simplicity in design application and because of the limited available data on the newer alloys, such data being confined to tensile creep tests with no available relaxation-test data.

The elastic displacement of any part of the structure is proportional to the elastic strain at that time, i.e.,

$$\delta = K\epsilon . \tag{62}$$

In a member with uniform stress, such as the bolts in tension, K is independent of plastic deformations. In the flanges, however, K is a function of plastic deformations since such deformation redistributes the stress. A conservative[5] assumption is that K is a constant for all parts of the fitting and ϵ is the maximum strain corresponding to the maximum calculated elastic stress. Use of K as a constant for all parts of the fitting implies that:

(1) All parts of the fitting operate at the same maximum stress level. (This may be accomplished by appropriate design of the fitting; however, if this is not the case, an alternative method is indicated later in this Appendix.)

(2) All parts are made of the same material.

(3) All parts operate at the same temperature.

(4) In parts subjected to bending stress, relaxation does not alter the stress distribution.

With the assumption of constant K:

$$\text{at } t = 0: \quad \delta_o = K\epsilon_o \tag{63}$$

$$\text{at } t = t: \quad \delta_t = K\epsilon_t , \tag{64}$$

where t = time, hr. The difference between δ_o and δ_t is the plastic displacement occurring in time t, giving

$$\delta_o - \delta_t = \delta_p \tag{65}$$

$$K\epsilon_o - K\epsilon_t = K\epsilon_p . \tag{66}$$

*References for Appendix II are listed on page 211.

201

The elastic strains ϵ_o and ϵ_t are proportional to the stresses S_o and S_t, giving

$$\epsilon_t = \epsilon_o \frac{S_t}{S_o} \tag{67}$$

Substitute ϵ_t from Equation (67) in Equation (66):

$$\epsilon_p - \epsilon_o \left(1 - \frac{S_t}{S_o}\right) = O \quad . \tag{68}$$

Differentiating Equation (68) with respect to time:

$$\frac{d\epsilon_p}{dt} + \frac{\epsilon_o}{S_o} \frac{dS_t}{dt} = O \quad . \tag{69}$$

The values of $d\epsilon_p/dt$ in Equation (69) are best obtained from relaxation tests of the material at the required temperature. However, in the absence of relaxation-test data, $d\epsilon_p/dt$ may be obtained from creep-test data, particularly when the effect of first-stage creep is handled separately. While Equation (69) could be integrated graphically from creep-test data, in order to expedite design work it is desirable to express $d\epsilon_p/dt$ analytically. A widely used expression is

$$\frac{d\epsilon_p}{dt} = C_1 S_t^n \quad , \tag{70}$$

where

ϵ_p = plastic strain, in in.

t = time, hr

S_t = stress, psi.

C_1 and n are material constants and are functions of the temperature. These constants can be obtained empirically from a series of creep tests of the material at the required temperature and at various stress levels.

The expression for $d\epsilon_p/dt$ in Equation (70) is independent of time; this is approximately true for second-stage creep but is not valid for first- or third-stage creep. The design method covers the effect of first-stage creep by means of a pseudo modulus of elasticity, E^1, obtained directly from experimental creep data by extrapolating the second-stage creep back to zero time as indicated by Figure 106.
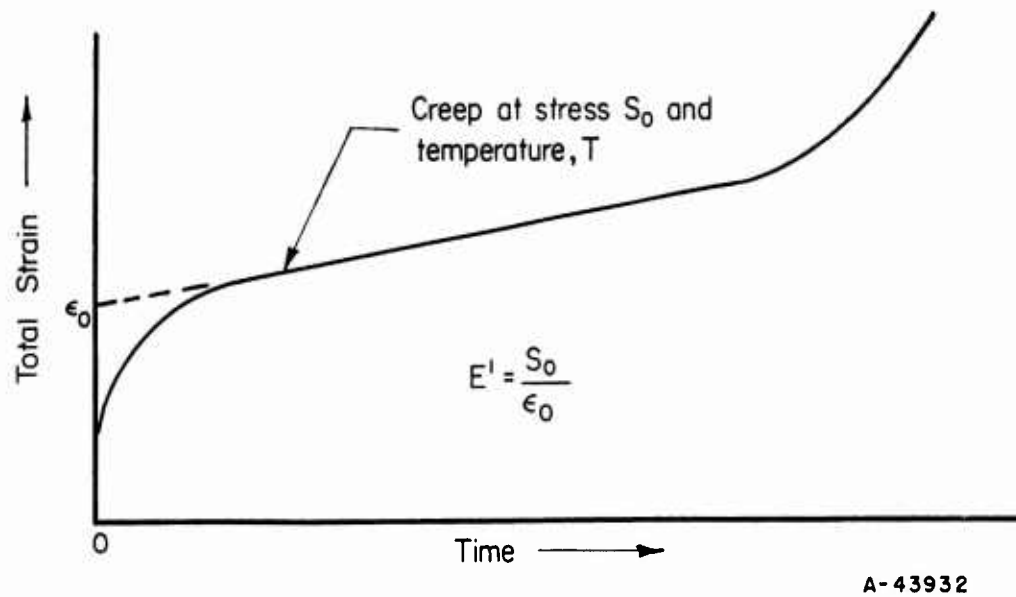
FIGURE 106. METHOD OF ESTABLISHING VALUE OF E^1

The initial preload F_1 is considered to be reduced (in zero time) to a new value $(F_1)_T$ as given by the equation

$$(F_1)_T = F_1 \times \frac{E^1}{E_r} \quad , \tag{71}$$

where E_r is the modulus of elasticity at room temperature, i.e., the temperature at which the preload F_1 was applied to the fitting.

Since the fitting structure by its nature is limited to very small strains, it is unlikely that third-stage creep will be encountered; hence, Equation (70) is adequate for the particular design problem.

Since $\epsilon_o / S_o = 1/E_T$, where E_T is the modulus of elasticity at the design temperature, inserting this relationship along with $d\epsilon_p / dt = C_1 S^n$ in Equation (69) we obtain

$$C_1 S_t^n + \frac{1}{E_T} \frac{dS}{dt} = 0 \quad , \tag{72}$$

which may be written

$$dt = - \frac{dS}{C_1 E_T S_t^n} \tag{73}$$

By integrating Equation 73:

$$t = \int_0^t dt = - \frac{1}{C_1 E_T} \int_{S_o}^{S_t} \frac{dS}{S_t^n} \quad . \tag{74}$$

$$t = \frac{1 - \left(\frac{S_t}{S_o}\right)^{n-1}}{C_1 E_T (n-1) S_t^{n-1}} \tag{75}$$

Equation (75) is the well-known equation for relaxation of a bolt under constant total strain. However, it was derived here to be applicable to a connection consisting of several parts, made of the same material, each of which is subjected to the same stress and temperature and where it is assumed that the stress-displacement relations do not change as a result of loadings* or creep. The restriction to the theory that all parts are operating at the same stress can be removed by a relatively simple extension of the theory. If the connection is considered as three parts (flanges, bolts, seal of a bolted-flanged connection), the equation for calculating service life becomes

$$t = \frac{\left[1 + \frac{K_2}{K_1} + \frac{K_3}{K_1}\right]\left[1 - \left(\frac{S_t}{S_o}\right)^{n-1}\right]}{\left[1 + \left(\frac{K_2}{K_1}\right)^n + \left(\frac{K_3}{K_1}\right)^n\right] C_1 E_T (n-1) S_t^{n-1}} \quad , \tag{76}$$

where the K's are defined by the elastic displacement-stress relations: $\delta_1 = K_1 S^1$, $\delta_2 = K_2 S^1$, $\delta_3 = K_3 S^1$ for flanges, bolts, and seal**, respectively, and S^1 is the stress in the flanges.

Removal of the restriction that all parts of the connections be made of the same material and operate at the same temperature requires considerable additional design effort since the resulting equation,

$$dt = \frac{-\left(1 + \frac{K_2}{K_1} + \frac{K_3}{K_1}\right) dS'}{C_{11} S_t^{n1} + C_{12}\left(\frac{K_2}{K_1} S_t'\right)^{n2} + C_{13}\left(\frac{K_3}{K_1} S_t'\right)^{n3}} \quad , \tag{77}$$

with the n's all different and noninteger, must be numerically or graphically integrated.

The removal of the restriction that the stress-displacement relations, for parts in bending, do not change with creep presents formidable difficulties. Some progress on this problem[5-6] has been made for the case of a ring in torsion. However, even for this comparatively simple structure numerical integration methods are required. The case of the ring with attached cylindrical shell is much more complex.

---

*Actually, the stresses in a fitting structure do vary with loads. The stress variation in the parts that contribute most to relaxation (bolts and flanges in bolted fittings, nuts and stub ends in threaded fittings), however, is relatively small. The stress in the seal decreases with increasing internal pressure so that the assumption that stress in the seal does not vary with loads is generally conservative from the standpoint of relaxation.

**It should be recognized that the K's may be functions of the internal pressure and external loads.

The theoretical refinements discussed above, along with other desirable refinements to the theory, are not within the scope of this project. Accordingly, the preliminary design work has been based on the simplified concept described above with the expectation that, due to a number of conservative assumptions, the resulting designs will be adequate.

Application of Creep-Design Procedure

The design procedure at temperatures where creep or relaxation is a dominant factor is essentially one of establishing pressure-time ratings at a specified temperature for a given fitting; i.e., a fitting with all dimensions established and made of a specified material. In this discussion, the "given fitting" is shown in Figure 107.

As noted previously, René 41 was selected as the recommended material for high-temperature design. The design analysis uses creep data from Figure 3.042 of Reference (7), "Master Curves for Creep and Creep Rupture for Sheet and Bar". Specifically, the data for bar stock, heat treated at 2150 F for 2 hours, air cooled and aged at 1650 F for 4 hours, were used. These data are given in the form of stress versus the Larson-Miller parameter $(T + 460)(20 + \log_{10}t)$, for the 0.2 per cent creep condition. With the assumption that $d\epsilon/dt$ is independent of time, the data can be converted to a graph of $d\epsilon/dt$ versus stress at 1500 F, as shown in Figure 108.

The relationship between creep rate and stress in the creep-stress range of 10,000 to 60,000 psi can be conservatively approximated by the equation

$$\frac{d\epsilon_p}{dt} = 1.3 \times 10^{-26} S^{4.82} \quad , \tag{78}$$

where

ϵ_p = strain, in./in.

t = time, hr

S = stress, psi.
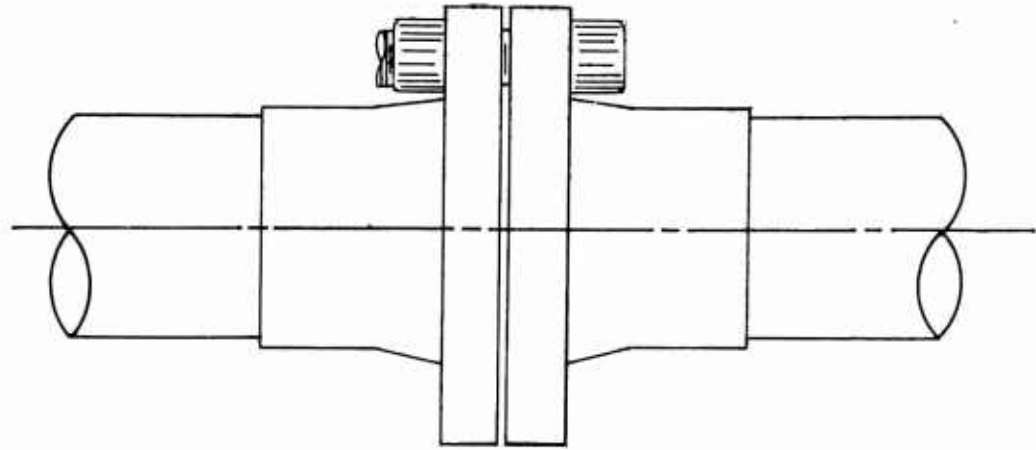
Actual size
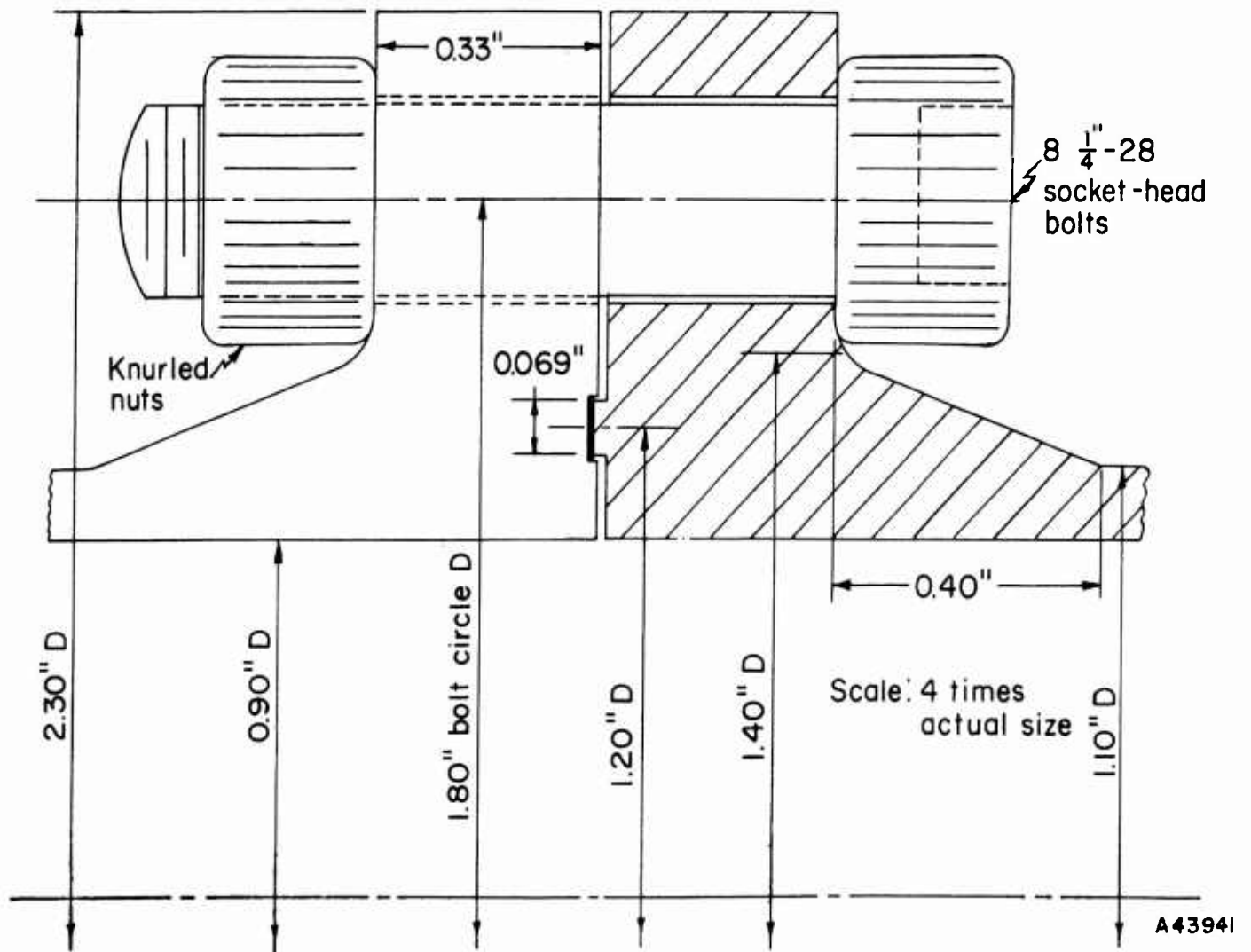
FIGURE 107. 1-IN. BOLTED FITTING

A43941
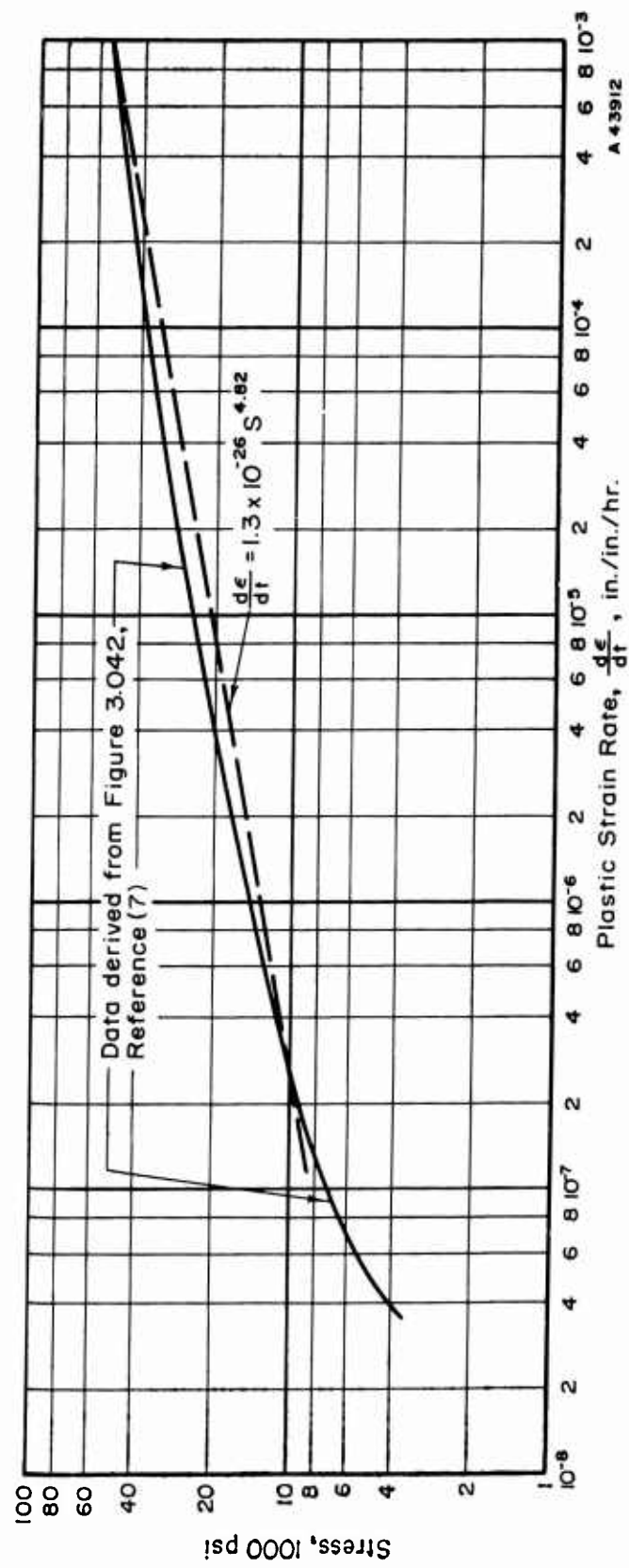
FIGURE 108. CREEP RATE OF RENÉ 41 BAR AT 1500 F

207

Equation (78), plotted in Figure 108, is of the form $\dfrac{d\epsilon_p}{dt} = C_1 S_t^n$, which forms the basis for the previous development. Additional data on René 41 needed for the analysis is presented in Table 25.

TABLE 25. DESIGN PROPERTIES OF RENÉ 41

	70 F	1500 F
Yield Strength[a], psi	120,000	97,000
Modulus of Elasticity, psi	3.2×10^7 (E_r)	2.4×10^7 (E_T)
Coefficient of Thermal Expansion, per F	6.8×10^{-6}	8.5×10^{-6}
Pseudo-Modulus[b], E^1, psi, Approximately 1.6×10^7 at $S_o = 60,000$ psi and 1500 F		

(a) From Reference (8).
(b) From Reference (9).

The creep design procedure will be applied to the bolted flanged joint with the dimensions shown in Figure 107. The procedure is characterized by the following steps: (1) determine maximum preload at room temperature, (2) determine effective preload at 1500 F, steady state, (3) compute a time-versus-residual-bolt-stress curve, and (4) consolidate maximum operating pressure corresponding to the residual bolt stresses for both steady state and transient thermal conditions.

Because maximum service life is obtained with the application of maximum initial preload, the bolts are considered to be initially tightened to their yield strength of 120,000 psi. The flanged joint shown in Figure 107 has eight 1/4-28 bolts, each bolt having a cross-sectional area at the root of the threads of 0.0326 square inch. The total cross-sectional area of the bolts of the flanged joint shown in Figure 107 is therefore 8 x 0.0326 or 0.261 square inch. The total bolt load corresponding to 120,000-psi bolt stress is then 120,000 x 0.261 = 31,400 lb. By using the stress-calculation methods shown in Appendix I, it can be shown that a total bolt load of 31,400 lb, applied to the flanged joint shown in Figure 107, produces a controlling stress in the flanges of 116,500 psi. Since this stress is almost equal to the bolt stress of 120,000 psi, it will be assumed that the initial stress in both the bolts and the flanges is 120,000 psi. This assumption permits the use of Equation (75) to calculate service life, t, rather than the more complex Equation (76). In the following, the decrease in bolt stress as a function of time will be determined; it should be kept in mind that this decrease in bolt stress is due to creep of all parts of the joint, not the bolts alone.

As the temperature is increased from ambient to 1500 F, the initial preload is reduced by a factor E^1/E_r, where E^1 is the pseudo-modulus of elasticity of 1500 F and E_r is the modulus of elasticity at room temperature. Gross yielding does not occur, since the yield strength decreases at a lesser rate than does the modulus of elasticity.

The values of the constants in Equation (75) for René 41 at 1500 F are: $C_1 = 1.3 \times 10^{-26}$, $n = 4.82$, and $E_T = 2.4 \times 10^7$. The bolt preload at 1500 F is one-half the initial preload of 120,000 psi; that is, S_o is 60,000 psi. By substitution of these values, Equation (75) becomes

$$t = \frac{1 - \left(\dfrac{S_t}{60,000}\right)^{3.82}}{(1.19 \times 10^{-18})(S_t)^{3.82}} \quad , \tag{79}$$

where S_t = residual stress in the bolts after t hours of service life.

The effective residual bolt load at any time is simply S_t multiplied by the bolt area of the flanged joint shown in Figure 107.

$$F = A_B S_t = 0.261 \, S_t \, . \tag{80}$$

Arbitrary values may be assigned to S_t and the corresponding time required for the stress to relax from 60,000 psi to the chosen value can be calculated from Equation (79). The corresponding residual bolt load given by Equation (80) can also be calculated for each assigned values of S_t. The structural loads carried by the connection, with this effective residual bolt load, can then be computed by the method outlined earlier, where temperature effects did not involve creep.

As an example, assume that S_t is assigned a value of 40,000 psi. From Equation (79), t is found to be 1.74 hours; i.e., it will take 1.74 hours for the bolt stress to decrease from 60,000 psi to 40,000 psi. From Equation (80), with $S_t = 40,000$, the residual bolt load at the end of 1.74 hours is 10,430 lb.

The residual bolt load of 10,430 lb at the end of 1.74 hours may now be considered as if it were an initial applied bolt load F_1. By using the method discussed earlier in designs in which creep was not a factor, a design pressure P corresponding to an initial load F, can be obtained. For the bolted fitting shown in Figure 107, the significant factors may be expressed by the equation

$$F_1 = F_i + \frac{\dfrac{R_B}{R_G} F_s}{1 + \dfrac{R_B}{R_G}} + \frac{2qh_G}{Q} P \quad , \tag{81}$$

where

F_1 = 10,430 lb (in this particular example).

F_i = seal load which, in the design procedures, is required to be such that the seal stress is not less than 3 times the pressure. On this particular bolted fitting, the seal area (See Figure 107) is 0.281 sq in., hence, a minimum value of F_i is 0.281 x 3 x P = 0.783 P.

R_B and R_G = spring constants of the bolted fitting discussed in the section "Preload".

F_s = structural load. This load is the sum of the hydrostatic end load, which is proportional to the pressure, and an external bending-moment load[*], which, while not necessarily proportional to the pressure, is considered as such in this evaluation.

---

[*] The bending-moment design limits at high (over 600 F) temperatures should be further investigated before final designs are established.
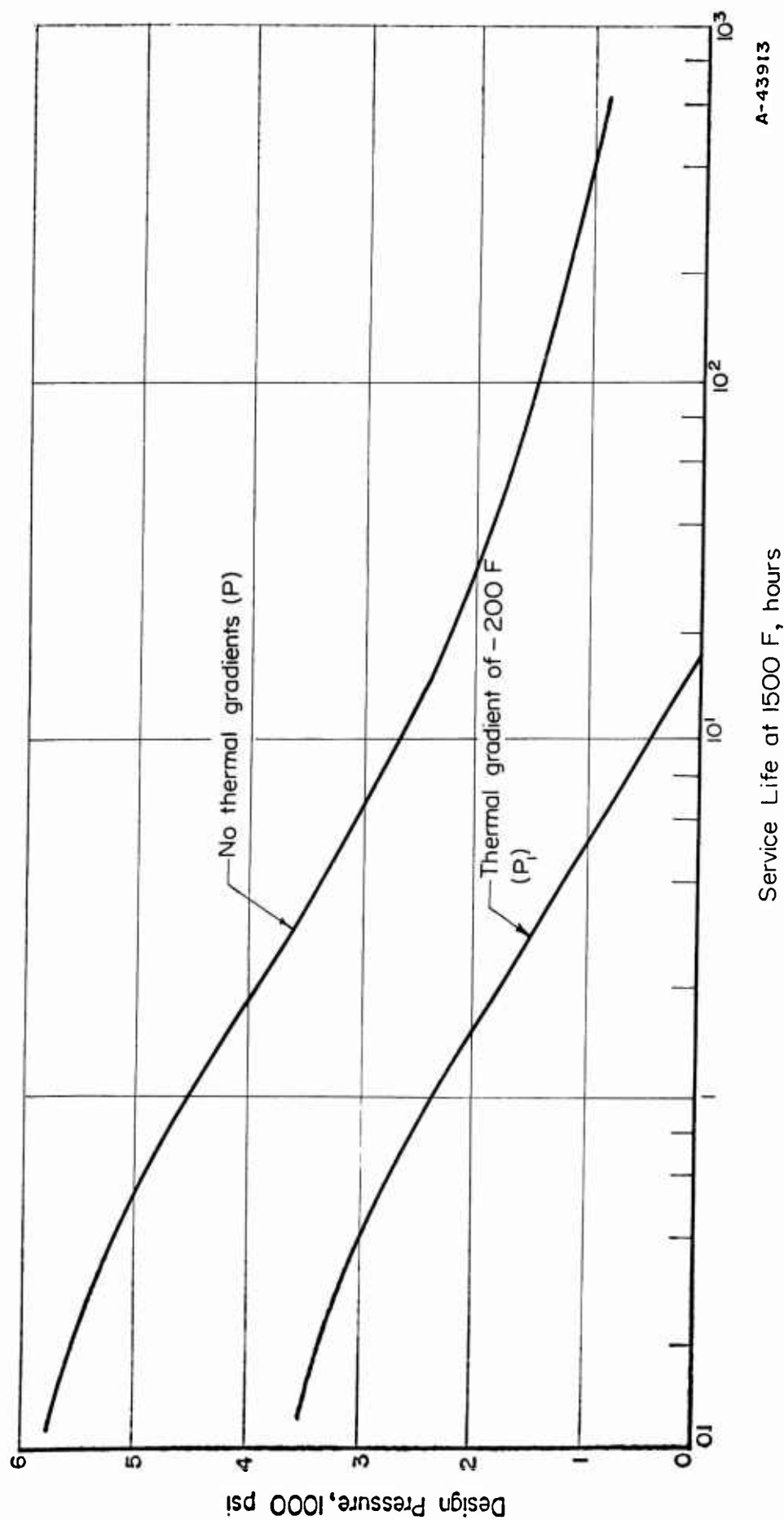
FIGURE 109. PRESSURE-SERVICE LIFE RATINGS OF THE BOLTED FITTING SHOWN IN FIGURE 107

A-43913

210

$\dfrac{2qh_G}{Q}$ = displacement characteristic of the bolted fitting giving bolt-load decrease due to the radial effect of internal pressure [See last term in definition of α under Equation (19).]

When the displacement characteristics are evaluated for the bolted fitting shown in Figure 107, and taking F_s as 1.9 P (its value in the temperature range -425 to 600 F), and using the design limit $F_i = 0.783$ P, Equation (81) becomes

$$F_1 = 0.783 \, P + 1.585 \, P + 0.206 \, P \quad . \tag{82}$$

For $F_1 = 10,430$ lb, Equation (82) gives P = 4050 psi. This means that the maximum design pressure for the bolted fitting shown in Figure 107, operating at 1500 F for 1.7 hours, is 4050 psi. A series of such calculations has been made for different values of S_t; the results are shown graphically in Figure 109.

The above analysis assumed that there were no temperature gradients in the flanged joint which, in general, probably is not a correct assumption. A critical condition occurs when the bolt load relaxes to 10,430 lb near the end of the service life along with a temperature fluctuation at that time which causes the flanges to be 200 F (design limit) cooler than the bolts. Under these conditions there will be a relative bolt expansion of:

$$\Delta T = 200 \times 0.86 \times 8.5 \times 10^{-6} = 1.46 \times 10^{-3} \text{ in.}$$

The residual bolt load, F_1, is further reduced by this thermal gradient from 10,430 lb to 4900 lb; the corresponding design pressure, P_1, must therefore be limited to 1900 psi. Figure 109 shows P_1 plotted against service life, P_1 being the maximum design pressure where the design procedure includes a 200 F thermal gradient.

References

(1) Marin, Joseph, Engineering Materials, Prentice-Hall, Inc., New York (1952).

(2) Finnie, Iain, and Heller, W. R., Creep of Engineering Materials, McGraw-Hill Book Company, New York (1959)

(3) Popov, E. P., "Correlation of Tension Creep Tests with Relaxation Tests", ASME J. Appl. Mech. (June, 1947).

(4) Robinson, E. L., "Steam-Piping Designs to Minimize Creep Concentrations", ASME Trans. (1955).

(5) Waters, E. O., "Analysis of Bolted Joints at High Temperature", ASME Trans. (1938).

(6) Marin, Joseph, discussion of paper, "Formulas for Stresses in Bolted-Flanged Connections", ASME Trans. (1937).

(7) "Air Weapons Materials Application Handbook, Metals and Alloys", ARDC TR59-66 (December, 1959).

(8) Engineering Data Bulletin VM-107, René 41 (May, 1958), Metallurgical Products
     Dept., General Electric Company, Detroit 32, Michigan.

(9) "Effect of Creep-Exposure on Mechanical Properties of René 41", University of
     Michigan, ASD TR 61-73 (August, 1961).

SELECTION OF THREAD PROFILES FOR FITTINGS

The selection of threads is a function of the over-all design of a specific fitting, and therefore the discussions and evaluations presented are qualitative rather than quantitative. These discussions are limited to a few basic factors without taking into consideration all of the factors that influence thread behavior and the behavior of the threaded connections. For example, materials properties and various means of improving thread behavior are not considered. The discussions are limited to the most common case, in which one of the threaded members is subjected to a tension load and the other to a compression load.

Bolted Fittings

When a bolted fitting is loaded or preloaded, the bolt elongates and the nut compresses axially. This is the primary cause for nonuniform load distribution along the threads, as shown in Figure 110, and it is the reason that the first thread next to the
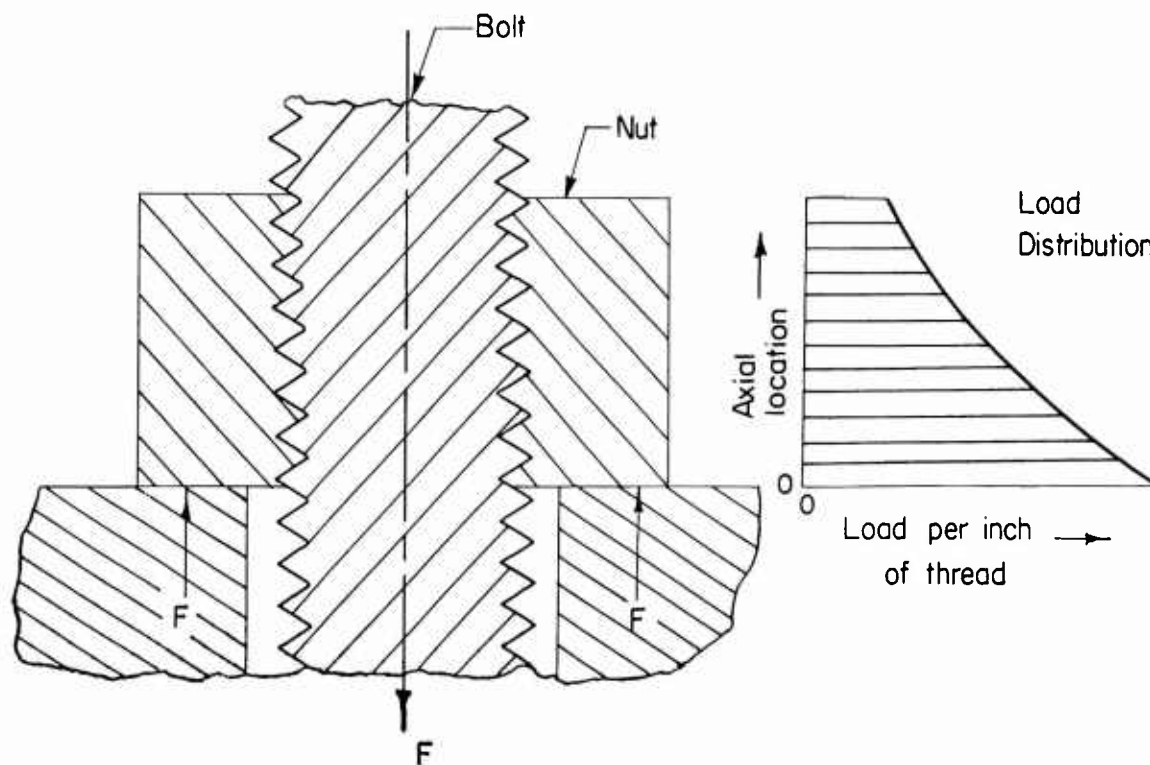
FIGURE 110. ILLUSTRATION OF NONUNIFORM LOAD DISTRIBUTION
IN A NUT TIGHTENED ON A BOLT

loaded nut surface carries more load than the other threads. The nonuniformity in load distribution is mitigated somewhat by cantilever-type bending of threads, by radial contraction of the bolt, and by radial expansion of the nut. The radial contraction and expansion are caused by two factors: (1) Poisson's effect from tension and compression and (2) the radial component on thread flank surfaces resulting from the axial bolt load. These radial movements or thread recessions occur mainly in the first threads and are beneficial from the standpoint of load distribution among the threads. However, they cause circumferential hoop stresses and a decrease in thread-engagement depth of the highest loaded critical threads. Thread bending increases the critical stresses at the roots of the threads.

The expansion of the nut may be restrained somewhat by the friction between the loaded-nut face and the flange surface. The thread recession could be decreased essentially to only that resulting from Poisson's effect if buttress threads were used instead of a basically triangular thread form. This would create, however, a trade-off condition because the elimination of circumferential hoop stresses and the decrease in nominal contact pressure (because of less thread recession) would be gained at the expense of less favorable load distribution along the threads and lower fatigue strength of the bolt.

Since the bolt accounts for most of the weight in a bolt-nut combination, it is advantageous, from the standpoint of the strength-weight ratio, to select a thread profile that permits use of the strongest bolts, particularly for fatigue loading. This leads to the conclusion that bolts with triangular threads with a 60-degree included angle and with full-radius roots should be used in flanged fittings, even if they do require higher tightening torques than buttress threads for the same axial load. Since almost all threaded fasteners are made with such threads, a practical advantage results in that commercial high-strength fasteners can be employed. At first it may appear that an Acme thread would constitute an acceptable compromise between the 60-degree triangular thread and a buttress thread. However, this is not the case. For the same thread pitch and, thus, roughly for the same major and minor diameters, the Acme thread is weaker than either the triangular or buttress threads.

Among the 60-degree thread profiles, the following were considered:

(1) Standard threads with basically flat roots (MIL-S-7742), having a nominal thread-engagement depth equal to 83.33 per cent of the theoretical depth (defined as $h = 3/4\ P \cos 30°$, where P is thread pitch)

(2) Threads with a full-radius root (MIL-B-7838), having a nominal thread-engagement depth equal to 83.33 per cent of the theoretical depth

(3) Reduced-depth threads with an increased full-radius root (MIL-S-8879), having a nominal thread-engagement depth equal to 75 per cent of the theoretical depth

(4) Reduced-depth threads proposed by Standard Pressed Steel Co., with a still greater full-radius root, having a nominal thread-engagement depth equal to 55 per cent of the theoretical depth.

For external bolt threads of the same size and pitch, the major diameter is nominally the same for all four profiles. The nominal minor diameter is essentially the same for the first two profiles. It becomes larger for the 75 per cent thread and still larger for the 55 per cent thread as a consequence of the increase in root radius and the decrease in thread depth. The major diameter of the internal threads is also essentially the same for all four profiles. The minor diameter of the internal threads is increased with the corresponding increase in the minor diameter of the external threads to avoid interference of the internal-thread crests with the root radius of the external threads.

The most common failures that occur with such preloaded bolted connections are:

(1) A transverse fracture of the bolt from overstress, creep, or fatigue, usually starting at the root of the first engaged thread

(2) Longitudinal failure of the nut due to excessive circumferential hoop stresses

(3) Stripping of the mating threads because of overload

(4) Seizure of the mating threads, caused by excessive contact pressure.

Considering only the strength of the bolt for all failure modes — overstress, creep, and fatigue — the reduced-depth thread is clearly superior to the full-depth thread. The larger minor diameter provides a larger load-carrying cross section, and the larger root radius has a lower stress concentration, which is important for fatigue strength. The published data support the above statement and show higher ultimate tensile strength, stress-rupture strength, and higher fatigue strength for the reduced-depth threads. It appears that the biggest gain for the reduced-depth thread lies in its improved fatigue characteristics, mainly due to the enlarged root radius. Because of the latter, the standard threads with a full-radius root (MIL-B-7838) are to be preferred in all cases over the standard threads with flat roots (MIL-S-7742). Whenever fatigue is the primary consideration, the 75 per cent threads (MIL-S-8879) or even the SPS-proposed 55 per cent threads may be the best unless considerations other than fatigue limit their use.

In the case of nut failures from excessive circumferential hoop stresses, there should be no essential differences between reduced-depth and full-depth threads, provided all other conditions are equal. The stripping strength of reduced-depth threads on the bolts should theoretically decrease with the thread depth but not necessarily in proportion, because of decrease in "shear" area. It is being claimed, however, that the stripping strength of reduced-depth threads on the bolts remains equal to that of full-depth threads until the engagement depth decreases to about 50 per cent of the theoretical depth, and then it drops off rather rapidly. Actually, there are not enough data available to make a valid conclusion. At any rate, it appears that the stripping strength of the 55 per cent thread on the bolt may be lower than that of full-depth or the 75 per cent thread if the thread recession is considered.

Because of lack of sufficient experience data, an uncertainty exists concerning the behavior of reduced-depth threads with respect to thread seizure. From an elementary point of view, the nominal contact pressures, defined as the axial force divided by the projected area of threads, are higher in the reduced-depth threads, and therefore such threads should be more susceptible to seizure and galling. Because of thread bending

under load, the actual contact between threads is concentrated in a limited area rather than being distributed uniformly over the entire thread flank. Galling and seizing of threads is thus governed mainly by the peak contact stresses. Because of the complexities involved, it is virtually impossible to predict analytically the quantitative peak contact stresses and subsequent amount of thread galling or seizing. Judging from the geometries involved, higher peak contact pressures can be expected in the 55 per cent thread than in the 75 per cent or full-depth threads, and therefore thread galling or seizing may become a problem in reduced-depth threads.

It becomes apparent that, from the viewpoint of bolt strength, the reduced-depth threads should be used unless galling, seizing, or stripping occurs. One of the requirements for all mechanical fittings is that they should be capable of sustaining several assemblies and disassemblies. If only thread galling or mild seizing would occur in some fasteners of the flanged connections, the damaged fasteners could probably be easily replaced during reassembly when needed. Since the 75 per cent thread (MIL-S-8879) is widely accepted by the aircraft industry, it can be reasonably assumed that its stripping strength is sufficient, and therefore it appears to be advantageous to use it for fasteners in flanged fittings.

Use of the 55 per cent thread in fasteners for flanged fittings is not recommended at this time because of the uncertainties concerning its stripping strength and thread seizure. Such a thread form, however, may be considered for future use, provided that these uncertainties are eventually resolved favorably.

Threaded Fittings

Here, the threaded members are "sleeves" with or without wrench flats. The internal member has the external threads and the external member has the internal threads. In most cases, the internal threads are loaded in tension and the external threads in compression, which is opposite to a normal bolt- and-nut combination. Regardless of the load directions, the primary function of the threads is to provide or sustain high axial forces. At the same time, the sleeves should be of a minimum weight design. Buttress threads fulfill both of these requirements because they develop the highest axial force for a given torque value and because they do not develop hoop stresses in the sleeves; therefore, they permit minimum wall thickness. The lower fatigue strength as compared with the 60-degree threads is of little consequence for this application because the critical location, as far as the fatigue strength of the fitting is concerned, is the tube-to-fitting connection. Since there is practically no disengagement of threads due to radial forces in buttress threads, they are also expected to be better from the standpoint of preload relaxation.

In view of these considerations, buttress threads are recommended for larger size threaded fittings. In smaller size threaded fittings, the increased cost of buttress threads as compared with that of NF threads may not be justified since, based on preliminary designs of a 1/8 in. threaded fitting, it appears that excess material will be present in the nut because of manufacturing requirements. If this occurs, the reduction of radial thrust by use of buttress threads would be only a minor advantage. Also, in small sizes, the advantage of high axial force for a given torque, which may be obtained with buttress

threads, is of less importance since in small sizes the required axial force is relatively small. The size division between threaded fittings with NF threads and those with buttress threads will depend upon required design details in intermediate sizes.

DETERMINATION OF POTENTIAL THERMAL GRADIENTS
FOR EXPERIMENTAL FITTING

A 1/2-inch commercial fitting was assembled and fitted with thermocouples as shown in Figure 111. The thermocouple measurements were recorded continuously by a Model 1108 Visicorder. Aroclors 1254 fluid was heated to 600 F and passed continuously through the fitting. The effect of cold fluids was evaluated by passing liquid nitrogen continuously through the fitting.
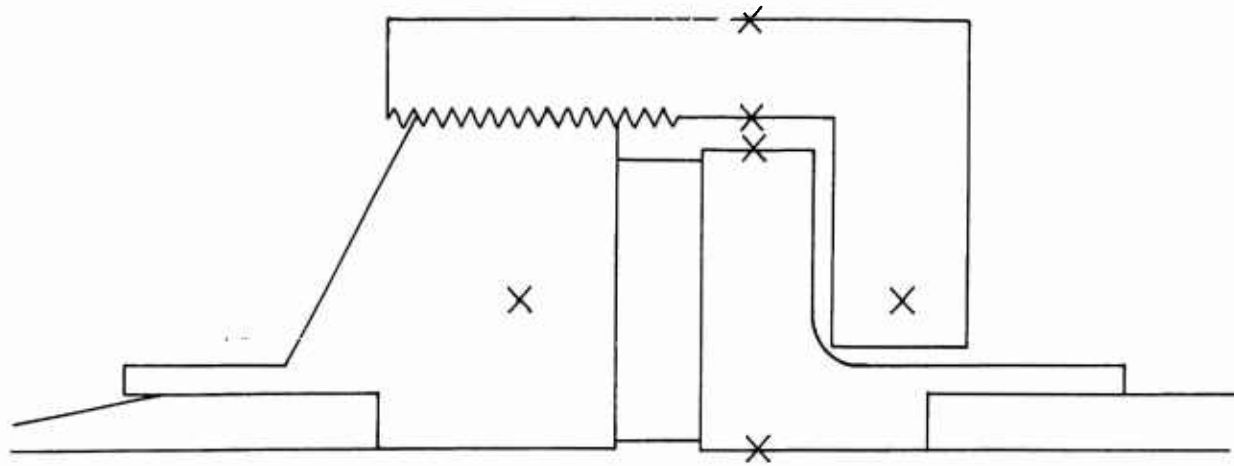
A-44076

FIGURE 111. LOCATION OF THERMOCOUPLES FOR THERMAL-GRADIENT EVALUATION

X designates location of thermocouples.

Eighteen tests were performed. The mean average temperature difference recorded between the tension and compression members is shown in Figure 112. The maximum average difference was +276 F and -162 F for the hot and cold tests, respectively. These values were used to determine the transient thermal displacements in the design for the experimental fitting.
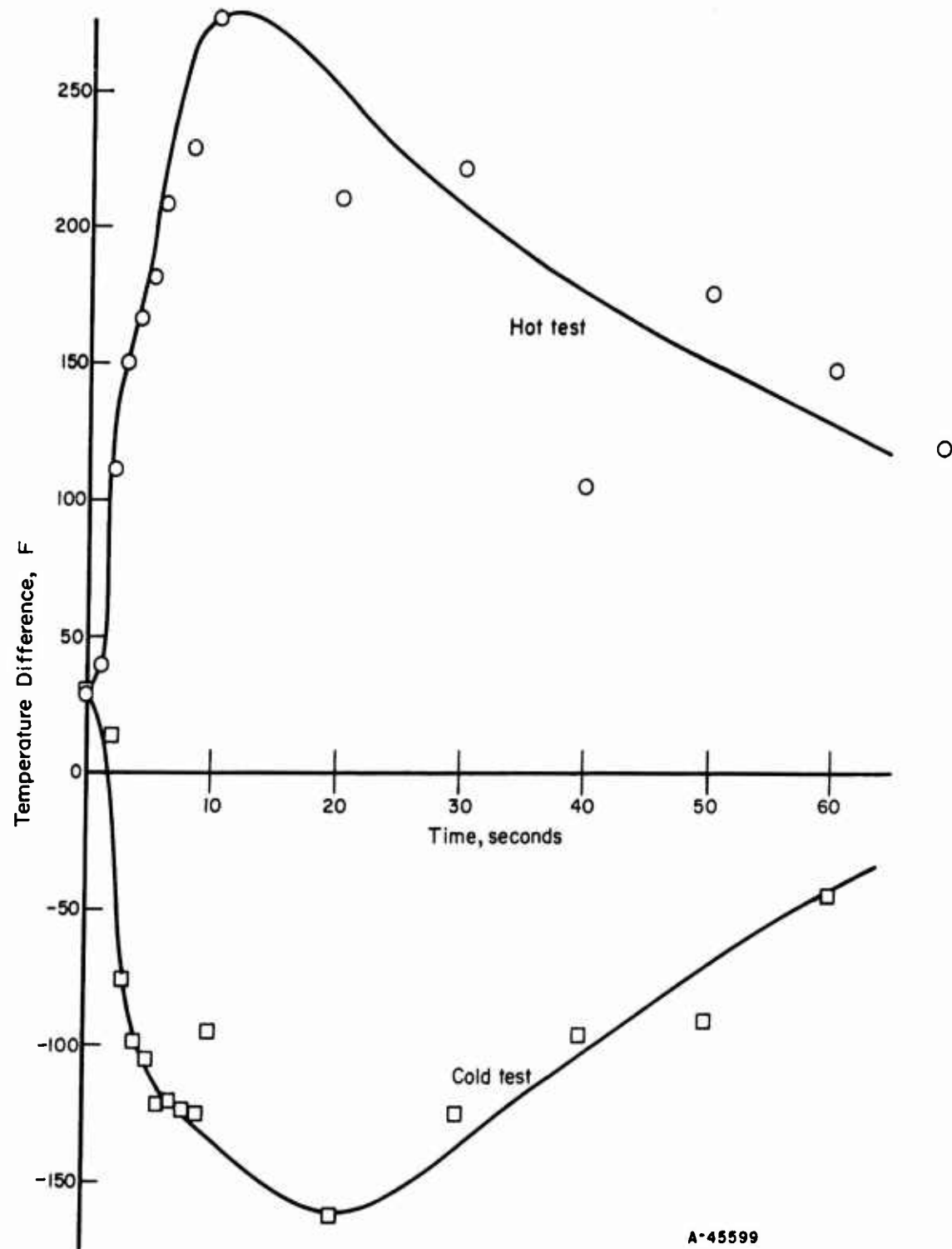
FIGURE 112. TEMPERATURE DIFFERENCE BETWEEN COMPRESSION
AND TENSION MEMBERS OF 1/2-INCH FITTING AS A
FUNCTION OF TIME

APPENDIX V

LABORATORY VERIFICATION OF THE THEORETICAL SPRING CONSTANT CHARACTERISTICS OF SELECTED NUT DESIGNS

Answers to the following questions were necessary to show that the actual spring constants of selected nut configurations could be predicted by theoretical considerations:

(1) Could the spring constant of the nut be controlled by variations of the nut hub and flange thicknesses?

(2) How closely would the theoretical spring constant of the nut match the actual spring constant?

(3) How closely would the theoretical yield point of the nut match the actual yield point?

Spring Constant Versus Hub and Flange Thickness

The test fixture shown in Figure 113 was used to load the nut on a standard tensile test machine. By using a calibrated extensometer and a recorder integral with the tensile test machine, a continuous curve of strain versus load was obtained during testing.

A commercially available 1/2-inch fitting nut made from Type 347 stainless steel was modified by removing the wrench flats, and a series of experiments was conducted in which only the hub thickness was modified while the flange thickness was kept constant. Figure 114 shows the decrease in spring rate (an increase in spring constant) as the hub thickness was decreased from 0.080 to 0.0190 in.

A second series of experiments was conducted to determine how changes in flange thickness affected the spring rate when the hub thickness was held constant. Figure 115 shows the decrease in spring rate as the flange thickness was reduced.

Theoretical Versus Experimental Spring Constant

The accuracy of the theoretical expressions for predicting the actual elastic behavior of the nut was determined by comparing calculated force-deflection curves with actual force-deflection curves obtained on a tensile-test machine by means of the test fixture described in Figure 113.

Several nut configurations determined by the computer program were selected and fabricated from AM-355 bar stock. The dimensions of two of these, Specimens AM-1-1 and AM-4-1, are shown in Table 26. Also shown are Specimens R-1-2 and R-1-6, fabricated as per Figure 89.

The theoretical and experimental spring constants for Specimens AM-1-1 and AM-4-1, R-1-2, and R-1-6, are given in Table 27. The theoretical spring constant listed in Table 27 includes the calculated spring constant for the test fixture. The percentage
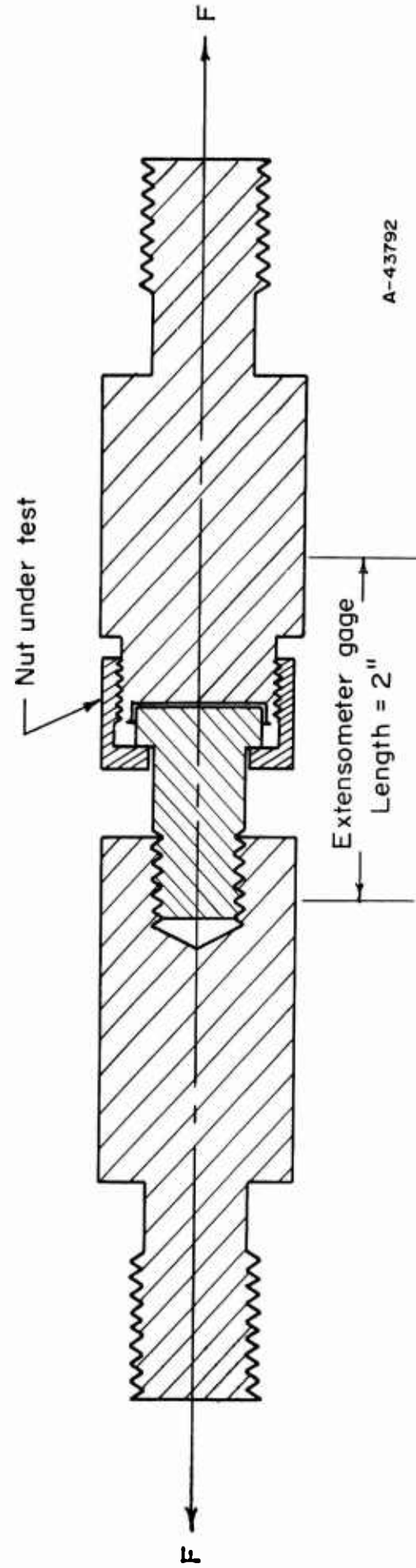
Note: Strain as measured by the extensometer was plotted versus force continuously during testing by means of a recorder integral with the tensile-test machine.

FIGURE 113. TEST FIXTURE USED TO OBTAIN LOAD-DEFLECTION CURVES ON TENSILE-TEST MACHINE

222
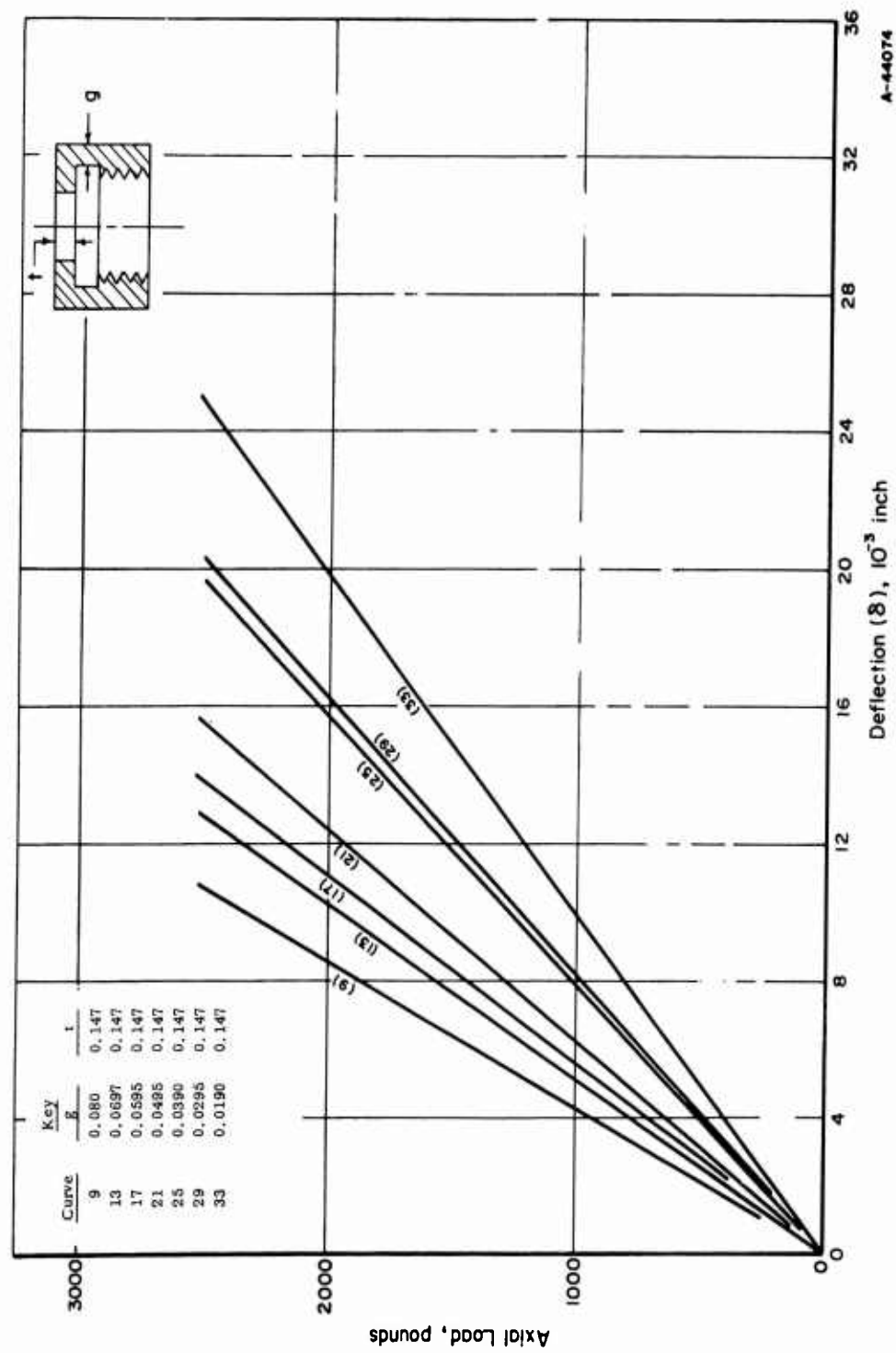
FIGURE 114. LOAD VERSUS DEFLECTION FOR MODIFIED COMMERCIAL NUT

223
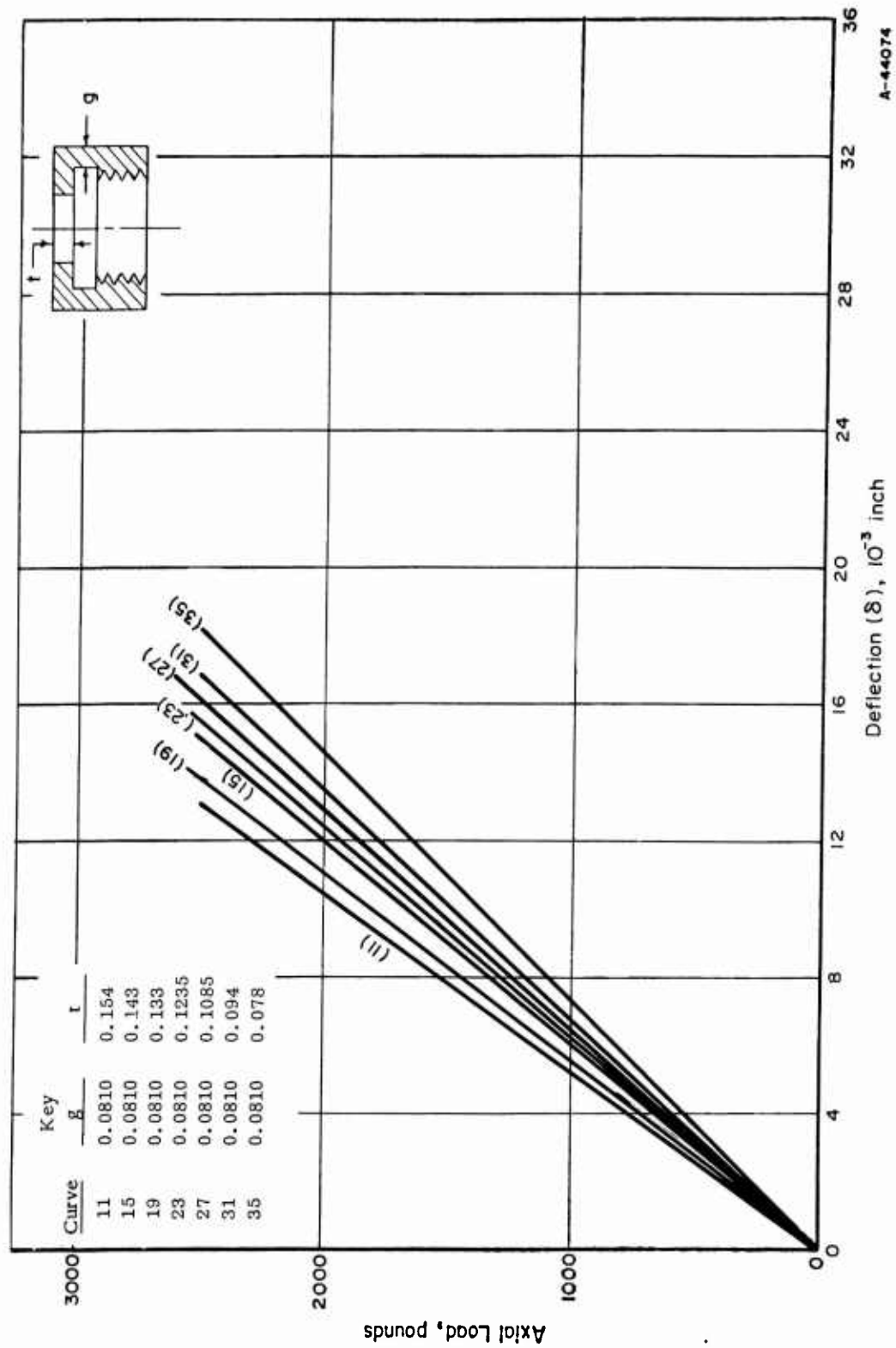
FIGURE 115. LOAD VERSUS DEFLECTION FOR MODIFIED COMMERCIAL NUT

224

difference of the theoretical versus experimental spring constants is also given in Table 27. The spring constant curves for Nuts R-1-2 and R-1-6 are shown in Figure 116, together with the theoretical curve. As can be seen, there is very good correlation between the theoretical and experimental slopes.

Theoretical Versus Actual Yield Point

Included in Table 27 are the theoretical and experimental yield points for the four specimens. The percentage difference of the theoretical versus the experimental yield points is also given. The theoretical yield point was determined by dividing the maximum allowable load by two-thirds, which was the basis for determining the maximum allowable stress. The experimental yield point was the load at which yielding apparently started, as evidenced by a change in slope of the curve plotted during the experiments. The theoretical and experimental yield points are also indicated in Figure 116. Again it can be seen that there is very good correlation between the theoretical and the experimental values.

TABLE 26. NUT DIMENSIONS

Specimen	Material	GA	T	FL5	F1	DG	D	DB
AM-1-1	AM-355	0.009	0.290	0.156	0.696	1.013	1.031	0.542
AM-4-1	AM-355	0.0085	0.300	0.250	0.706	1.032	1.049	0.542
R-1-2	René 41	0.0253	0.246	0.255	0.290	1.013	1.0625	0.570
R-1-6	René 41	0.0253	0.246	0.255	0.290	0.012	1.0625	0.570

A-45609
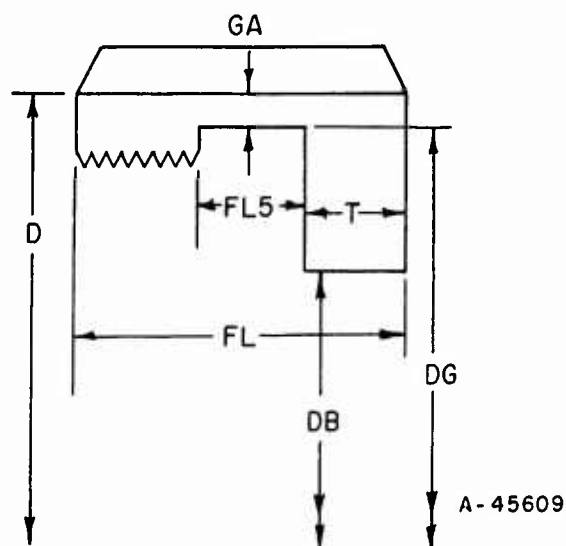
TABLE 27. SPRING CONSTANTS AND MAXIMUM ALLOWABLE LOADS

		Spring Constant			Yield Point		
Specimen	Material	Theoretical	Experi-mental	Per Cent Differ-ence	Theoretical	Experi-mental	Per Cent Differ-ence
AM-1-1	AM-355	4.27×10^{-7}	4.64×10^{-7}	-7.97	10,200	11,100	-8.10
AM-4-1	AM-355	4.31×10^{-7}	5.12×10^{-7}	-15.82	10,700	9,500	+12.63
R-1-2	René 41	3.93×10^{-7}	4.03×10^{-7}	-2.48	9206.9	9795	-6.00
R-1-6	René 41	3.93×10^{-7}	4.18×10^{-7}	-5.98	9206.9	9390	-1.94
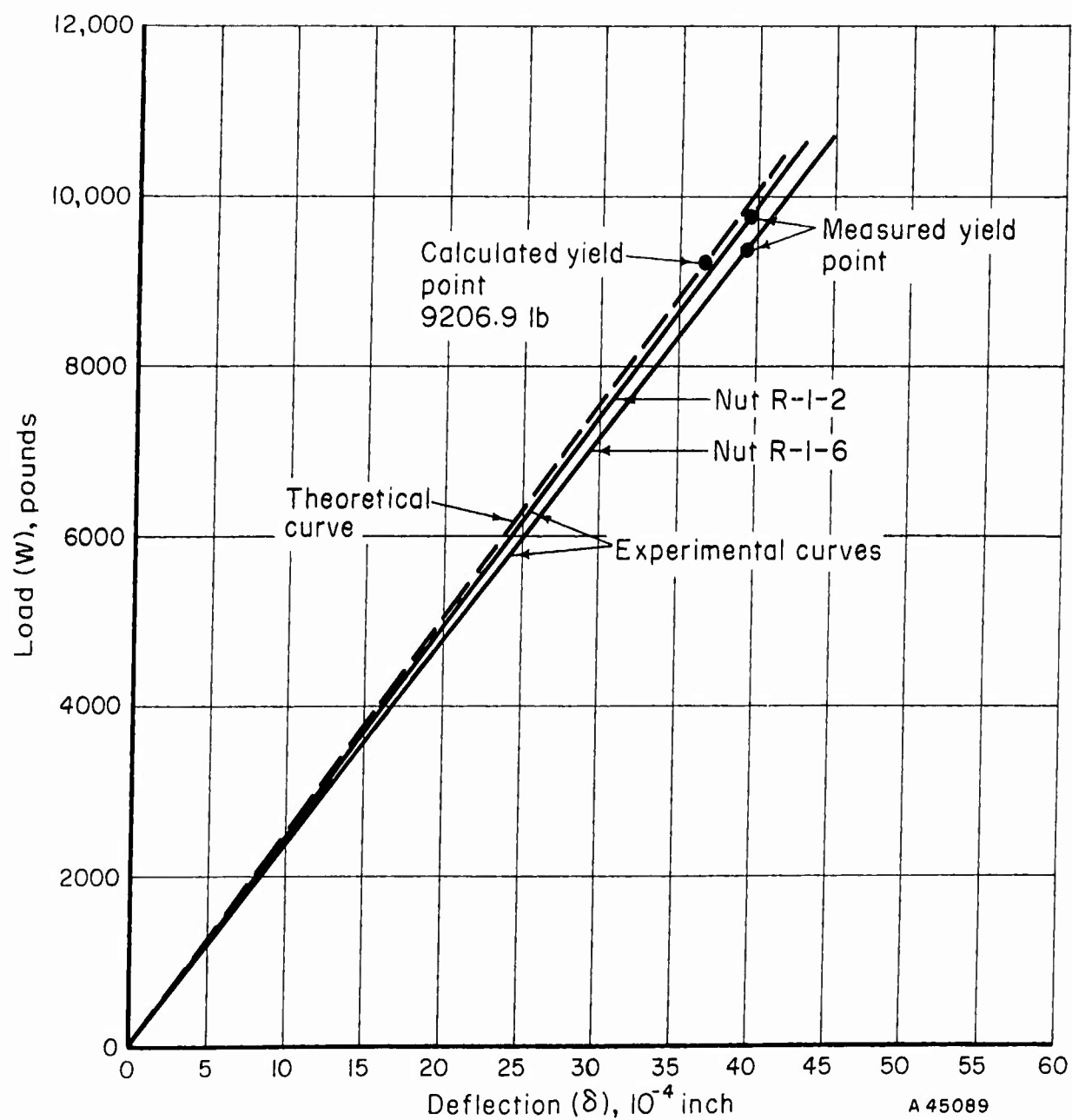
FIGURE 116. LOAD VERSUS DEFLECTION FOR EXPERIMENTAL NUT

APPENDIX VI

DIGITAL COMPUTER PROGRAMS

Introduction

Three digital computer programs are given in the following order:

(1) Input Data Sheet and Operating Instructions

(2) Symbol Definitions

(3) Drawings showing Nomenclature

(4) Source Card Listing including Data Card Listing

(5) Typical Outputs

The Source Card Listing includes the control cards necessary for operation on the Bendix G-20 computer.   Modification of these control cards may be necessary for operation on other computer systems.   The algebraic symbols are written with the following symbols:

Exponentiation	**
Multiplication	*
Division	/
Addition	+
Subtraction	-
Opening Parenthesis	(
Closing Parenthesis	)

Each line represents one source card with the algebraic statements beginning in Column 7.

The output of the programs requires 120-character paper.

Input Data Sheet and Operating Instructions

Flanged-Connector Design Program

PROJECT   G-6201-1   Date of Run _____ __, 19

DECK NO.   FLGDSN

DATE   July 10, 1963

PREPARED BY J. W. Adam

Data Cards (4 cards/run)

CARD 1

Col.				
1-12	+/- . _ _ _ _ _ _	E +/- _ _	D
13-24	+/- . _ _ _ _ _ _	E +/- _ _	TT
25-36	+/- . _ _ _ _ _ _	E +/- _ _	STE
37-48	+/- . _ _ _ _ _ _	E +/- _ _	PT
49-60	+/- . _ _ _ _ _ _	E +/- _ _	GO
61-72	+/- . _ _ _ _ _ _	E +/- _ _	AMC

CARD 2

Col.				
1-12	+/- . _ _ _ _ _ _	E +/- _ _	SG
13-24	+/- . _ _ _ _ _ _	E +/- _ _	SFA
25-36	+/- . _ _ _ _ _ _	E +/- _ _	SBA
37-48	+/- . _ _ _ _ _ _	E +/- _ _	AM
49-60	+/- . _ _ _ _ _ _	E +/- _ _	SFT
61-72	+/- . _ _ _ _ _ _	E +/- _ _	SBT

CARD 3

Col.				
1-12	+/- . _ _ _ _ _ _	E +/- _ _	SFYS
13-24	+/- . _ _ _ _ _ _	E +/- _ _	SSEYS
25-36	+/- . _ _ _ _ _ _	E +/- _ _	SBYS
37-48	+/- . _ _ _ _ _ _	E +/- _ _	CAPX
49-60	+/- . _ _ _ _ _ _	E +/- _ _	CAPY
61-72	+/- . _ _ _ _ _ _	E +/- _ _	CAPZ

CARD 4

Col.				
1-12	+/- . _ _ _ _ _ _	E +/- _ _	P

Data must be entered as ±.XXXXXX times some power of 10., e.g., -372.56 goes in as +/θ . 3 7 2 5 6 0 E θ/- 0 3

      The deck is a space FORTRAN absolute deck. All the control cards necessary for a compilation and execution are included. Just put the 4 data cards in place of the index card. Running time is about 30 seconds per set of data. Another ABS Deck is available which prints out intermediate values if desired. Multiple sets of data can be stacked.

Note: (1) AMC = 0 if not known

      (2) CAPX = 1 for nonmetallic gaskets
                    2 for metallic gaskets

      (3) CAPY = 1 for integral (Type I) flanges
                  = 2 for loose ring (Type II) flanges

      (4) CAPZ = 1→5 (see Figure 119) for Type I flanges
                  = 1 for Type II flanges

Definition of Symbols Used in FLGDSN Program

Flanged-Connector Design Program

A	Outside diameter of flange, in.
AB	Total required bolt area (max of ABG, ABS), sq in.
ABG	Required bolt area for operating conditions, sq in.
ABS	Required bolt area for seating gasket, sq in.
AB1	Thread root area of one bolt, sq in.
AG	Gasket seating area, sq in.
AK	Dimensional ratio A/B
*AM	Residual gasket stress factor
*AMC	External bending moment, in-lb
ANS	Nominal bolt size
ANU	Approximation factor
AS	Outside diameter of stub and flange
A1	Stress calculation parameter
A2	Stress calculation parameter
A3	Stress calculation parameter
A4	Stress calculation parameter
A5	Stress calculation parameter
A6	Stress calculation parameter
A7	Stress calculation parameter
A8	Stress calculation parameter
A9	Stress calculation parameter
A10	Stress calculation parameter

* signifies input quantities.

231

B	Inside diameter of flange, in.
BETA	Inside diameter of stub end, in.
BS	Inside diameter of stub end, in.
C	Bolt circle diameter, in.
*CAPX	Gasket type identification factor
*CAPY	Flange type identification factor
*CAPZ	Facing type identification factor
*D	Outside diameter of tube, in.
DELT	Incremental variation in flange thickness, in.
DH	Bolt hole diameter, in.
FMG	Total flange moment, gasket seating conditions, in-lb
FMO	Total flange moment, operating conditions, in-lb
FMT	Total flange moment, test conditions, in-lb
F14	Stress calculation parameter (table designation)
F14A	Stress calculation factor (interpolated value)
F15	Stress calculation parameter (table designation)
F15A	Stress calculation parameter (interpolated value)
G	Average diameter of gasket, in.
*GO	Thickness of hub at small end, in.
GS	Thickness of hub at stub end, in.
G1	Thickness of hub at back of flange, in.
G14	Stress calculation parameter (table designation)
G41	Stress calculation parameter (table entry)
H	Hub length, in.
HD	Load moment arm, in.
HDM	Bolt maximum head diameter, in.

* Signifies input quantities.

HG	Load moment arm, in.
H1	Straight portion hub length, loose ring flange, in.
H14	Stress calculation parameter (table designation)
H2	Tapered portion hub length, loose ring flange, in.
H41	Stress calculation parameter (table entry)
I	Counting factor (bolt table identification)
J	Counting factor (bolt table entry)
K	Counting factor (iteration limitation)
K1	Gasket type identification factor = CAPX
K2	Flange type identification factor = CAPY
K3	Facing type identification factor = CAPZ
L	Counting factor (iteration limitation)
M	Stress calculation designation factor
N	Number of bolts (fixed point designation)
O	Number of bolts (floating point designation)
*P	Maximum operating pressure, psi
PB	Internal pressure equivalent to external bending moment, psi
PB1	Internal pressure equivalent to external bending moment, psi
PB2	Internal pressure equivalent to external bending moment, psi
PPRM	Smaller of P and 2/3 PT, psi
*PT	Maximum test pressure (ambient temp), psi
RG	Radial clearance between flange and stub end hub, in.
RR	Minimum radial clearance between bolt circle and hub, in.
RS	Minimum space between bolts, in.
*SBA	Allowable stress bolt material — ambient temp, psi

---

* Signifies input quantities.

*SBT	Allowable stress bolt material – max operating temp, psi
*SBYS	Yield stress – bolt material – ambient temp, psi
*SFA	Allowable stress – flange material – ambient temp, psi
*SFT	Allowable stress – flange material – max operating temp, psi
*SFYS	Yield strength – flange material – ambient temp, psi
*SG	Gasket seating stress, psi
SGC1	Stress resulting from FMG – Type I flanges, psi
SGC2	Stress resulting from FMG – Type II flanges, psi
SIGC	Stress per unit moment, $1/\text{in.}^3$
SIG1	Stress per unit moment, $1/\text{in.}^3$
SIG2	Stress per unit moment, $1/\text{in.}^3$
SIG3	Stress per unit moment, $1/\text{in.}^3$
SOC1	Stress resulting from FMO – Type I flanges, psi
SOC2	Stress resulting from FMO – Type II flanges, psi
*SSEYS	Yield stress – stub end material – ambient temp, psi
STC1	Stress resulting from FMT – Type I flanges, psi
STC2	Stress resulting from FMT – Type II flanges, psi
*STE	Endurance strength of tubing material, psi
TEMP	Two-thirds of PT, psi
THETA	Inside diameter of Flange=B, in.
THPI	Bolt threads per in.
TO	Flange thickness estimate
TOA	Flange thickness after change due to stress condition, in.
TOB	Flange thickness after change due to stress condition, in.
TOC	Flange thickness after change due to stress condition, in.

* Signifies input quantities.

234

TOD   Flange thickness after change due to stress condition, in.

TOE   Flange thickness after change due to stress condition, in.

TOF   Flange thickness after change due to stress condition, in.

TØMIN Minimum acceptable flange thickness based on stresses and spacing

TØMSP Minimum acceptable flange thickness based on spacing

TO1   Flange thickness estimate, in.

TO2   Flange thickness estimate, in.

TS   Thickness of lap on stub end, in.

*TT   Wall thickness of tube, in.

T13   Stress calculation factor

U13   Stress calculation factor

V1   Flange and hub volume — Type I flange, in.^{3}

V14   Stress calculation parameter (table designation)

V14A   Stress calculation factor (interpolated value)

V2   Flange and hub volume — Type II flange, in.^{3}

V2F   Flange volume — Type II flange, in.^{3}

V2H   Hub volume — Type II flange, in.^{3}

W   Gasket width, in.

WS   Load due to internal pressure plus external bending moment

W1   Suggested gasket width, in.

W2   Suggested gasket width, in.

X   Average diameter of contact area between loose flange and stub end, in.

Y13   Stress calculation factor

ZT   Section modulus of tube, in.$^{-3}$

Z13   Stress calculation factor

---

* Signifies input quantities.

235

FIGURE 117. TYPE I FLANGE, SHOWING NOMENCLATURE FOR
FLANGED-CONNECTOR DESIGN PROGRAM

FIGURE 118. TYPE II FLANGE, SHOWING NOMENCLATURE FOR
FLANGED CONNECTOR DESIGN PROGRAM

236
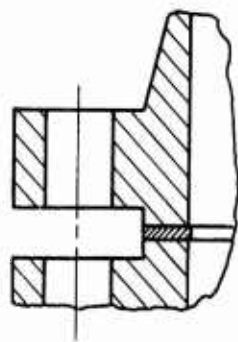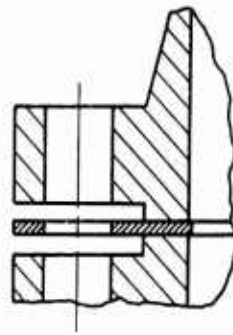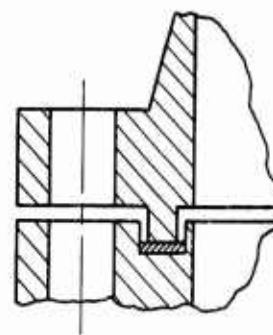
CAP Z = 1   CAP Z = 2   CAP Z = 3
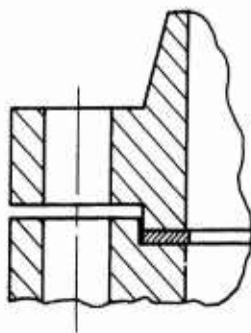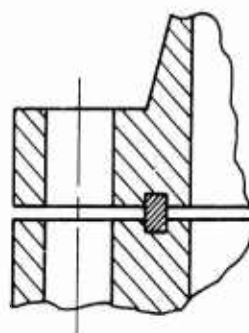
CAP Z = 4   CAP Z = 5

1. Raised face, gasket on facing only
2. Raised face, gasket extending to flange OD
    for ease in centering

3. Tongue and groove facing
4. Male-female facing
5. Double-groove facing, with plated metal gasket   A-45644

FIGURE 119. TYPICAL FLANGE-GASKET CONFIGURATIONS

237

```
I     BILIN                    0010
E     INPUT SOURCE CARDS
E     EXECUTE
E     OUTPUT SUBROUTINE TAPE
E     FORTRAN
H     NAME BILIN
C     BIVARIATE LINEAR INTERPOLATION FUNCTION SUBPROGRAM        BILIN010
C     CALLING SEQUENCE                                          BILIN020
C      BILIN(X,Y,Z,NX,NY,ARGX,ARGY)                             BILIN030
C       WHERE X IS A LINEAR ARRAY OF THE FIRST INDEPENDENT VARIABLE  BILIN040
C              THE VALUES OF X ARE LISTED IN INCREASING SEQUENCE     BILIN050
C           Y IS A LINEAR ARRAY OF THE SECOND INDEPENDENT VARIABLE   BILIN060
C              THE VALUES OF Y ARE LISTED IN INCREASING SEQUENCE     BILIN070
C           Z IS A LINEAR ARRAY OF THE DEPENDENT VARIABLE           BILIN080
C              Z IS ORDERED BY CHOOSING AN X AND LISTING THE VALUES  BILIN090
C              OF THE DEPENDENT VARIABLE FOR ALL VALUES OF Y        BILIN100
C           NX IS THE NUMBER OF X VALUES                            BILIN110
C           NY IS THE NUMBER OF Y VALUES                            BILIN120
C           ARGX IS THE X FUNCTION ARGUMENT                         BILIN130
C           ARGY IS THE Y FUNCTION ARGUMENT                         BILIN140
      FUNCTION BILIN(X,Y,Z,NX,NY,ARGX,ARGY)                          BILIN150
      DIMENSION X(5),Y(5),Z(5)                                       BILIN160
      COMMON I,J,K,TEMP,TEMP1                                        BILIN170
C     THREE SP VARIABLES OF COMMON                                   BILIN180
C     TWO DP VARIABLES OF COMMON                                     BILIN190
      DO 1 I=2,NX                                                     BILIN200
      IF (ARGX-X(I))2,2,1                                            BILIN210
    1 CONTINUE                                                       BILIN220
      I=NX                                                           BILIN230
    2 DO 3 J=2,NY                                                    BILIN240
      IF (ARGY-Y(J))4,4,3                                           BILIN250
    3 CONTINUE                                                       BILIN260
      J=NY                                                           BILIN270
    4 K=I*NY-NY+J                                                    BILIN280
      TEMP=((Z(K)-Z(K-1))*ARGY+Z(K-1)*Y(J)-Z(K)*Y(J-1))/(Y(J)-Y(J-1))  BILIN290
      K=K-NY                                                         BILIN300
      TEMP1=((Z(K)-Z(K-1))*ARGY+Z(K-1)*Y(J)-Z(K)*Y(J-1))/(Y(J)-Y(J-1)) BILIN310
      BILIN=((TEMP-TEMP1)*ARGX+TEMP1*X(I)-TEMP*X(I-1))/(X(I)-X(I-1))    BILIN320
      RETURN                                                        BILIN330
      END                                                           BILIN340
L                                                                   BILIN350

E     END OF JOB                                                         7
I     FLANGE DESIGN              0060
E     INPUT SOURCE CARDS
E     EXECUTE
E     OUTPUT DEBUG TAPE
E     FORTRAN
H     NAME FLGDSN
H     EQUIP= CARDRE,PRINTE;
      DIMENSION ANS(15),THPI(15),AB1(15),RR(15),RS(15),DH(15),HDM(15)
      DIMENSION G14(9),H14(14),V14(126),F14(126),F15(126)
    1 FORMAT(6E12.6)
    2 FORMAT(27H BEARING AREA NOT SATISFIED)
    3 FORMAT (8H      D=,E12.6,6H   TT=,E12.6,6H  STE=,E12.6,6H    PT=,E1
     12.6,6H   GO=,E12.6,6H  AMC=,E12.6/8H       SG=,E12.6,6H  SFA=,E12.6,
```

```
      24H   SBA=,E12.6,6H   AM=,E12.6,6H  SFT=,E12.6,6H  SBT=,E12.6/8H   S
     1FYS=,E12.6,6HSSEYS=,E12.6,6H SBYS=,E12.6,6H CAPX=,E12.6,6H CAPY=,E
     412.6,6H CAPZ=,E12.6/8H       P=,E12.6/)
    4 FORMAT (18H NO BOLT AVAILABLE)
    5 FORMAT (9H     RG=,F12.6,6H   ZT=,E12.6,6H   BS=,E12.6,6H    B=,E1
     13.6,6H   PH=,E12.6,6H TEMP=,E12.6/8H   PPRM=,E12.6,6H   WS=,E12.6,
     24H   W1=,E12.6,6H   W2=,E12.6,6H    W=,E12.6/)
  186 FORMAT(20H1 TYPE 2 FLANGE FOR;//)
  187 FORMAT (40H   WE HAVE,I3,F6.2,13H BOLTS WITH ;//15H             A=
     1,E12.6,8H     AS=,E12.6,8H      B=,E12.6,8H      BS=,E12.6,8H
     2D=,E12.6/15H            DH=,E12.6,8H      G=,E12.6,8H     GS=,E12.
     36,8H      H=,E12.6,8H     H1=,E12.6/15H            H2=,E12.6,8H
     4   HG=,F12.6,8H   THPI=,E12.6,8H  TOMIN=,F12.6,8H  TOMSP=,E12.6/15H
     5            TS=,F12.6,8H     V1=,E12.6,8H     V2=,E12.6,8H      W=
     6,E12.6,8H     WS=,E12.6//)
  188 FORMAT(20H1 TYPE 1 FLANGE FOR;/)
  189 FORMAT(10H  WE HAVE //8H   TOMIN=,E12.6,6H    B=,E12.6,6H    A=,E12
     1.6,6H BETA=,F12.6,6H   BS=,E12.6,6H   V1=,E12.6/8H  THETA=,E12.6,6
     2H    J=,F12.6,6H    C=,E12.6,6H    W=,E12.6,6H    N=,E12.6,6H     G
     3=,F12.6/8H  TOMSP=,F12.6//////)
 1000 FORMAT(7F10.5)
 1001 FORMAT(12F6.3)
      READ 1000,(ANS(I),THPI(I),AB1(I),RR(I),RS(I),DH(I),HDM(I),I=1,15)
      READ 1001,((G14(I),I=1,9),(H14(I),I=1,14),(V14(I),I=1,126),(F14(I)
     1,I=1,126),(F15(I),I=1,126))
      PRINT 1000,(ANS(I),THPI(I),AB1(I),RR(I),RS(I),DH(I),HDM(I),I=1,18)
      PRINT 1001,((G14(I),I=1,9),(H14(I),I=1,14),(V14(I),I=1,126),(F14(I
     1),I=1,126),(F15(I),I=1,126))
  999 READ 1, D,TT,STE,PT,GO,AMC,SG,SFA,SBA,AM,SFT,SBT,SFYS,SSEYS,SBYS,C
     1APX,CAPY,CAPZ,P
      K1=CAPX
      K2=CAPY
      K3=CAPZ
      AS=0.
      GS=0.
      H=0.
      H1=0.
      H2=0.
      RG=0.
      TS=0.
      V1=0.
      V2=0.
      TOMSP=0.
      ZT=.09817477D4*((D**4.)-((D-2.*TT)**4.))/D
      BS=D-2.*TT
      GO TO (17,18),K2
   17 G=BS
      PRINT 188
      PRINT 1,D,TT,STE,PT,GO,AMC,SG,SFA,SBA,AM,SFT,SBT,SFYS,SSEYS,SBYS,C
     1APX,CAPY,CAPZ,P
      GO TO 19
   18 RG=.020,.0025*D
      G=BS+2.*RG+4.*TT
      PRINT 186
      PRINT 1,D,TT,STE,PT,GO,AMC,SG,SFA,SBA,AM,SFT,SBT,SFYS,SSEYS,SBYS,C
     1APX,CAPY,CAPZ,P
```

```
   19 IF (AMC-0.)21,21,20
   20 PB=4.*AMC*TT/(D*ZT)
      GO TO 22
   21 PB1=4.*STE*TT/(3.*D)
      PB2=240.*((D+3.)**3.)*TT/(ZT*D)
      PB=MIN1F(PB1,PB2)
   22 GO TO (23,24),K2
   23 BETA=B
      GO TO 25
   24 BETA=BS
   25 TEMP=2.*PI/3.
      PPRM=MAX1F(P,TEMP)
      WS=(BETA**2.)*(PPRM+PB)
      GO TO (26,29),K1
   26 W1=.07+.0310*D
      IF (W1-.1)27,28,28
   27 W1=.1
   28 W2=WS/(16.*D*SG)
      W=MAX1F(W1,W2)
      L=1
      GO TO 32
   29 W1=.04+(.0069230762*D)
      IF(W1-.05)30,31,31
   30 W1=.05
   31 W2=WS/(8.*D*SG)
      W=MAX1F(W1,W2)
      GO TO (32,35),K2
   32 GO TO (35,33,34,33,34),K3
   33 G=BETA+W
      GO TO 39
   34 G=BETA+W+2.*(.05+.00666667*D)
      GO TO 39
   35 G=BS+W
   39 AG=3.141592654*W*G
      ABS=(WS+AM*PPRM*AG)/SBT
      ABG=AG*SG/SBA
      AB=MAX1F(ABS,ABG)
      J=1
   40 N=(AB/AB1(J))+.9999999
  145 D=N
      G1=1000.
      GO TO (41,42),K2
   41 G1=MIN1F(4.*GO,.6666667*((B*GO)**.5)+GO)
      C=MAX1F(B+2.*(G1+RR(J)),G+W+DH(J))
      GO TO 43
   42 C=MAX1F(BS+2.*(2.*TT+RG+DH(J)),G+W+DH(J))
   43 IF(RS(J)-3.141592654*C/0)45,45,44
   44 GO TO 444
  444 J=J+1
      IF (J-15 )40,40,52
   52 PRINT 4
      GO TO 200
   45 A=C+2.*DH(J)
      GO TO (47,46),K2
   46 THETA=B
      ANU=1.0
```

```
      A3=G+M
      IF (A3**.5)*F/((A8*SBYS*4./(SSEYS*3.141592654))+(THETA**2.)))61,48,4
      39
  61  IF( G  GT
  61  A3=1.02*A3
      F=(A**1.02-THETA)/2.
      C=E+A1
      IF (C   5 )45 35,44
  44  B=A1*C 2
      GO TO 35
  47  AM1=.6664447
      C=DELTA-FA
  48  HG=.5*(C-A)
      AK=A/THETA
      Z13=(1./(AK-1.))*(0.66845+5.71690*((AK*AK*LOG10F(AK))/(AK*AK-1.)))
      FO1=AM1*(((1.*(WS+AM*P*AG)*HG/(SFT*THETA))**.5)
      FO2=AM1*(((1.*AG*SG*HG/(SFA*THETA))**.5)
      Z=Z1
  66  TO=MA/1F (FO1,FO2)
  45  IF((2.*(DH(J)+T0))-3.141592654*C/0)53,50,50
  53  J=N+1
      J=N
      IF(PG(J)-3.141592654*C/0)49,49,152
 152  J=N-1
      J=N
      TO=(3.141592654*C/(2.*0))-DH(J)
      TOMSP=TO
  51  GO TO (51,101),K2
  51  H=1.5*((B*G0)**.5)
      Z13=(AK*AK*(1.+8.55246*LOG10F(AK))-1.)/(1.36136*(AK*AK-1.)*(AK-1.)
      1)
      T13=(AK*AK+1.)/(AK*AK-1.)
      T13=((AK*AK*(1.+8.55246*LOG10F(AK))-1.)/((AK-1.)*(1.04720+1.94480*
      1(AK*AK)))
      H41=H/((THETA*G0)**.5)
      G41=G1/G)
      F14A=BILIN(G14,H14,F14,9,14,G41,H41)
      V14A=BILIN(G14,H14,V14,9,14,G41,H41)
      F15A=BILIN(G14,H14,F15,9,14,G41,H41)
      IF(F15A-1.)149,151,151
 149  F15A=1.
 151  GO TO 55
    2  TYPE 1 FLANGES
  55  DELT=.02*TO
      A1=F14A/(SQRTF(THETA*G0))
      A2=(T13*G0*G1*SQRTF(THETA*G0))/V14A
      N=1
  55  A3=T0*A1+1.
      A4=A3/(11)
      A5=(T0**3.)/A2
      A8=A4+A5
      SIG1=F15A/(A6*G1*G1*THETA)
      A7=(4.*T0*A1/3.)+1.
      SIG2=A7/(A6*T0*T0*THETA)
      A9=F15/(T0*T0*THETA)
      SIG3=A8*(T13*SIG2)
```

```
      SIGC=MAX1F (SIG2,SIG3,2.*SIG1/3,.5*(SIG1+SIG2),.5*(SIG1+SIG3))
C     MOMENT CALCULATIONS
      HG=.5*(C-G)
      HD=.5*(C-THETA-GO)
      FMG=AG*SG*HG
      A9=.785*G*G*(P+PB)*HD
      A10=AM*P*AG*HG
      FMO=A9+A10
      FMT=(FMO*(PT+PB))/(P+PB)
C     STRESS CALCULATIONS
  150 GO TO (70,80,90,98),M
   70 SGC1=SIGC*FMG
   71 IF(SGC1-SFA)72,73,75
   72 IF(SGC1-.95*SFA)76,76,73
   73 GO TO 74
   74 M=2
      GO TO 66
   75 TOA=TO+DELT
      K=K+1
      IF (K-30)146,146,73
  146 TO=TOA
      GO TO 65
   76 TOA=TO-DELT
      K=K+1
      IF (K-30)146,146,73
   80 SOC1=SIGC*FMO
   81 IF (SOC1-SFT)82,83,85
   82 IF(SOC1-.95*SFT)86,86,83
   83 GO TO 84
   84 M=3
      GO TO 66
   85 TOB=TO+DELT
      K=K+1
      IF (K-30)147,147,83
  147 TO=TOB
      GO TO 65
   86 TOB=TO-DELT
      K=K+1
      IF (K-30)147,147,83
   90 STC1=SIGC*FMT
   91 IF(STC1-.9*SFYS)92,93,95
   92 IF(STC1-.85*SFYS)96,96,93
   93 GO TO 94
   94 M=4
      GO TO 150
   95 TOC=TO+DELT
      K=K+1
      IF(K-30)148,148,93
  148 TO=TOC
      GO TO 65
   96 TOC=TO-DELT
      K=K+1
      IF(K-30)148,148,93
   98 TOMIN=MAX1F(TOA,TOB,TOC,TOMSP)
      V1=(.785398160*((A*A-THETA*THETA)*TOMIN+(((THETA+GO)**2.)-(THETA*T
     1HETA))-((DH(J)**2.)*0*TOMIN))+((G1-GO)*H/2.)*(THETA+GO+((G1-GO)/3.
```

```
      2)))
       PRINT 187,N,ANS(J),A,AS,B,BS,C,DH(J),G,GS,H,H1,H2,RG,THPI(J),TOMIN
      1,IOMSP,IS,V1,V2,W,WS
    99 IF(J-15 )44,200,200
C  TYPE 2 FLANGES
   100 DELT=.02*TO
       K=0
       X=.5*(AS+THETA)
       HG=.5*(C-X)
       HD=.5*(C-THETA)
       FMG=AG*SG*HG
       A1=.7853981L6*G*G*(P+PB)*HD
       A2=AM*P*AG*HG
       FMO=A1+A2
       FMT=FMO*(PT+PB)/(P+PB)
   101 SIGC=Y13/(TO*TO*THETA)
C   STRESS CALCULATIONS
   102 GO TO (110,120,130,138),M
   110 SGC2=SIGC*FMG
   111 IF(SGC2-SFA)112,113,115
   112 IF(SGC2-.95*SFA)116,116,113
   113 GO TO 114
   114 M=2
       GO TO 66
   115 TOD=TO+DELT
       K=K+1
       IF(K-30)142,142,113
   142 TO=TOD
       GO TO 101
   116 TOD=TO-DELT
       K=K+1
       IF(K-30)142,142,113
   120 SOC2=SIGC*FMO
   121 IF(SOC2-SFT)122,123,125
   122 IF(SOC2-.95*SFT)126,126,123
   123 GO TO 124
   124 M=3
       GO TO 66
   125 TOE=TO+DELT
       K=K+1
       IF(K-30)143,143,123
   143 TO=TOE
       GO TO 101
   126 TOE=TO-DELT
       K=K+1
       IF(K-30)143,143,123
   130 STC2=SIGC*FMT
   131 IF(STC2-.9*SFYS)132,133,135
   132 IF(STC2-.85*SFYS)136,136,133
   133 GO TO 134
   134 M=4
       GO TO 102
   135 TOF=TO+DELT
       K=K+1
       IF(K-30)144,144,133
   144 TO=TOF
```

```
      GO TO 101
  136 TOF=TO-DELT
      K=K+1
      IF(K-30)144,144,133
  138 TOMIN=MAX1F(TOD,TOE,TOF,TOMSP)
      V2F=(.78539816*((A*A-THETA*THETA)*TOMIN-(DH(J)**2.)*0*TOMIN))
      TS=2.*TT
      GS=2.*TT
      H1=((THETA*GS)**.5)*2.
      IF(H1-2.*TOMIN)139,139,140
  139 H1=2.*TOMIN
  140 H2=.5*H1
      V2H=(.78539816*((AS*AS-BS*BS)*TS+(((BS+2.*GS)**2.)-BS*BS)*H1+((((B
     1S+G0*2.)-BS*BS)*H2))+(((GS-G0)*H2/2.)*(GS-G0)/3.)))
      V2=V2F+V2H
      PRINT 187,N,ANS(J),A,AS,B,BS,C,DH(J),G,GS,H,H1,H2,RG,THPI(J),TOMIN
     1,TOMSP,TS,V1.V2,W,WS
  141 IF(J-15 )44,200,200
  200 GO TO 999
      END
```

L

5.00000	44.00000	.00716	.13200	.39600	.14100	.20000
6.00000	40.00000	.00874	.14300	.42900	.15200	.22100
8.00000	36.00000	.01285	.16500	.49500	.18000	.26500
10.00000	32.00000	.01750	.18600	.55800	.20900	.30600
12.00000	28.00000	.02260	.20200	.60600	.24000	.33700
4.16000	28.00000	.03260	.25900	.65700	.28100	.43800
5.16000	24.00000	.05240	.30600	.79600	.34400	.53100
6.16000	24.00000	.08090	.36500	.97400	.40600	.64900
7.16000	20.00000	.10900	.41500	1.12500	.46900	.75000
8.16000	20.00000	.14900	.46400	1.24200	.53200	.82800
9.16000	18.00000	.18900	.51900	1.40700	.59400	.93800
10.16000	18.00000	.24000	.57500	1.57500	.68700	1.05000
12.16000	16.00000	.35100	.66500	1.84500	.81200	1.23000
14.16000	14.00000	.48000	.77900	2.15700	.93700	1.43800
16.16000	12.00000	.62500	.87000	2.43700	1.06200	1.62000

1.000	1.500	2.000	2.500	3.000	3.500	4.000	4.500	5.000	.250	.300	.350
.400	.450	.500	.600	.700	.800	.900	1.000	1.250	1.500	2.000	.550
.550	.550	.550	.550	.550	.550	.550	.550	.550	.550	.550	.550
.550	.390	.370	.350	.335	.320	.310	.300	.280	.275	.265	.255
.240	.230	.220	.330	.300	.270	.250	.230	.220	.205	.190	.175
.160	.150	.135	.130	.125	.295	.265	.235	.215	.200	.180	.160
.135	.125	.110	.100	.090	.080	.070	.280	.245	.220	.190	.173
.160	.132	.120	.100	.090	.080	.070	.060	.052	.265	.230	.200
.175	.160	.140	.115	.095	.080	.070	.062	.052	.048	.040	.250
.220	.185	.165	.142	.125	.100	.082	.070	.061	.055	.042	.040
.030	.240	.210	.175	.160	.135	.120	.095	.078	.063	.055	.050
.040	.035	.027	.230	.200	.170	.150	.134	.119	.090	.075	.062
.054	.044	.039	.030	.025	.909	.909	.909	.909	.909	.909	.909
.909	.909	.909	.909	.909	.909	.909	.875	.870	.862	.853	.846
.840	.833	.825	.820	.810	.800	.790	.780	.770	.870	.856	.852
.833	.823	.815	.800	.799	.780	.765	.750	.725	.700	.685	.870
.860	.840	.830	.820	.810	.791	.772	.750	.735	.715	.680	.660
.630	.880	.870	.855	.835	.825	.810	.790	.765	.735	.715	.690
.655	.630	.590	.890	.875	.862	.840	.830	.815	.785	.760	.730

244

```
    .700    .675    .635    .600    .565    .895    .880    .867    .845    .832    .816    .786
    .755    .720    .685    .665    .625    .585    .540    .900    .881    .870    .850    .835
    .818    .786    .751    .720    .682    .660    .615    .575    .530    .900    .882    .872
    .855    .838    .820    .786    .749    .720    .681    .655    .605    .565    .515   1.000
   1.      1.      1.      1.      1.      1.      1.      1.      1.      1.      1.      1.
   1.      1.3     1.2     1.1     1.      1.      1.      1.      1.      1.      1.      1.
   1.      1.      1.      2.2     2.0     1.8     1.6     1.4     1.3     1.      1.      1.
   1.      1.      1.      1.      1.      3.6     3.1     2.8     2.5     2.2     2.0     1.5
   1.2     1.      1.      1.      1.      1.      1.      5.2     4.7     4.2     3.7     3.3
   3.0     2.3     1.7     1.3     1.      1.      1.      1.      1.      7.2     6.5     5.7
   5.1     4.5     4.0     3.2     2.5     1.8     1.5     1.2     1.      1.      1.      9.5
   8.3     7.5     6.8     6.0     5.3     4.2     3.3     2.6     2.0     1.6     1.05    1.0
   1.     12.     11.      9.2     8.4     7.5     6.9     5.3     4.2     3.3     2.7     2.1
   1.4     1.0     1.     14.     13.     12.     11.      9.3     8.2     6.7     5.2     4.1
   3.2     2.7     1.6     1.2     1.0
+.300000E+01+.300000E-01+.900000E+05+.150000E+04+.900000E-01+.000000E+00
+.300000E+05+.100000E+06+.750000E+05+.300000E+01+.730000E+05+.540000E+05
+.150000E+06+.150000E+06+.150000E+06+.100000E+01+.100000E+01+.100000E+01
+.100000E+04
+.300000E+01+.300000E-01+.900000E+05+.150000E+04+.900000E-01+.000000E+00
+.300000E+05+.100000E+06+.750000E+05+.300000E+01+.730000E+05+.540000E+05
+.150000E+06+.150000E+06+.150000E+06+.100000E+01+.200000E+01+.100000E+01
+.100000E+04
E     END OF JOB
E     PAUSE
```

TABLE 28. TYPICAL INTEGRAL FLANGE DESIGNS

TYPE 1 FLANGE FOR:

D= .360000.+31 TI= .300000.-01 STE= .900000.+05 PT= .150000.+04 GO= .900000.-01 AMC=   .0
SG= .360000.+15 SFA= .100000.+06 SBA= .750000.+05 AM= .300000.+01 SFT= .730000.+05 SBT= .540000.+05
SFYS= .150000.+06 SSEYS= .150000.+16 SBYS= .150000.+06 CAPX= .100000.+01 CAPY= .100000.+01 CAPZ= .100000.+01
P= .150000.+04

WE HAVE 13 5.16 BOLTS WITH :

A= .496000.+01	AS= .0	B= .294000.+01	BS= .294000.+01	C= .427200.+01
DH= .344600.+00	G= .310300.+01	GS= .0	H= .771589.+00	H1= .0
H2= .0	RG= .0	THPI= .240000.+02	TOMIN= .388415.+00	TOMSP= .0
TS= .0	V1= .514584.+01	V2= .0	W= .163000.+00	WS= .190159.+05

WE HAVE 9 6.16 BOLTS WITH :

A= .520200.+01	AS= .0	B= .294000.+01	BS= .294000.+01	C= .439000.+01
DH= .406900.+00	G= .310300.+01	GS= .0	H= .771589.+00	H1= .0
H2= .0	RG= .0	THPI= .240000.+02	TOMIN= .398990.+00	TOMSP= .0
TS= .0	V1= .605342.+01	V2= .0	W= .163000.+00	WS= .190159.+05

WE HAVE 9 7.16 BOLTS WITH :

A= .542800.+01	AS= .0	B= .294000.+01	BS= .294000.+01	C= .449000.+01
DH= .469000.+00	G= .310300.+01	GS= .0	H= .771589.+00	H1= .0
H2= .0	RG= .0	THPI= .200000.+02	TOMIN= .398990.+00	TOMSP= .0
TS= .0	V1= .655078.+01	V2= .0	W= .163000.+00	WS= .190159.+05

WE HAVE 8 8.16 BOLTS WITH :

A= .565200.+01	AS= .0	B= .294000.+01	BS= .294000.+01	C= .458800.+01
DH= .532900.+00	G= .310300.+01	GS= .0	H= .771589.+00	H1= .0
H2= .0	RG= .0	THPI= .200000.+02	TOMIN= .417850.+00	TOMSP= .0
TS= .0	V1= .765098.+01	V2= .0	W= .163000.+00	WS= .190159.+05

WE HAVE 8 9.16 BOLTS WITH :

A= .588600.+01	AS= .0	B= .294000.+01	BS= .294000.+01	C= .469800.+01
DH= .594000.+00	G= .310300.+01	GS= .0	H= .771589.+00	H1= .0
H2= .0	RG= .0	THPI= .180000.+02	TOMIN= .420612.+00	TOMSP= .0
TS= .0	V1= .840402.+01	V2= .0	W= .163000.+00	WS= .190159.+05

WE HAVE 7 10.16 BOLTS WITH :

A= .618400.+01	AS= .0	B= .294000.+01	BS= .294000.+01	C= .481000.+01
DH= .627000.+00	G= .310300.+01	GS= .0	H= .771589.+00	H1= .0
H2= .0	RG= .0	THPI= .180000.+02	TOMIN= .429078.+00	TOMSP= .0
TS= .0	V1= .960814.+01	V2= .0	W= .163000.+00	WS= .190159.+05

WE HAVE 7 12.16 BOLTS WITH :

A= .661400.+01	AS= .0	B= .294000.+01	BS= .294000.+01	C= .499000.+01
DH= .812000.+00	G= .310300.+01	GS= .0	H= .771589.+00	H1= .0
H2= .0	RG= .0	THPI= .160000.+02	TOMIN= .440713.+00	TOMSP= .0
TS= .0	V1= .112993.+02	V2= .0	W= .163000.+00	WS= .190159.+05

WE HAVE 7 14.16 BOLTS WITH :

A= .709200.+01	AS= .0	B= .294000.+01	BS= .294000.+01	C= .521800.+01
DH= .937000.+00	G= .310300.+01	GS= .0	H= .771589.+00	H1= .0
H2= .0	RG= .0	THPI= .140000.+02	TOMIN= .447873.+00	TOMSP= .0
TS= .0	V1= .132369.+02	V2= .0	W= .163000.+00	WS= .190159.+05

WE HAVE 6 16.16 BOLTS WITH :

A= .752400.+01	AS= .0	B= .294000.+01	BS= .294000.+01	C= .540000.+01
DH= .106200.+01	G= .310300.+01	GS= .0	H= .771589.+00	H1= .0
H2= .0	RG= .0	THPI= .120000.+02	TOMIN= .460291.+00	TOMSP= .0
TS= .0	V1= .156412.+02	V2= .0	W= .163000.+00	WS= .190159.+05

TABLE 29. TYPICAL LOOSE RING FLANGE DESIGN

```
;TYPE 2 FLANGE FOR;

9
    D= .300000.+1   TI= .300000.-01   STE= .900000.+05   PT= .150000.+04   GO= .900000.-01   AMC=          .0
    SG= .300000.+05  SFA= .100000.+06  SBA= .750000.+05   AM= .300000.+01   SFT= .730000.+05  SBT= .540000.+05
    SFYS= .150000.+06SSEYS= .150000.+06 SBYS= .150000.+06 CAPX= .100000.+01 CAPY= .200000.+01 CAPZ= .100000.+01
    P= .150000.+04
```

WE HAVE 13 5.16 BOLTS WITH ;

A= .449100.+01	AS= .326600.+01	B= .311500.+01	BS= .294000.+01	C= .380300.+01
DH= .344000.+00	G= .310300.+01	GS= .600000.-01	H= .0	H1= .101815.+01
H2= .509077.+00	RG= .275000.-01	THPI= .240000.+02	TOMIN= .509077.+00	TOMSP= .0
TS= .600000.-01	V1= .0	V2= .203212.+01	W= .163000.+00	WS= .190159.+05

WE HAVE 8 6.16 BOLTS WITH ;

A= .473900.+01	AS= .326600.+01	B= .311500.+01	BS= .294000.+01	C= .392700.+01
DH= .406000.+00	G= .310300.+01	GS= .600000.-01	H= .0	H1= .105630.+01
H2= .528150.+00	RG= .275000.-01	THPI= .240000.+02	TOMIN= .528150.+00	TOMSP= .0
TS= .600000.-01	V1= .0	V2= .314532.+01	W= .163000.+00	WS= .190159.+05

WE HAVE 7 7.16 BOLTS WITH ;

A= .499100.+01	AS= .326600.+01	B= .311500.+01	BS= .294000.+01	C= .405300.+01
DH= .469000.+00	G= .310300.+01	GS= .600000.-01	H= .0	H1= .107261.+01
H2= .536303.+00	RG= .275000.-01	THPI= .200000.+02	TOMIN= .536303.+00 × TOMSP= .0
TS= .600000.-01	V1= .0	V2= .413209.+01	W= .163000.+00	WS= .190159.+05

WE HAVE 6 8.16 BOLTS WITH ;

A= .524300.+01	AS= .326600.+01	B= .311500.+01	BS= .294000.+01	C= .417900.+01
DH= .532000.+00	G= .310300.+01	GS= .600000.-01	H= .0	H1= .111108.+01
H2= .555541.+00	RG= .275000.-01	THPI= .200000.+02	TOMIN= .555541.+00	TOMSP= .0
TS= .600000.-01	V1= .0	V2= .533303.+01	W= .163000.+00	WS= .190159.+05

WE HAVE 6 9.16 BOLTS WITH ;

A= .549100.+01	AS= .326600.+01	B= .311500.+01	BS= .294000.+01	C= .430300.+01
DH= .594001.+00	G= .310300.+01	GS= .600000.-01	H= .0	H1= .112643.+01
H2= .563216.+00	RG= .275000.-01	THPI= .180000.+02	TOMIN= .563216.+00	TOMSP= .0
TS= .600000.-01	V1= .0	V2= .639766.+01	W= .163000.+00	WS= .190159.+05

WE HAVE 6 10.16 BOLTS WITH ;

A= .586300.+01	AS= .326600.+01	B= .311500.+01	BS= .294000.+01	C= .448900.+01
DH= .687000.+00	G= .310300.+01	GS= .600000.-01	H= .0	H1= .114850.+01
H2= .574250.+00	RG= .275000.-01	THPI= .180000.+02	TOMIN= .574250.+00	TOMSP= .0
TS= .600000.-01	V1= .0	V2= .810368.+01	W= .163000.+00	WS= .190159.+05

WE HAVE 6 12.16 BOLTS WITH ;

A= .636300.+01	AS= .326600.+01	B= .311500.+01	BS= .294000.+01	C= .473900.+01
DH= .812000.+00	G= .310300.+01	GS= .600000.-01	H= .0	H1= .117643.+01
H2= .588214.+00	RG= .275000.-01	THPI= .160000.+02	TOMIN= .588214.+00	TOMSP= .0
TS= .600000.-01	V1= .0	V2= .106331.+02	W= .163000.+00	WS= .190159.+05

WE HAVE 5 14.16 BOLTS WITH ;

A= .686300.+01	AS= .326600.+01	B= .311500.+01	BS= .294000.+01	C= .498900.+01
DH= .937000.+00	G= .310300.+01	GS= .600000.-01	H= .0	H1= .117643.+01
H2= .588214.+00	RG= .275000.-01	THPI= .140000.+02	TOMIN= .588214.+00	TOMSP= .0
TS= .600000.-01	V1= .0	V2= .130522.+02	W= .163000.+00	WS= .190159.+05

WE HAVE 5 16.16 BOLTS WITH ;

A= .736300.+01	AS= .326600.+01	B= .311500.+01	BS= .294000.+01	C= .523900.+01
DH= .106200.+01	G= .310300.+01	GS= .600000.-01	H= .0	H1= .117643.+01
H2= .588214.+00	RG= .275000.-01	THPI= .120000.+02	TOMIN= .588214.+00	TOMSP= .0
TS= .600000.-01	V1= .0	V2= .161667.+02	W= .163000.+00	WS= .190159.+05

247

Input Data Sheet and Operating Instructions

Threaded-Fitting Design Program

PROJECT   G-6201   Date of Run _____ __, 19

DECK NO.   TFD

DATE   July 10, 1963

PREPARED BY J. W. Adam

Data Cards (5 cards/run)

CARD 1

Col.

1-14 +/- .	E +/-	GS
15-28 +/- .	E +/-	P
29-42 +/- .	E +/-	DO
43-56 +/- .	E +/-	SY
57-70 +/- .	E +/-	FS

CARD 2

Col.

1-14 +/- .	E +/-	DP
15-28 +/- .	E +/-	FL
29-42 +/- .	E +/-	PSI
43-56 +/- .	E +/-	FN
57-70 +/- .	E +/-	WZ

CARD 3

1-14 +/- .	E +/-	FL2
15-28 +/- .	E +/-	D2
29-42 +/- .	E +/-	DELTC
43-56 +/- .	E +/-	FL3
57-70 +/- .	E +/-	E

CARD 4

1-14 +/- .	E +/-	FL5
15-28 +/- .	E +/-	ALPHA
29-42 +/- .	E +/-	SB
43-56 +/- .	E +/-	DELTH
57-70 +/- .	E +/-	DG

CARD 5

| 1-14 +/- . | E +/- | DT |
| 15-28 +/- . | E +/- | TO |

Data must be entered as ±.XXXXXXXX times some power of 10., e.g., -372.56 goes in as +/θ . 3 7 2 5 6 0 0 0 E θ/- 0 3

The deck is a systems FORTRAN source deck. All the control cards necessary for a compilation and execution are included. Just put the 4 data cards in place of the index card. Running time depends on DG and DT, but it is about 2 to 4 minutes per set of data. Multiple sets of data can be stacked.

Note: DG and DT should be entered as negative.

Definition of Symbols Used for Threaded-Fitting-Design Program

A	Nut equivalent outside radius	in.
*ALPHA	Coefficient of thermal expansion	in./in./F
AM	External bending moment	in-lb
AMT	External bending moment	in-lb
AU	Poissons ratio	
B	Inside radius of nut inwardly projecting flange	in.
BETA	Calculation variable	1/in.
BT1	Calculation variable	
BT2	Calculation variable	
BT3	Calculation variable	
*D	Nut dimension across wrench flats	in.
DCAPI	Minor thread diameter	in.
DCAPO	Minimum nut equivalent outside diameter based on radial thread force	in.
DE	Nut equivalent outside diameter	in.
DELA	Calculation variable	in.
DELCLD	Nut elongation due to cold thermal gradient	in.
DELHT	Nut elongation due to hot thermal gradient	in.
*DELTC	Cold thermal gradient	F
*DELTH	Hot thermal gradient	F
DELTOT	Total nut flange deflection	in.
DEL4	Nut elongation in threaded portion at maximum load	in.
DEL5	Nut elongation in hub at maximum load	in.
DEL6	Nut elongation at maximum load due to flange rotation	in.
*DG	Incremental variation in nut hub thickness	in.

* Designates input data.

249

DI	Inside tube diameter	in.
DM	Major thread diameter	in.
*DO	Outside tube diameter	in.
*DP	Thread pitch diameter	in.
DSG	Inside diameter of nut hub	in.
*DT	Incremental variation in nut flange thickness	in.
D1	Average diameter of threaded stub end	in.
*D2	Average diameter of seal tang	in.
D3	Average diameter of flanged stub end	in.
D4	Average diameter of threaded portion of nut	in.
D5	Average diameter of nut hub	in.
*E	Modulus of elasticity	psi
FE	End load due to pressure	lb
FKC	Deflection rate of compression members	in-lb
FKT	Actual deflection rate of tension members	in-lb
FKTD	Desired deflection rate of tension members	in-lb
*FL	Length of nut thread	in.
FLPRM	Length of nut thread plus hub length	in.
FL1	Length of threaded stub end under compression	in.
*FL2	Length of seal tang	in.
*FL3	Length of flanged stub end under compression	in.
FL4	Length of nut thread under tension	in.
*FL5	Length of nut hub	in.
FM	Equivalent end load due to bending moment	lb
FMH	Bending moment at nut hub-flange intersection	in-lb
FMHO	Calculation variable	

* Designates input data.

250

FMO	Restraining bending moment at nut hub-flange intersection	in-lb
* FN	Number of threads per in.	
* FS	Required seal seating load	lb
G	Equivalent nut hub thickness	in.
GA	Minimum nut hub thickness	in.
GO	Initial hub thickness	in.
* GS	Maximum seal line diameter	in.
HG	Moment arm	in.
I	Controlling stress identification factor	
I1	Controlling stress identification factor	
I2	Controlling stress identification factor	
I3	Controlling stress identification factor	
* P	Operating pressure	psi
PB	Pressure equivalent of bending moment	psi
* PSI	Thread angle (bearing face to perpendicular to axis)	degrees
* SB	Fitting material 200,000 cycle fatigue strength	psi
SCAPH	Longitudinal hub stress (designated SH in output list heading)	psi
SH	Maximum allowable stress	psi
SHP	Bending stress	psi
SHT	Allowable stress based on SB	psi
SR	Radial ring stress	psi
ST	Tangential ring stress	psi
STHF	Thread shear stress	psi
STHG	Tensile stress in nut hub	psi
STTF	Tensile stress in nut thread section	psi

* Designates input data.

251

*SY	Fitting material yield stress	psi
T	Nut flange thickness	in.
TEMP	Calculation variable	
THETM	Nut flange rotation	degrees
TN	Minimum nut thickness of threads based on radial thread force	in.
*TO	Initial nut flange thickness	in.
TT	Minimum tube thickness	in.
V	Nut volume	in.^{3}
W	Nut load (based on either FS or WSTR)	lb
WMAX	Maximum allowable nut load	lb
WMAX 1	Maximum allowable nut load (based on SCAPH)	lb
WMAX 2	Maximum allowable nut load (based on SR)	lb
WMAX 3	Maximum allowable nut load (based on ST)	lb
WMAX 4	Maximum allowable nut load (based on STTF)	lb
WMAX 5	Maximum allowable nut load (based on STHF)	lb
WMAX 6	Maximum allowable nut load (based on STHG)	lb
WMAX 7	Maximum allowable nut load (based on SCAPH and SR)	lb
WMAX 8	Maximum allowable nut load (based on ST and STTF)	lb
WMAX 9	Maximum allowable nut load (based on STHF and STHG)	lb
WPRLD	Recommended preload for assembly	lb
WSL	Minimum allowable seal load	lb
WSTR	Nut load (based on FE and FM)	lb
W 1	Thickness of threaded stub end	in.
*W 2	Thickness of seal tang	in.
W 3	Thickness of flanged stub end	in.

* Designates input data.

W 4	Average thickness of threaded portion of nut	in.
W 5	Average thickness of nut hub	in.
ZB	Section modulus of tube	in.^{3}
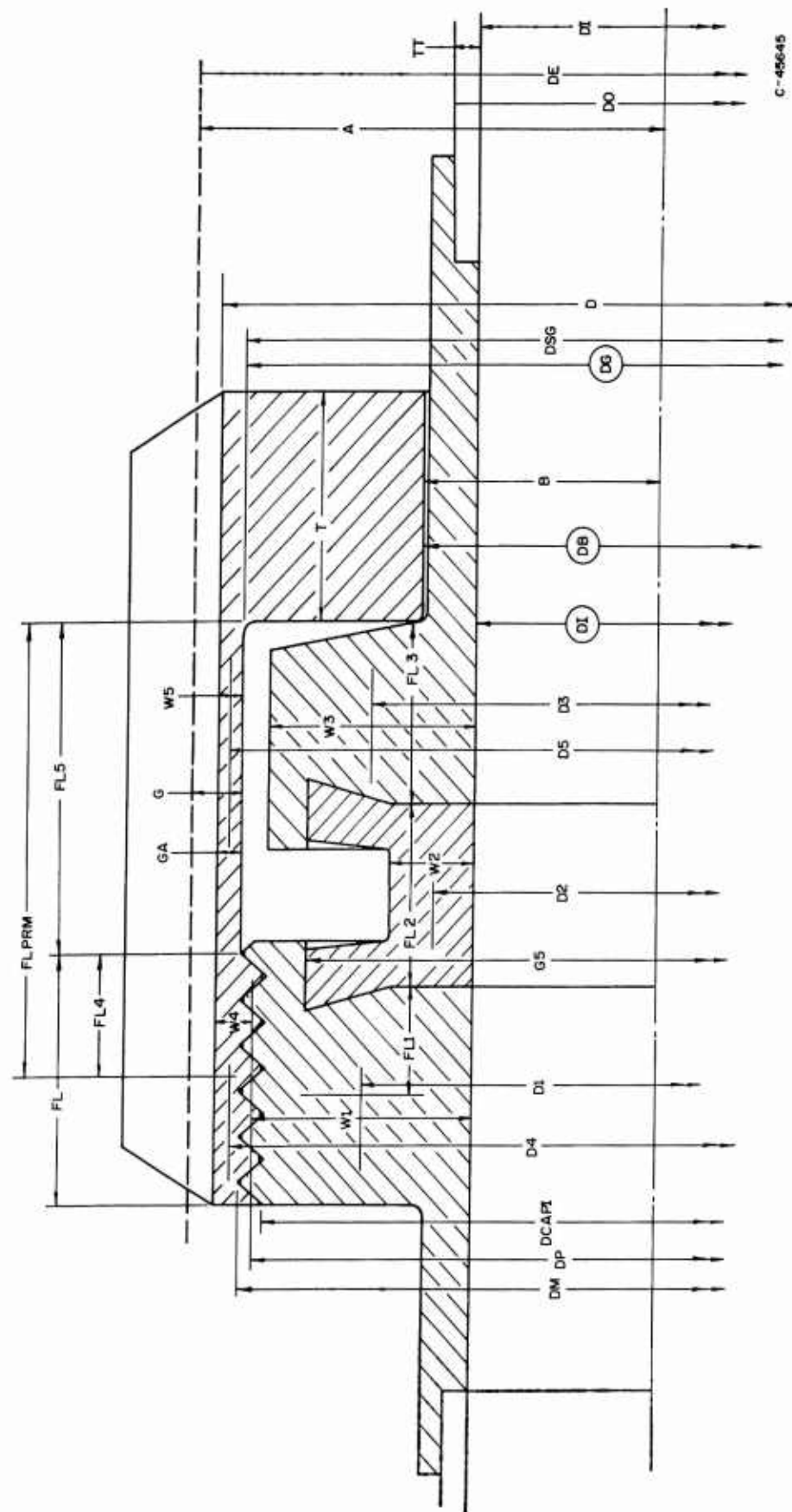
FIGURE 120. DRAWING SHOWING NOMENCLATURE FOR THREADED-FITTING DESIGN PROGRAM AND FOR THREADED-FITTING CAPABILITIES PROGRAM (SEE CIRCLED ITEMS)

254

```
I  THREADED FITTING DESIGN   0030                                                    3016C
E     INPUT SOURCE CARDS
E     EXECUTE
E     OUTPUT DEBUG TAPE
E     FORTRAN
H     NAME TFD
H     EQUIP=CARDRE,PRINTE;
C     DECK NUMBER 3016C
   1 FORMAT (5E14.8)
   2 FORMAT (25H1THREADED FITTING DESIGN //8H      GS=,E12.6,6H      P=,E1
     12.6,6H   DO=.E12.6,6H   SY=,E12.6,6H   FS=,E12.6,6H   DP=,E12.6/8H
     2    FL=,E12.6,6H   PSI=,E12.6,6H   FN=,E12.6,6H   W2=,E12.6,6H   FL
     32=,E12.6,6H   D2=,E12.6/8H   DELTC=,E12.6,6H   FL3=,E12.6,6H   E=,E
     412.6,6H   FL5=,E12.6,6HALPHA=,E12.6,6H   SB=,E12.6/8H   DELTH=,E12.6
     5,6H   DG=,E12.6,6H   DT=,E12.6,6H   TO=,E12.6,6H    D=,E12.6///)
   3 FORMAT (8H1 FOR D=,E12.6,10H   WE HAVE //8H      FE=,E12.6,6H   FM=,
     1E12.6,6H WSTR=,E12.6,6H      W=,E12.6,6H   DE=,E12.6,6H    A=,E12.6/
     28H      DI=,E12.6,6H   TT=,E12.6,6H    B=,E12.6,6H   SH=,E12.6,6H
     3 DM=,E12.6,8H   DCAPI=,E12.6///////)
   4 FORMAT (10H      W1=,E12.6,8H      D1=,E12.6,8H    FL1=,E12.6,8H
     1   FKC=,E12.6/10H      W2=,E12.6,8H      D2=,E12.6,8H    FL2=,E12.6
     2,8H DELCLD=,E12.6/10H      W3=,E12.6,8H      D3=,E12.6,8H    FL3=,
     3E12.6,8H   DELHT=,E12.6/10H      W4=,E12.6,8H      D4=,E12.6,8H
     4FL4=,E12.6,8H    WSL=,E12.6/50H
     5          FL5=,E12.6//)
   5 FORMAT (1H1,10H      FOR  G=,E12.6,15H   WE   HAVE   HG=,E12.6,10H   AND
     1 GA=,E12.6//)
   6 FORMAT(116H   T      I      WMAX    WPRLD       SH          SR          ST
     1     STTF        STHF        STHG       FKT         FKTD         V//)
   7 FORMAT(F5.3,I3,2F8.1,8E11.5,F7.4)
  45 READ 1,GS,P,DO,SY,FS,DP,FL,PSI,FN,W2,FL2,D2,DELTC,FL3,E,FL5,ALPHA,
     1SB,DELTH,DG,DT,TO,D
     PRINT 2,GS,P,DO,SY,FS,DP,FL,PSI,FN,W2,FL2,D2,DELTC,FL3,E,FL5,ALPHA
     1,SB,DELTH,DG,DT,TO,D
     FE=GS*GS*P*0.785398163
     DCAPI=DP-(.649519/FN)
     DM=2.*DP-DCAPI
     SH=.6666666667*SY
     SHT=.5*SB
     IF (SHT-SH)10,11,11
  10 SH=SHT
  11 TT=(P*DO)/(2.*SH)
     IF (TT-.005)12,13,13
  12 TT=.005
  13 DI=DO-2.*TT
     ZB=.0981747704*((DO**4.)-(DI**4.))/DO
     B=.285
     AM=SH*ZB
     AMT=60.*(DO+3.)**3.
     IF (AM-AMT)15,15,14
  14 AM=AMT
  15 SHP=AM/ZB
     PB=4.*TT*SHP/DO
     FM=.785398163*DO*DO*PB
     WSTR=FM+FE
     IF (WSTR-FS)16,17,17
```

```
   16 W=FS
      GO TO 18
   17 W=WSTR
   18 TN= W*TANF(PSI/57.295780)/(3.141592654*FL*SY)
      DCAPO=DM+2.*TN
  177 DE=D*1.050075135
      A=DE*.5
      PRINT 3,D,FE,FM,WSTR,W,DE,A,DI,TT,B,SH,DM,DCAPI
      W1=.5*(DP-DI)
      W3=.5*(DCAPI-.03-DI)
      W4=.5*(DE-DP)
      WSL=.1*WSTR
      D1=.5*(DP+DI)
      D3=.5*(DCAPI-.03+DI)
      D4=.5*(DE+DP)
      FL1=.5*FL
      FL4=FL1
      FKC=((FL1/(W1*D1))+(FL2/(W2*D2))+(FL3/(W3*D3)))/(3.141592654*E)
      FLPRM=FL4+FL5
      DELCLD=ALPHA*DELTC*FLPRM
      DELHT=ALPHA*DELTH*FLPRM
      PRINT 4,W1,D1,FL1,FKC,W2,D2,FL2,DELCLD,W3,D3,FL3,DELHT,W4,D4,FL4,W
     1SL,FL5
      GO=A-DM/2.
      G=GO
   50 HG=A-G/2.-B
      DSG=2.*(A-G)
      GA=(D-DSG)/2.
      AU=.3
      PRINT 5,G,HG,GA
      PRINT 6
      T=TO
   20 BT1=3.*(1.-AU*AU)
      BT2=A*A*G*G
      BT3=BT1/BT2
      BETA=BT3**.25
   22 TEMP=LOGF(A/B)
      FMHO=HG/(A*6.283185308*((((1.-AU*AU)*TEMP*((T/G)**3.))/(2.*BETA*A)
     1)+1.+(BETA*T/2.)))
      WMAX1=SH*G*G/(6.*FMHO)
      WMAX2=SH*T*T/(6.*(1.+BETA*T/2.)*FMHO)
      WMAX3=(B*T*T*SH*TEMP)/(3.*((HG/3.141592654)-2.*A*FMHO*(1.+BETA*T/2
     1.)))
      WMAX4=(SH*3.141592654*(DE*DE-DM*DM))/4.
      WMAX5=SH*2.513274123?*FL*DP
      WMAX6=SH*3.141592654*(A*A-(A-G)* (A-G))
      IF(WMAX1-WMAX2)400,401,401
  400 WMAX7=WMAX1
      I1=1
      GO TO 420
  401 WMAX7=WMAX2
      I1=2
  420 IF(WMAX3-WMAX4)402,403,403
  402 WMAX8=WMAX3
      I2=3
      GO TO 421
```

```
403 WMAX8=WMAX4
    I2=4
421 IF(WMAX5-WMAX6)404,405,405
404 WMAX9=WMAX5
    I3=5
    GO TO 422
405 WMAX9=WMAX6
    I3=6
422 IF(WMAX7-WMAX8)406,407,407
406 IF(WMAX7-WMAX9)408,409,409
408 WMAX=WMAX7
    I=I1
    GO TO 415
409 WMAX=WMAX9
    I=I3
    GO TO 415
407 IF(WMAX8-WMAX9)410,411,411
417 IF(WMAX8-WMAX9)410,411,411
410 WMAX=WMAX8
    I=I2
    GO TO 415
411 WMAX=WMAX9
    I=I3
415 DEL4=(WMAX*FL4)/(3.141592654*E*W4*D4)
    W5=G
    D5=2.*(A-G/2.)
    DEL5=(WMAX*FL5)/(3.141592654*E*W5*D5)
    DELA=FKC*(WMAX-WSL-WSTR)
    FKTD=(DELCLD+DELHT-DELA)/(WMAX-WSL-WSTR)
    FMO=WMAX*HG
225 FMH=FMO/(6.28318530B*A*(((1.-AU*AU)/(2.*BETA*A))*(T/G)**3.*
   1TEMP    +1.+BETA*T/2.))
    SCAPH=(6.*FMH)/(G*G)
    SR=(6./(T*T))*(1.+BETA*T/2.)*FMH
    ST=(3./(T*T*R*TEMP))*(FMO/3.141592654-2.*A*FMH*(1.+BETA*T/2.))
    STTF=(4.*WMAX)/(3.141592654*(DE*DE-DM*DM))
    STHF=WMAX/(2.5132741232*FL*DP)
    STHG=WMAX/(3.141592654*(A*A-(A-G)**2.))
    V=3.141592654*((A*A-B*B)*T+(A*A-(A-G)**2.)*FL5+(A*A-DP*DP/4.)*FL)
    DEL6=(2.*HG*R*ST)/(E*T)
    FKT=(DEL4+DEL5+DEL6)/WMAX
    DELTOT=FKT*WMAX+FKC*(WMAX-WSTR)
    WPRLD=(DELTOT-DELHT)/(FKC+FKT)
    THETM=DEL6*57.295780/HG
    PRINT 7,T,I,WMAX,WPRLD,SCAPH,SR,ST,STTF,STHF,STHG,FKT,FKTD,V
    IF(FKTD-0)30,70,70
70  T=T+DT
    IF(T+DT)30,20,20
30  G=G+DG
    IF (GA-0)40,40,29
29  GO TO 50
40  GO TO 41
41  GO TO 45
    END
```

```
+.82000000E+00+.30000000E+04+.50000000F+00+.15000000E+06+.12000000E+04
+.96750000E+00+.29000000E+00+.30000000E+02+.20000000E+02+.95000000E-01
+.20000000E+00+.53200000E+00+.16200000E+03+.80000000E-01+.29000000E+08
+.25500000E+00+.75000000E-05+.23000000E+06+.30000000E+03-.30000000E-02
-.30000000E-02+.30000000E+00+.10625000E+01
```
```
E     END OF JOB
E     PAUSE
```

THREADED FITTING DESIGN

$GS=.820000_{10}+00$ $P=.300000_{10}+04$ $DO=.500000_{10}+00$ $SY=.1500000_{10}+06$ $FS=.1200000_{10}+04$ $DP=.967500_{10}+00$

$FL1=.290000_{10}+00$ $PSI=.300000_{10}+02$ $FN=.200000_{10}+02$ $W2=.950000_{10}-01$ $FL2=.200000_{10}+00$ $D2=.5320000_{10}+00$

$DELTC=.162000_{10}+03$ $FL3=.800000_{10}-01$ $E=.290000_{10}+08$ $FL5=.2550000_{10}+00$ $ALPHA=.750000_{10}-05$ $SB=.2300000_{10}+06$

$DELTH=.300000_{10}+03$ $DG=.300000_{10}-02$ $DT=.300000_{10}-02$ $TO=.300000_{10}+00$ $D=.10625_{10}+01$

FOR $D=.106250_{10}+01$ WE HAVE

$FE=.158431_{10}+04$ $FM=.117810_{10}+04$ $WSTR=.276240_{10}+04$ $W=.276240_{10}+04$ $DE=.111570_{10}+01$ $A=.557852_{10}+00$

$DI=.485000_{10}+00$ $TT=.750000_{10}-02$ $B=.285000_{10}+00$ $SH=.100000_{10}+06$ $DM=.999976_{10}+00$ $DCAPI=.935024_{10}+00$

$W1=.241250_{10}+00$ $D1=.726250_{10}+00$ $FL1=.145000_{10}+00$ $FKC=.585355_{10}-07$

$W2=.950000_{10}-01$ $D2=.532000_{10}+00$ $FL2=.200000_{10}+00$ $DELCLD=.486000_{10}-03$

$W3=.210012_{10}+00$ $D3=.695012_{10}+00$ $FL3=.800000_{10}-01$ $DELHT=.900000_{10}-03$

$W4=.741024_{10}-01$ $D4=.104160_{10}+01$ $FL4=.145000_{10}+00$ $WSL=.276240_{10}+03$

$FL5=.255000_{10}+00$

FOR G=.51864410-01 WE HAVE HG=.24692010+00 AND GA=.25262010-01

T	I	WMAX	WPRLD	SH	SR	ST	STTF	STHF	STHG	FKT	FKTD	V
.300	3	8417.0	5120.7	.8183310+05	.5218310+04	.1000010+06	.4377010+05	.1193610+05	.4855810+05	.2635510-06	.1991610-06	0.3313
.297	3	8276.9	5033.2	.8266010+05	.5349410+04	.1000010+06	.4304110+05	.1173810+05	.4775010+05	.2687810-06	.2060610-06	0.3291
.294	3	8138.3	4947.4	.8350310+05	.5485410+04	.1000010+06	.4232110+05	.1154110+05	.4695010+05	.2741910-06	.2132510-06	0.3269
.291	3	8001.3	4863.2	.8436410+05	.5626410+04	.1000010+06	.4160810+05	.1134710+05	.4616010+05	.2797910-06	.2207510-06	0.3248
.288	3	7865.9	4780.7	.8524310+05	.5772810+04	.1000010+06	.4090410+05	.1115510+05	.4537910+05	.2855810-06	.2285810-06	0.3226
.285	3	7732.1	4699.7	.8614010+05	.5924610+04	.1000010+06	.4020810+05	.1096510+05	.4460710+05	.2915910-06	.2367710-06	0.3204
.282	3	7599.8	4620.4	.8705610+05	.6082410+04	.1000010+06	.3952110+05	.1077710+05	.4384410+05	.2978010-06	.2453310-06	0.3183
.279	3	7469.2	4542.6	.8799210+05	.6246210+04	.1000010+06	.3884110+05	.1059210+05	.4309010+05	.3042410-06	.2542910-06	0.3161
.276	3	7340.1	4466.4	.8894910+05	.6416510+04	.1000010+06	.3817010+05	.1040910+05	.4234510+05	.3109110-06	.2636810-06	0.3139
.273	3	7212.6	4391.7	.8992610+05	.6593610+04	.1000010+06	.3750710+05	.1022810+05	.4161010+05	.3178210-06	.2735210-06	0.3118
.270	3	7086.8	4318.5	.9092510+05	.6777810+04	.1000010+06	.3685210+05	.1005010+05	.4088410+05	.3249910-06	.2838510-06	0.3096
.267	3	6962.5	4246.8	.9194710+05	.6969510+04	.1000010+06	.3620610+05	.9873610+04	.4016710+05	.3324210-06	.2946910-06	0.3074
.264	3	6839.8	4176.6	.9299210+05	.7169110+04	.1000010+06	.3556810+05	.9699610+04	.3945910+05	.3401210-06	.3060910-06	0.3053
.261	3	6718.8	4107.9	.9406110+05	.7377110+04	.1000010+06	.3493910+05	.9528010+04	.3876110+05	.3481110-06	.3180810-06	0.3031
.258	3	6599.3	4040.6	.9515510+05	.7593910+04	.1000010+06	.3431810+05	.9358610+04	.3807210+05	.3563910-06	.3307110-06	0.3009
.255	3	6481.5	3974.7	.9627410+05	.7819910+04	.1000010+06	.3370510+05	.9191510+04	.3739210+05	.3649910-06	.3440310-06	0.2988
.252	3	6365.4	3910.2	.9742010+05	.8055710+04	.1000010+06	.3310110+05	.9026810+04	.3672210+05	.3739110-06	.3580910-06	0.2966
.249	3	6250.8	3847.1	.9859410+05	.8302010+04	.1000010+06	.3250510+05	.8864410+04	.3606110+05	.3831610-06	.3729510-06	0.2944
.246	3	6137.9	3785.4	.9979610+05	.8559110+04	.1000010+06	.3191810+05	.8704310+04	.3541010+05	.3927710-06	.3886710-06	0.2923
.243	1	5965.3	3663.7	.1000010+06	.8738010+04	.9898210+05	.3102110+05	.8459510+04	.3441410+05	.4027510-06	.4150410-06	0.2901
.240	1	5784.6	3533.5	.1000010+06	.8904910+04	.9776010+05	.3008110+05	.8203210+04	.3337110+05	.4131010-06	.4462210-06	0.2879
.237	1	5608.1	3407.2	.1000010+06	.9077510+04	.9653810+05	.2916310+05	.7952910+04	.3235310+05	.4238610-06	.4808910-06	0.2858
.234	1	5435.8	3284.7	.1000010+06	.9256110+04	.9531610+05	.2826710+05	.7708610+04	.3135910+05	.4350310-06	.5196510-06	0.2836
.231	1	5267.7	3166.0	.1000010+06	.9440910+04	.9409410+05	.2739310+05	.7470210+04	.3039010+05	.4466310-06	.5632510-06	0.2814
.228	1	5103.8	3051.1	.1000010+06	.9632310+04	.9287210+05	.2654010+05	.7237710+04	.2944410+05	.4586910-06	.6126210-06	0.2792

Input Data Sheet and Operating Instructions

Threaded-Fitting Capabilities Program

PROJECT   G-6201-1   Date of Run _____ __ , 19

DECK NO.   TFC

DATE   July 10, 1963

PREPARED BY J. W. Adam

Data Cards (5 cards/run)

CARD 1

Col.

1-14 +/- . _ _ _ _ _ _ _ _ _ _	E +/- _	SY
15-28 +/- . _ _ _ _ _ _ _ _ _ _	E +/- _	DE
29-42 +/- . _ _ _ _ _ _ _ _ _ _	E +/- _	D
43-56 +/- . _ _ _ _ _ _ _ _ _ _	E +/- _	DP
57-70 +/- . _ _ _ _ _ _ _ _ _ _	E +/- _	FN

CARD 2

Col.

1-14 +/- . _ _ _ _ _ _ _ _ _ _	E +/- _	FL
15-28 +/- . _ _ _ _ _ _ _ _ _ _	E +/- _	DG
29-42 +/- . _ _ _ _ _ _ _ _ _ _	E +/- _	DB
43-56 +/- . _ _ _ _ _ _ _ _ _ _	E +/- _	T
57-70 +/- . _ _ _ _ _ _ _ _ _ _	E +/- _	E

CARD 3

| 1-14 +/- . _ _ _ _ _ _ _ _ _ _ | E +/- _ | FL5 |

CARD 4

1-14 +/- . _ _ _ _ _ _ _ _ _ _	E +/- _	DI
15-28 +/- . _ _ _ _ _ _ _ _ _ _	E +/- _	W2
29-42 +/- . _ _ _ _ _ _ _ _ _ _	E +/- _	FL2
43-56 +/- . _ _ _ _ _ _ _ _ _ _	E +/- _	FL3
57-70 +/- . _ _ _ _ _ _ _ _ _ _	E +/- _	TQ

CARD 5

Col.

1-14 +/- . _ _ _ _ _ _ _ _ _ _	E +/- _	P
15-28 +/- . _ _ _ _ _ _ _ _ _ _	E +/- _	GS
29-42 +/- . _ _ _ _ _ _ _ _ _ _	E +/- _	ALPHA
43-56 +/- . _ _ _ _ _ _ _ _ _ _	E +/- _	D2

Data must be entered as ±. XXXXXXXX times some power of 10. , e. g. , -372. 56 goes in as +/θ . 3 7 2 5 6 0 0 0 E θ/- 0 3

The deck is a systems FORTRAN source deck. All the control cards necessary for a compilation and execution are included. Just put the 5 data cards in place of the index card. Running time is about 2 minutes per set of data. Multiple sets of data can be stacked.

Note: Either DE or D must equal zero.

Definition of Symbols Used for Threaded-Fitting Capabilities Program

A	Nut equivalent outside radius	in.
*ALPHA	Coefficient of thermal expansion	in./in./F
AU	Poisson's ratio	
B	Inside radius of nut inwardly projecting flange	in.
BETA	Calculation variable	1/in.
BT1	Calculation variable	
BT2	Calculation variable	
BT3	Calculation variable	
*D	Nut dimension across wrench flats	in.
*DB	Inside diameter of nut inwardly projecting flange	in.
DCAPI	Minor thread diameter	in.
*DE	Nut equivalent outside diameter	in.
DELCLD	Nut elongation due to cold thermal gradient	in.
DELHT	Nut elongation due to hot thermal gradient	in.
DELTC	Cold thermal gradient	F
DELTH	Hot thermal gradient	F
DEL4	Nut elongation in threaded portion at maximum load	in.
DEL5	Nut elongation in hub at maximum load	in.
DEL6	Nut elongation at maximum load due to flange rotation	in.
*DG	Inside diameter of nut hub	in.
*DI	Inside fitting diameter	in.
DM	Major thread diameter	in.
*DP	Thread pitch diameter	in.
D1	Average diameter of threaded stub end	in.
*D2	Average diameter of seal tang	in.

* Designates input data.

262

D3	Average diameter of flanged stub end	in.
D4	Average diameter of threaded portion of nut	in.
D5	Average diameter of nut hub	in.
*E	Modulus of elasticity	psi
FE	End load due to pressure	lb
FKC	Deflection rate of compression members	in-lb
FKT	Actual deflection rate of tension members	in-lb
*FL	Length of nut thread	in.
FLPRM	Length of nut thread plus hub length	in.
FL1	Length of threaded stub end under compression	in.
*FL2	Length of seal tang	in.
*FL3	Length of flanged stub end under compression	in.
FL4	Length of nut thread under tension	in.
*FL5	Length of nut hub	in.
FM	Equivalent end load due to bending moment	lb
FMH	Bending moment at nut hub-flange intersection	in-lb
FMHO	Calculation variable	
FMO	Restraining bending moment at nut hub-flange intersection	in-lb
*FN	Number of threads per inch	
G	Equivalent nut hub thickness	in.
GA	Minimum nut hub thickness	in.
*GS	Maximum seal line diameter	in.
HG	Moment arm	in.
I	Controlling stress identification factor	
I1	Controlling stress identification factor	
I2	Controlling stress identification factor	

* Designates input data.

I3	Controlling stress identification factor	
K	Counting factor	
*P	Operating pressure	psi
SCAPH	Longitudinal hub stress (designated SH in output list heading)	psi
SH	Maximum allowable stress	psi
SR	Radial ring stress	psi
ST	Tangential ring stress	psi
STHF	Thread shear stress	psi
STTF	Tensile stress in nut thread section	psi
*SY	Fitting material yield stress	psi
*T	Nut flange thickness	in.
TEMP	Calculation variable	
*TQ	Recommended preload torque	in-lb
V	Nut volume	in.^{3}
WMAX	Maximum allowable nut load	lb
WMAX1	Maximum allowable nut load (based on SCAPH)	lb
WMAX2	Maximum allowable nut load (based on SR)	lb
WMAX3	Maximum allowable nut load (based on ST)	lb
WMAX4	Maximum allowable nut load (based on STTF)	lb
WMAX5	Maximum allowable nut load (based on STHF)	lb
WMAX6	Maximum allowable nut load (based on STHG)	lb
WMAX7	Maximum allowable nut load (based on SCAPH and SR)	lb
WMAX8	Maximum allowable nut load (based on ST and STTF)	lb
WMAX9	Maximum allowable nut load (based on STHF and STHG)	lb
WPLD	Preload based on TQ	lb
WSL	Minimum allowable seal load	lb

* Designates input data.

264

WSTR	Nut load (based on FE and FM)	lb
W1	Thickness of threaded stub end	in.
*W2	Thickness of seal tang	in.
W3	Thickness of flanged stub end	in.
W4	Average thickness of threaded portion of nut	in.
W5	Average thickness of nut hub	in.

---

* Designates input data.

```
I  THREADED FITTING CAPABILITIES    0030
E     INPUT SOURCE CARDS
E     EXECUTE
E     OUTPUT DEBUG TAPE
E     FORTRAN
H      NAME TFC
H      EQUIP=CARDRE,PRINTE;
C  DECK 3016D PLUS THERMAL
   1 FORMAT (5E14.8)
   2 FORMAT (31H1THREADED FITTING CAPIBILITIES //8H      SY=,E12.6,6H
     1DE=,E12.6,6H    D=,E12.6,6H   DP=,E12.6,6H   FN=,E12.6/8H      FL=,
     2E12.6,6H   DG=,E12.6,6H   DB=,E12.6,6H    T=,E12.6,6H    E=,E12.6/
     38H    FL5=,E12.6//)
   3 FORMAT (10H      SH=,E12.6,8H      DE=,E12.6,8H      D=,E12.6,8H
     1    A=,E12.6,8H      W4=,E12.6/10H      D4=,E12.6,8H    FL4=,E12.6
     2,8H    W5=,F12.6,8H      D5=,E12.6,8H    FL5=,E12.6/10H      G=,
     3E12.6,8H      GA=,E12.6,8H      B=,E12.6,8H    HG=,E12.6,8H    AU
     4=,E12.6/10H    WMAX1=,E12.6,8H  WMAX2=,E12.6,8H  WMAX3=,E12.6,8H
     5WMAX4=,E12.6,8H  WMAX5=,E12.6)
   4 FORMAT (10H    WMAX6=,E12.6,8H  DEL 4=,E12.6,8H  DEL 5=,E12.6,8H
     1DEL 6=,E12.6,8H  SCAPH=,E12.6/10H      SR=,E12.6,8H      ST=,E12.6
     2,8H    STTF=,E12.6,8H    STHF=,E12.6,8H    STHG=,E12.6/10H      V=,
     3E12.6,8H    FKT=,E12.6,8H    WMAX=,E12.6/)
   5 FORMAT (8H      DI=,F12.6,6H    W2=,E12.6,6H  FL2=,E12.6,6H  FL3=,E1
     12.6,6H    TQ=,E12.6/8H      P=,E12.6,6H    GS=,E12.6,6HALPHA=,E12.6,
     26H    D2=,E12.6/)
   8 FORMAT (11H      W1=,E12.6,8H      W3=,F12.6,8H      D1=,E12.6,8H
     1    D3 =,F12.6/10H    FKC=,E12.6,8H    WPLD=,E12.6,8H    WSI=,E12.
     26,8H    FE=,E12.6/10H      FM=,E12.6,8H    WSTR=,E12.6,8H  DELHT=
     3,E12.6,8H  DELCLD=,E12.6/10H    DELTH=,E12.6,8H  DELTC=,E12.6///)
  45 READ 1,SY,DE,D,DP,FN,FL,DG,DB,T,E,FL5
     PRINT 2,SY,DE,D,DP,FN,FL,DG,DB,T,E,FL5
     READ 1,DI,W2,FL2,FL3,TQ,P,GS,ALPHA,D2
     PRINT 5,DI,W2,FL2,FL3,TQ,P,GS,ALPHA,D2
     SH=.6666666667*SY
     IF (DE-0)177,177,41
 177 DE=D*1.050075135
     GO TO 42
  41 D=DE/1.050075135
  42 A=DE*.5
     DCAPI=DP-(.649519/FN)
     DM=2.*DP-DCAPI
     W4=.5*(DE-DP)
     D4=.5*(DE+DP)
     FL1=.5*FL
     FL4=FL1
     GA=(D-DG)/2.
     G=A-DG/2.
     B=DB/2.
  50 HG=A-G/2.-B
     AU=.3
  20 BT1=3.*(1.-AU*AU)
     BT2=A*A*G*G
     BT3=BT1/BT2
     BETA=BT3**.25
  22 TEMP=LOGF(A/B)
```

```
      FMHO=HG/(A*6.283185308*(((1.-AU*AU)*TEMP*((T/G)**3.))/(2.*BETA*A)
     1)+1.+(BETA*T/2.)))
      WMAX1=SH*G*G/(6.*FMHO)
      WMAX2=SH*T*T/(6.*(1.+BETA*T/2.)*FMHO)
      WMAX3=(B*T*T*SH*TEMP)/(3.*((HG/3.141592654)-2.*A*FMHO*(1.+BETA*T/
     12.)))
      WMAX4=(SH*3.141592654*(DE*DE-DM*DM))/4.
      WMAX5=SH*2.5132741232*FL*DP
      WMAX6=SH*3.141592654*(A*A-(A-G)*  (A-G))
      IF(WMAX1-WMAX2)400,401,401
  400 WMAX7=WMAX1
      I1=1
      GO TO 420
  401 WMAX7=WMAX2
      I1=2
  420 IF(WMAX3-WMAX4)402,403,403
  402 WMAX8=WMAX3
      I2=3
      GO TO 421
  403 WMAX8=WMAX4
      I2=4
  421 IF(WMAX5-WMAX6)404,405,405
  404 WMAX9=WMAX5
      I3=5
      GO TO 422
  405 WMAX9=WMAX6
      I3=6
  422 IF(WMAX7-WMAX8)406,407,407
  406 IF(WMAX7-WMAX9)408,409,409
  408 WMAX=WMAX7
      I=I1
      GO TO 415
  409 WMAX=WMAX9
      I=I3
      GO TO 415
  407 IF(WMAX8-WMAX9)410,411,411
  417 IF(WMAX8-WMAX9)410,411,411
  410 WMAX=WMAX8
      I=I2
      GO TO 415
  411 WMAX=WMAX9
      I=I3
  415 DEL4=(WMAX*FL4)/(3.141592654*E*W4*D4)
      W5=G
      D5=2.*(A-G/2.)
      DEL5=(WMAX*FL5)/(3.141592654*E*W5*D5)
      FMO=WMAX*HG
  225 FMH=FMO/(6.283185308*A*(((1.-AU*AU)/(2.*BETA*A))*(T/G)**3.*
     1TEMP    +1.+BETA*T/2.))
      SCAPH=(6.*FMH)/(G*G)
      SR=(6./(T*T))*(1.+BETA*T/2.)*FMH
      ST=(3./(T*T*B*TEMP))*(FMO/3.141592654-2.*A*FMH*(1.+BETA*T/2.))
      STTF=(4.*WMAX)/(3.141592654*(DE*DE-DM*DM))
      STHF=WMAX/(2.5132741232*FL*DP)
      STHG=WMAX/(3.141592654*(A*A-(A-G)**2.))
      V=3.141592654*((A*A-B*B)*T+(A*A-(A-G)**2.)*FL5+(A*A-DP*DP/4.)*FL)
```

267

```
      DEL6=(2.*HG*R*ST)/(E*T)
      FKT=(DEL4+DEL5+DEL6)/WMAX
      PRINT 3,SH,DE,D,A,W4,D4,FL4,W5,D5,FL5,G,GA,B,HG,AU,WMAX1,WMAX2,WMA
     1X3,WMAX4,WMAX5
      PRINT 4,WMAX6,DEL4,DEL5,DEL6,SCAPH,SR,ST,STTF,STHF,STHG,V,FKT,WMAX
C     THERMAL CAPABILITIES
      K=0.
   30 W1=.5*(DP-DI)
      W3=.5*(DCAPI-.03-DI)
      D1=.5*(DP+DI)
      D3=.5*(DCAPI-.03+DI)
      FKC=((FL1/(W1*D1))+(FL2/(W2*D2))+(FL3/(W3*D3)))/(3.141592654*E)
      WPLD=TQ/(0.2*DP)
      WSL=.1*WPLD
      FE=GS*GS*P*0.785398163
   31 FM=.5*FE
      GO TO 33
   32 FM=0.
   33 WSTR=FM+FE
      K=K+1.
      DELHT=FKT*(WMAX-WPLD)+FKC*(WMAX-WSTR-WPLD)
      FLPRM=FL4+FL5
      DELTH=DELHT/(ALPHA*FLPRM)
      DELCLD=FKC*(WPLD-WSL)+FKT*(WPLD-WSL-WSTR)
      DELTC=DELCLD/(ALPHA*FLPRM)
      PRINT 8,W1,W3,D1,D3,FKC,WPLD,WSL,FE,FM,WSTR,DELHT,DELCLD,DELTH,DEL
     1TC
      GO TO (32,34),K
   34 GO TO 45
      END
L
+.48000000E+05+.00000000E+00+.11260000E+01+.96750000E+00+.20000000E+02
+.25000000E+00+.93800000E+00+.65600000E+00+.15200000E+00+.29000000E+08
+.12500000E+00
+.40600000E+00+.12500000E+00+.20000000E-01+.21500000E+00+.40000000E+03
+.30000000E+04+.80300000E+00+.10400000E-04+.53800000E+00
E     END OF JOB
E     PAUSE
```

Typical Output for Threaded-Fitting Capabilities Program

THREADED FITTING CAPABILITIES

```
SY= .480000.+05    DE=                 D= .112600.+01    DP= .967500.+00    FN= .200000.+02
FL= .250000.+00    DG= .938000.+00     DB= .656000.+00    T= .152000.+00    E= .290000.+08
FL5= .125000.+00


D1= .406000.+00    W2= .125000.+00     FL2= .200000.-01    FL3= .215000.+00    TQ= .400000.+03
P= .300000.+04     GS= .803000.+00     ALPHA= .104000.-04    D2= .538000.+00


SH= .320000.+05    DE= .118238.+01     D= .112600.+01      A= .591192.+00    W4= .107442.+00
D4= .107494.+01    FL4= .125000.+00    W5= .122192.+00    D5= .106019.+01    FL5= .125000.+00
G= .122192.+00     GA= .940000.-01     B= .328000.+00     HG= .202096.+05    AU= .300000.+00
WMAX1= .226274.+04  WMAX2= .256796.+04  WMAX3= .627122.+04  WMAX4= .100049.+05  WMAX5= .194527.+05
WMAX6= .130235.+05  DEL 4= .268805.-04  DEL 5= .239645.-04  DEL 6= .347259.-03  SCAPH= .320000.+05
SR= .281965.+05    ST= .115460.+05     STIF= .723724.+04   STHF= .372224.+04   STHG= .555977.+04
V= .257106.+00     FKT= .175939.-06    WMAX= .226274.+04


W1= .280750.+00    W3= .249512.+00     D1= .686750.+00    D3 = .655512.+00
FKC= .248088.-07   WPLD= .206718.+04   WSL= .206718.+03   FE= .151930.+04
FM= .759648.+03    WSTR= .227894.+04   DELHT=-.172802.-04  DELCLD=-.274705.-04
DELTH=-.664623.+01  DELTC=-.105656.+02


W1= .280750.+00    W3= .249512.+00     D1= .686750.+00    D3 = .655512.+00
FKC= .248088.-07   WPLD= .206718.+04   WSL= .206718.+03   FE= .151930.+04
FM= .0             WSTR= .151930.+04   DELHT= .156577.-05  DELCLD= .106181.-03
DELTH= .602219.+00  DELTC= .408388.+02
```

LEAKAGE FLOW ANALYSIS

The flow through a seal can be analyzed as a laminar flow of a viscous fluid if the mean free path of the gas molecules is less than the smallest passage dimension. If the mean free path is the same order of magnitude as the passage dimension, the flow becomes molecular rather than laminar, and a correction for slip flow at the wall must be applied to the laminar-flow analysis. In general the flow is laminar if

$$\frac{\lambda}{h} < 1 = \text{Knudsen's number}$$

$$\lambda = \text{Mean free path of molecule, in.}$$

$$h = \text{Passage height, in.}$$

It is possible to analyze the flow through a seal on the basis of laminar flow, applying a correction which is a function of Knudson's number if Knudsen's number approaches 1.0.

The Laminar-Flow Analysis

In the following the complete derivation is given since the case of flow through slots is not given in the literature, which discusses flow through capillary tubes. [1]*

Consider a narrow slot of height h, width w, and length ℓ, as shown in Figure 121. Flow is in the direction of ℓ, and the width w would correspond to the periphery of a circular seal.

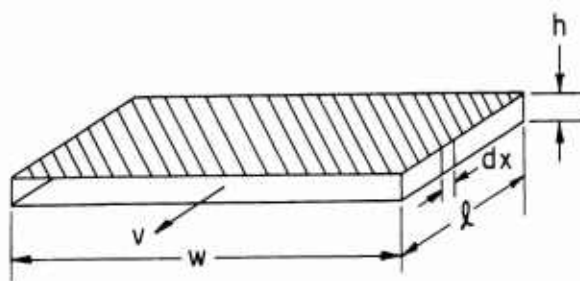

FIGURE 121. SLOT ASSUMED FOR LAMINAR-FLOW ANALYSIS

Consider now a section dx in length and of unit width through Figure 121 in the plane of ℓ, as shown in Figure 122. Since the flow is laminar, the velocity must be zero at the walls, and the velocity profile will be symmetrical about the center line of the passage. A pressure difference, dp, acts across the length dx. If we now consider a section δh in height, we can write the pressure force on the segment,
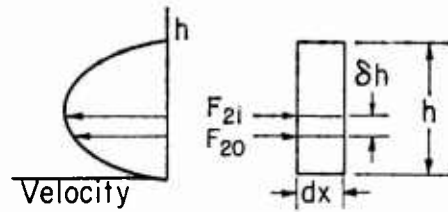
$$F_1 = -\delta h dp.$$

FIGURE 122. FLOW AT SECTION dx OF SLOT

The pressure force must be equal and opposite to the viscous shearing forces on the segment if the flow is to be steady. The viscosity is defined as the ratio of shear stress to velocity gradient. Thus the shearing forces must have the form

$$F_2 = \eta dx \frac{dv}{dy},$$

where

η = viscosity
v = velocity
y = ordinant in h direction.

At the outer surface of the element δh, the shearing force will be

$$F_{2o} = \eta dx \frac{dv}{dy}.$$

Since the velocity increases as the center line is approached, the force on the inner surface of the element will be

$$F_{2i} = \eta dx \frac{d}{dy} (v + \frac{dv}{dy} \delta h).$$

Also, the velocity gradient, dv/dh, is greater at the outer surface of the element, and the net shearing force on the element will be

$$F_2 = F_{2o} - F_{2i} = \eta dx \left[\frac{dv}{dy} - \frac{d}{dy}(v + \frac{dv}{dy} \delta h) \right].$$

If the element is not accelerating, the pressure force must equal the shearing force:

$$F_1 = F_2$$

$$- \delta h dp = \eta dx \left[\frac{dv}{dy} - \frac{d}{dy}(v + \frac{dv}{dy} \delta h) \right]$$

$$= \eta dx \left[\frac{dv}{dy} - \frac{dv}{dy} - \delta h \frac{d^2 v}{dy^2} - \frac{dv}{dy} \frac{d\delta h}{dy} \right].$$

Leaving out the second-order term results in

$$-\delta h dp = \eta dx \delta h \frac{d^2 v}{dy^2}$$

$$\frac{1}{\eta} \frac{dp}{dx} = \frac{d^2 v}{dy^2} .$$

272

Considering first the right side of this equation, assume a solution of the form

$$v = A + By + Cy^2$$

$$\frac{dv}{dy} = B + 2Cy , \quad \frac{d^2v}{dy^2} = 2C$$

and

$$2C = \frac{1}{\eta} \frac{dp}{dx} .$$

From the laminar flow requirement, $v = 0$ when $y = 0$; therefore, $A = 0$.

The flow must also be symmetrical about the center line. Therefore,

$$\frac{dv}{dy} = 0 \text{ when } y = \frac{h}{2}$$

$$0 = B + 2Cy = B + \frac{1}{\eta} \frac{dp}{dx} \frac{h}{2}$$

and

$$B = - \frac{h}{2\eta} \frac{dp}{dx} .$$

The equation for the velocity profile is therefore

$$v = - \frac{h}{2\eta} \frac{dp}{dx} y + \frac{1}{2\eta} \frac{dp}{dx} y^2$$

$$= - \frac{1}{2\eta} \frac{dp}{dx} (hy - y^2).$$

The volume flow rate through the slit will be

$$Q = 2w \int_0^{h/2} v\,dy = - \frac{w}{\eta} \frac{dp}{dx} \int_0^{h/2} (hy - y^2)\,dy$$

$$= - \frac{w}{\eta} \frac{dp}{dx} \left[\frac{hy^2}{2} - \frac{y^3}{3} \right]_0^{h/2}$$

$$= - \frac{w}{12\eta} \frac{dp}{dx} h^3.$$

The mass flow rate through the slit is

$$M = \rho Q = - \frac{p}{12RT} \frac{wh^3}{\eta} \frac{dp}{dx} .$$

Since, from continuity, the mass flow must be constant

$$\frac{dM}{dx} = 0 = \frac{wh^3}{12RT\eta} \left[p \frac{d^2p}{dx^2} + \left(\frac{dp}{dx}\right)^2 \right] , \tag{83}$$

an isothermal process being assumed.

Let

$$Z = - \frac{dp}{dx} ;$$

then,

$$\frac{dZ}{dx} = - \frac{d^2p}{dx^2} = \frac{dZ}{dp} \frac{dp}{dx} = -Z \frac{dZ}{dp} .$$

273

The bracketed term in Equation (83) then becomes

$$p\, Z\, \frac{dZ}{dp} + Z^2 = 0$$

or

$$\frac{dZ}{Z} + \frac{dp}{p} = 0\ ,$$

which can be integrated to

$$\log Z + \log p = \log C_1$$

or

$$Zp = C_1\ .$$

Since

$$Z = -\frac{dp}{dx}$$

$$p\frac{dp}{dx} = -C_1,$$

which can be integrated to

$$\frac{p^2}{2} = -C_1 x + C_2\ .$$

From the boundary conditions

$$p = p_1 \text{ when } x = 0$$

and

$$p = p_2 \text{ when } x = \ell\ .$$

Therefore,

$$C_2 = \frac{p_1^{\,2}}{2}\ ,$$

and

$$C_1 = \frac{1}{2\ell}\left(p_1^{\,2} - p_2^{\,2}\right).$$

The equation for the pressure variation lengthwise in the slit is therefore

$$p^2 = p_1^{\,2} - \frac{x}{\ell}\left(p_1^{\,2} - p_2^{\,2}\right)\ .$$

Referring again to the mass-flow equation

$$M = \rho Q = -\frac{pwh^3}{12RT\eta}\frac{dp}{dx}\ ,$$

274

we can write

$$-p\frac{dp}{dx} = \frac{1}{2\ell}(p_1^2 - p_2^2)$$

$$M_L = \frac{wh^3(p_1^2 - p_2^2)}{24RT\eta\ell} .$$

Since $p_1^2 - p_2^2 = (p_1 - p_2)(p_1 + p_2)$, this can be written in terms of the average pressure or density;

$$M_L = \frac{wh^3(p_1 - p_2)\,p_{avg}}{12\,RT\eta\ell}$$

$$M_L = \frac{wh^3(p_1 - p_2)\,\rho_{avg}}{12\eta\ell}$$

Since leakage rates are usually measured at the discharge pressure, p_2, it is also useful to write the mass-flow equation in terms of the discharge pressure

$$M_L = \frac{wh^3\left[\left(\dfrac{p_1}{p_2}\right)^2 - 1\right]p_2\rho_2}{24\eta\ell} . \tag{84}$$

Molecular Flow

The flow is molecular if the mean free path of the gas molecules is large compared with the passage height. In this case the laminar-flow boundary condition of zero velocity at the wall is no longer true. There is some slip along the wall.

Knudson develops an equation[1] for the flow in this regime as

$$M = -\frac{8}{3}\sqrt{\frac{2}{\pi}}\sqrt{\frac{\rho}{p}}\frac{A^2}{O}\frac{dp}{dx} .$$

where

A = flow area of passage

O = parameter of passage.

If the passage is in the form of a slot, of height h and width w,

$$\frac{A^2}{O} = \frac{w^2h^2}{2(w + h)} .$$

If h<<w

$$\frac{A^2}{O} \approx \frac{wh^2}{2}$$

from which

$$M = -\frac{4}{3}\sqrt{\frac{2}{\pi}}\sqrt{\frac{\rho}{p}}\,wh^2\frac{dp}{dx} .$$

275

Since the mass flow is constant,

$$\frac{dM}{dx} = 0 = -\frac{4}{3} \sqrt{\frac{2}{\pi}} \sqrt{\frac{\rho}{p}} \, wh^2 \frac{d^2p}{dk^2}$$

or

$$\frac{d^2p}{dx^2} = 0 \; .$$

This differential equation has a solution of the form

$$p = a + bx$$

$$\frac{dp}{dx} = b \; .$$

But,

$$\frac{dp}{dx} = -\frac{3}{4} \sqrt{\frac{\pi}{2}} \frac{M}{wh^2} \sqrt{\frac{p}{\rho}} = b \; .$$

Therefore,

$$p = a - \frac{3}{4} \sqrt{\frac{\pi}{2}} \sqrt{\frac{p}{\rho}} \frac{Mx}{wh^2} \; .$$

Using the boundary conditions

$$p = p_1 \quad \text{at } x = 0$$

and

$$p = p_2 \quad \text{at } x = \ell \; ,$$

it follows that

$$a = p_1$$

$$M_M = \frac{4}{3} \frac{\sqrt{2} \, wh^2}{\sqrt{\pi} \, \ell} \sqrt{\frac{\rho}{p}} \, (p_1 - p_2)$$

$$p = p_1 - \frac{3}{4} \sqrt{\frac{2}{\pi}} \sqrt{\frac{p}{\rho}} \frac{Mx}{wh^2} \; .$$

Note that the pressure distribution along the length of the passage is linear for the molecular-flow case, rather than parabolic as in the laminar-flow case. The mass flow rate is proportional to the square of the passage height, rather than the cube.

Comparison of Laminar and Molecular Flows

The flow equation for the laminar-flow case is

$$M_L = \frac{wh^3 \, (p_1 - p_2) \, p_{avg}}{12RT\eta\ell}$$

and for the molecular flow case

$$M_M = \frac{4}{3} \sqrt{\frac{2}{\pi}} \frac{wh^2}{\ell} \sqrt{\frac{\rho}{p}} \, (p_1 - p_2) \; .$$

From kinetic theory of gases, an approximate relationship between viscosity and mean free path is found:

$$\eta = \frac{1}{3}\rho \, \overline{C} \, \lambda \, ,$$

where

$\overline{C}$ = mean velocity of the gas molecules

$$= \sqrt{\frac{8}{\pi}} RT$$

ρ = density = $\dfrac{p}{RT}$.

The equation for mass flow rate in the molecular case can therefore be written

$$M_M = \frac{4}{3} \sqrt{\frac{2}{\pi}} \times \frac{1}{3} \sqrt{\frac{8}{\pi}} \; \frac{wh^2 \, (p_1 - p_2) \, P_{avg} \, \lambda}{\eta RT}$$

$$= \frac{16 \, wh^2 \, (p_1 - p_2) \, P_{avg} \, \lambda}{9\pi \, \eta RT} \; .$$

The ratio of molecular to laminar flow can then be written

$$\frac{M_M}{M_L} = \frac{16 \times 12}{9\pi} \frac{\lambda}{h} = 6.8 \frac{\lambda}{h} \; .$$

Transition Flows

For the transition region of flow between laminar and molecular flow, a relationship of the form

$$M = M_L + E \, M_M$$

is used, where E is a constant found experimentally to be approximately 0.9 for single gases and 0.66 for mixtures of gases.[1]

Using the ratio of molecular to laminar flow and E = 0.9, the total flow is

$$M = M_L \, (1 + 0.9 \times 6.8 \frac{\lambda}{h}) = M_L \, (1 + 6.1 \frac{\lambda}{h}).$$

The mean free path should be evaluated at the average pressure in the passage.

References

(1) Loeb, L. B., The Kinetic Theory of Gases, 3d Edition, Dover Publications, Inc., New York (1961).

277

EXPERIMENTAL EVALUATION OF
CONOSEAL SEALING ACTION

Experiments Performed

Two types of experimental evaluations were performed. In the first series of experiments -2, -8, and -16 Conoseal gaskets were assembled at prescribed axial loads in the tensile-test machine as shown in Figure 123. The force-deflection curves for each size gasket were determined. The gaskets were removed from the fitting after each assembly, and were examined visually and with the aid of a 250-power microscope. Changes in dimension and geometry were recorded and these changes were correlated with the gasket's corresponding force-deflection curve.

In the second series of experiments, Conoseal fittings were (1) assembled to prescribed gasket loads chosen from the force-deflection curve, (2) encapsulated in a plastic material, (3) sectioned along their axial length, and (4) polished. Afterward the specimens were examined with the 250-power microscope. As a result of this examination technique the physical changes in the gasket were revealed. Also the microscopic interrelationships at the sealing surfaces were made clearly visible.

Evaluation of Results

Force-Deflection Curves

Force-deflection curves for the -8 and -16 Conoseal gaskets are shown in Figure 124. The force-deflection curve for the -2 gasket is shown in Figure 125. The thin continuous lines are curves obtained for specific gaskets. The broad lines represent the approximate straight-line average for all specimens evaluated.

One-Inch Gasket. There are five distinct slopes which make up the force-deflection curve for the -16 gasket. The 0.0075-inch axial travel from Point 6 to 7 serves to seat the gasket at all four corners (Figure 126a), and to take up tolerances and misalignments. The 0.0065-inch travel from Point 7 to 8 represents elastic displacement as the gasket is rotated. Buckling apparently begins between 1500- and 2000-lb force (Figure 126b), and continues for a travel of 0.016 inch (Figure 126c). At Point 9 the slope suddenly becomes steeper even though buckling sometimes may continue to about 3000 lb. However, it is presumed that at Point 9 or thereabouts the gasket is being flattened. This continues for a travel of 0.027 inch to Point 10 on Figure 124. Apparently, as shown in Figure 126d, the OD of the gasket is firmly seated and continued application of force causes the ID of the gasket to flatten. At Point 10, the seal responds like a flat gasket under continuous load (Figure 126e) and the slope becomes almost vertical.

One-Half-Inch Gasket. Examination of the 1/2-inch gasket at various prescribed loads revealed a slight bulking of the gasket between 800 and 1000-lb force (Figure 127b).

279
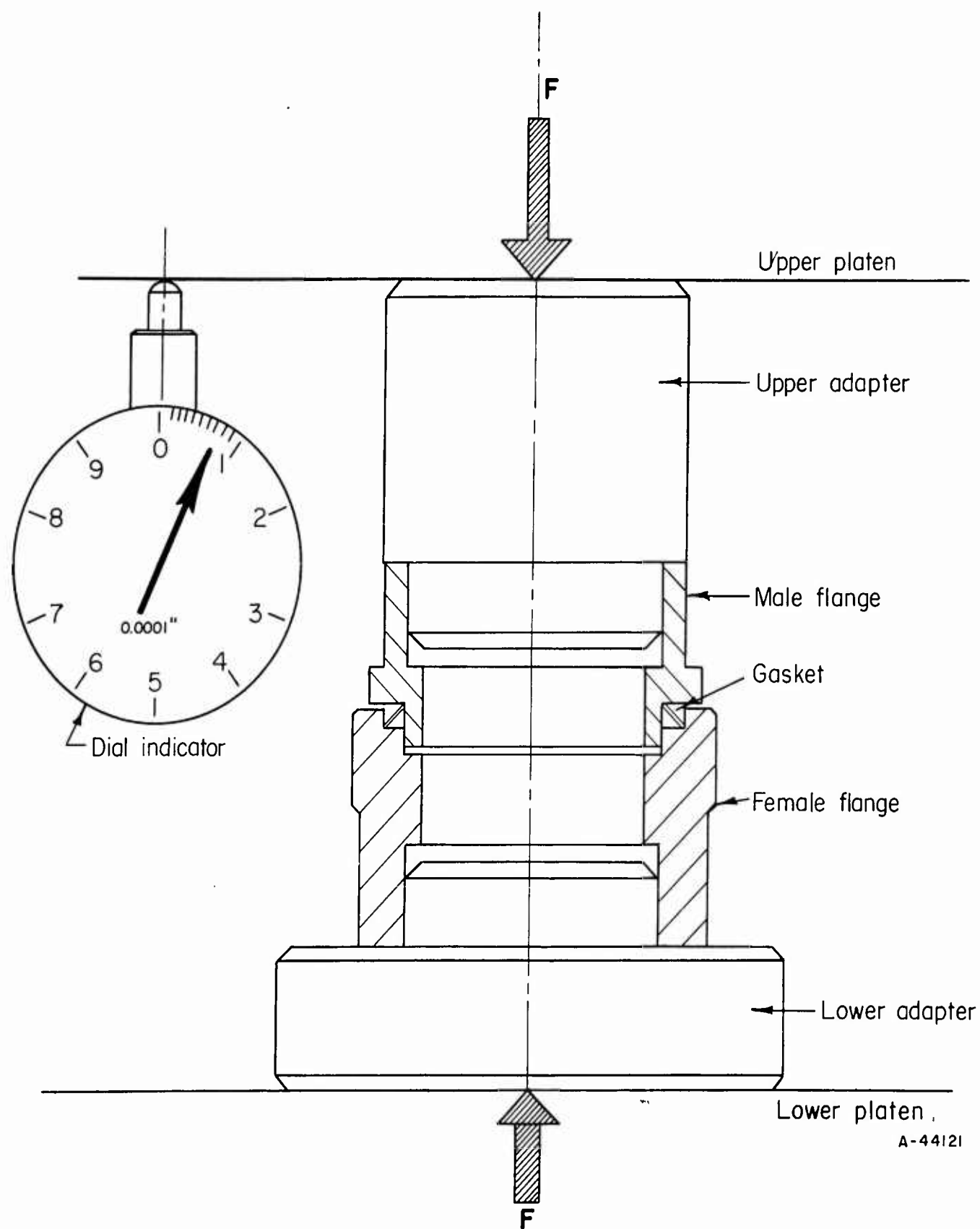
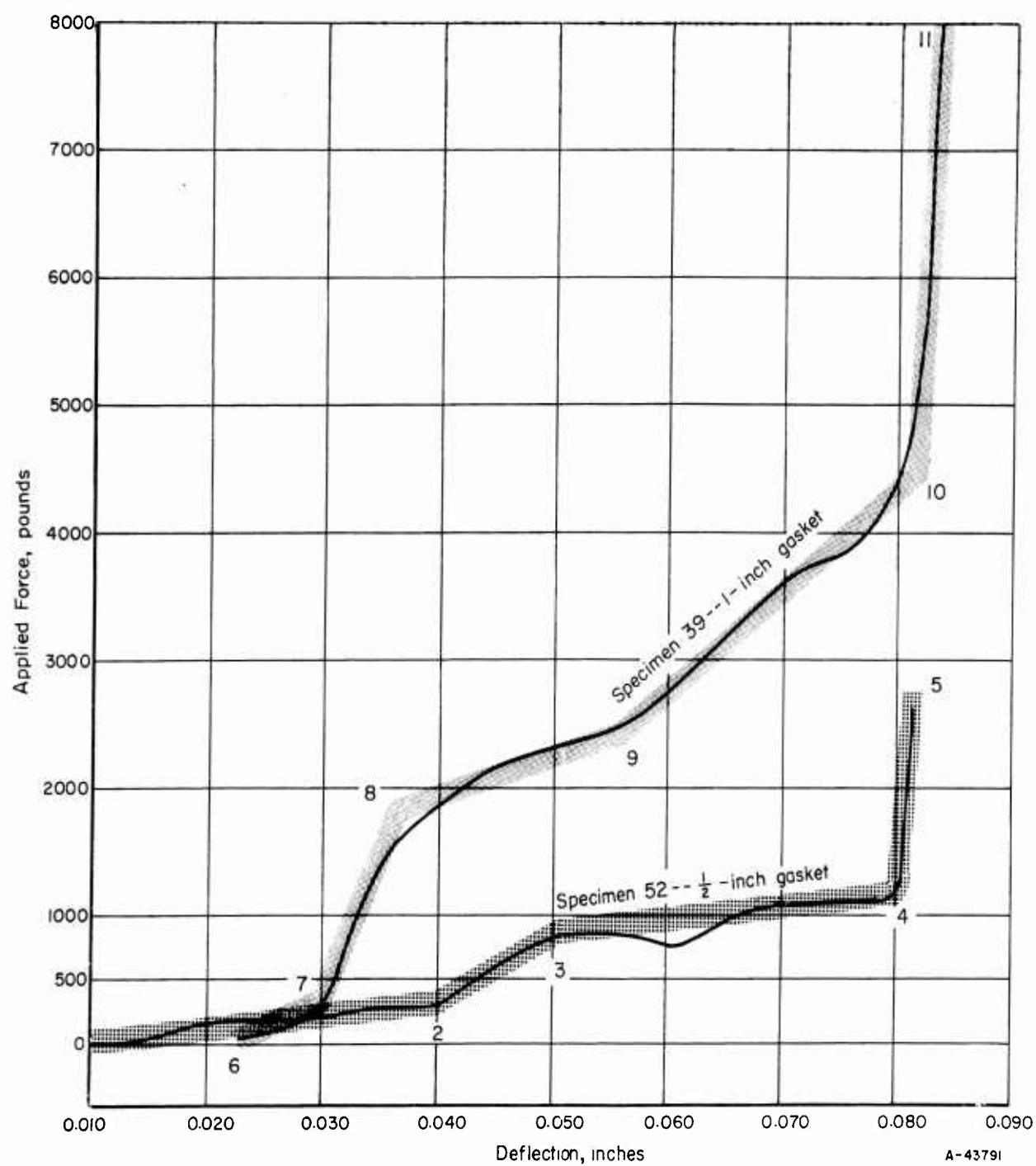FIGURE 123. SETUP FOR DETERMINATION OF FORCE-DEFLECTION CURVES

FIGURE 124. FORCE-DEFLECTION CURVES FOR MECHANICAL SEALS,
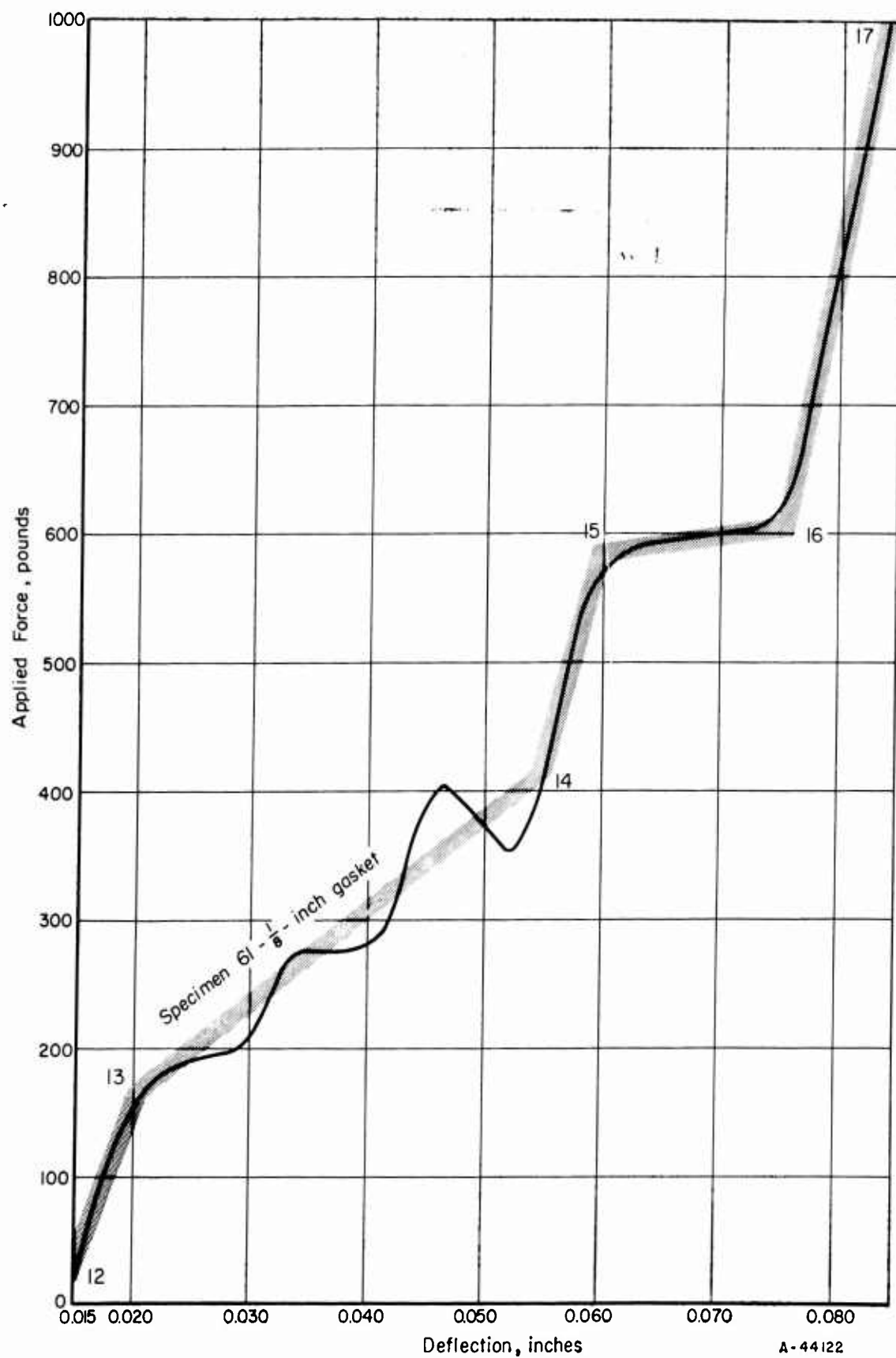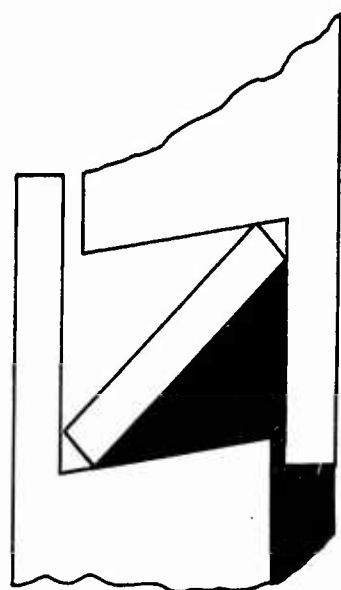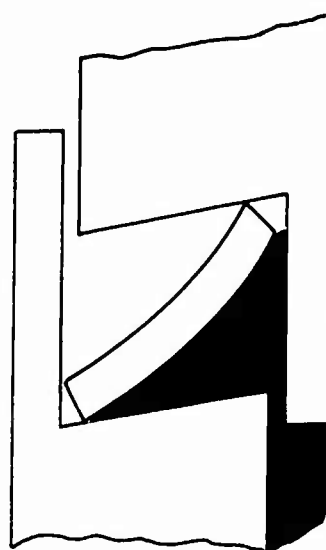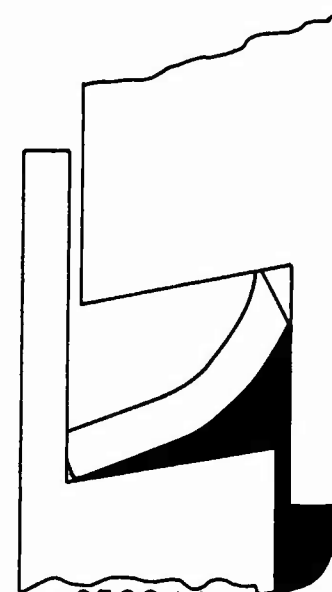SPECIMENS 39 AND 52

281

FIGURE 125. FORCE-DEFLECTION CURVE FOR MECHANICAL SEALS,
SPECIMEN 61

FIGURE 126. SEQUENTIAL DEFORMATION OF 1-INCH CONOSEAL GASKET

Shaded areas represent pressurized fluid.

This phenomenon occurs during a travel of 0.030 inch from Point 3 to 4 on Figure 124 and explains the presence of dips and momentary fall-offs in applied force. Elastic displacements at all the contacting surfaces and throughout the gasket body probably cause the steep rise in the curve from Point 2 to 3. At Point 4 the ID of the gasket was seated firmly whereas the OD was only partially seated (Figure 127c). Some curvature is still visible. At Point 4 on Figure 124 the gasket behaves more like a flat metal gasket under continued application of force although intimate contact is still not achieved on both flat faces (Figure 127d). However, it appears that in order to firmly seat the gasket on both faces, the fitting might be overstressed.

One-Eighth-inch Gasket. The force-deflection curve for the 1/8-inch gasket differs from the pattern of the two larger gaskets. The differences noted are:

(1) The initial seating slope (Point 12 to 13, Figure 125) is steep. This is probably caused by the greater stiffness of the 1/8-inch gasket.

(2) Although buckling first becomes apparent with a load between 350 and 400 lb (Figure 128b) the slope from Point 13 to 14 (Figure 125) is quite erratic and nonlinear. Generally this portion of the slope would represent elastic displacement which should be characterized by a straight steep slope.

(3) As shown in Figures 128b and 128c, buckling apparently occurs between Point 14 and 15 (Figure 125). However, this portion of the curve is a steep straight slope which is unexpected.

(4) At 600-lb load the gasket apparently collapses and the slope of the force-deflection curve is essentially horizontal for 0.015-inch travel.

Geometrical Effects

The behavior of the Conoseal gaskets is apparently dependent upon the geometrical relationships of the critical dimensions shown in Figure 129. The average values of these dimensions for each size gasket are shown in Table 30.

It is readily seen that in each gasket three of the dimensions are nearly constant: t, L, and θ. Therefore, the variations in plastic behavior are probably attributable to the variations in diameter ratios. The D_2/D_1 ratio for the -2 gasket is approximately equal to a similar ratio for standard Belleville disk springs. The D_2/D_1 ratio for the -16 gasket, however, is not much greater than unity.

On the basis of the evidence, the dimensional relationships of the -8 gasket would appear to be best if buckling of the gasket were to be prevented. If convex buckling is required, the change in dimensional ratios should tend toward the -2 gasket. Concave buckling is best achieved with the -16 gasket.
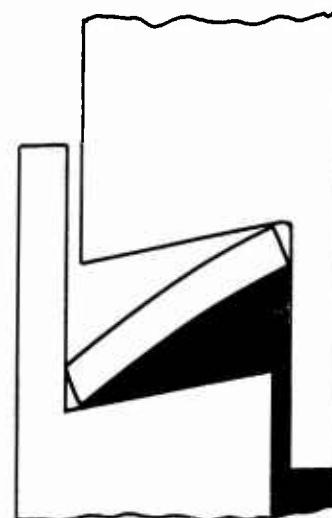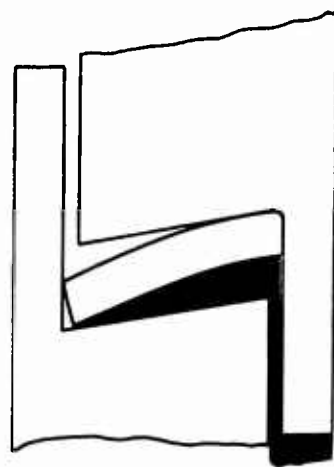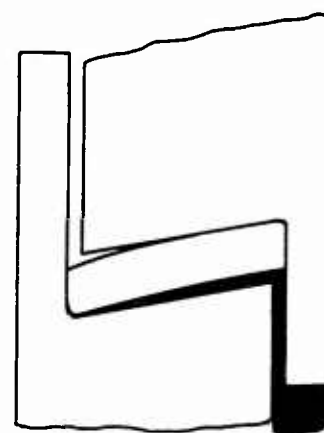
FIGURE 127. SEQUENTIAL DEFORMATION OF 1/2-INCH CONOSEAL GASKET

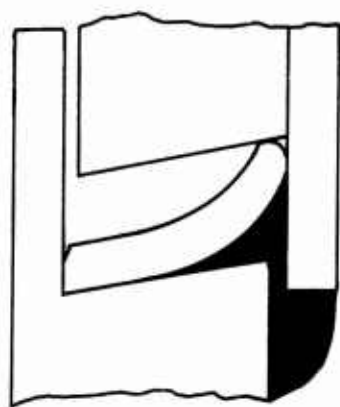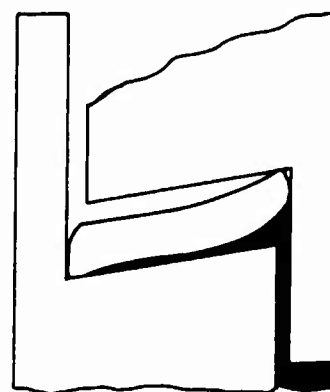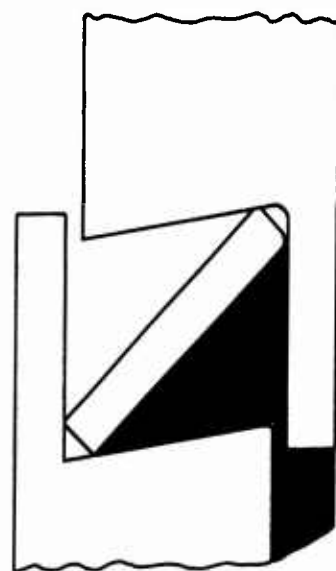Shaded areas represent pressurized fluid.

285
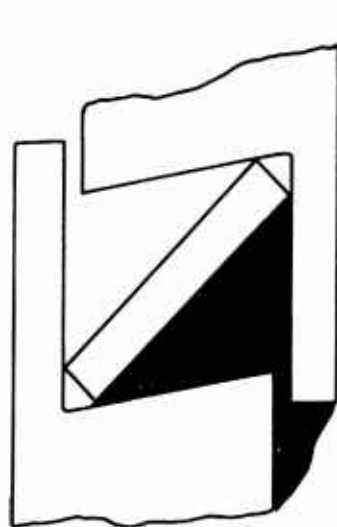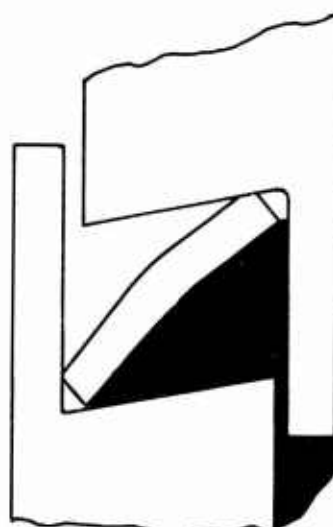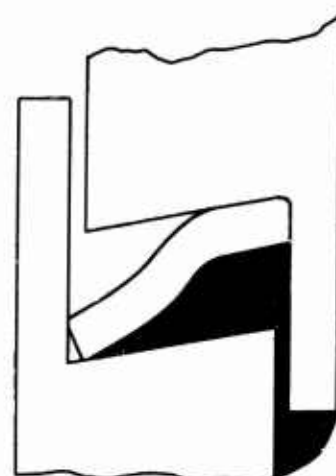
a. 300 Lb   b. 400 Lb   c. 600 Lb
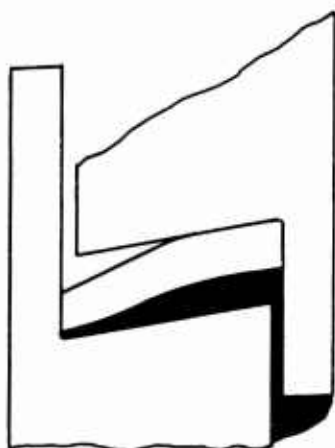
d. 800 Lb   e. 1200 Lb   A-44125

FIGURE 128.   SEQUENTIAL DEFORMATION OF 1/8-INCH CONOSEAL GASKET

Shaded areas represent pressurized fluid.
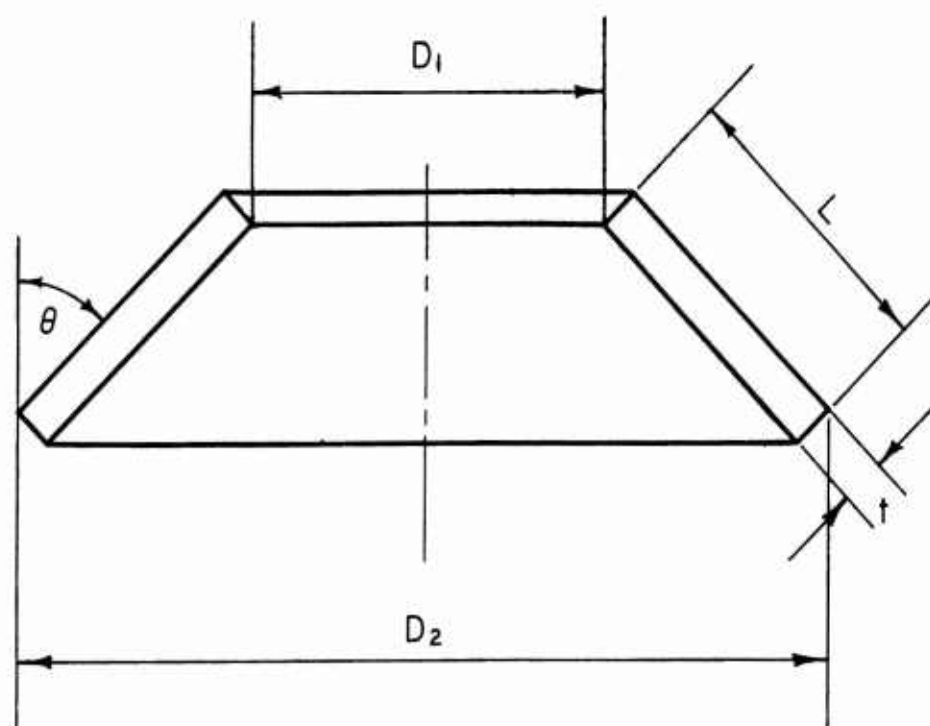
A-44126

FIGURE 129. CRITICAL DIMENSIONS OF CONOSEAL GASKETS

TABLE 30. AVERAGE VALUES FOR CRITICAL DIMENSIONS

	-2	-8	-16
t	0.0199	0.0213	0.0202
L	0.1270	0.1252	0.1265
D_1	0.1867	0.5974	1.0780
D_2	0.3922	0.8024	1.2857
θ	49°	48°	50°
D_2/D_1	2.100	1.343	1.193

Microscopic Analysis

Surface Finish. The gaskets were delivered in two lots. Generally those in the first lot had received a secondary machining operation on both the ID and OD. Those in the second lot had not. Inspection with the 250-power microscope revealed that the gaskets in the first lot were free of all burrs and that the machining marks on the sealing surfaces were concentric rings normal to the flow path. (Figure 130b).
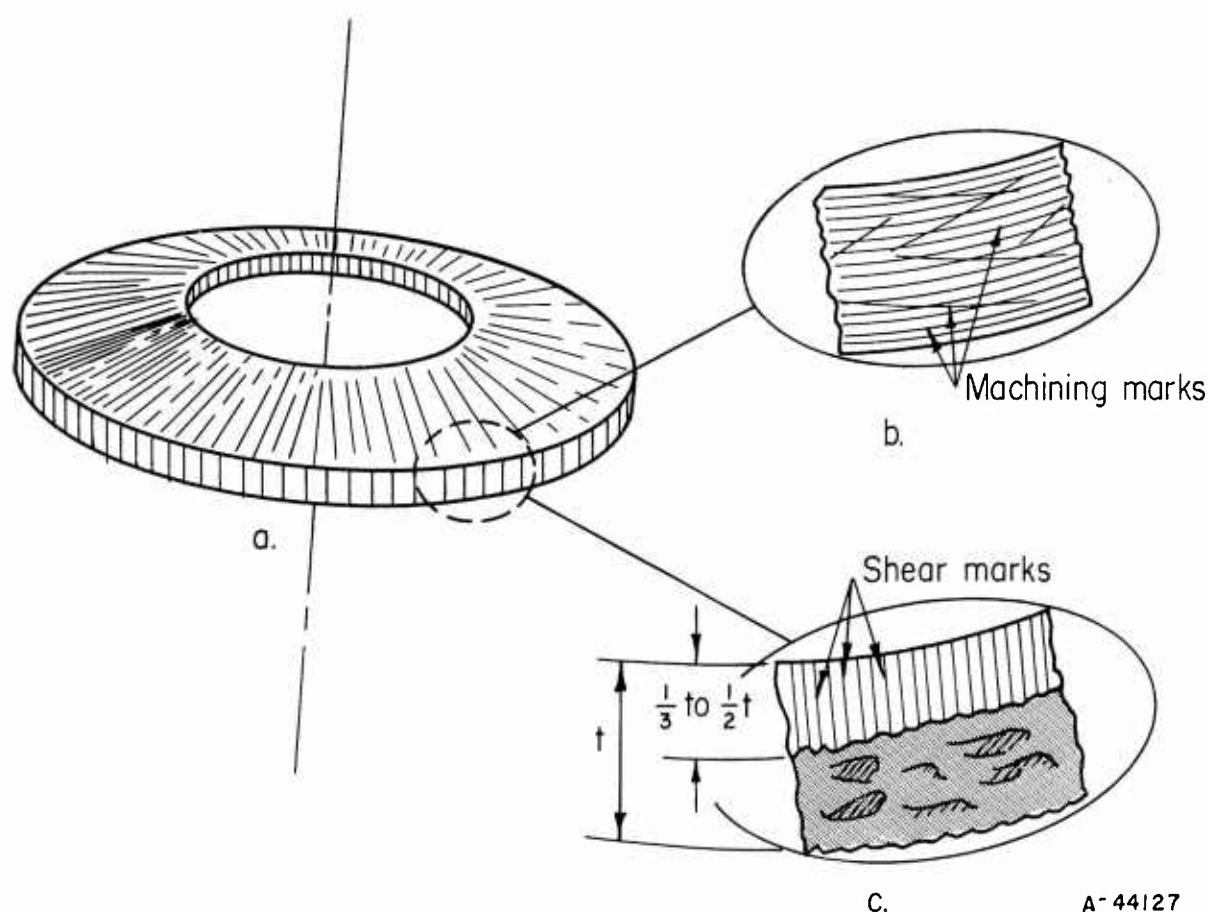
FIGURE 130. INSIDE- AND OUTSIDE-DIAMETER SURFACE FINISHES ON CONOSEAL GASKETS

The sealing surfaces of the gaskets in the second lot, however, were quite different. Deep scratches and shear grooves parallel to the flow path were present. These extended across 1/3 to 1/2 the width of the sealing face (Figure 130c). The remaining 1/2 to 2/3 of the sealing face was rough, ragged, and irregular (the gray area in Figure 130c). This type of surface is typical with sheet metal sheared in a power press. Edge A in Figure 130c was quite irregular and ragged and there was a heavy burr on the entire circumference along this edge. The same type of surface existed at the ID which also serves as a seal.

Re-examination of the sealing faces after assembly revealed that the shear marks and rough areas were still evident even when the gasket was assembled with a force 175 per cent greater than the recommended maximum torque. It should be noted that the gasket and the retaining flanges are fabricated from stainless steels with approximately

288

the same yield point and the same degree of hardness. Even though plastic yielding and deformation did occur, apparently plastic deformation in itself will not assure a good seal or adequate surface conformity. The photomicrographs in Figures 131 through 134 show clearly that for the -8 gasket, even at 2000 lb load (175 per cent overload) the gasket does not mate properly at the OD with the retainer flange.

Although leakage tests have not been performed, it appears from microscopic examinations that failure to machine the sealing faces and to remove all burrs will sharply reduce the reliability of the seal.

Surface Conformity. The photomicrographs in Figures 131 through 134 show at 100X the actual surface conformity achieved at the ID and OD for various axial loads. The location of Plates 1 through 4 in each of these figures with respect to the total fitting configuration is shown below. Figure 131 shows that at a 280-lb load the seal mates with the flanges only at the four corners. Note the hanging burr on the OD and the tear on the ID where the shearing punch broke through. The seal pictured in Figure 132 was assembled at 900 lb. Although there is a greater contact area, it is still restricted to the four corners. The hanging burr has been rolled under. Figure 133 assembled at 1040 lb reveals that contact has shifted from the corners to the seal faces. There is evide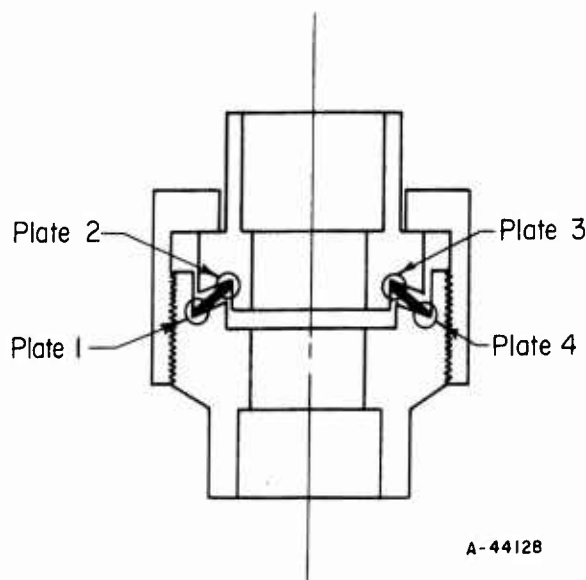nce of the flange member yielding plastically on the seal's OD (marked with arrows). The gasket assembled at 2000 lb (Figure 134)* has achieved excellent surface conformity on the ID and along part of the convex surface. However, only partial contact has been achieved on the OD.

A-44128

Although the -2 and the -16 gaskets buckled differently, both nevertheless achieved approximately the same degree of conformity except on opposite diameters. In general both the -2 and -16 size gaskets appear to have sealed better than the -8 gasket. The degree of conformity achieved with the -16 gasket is shown in Figures 135 through 137. At 2000 lb (Figure 135), which is about 1/2 the maximum load, the seal at the OD is nearly equivalent to the best seal obtained with the -8 gasket even at 175 per cent recommended load. Even the seal on that portion of the ID in contact appears to be quite

---

*This gasket (Figure 134) had received a secondary machining operation, whereas the others (Figures 131, 132, and 133) had not.

100X   N96504   100X   N96503

a. Plate 1. OD   b. Plate 2. ID

100X   N96502   100X   N96501

c. Plate 3. ID   d. Plate 4. OD
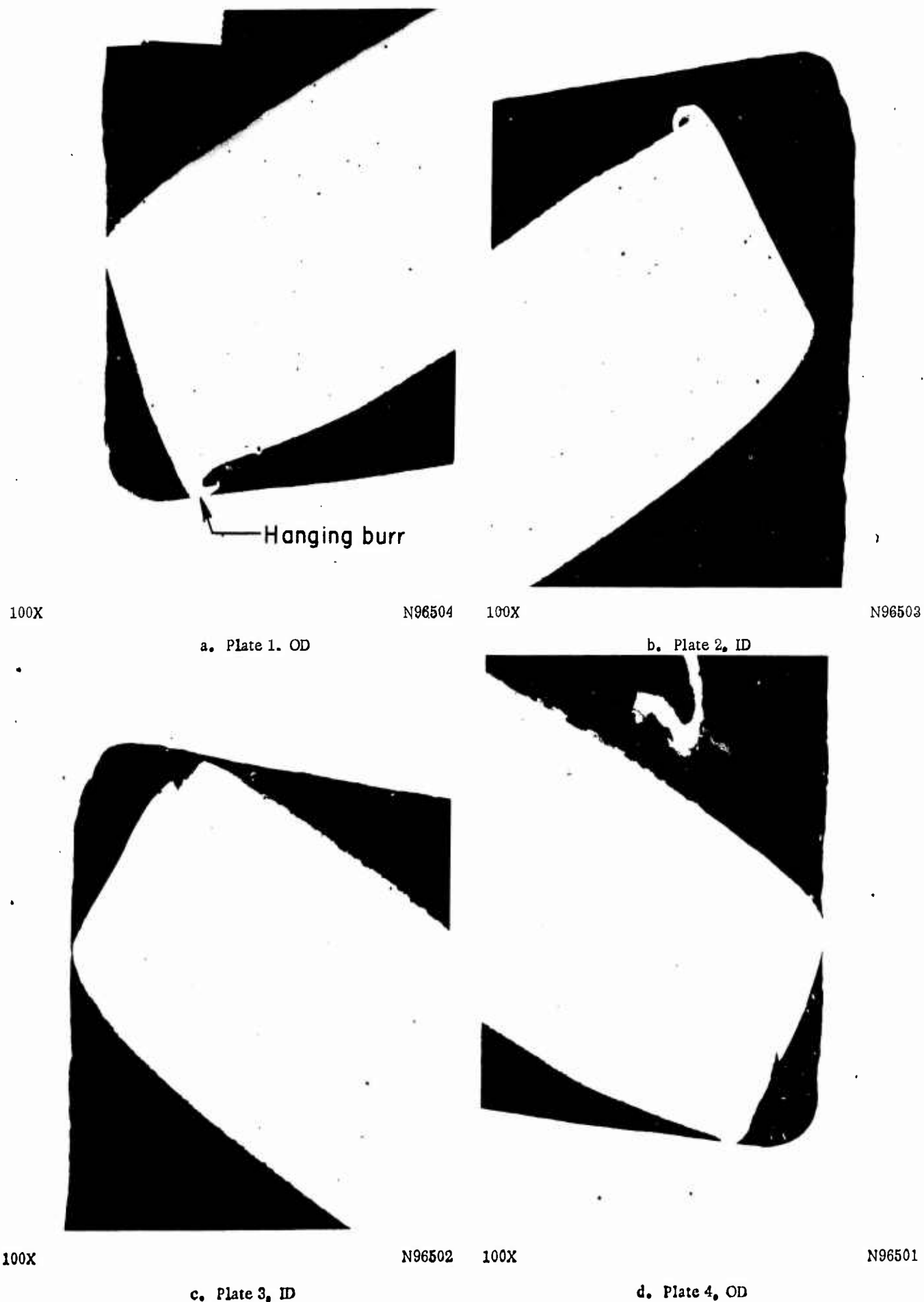
FIGURE 131. PHOTOMICROGRAPHS OF 1/2-INCH CONOSEAL (SPECIMEN 57) AT 280-POUND AXIAL LOAD

100X   N96508   100X   N96507

a. Plate 1, OD   b. Plate 2, ID

Hanging
burr

100X   N96506   100X   N96505

a. Plate 3, ID   d. Plate 4, OD

FIGURE 132. PHOTOMICROGRAPHS OF 1/2-INCH CONOSEAL (SPECIMEN 58)
AT 900-POUND AXIAL LOAD

100X   N96512   100X   N96511

a. Plate 1, OD   b. Plate 2, ID

100X   N96510   100X   N96509

c. Plate 3, ID   d. Plate 4, OD
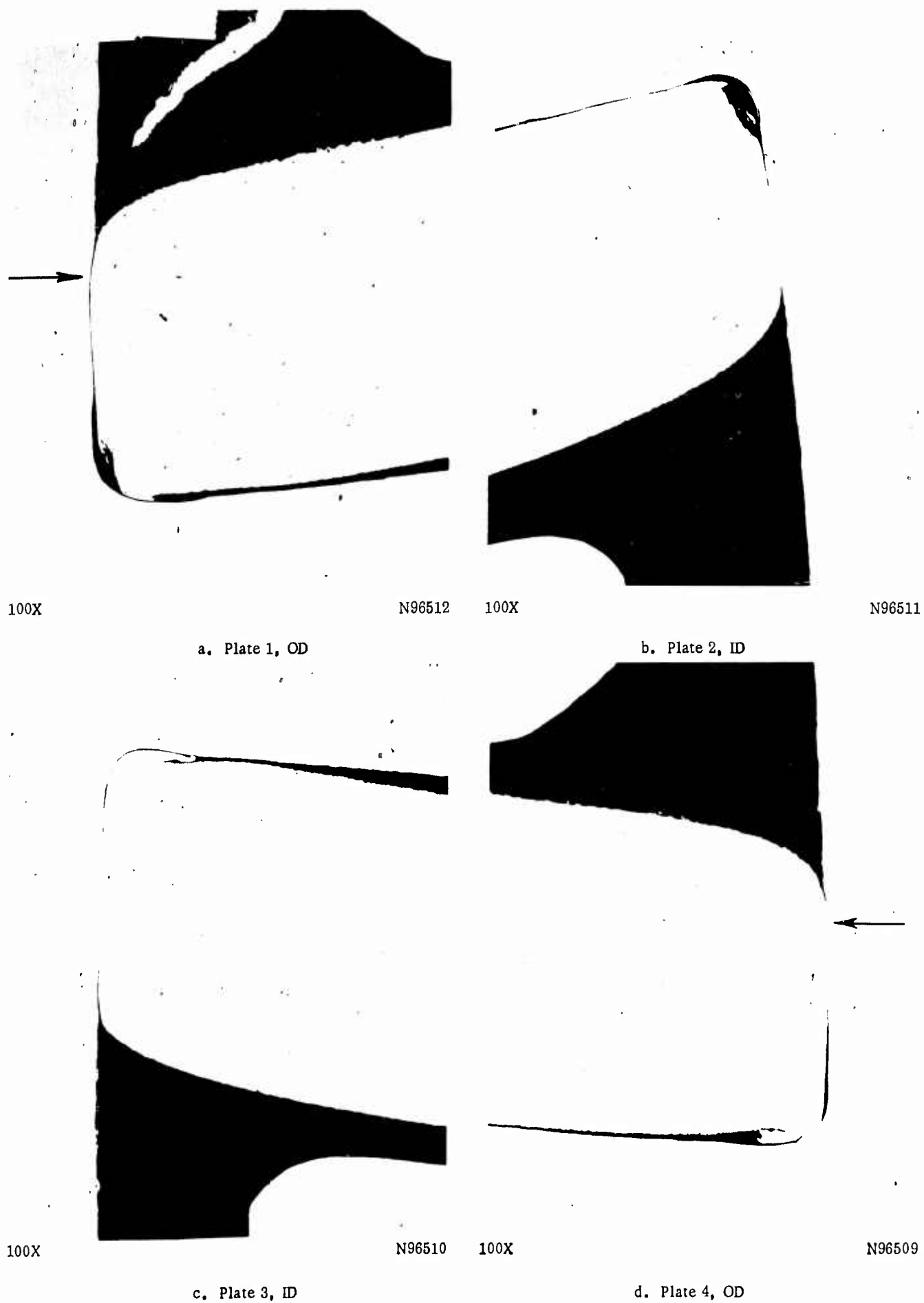
FIGURE 133.   PHOTOMICROGRAPHS OF 1/2-INCH CONOSEAL (SPECIMEN 59) AT 1040-POUND AXIAL LOAD

100X   N96488   100X   N96487

a. Plate 1, OD   b. Plate 2, ID

100X   N96486   100X   N96485

c. Plate 3, ID   d. Plate 4, OD
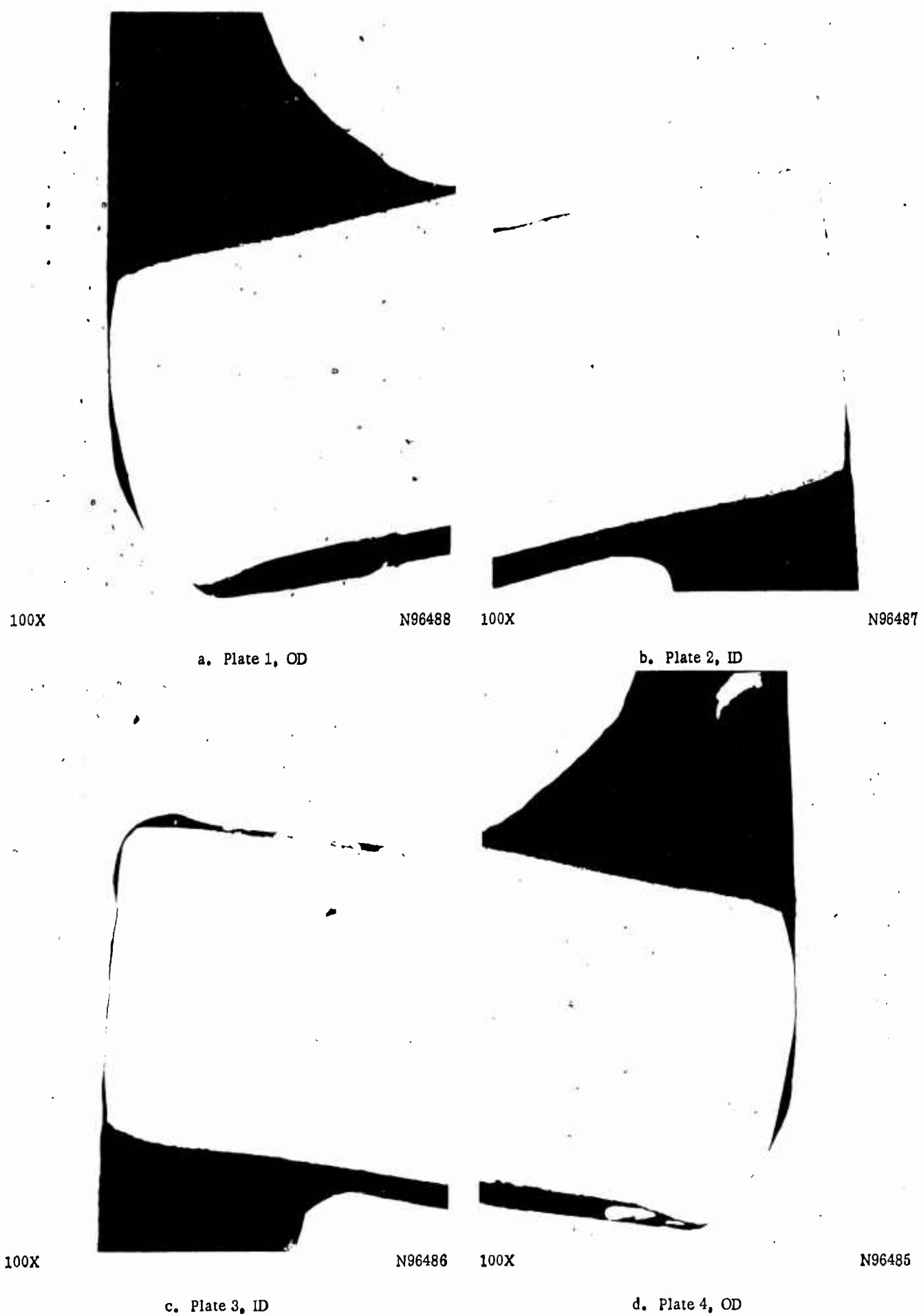
FIGURE 134. PHOTOMICROGRAPHS OF 1/2-INCH CONOSEAL (SPECIMEN 17)
AT 2000-POUND AXIAL LOAD

OD

ID

75X

N96674, N96675, and N96676

FIGURE 135. PHOTOMICROGRAPH OF 1-INCH CONOSEAL (SPECIMEN 40) AT 2000-POUND AXIAL LOAD

294

N96671, N96672, and N96673

75X

OD

FIGURE 136. PHOTOMICROGRAPH OF 1-INCH CONOSEAL (SPECIMEN 8) AT 3000-POUND AXIAL LOAD
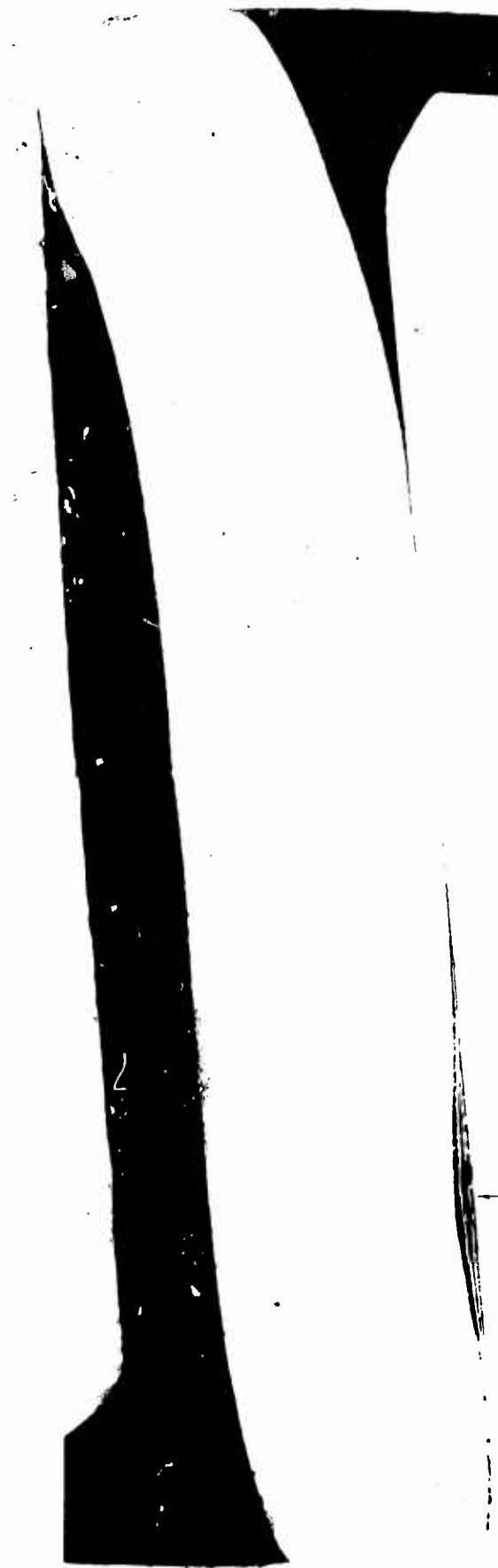
OD   75X

N96732 and N96733

FIGURE 137. PHOTOMICROGRAPH OF 1-INCH CONOSEAL (SPECIMEN 41)
AT 4000-POUND AXIAL LOAD

296

good. At 3000 lb (Figure 136) the seal on the OD and the convex face is excellent, whereas only a partial seal is evident on the ID. At 4000 lb (Figure 137) the applied load has caused a reverse buckling of the seal. This phenomenon probably caused the separation at the convex surface (marked with arrow). Both the ID and OD have sealed along the entire sealing face.

INFORMATION REVIEW AND BIBLIOGRAPHY

Considerable effort was expended to determine the extent of available knowledge in the open literature and the experience of manufacturers, users, and designers relative to fittings and similar components. This effort is described briefly. A selected bibliography is given of the references which have been of assistance in Phases I and II.

Information Review

Technical information was obtained through personal interviews with engineers and designers and from written reports of test and development programs on fittings. Additional related data basic to fitting design were collected and reviewed.

Technical Interviews

During the first month of the project the Battelle staff visited various organizations with experience in the design, manufacture, and use of aircraft and missile fittings. The organizations visited were:

(1) Aerojet-General
(2) Aerospace Corp.
(3) Armour Research Foundation
(4) Astronautics Division, General Dynamics
(5) Douglas Aircraft
(6) Flexonics Division, Calumet and Hecla Co.
(7) General Electric Co.
(8) Jet Propulsion Laboratory
(9) Lockheed Aircraft Co., Burbank
(10) Lockheed Missile and Space Division
(11) Marman Division, Aeroquip Corp.
(12) Parker-Hanifin Corp.
(13) Resistoflex Corp.
(14) Rocketdyne Division, North American Aviation
(15) Space Technology Laboratory
(16) Stanford Research Institute
(17) Weatherhead Corp.

The data sought during these visits related primarily to specific past experience with and knowledge of fitting failures. The types of failure, possible causes, and the location in the piping system were items of major interest. Design philosophy was discussed only in general terms. Unfortunately, little failure-analysis work had been done in this area. Moreover, results of the work which had been done had not been published. When failure data were available, they were very general.

Most of the information received consisted of technical reports of laboratory tests and analytical studies of present and new designs. The most frequent comments of the engineers interviewed were:

(1) The basic seal design of flared type fittings is inadequate, and the seal is subject to deterioration with increased pressure and temperature.

(2) Human error during assembly is the major source of difficulties with "zero-leak" fittings.

(3) Stricter quality control should be imposed on the manufacturers of fittings.

(4) Future specifications should classify the fitting according to the application.

Technical Literature

During the first 2 months a literature survey was conducted. Documents were collected, analyzed, and catalogued. Thereafter, additional pertinent documents were added to the file as they were noted. The file presently consists of more than 500 documents and is divided into nine major categories:

(1) Bolts
(2) Design
(3) Fittings
(4) Flanges
(5) Materials
(6) Manufacturing
(7) Seals
(8) Testing
(9) Threads.

The major sources of data are Armed Services Technical Information Agency, Interservice Data Exchange Program, Machine Design, Mechanical Engineering, Defense Metals Information Center, Transactions of American Society of Mechanical Engineers, Society of Automotive Engineers, and internal reports and memos from individual companies.

A comprehensive literature search, even if restricted to just one or two of the major categories, would have been beyond the scope of the Phase I program. New and typical information only was gathered. When it appeared that a document contained redundant information, it was usually omitted.

Reports dealing with the state of the art of flared and flareless fittings were conducted on a restricted basis also. Only major reports known to contain original test data were collected. The state-of-the-art study was intended to provide only sufficient data for failure analysis or analytical evaluation.

Bibliography

The references listed below are those which proved to be of greatest value in conducting the Phase I work.

Bolts

Appleberry, W. T., "How Fastener Tension Varies with External Joint Loads, Part I", Assembly and Fastener Engineering, 26-30 (April, 1961).

Appleberry, W. T., "How Fastener Tension Varies with External Joint Loads, Part II", Assembly and Fastener Engineering, 32-36 (May, 1961.

Appleberry, W. T., "How Fastener Tension Varies with External Joint Loads, Part III", Assembly and Fastener Engineering, 32-36 (June, 1961).

Dolan, T. J., and McClow, J. H., "The Influence of Bolt Tension and Eccentric Tensile Loads on the Behavior of a Bolted Joint", Procedures of Society of Experimental Stress Analysis, 29-43 (1959).

Harker, T. W., "Manufacture and Characteristics of High-Temperature Bolts", Metal Progress, 125-128 (October, 1953).

Lenzen, K. H., "Strength and Clamping Force of Bolts", Product Engineering, 130-133 (December, 1947).

Mordfin, L., "Some Problems of Fatigue of Bolts and Bolted Joints in Aircraft Applications", National Bureau of Standards, OTS PB 161637 (January, 1962).

Paslay, P. R., "On the Determination of the Influence of an Axial Preload Owing to Bolting on a Cylindrical Pressure Vessel", Journal of Engineering for Industry, 215-218 (May, 1961).

Pringle, O. A., "Loosening of Bolted Joints", Machine Design, 135-136 (February 2, 1961).

Silwones, S. S., Degen, Robert, A., "Test Results Guide – High Temperature Design of Bolted Assemblies", Product Engineering, 79-83 (September 30, 1957).

Smoley, E. M., and Kessler, F. J., "Retaining Tension in Gasketed Joints, Part II", Assembly and Fastener Engineering, 33-36 (October, 1961).

Spiotta, R. H., "Thread Rolling May be for You", Machinery, 182-194 (November, 1957).

Sproat, R. L., "A Checklist on Fasteners Reliability", Missile Design & Development, 58 (June, 1960).

Design

American Society of Mechanical Engineers Boiler and Pressure Vessel Code, Section VIII, "Unfired Pressure Vessels", American Society of Mechanical Engineers, 345 East 47th Street, New York 17, N. Y. (1959).

American Standards Association, Standards ASA B16. 1, ASA B16. 2, ASA B16. 5 American Society of Mechanical Engineers, 345 East 47th Street, New York.

"Design Criteria for Zero-Leakage Connectors for Launch Vehicles", General Electric Laboratories, Quarterly Progress Report No. 2, Contract NAS 8-4012 (October 11, 1962).

"Design Criteria for Zero-Leakage Connections for Launch Vehicles", Quarterly Progress Report No. 3, January 11, 1963, Contract NAS-8-4012, General Electric Company.

Flieder, W. G. , Loria, J. C. , Smith, W. J. , "Bowing of Cryogenic Pipelines", Journal of Applied Mechanics, 409-416 (September, 1961).

Jacobs, Robert B. , "Cryogenic Piping System Design Considerations", Heating, Piping, and Air Conditioning, 130-140 (February, 1960).

Lake, G. F. , and Boyd, G. , "Design of Bolted, Flanged Joints of Pressure Vessels", Proc. Institute of Mechanical Engineers (1957).

Le Fevre, William Jr. , "Torsional Strength of Steel Tubing as Affected by Length", Product Engineering, 133-136 (March, 1949).

Lewis, S. , Leakage Problems With Conventional Fittings", Space Technology Laboratories, 1-7 (May 24, 1961).

Loeb, L. B. , The Kinetic Theory of Gases, Chapter 7, Dover Publications, Inc. , New York (1961).

Marin, J. , "Design for Fatigue Loading, Part I", Machine Design, 88-94 (Jan. 24, 1957)

Marin, J. , "Design for Fatigue Loading, Part II", Machine Design, 95-99 (February 7, 1957).

Marin, J. , "Design for Fatigue Loading, Part III", Machine Design, 124-134 (February 21, 1957).

Marin, J. , "Design for Fatigue Loading, Part IV", Machine Design, 95-99 (March 7, 1957).

Marin, J. , "Design for Fatigue Loading, Part V", Machine Design, 154-157 (March 21, 1957).

"Mechanical-Drive Steam Turbines", National Electrical Manufacturers Association (NEMA) Standards Publication No. SM20-1958 (revised November, 1959).

Middleton, R. E. , "Hydraulic and Pneumatic Problems in High-Performance Aircraft", Applied Hydraulics, 98-101 (December 1956).

National Standards Association Standard NAS-624, "High Strength Air Frame Bolts".

Robinson, E. L. , "Steam-Piping Designs to Minimize Creep Concentrations", ASME Trans. (1955).

Ross, D. T. , Coons, S. A. , "Investigations in Computer-Aided Design", Massachusetts Institute of Technology", 1-81 (November 1961) (ASTIA AD269 573).

Rossheim, D. B. , and Markl, A. R. C. , "The Significance of and Suggested Limits for the Stress in Pipe Lines Due to the Combined Effects of Pressure and Expansion", ASME Trans. (July, 1940).

Smoley, E. M. , and Kessler, F. J. , "Retaining Tension in Gasketed Joints, Part I", Assembly and Fastener Engineering, 30-34 (September, 1961).

Timoshenko, S. , Strength of Materials, Part II, D. Van Nostrand Co. , 250 Fourth Avenue, New York 3, New York.

"Torque Manual", Third Edition, 1962, P. A. Sturtevant Co. , Addison, Illinois.

Wesstrom, D. B. , and Bergh, S. E. , "Effect of Internal Pressure on Stresses and Strains in Bolted-Flanged Connections", ASME Trans. (July, 1951).

Fittings

Allin, F. R. , and Courtot, L. B. , "Evaluation of Flareless Fittings for Low Density Gas Applications", Weatherhead Company, Test Report No. 69, 460-F (September 8, 1958.)

Beachley, N. H. , "Survey of Hydraulic Fittings in Air Force Ballistic Missile Programs", Space Tech. Lab. , Report 7431. 2-289, 1-9 (August 25, 1960).

"Buttress-Threaded Tube Ends Raise Coupler-Joint Efficiency", Iron Age, 90-91 (November 24, 1960).

Clark, K. , "Selection of Flareless Fittings . . . for Aircraft Circuits", Applied Hydraulics and Pneumatics, 10, 5, May, 1957, pp 158, 160-161, 3 figures.

Cornish, H. E. , and Bloom, J. C. , "Development of High Pressure Seals For AN Straight Thread Fittings", Applied Hydraulics, (18-24) (November, 1949).

Courtot, L. B. , "Refinement of Precision Flareless Fittings", Weatherhead Company, Engineering Progress Report (September, 1958).

Cowdrey, F. W. , "Flareless Hydraulic Fittings Keep F-104 'Dry'", Aviation Age (July, 1957).

Davenport, C. R. , "The Why and How of Weatherhead Ermeto Flareless Fittings", Weatherhead Company by special permission of Lockheed Aircraft Corporation.

"Design Criteria for Zero-Leakage Connectors for Launch Vehicles", General Electric Co. , General Engineering Lab, Schenectady, New York, Quarterly Progress Report No. 4, Contract NAS 8-4012, June 15, 1963.

Military Specification MIL-F-5509A, "Fittings; Fluid Connection", (March 13, 1951).

Military Specification MIL-F-1280A (A56), "Fittings, Flareless, Fluid Connection" (April 24, 1956).

Hallesy, H. W. , "Development of a Permanent and a Reconnectable Tube Fitting for High Pressures and/or High Temperatures", Boeing Aircraft, Report D6-5327 (March, 1960).

"Integrated Pressure Systems and Components", USAF P I-I0. 4, T. 0. 00-25-223 (February 1, 1962).

Lewis, S. , "Leakage Problems with Conventional Fittings", Space Tech. Lab. Report 9733.5-460, 1-7 (May 24, 1961).

Lewis, S. , "MS & AN Fittings", Space Tech. Lab. , Report GM60-7640.5-507, 1-4 (August 22, 1960).

Mayhew, W. E. , "Design and Development of a 1000 F Hydraulic System", Republic Aviation Report, AD 231 731 (July, 1959).

Mayhew, W. E. , "Design and Development of a 1000 F Hydraulic System", Republic Aviation Report, AD 257 940 (June, 1960).

Nicol, J. , "Tube Fittings, 1500 F Pneumatic System", Weatherhead Company (July, 1961).

Nicol, J. , "Hot Gas Line Fittings 1800 F for Dynasoar Reaction Contkol Systems", Weatherhead Company (July, 1961).

Parker, W. E. , "Fitting, Tubing, and Line Support Test Program Status Program", North American Aviation, 1-297, AD 131845 (April, 1957).

Phillips, R. W. , "Flareless Fittings", Applied Hydraulics and Pneumatics, 6, 5, May, 1953, pp 84, 86, 2 figures.

Phillips, R. W. , "Design and Application of Flared Fittings – Part 6 of a Series on Fluid Lines", Applied Hydraulics, 5, 12, December'52, pp 48, 50, 76, 5 figures.

Richards, C. M. , "Positive Gas Sealing With Flared Fittings", SAE Journal, 77-79 (October, 1960).

Richards, C. M. , "Precision Sleeves Improve Flareless Fittings", Hydraulic & Pneumatics, 120-122 (April, 1962).

Seibel, L. L. , and McGillen, V. W. , "Hydraulic and Pneumatic Fitting and Tubing Test Program", North American Aviation Report, AD 235 024 (November, 1959).

Flanges

American Society of Mechanical Engineers Boiler and Pressure Vessel Code Section VIII, Rules for Construction of Unfired Pressure Vessels, 1959 Edition   American Society of Mechanical Engineers, 345 East 47th Street, New York 17, New York.

Begg, G. A. J. , Discussion of "Second Report of the Pipe Flanges Research Committee", Proceedings of the Institute of Mechanical Engineers, 141, p. 461, 1939.

"Development of Mechanical Fittings, Phase I", Technical Documentary Report No. RTD-TDR-63-14, February, 1963, Air Force Flight Test Center, Rocket Propulsion Laboratories, Edwards Air Force Base, California.

Dittoe, T. A. , "Structural Test Requirements, Bolted Flanged Joints for Ducts", Convair Astronautics, General Dynamics Corp. , Report AZS-27-250 (March 25, 1956) Contract AF 04(645)-4.

Donald, M. B. , Salomon, J. M. , "Behaviour of Compressed Asbestos Fibre Gaskets in Narrow-Faced, Bolted, Flanged Joints", Proc. of Instru. Mech. Engrs. , 829-858 (December, 1957).

Donald, M. B. , and Salomon, J. M. , "The Behavior of Narrow-Faced, Bolted, Flanged Joints Under the Influence of Internal Pressure", Proc. Inst. Mech. Eng. (London) 173 (17), 461-468 (1959).

Dudley, W. M. , "Deflection of Heat Exchanger Flanged Joints as Affected by Barreling and Warping", Trans. of ASME, November, 1961.

George, H. J. , Rodabaugh, E. C. , and Holt, M. , "Aluminum Alloy Welding Neck Flanges Performance Equal to Carbon Steel", Heating, Piping and Air Conditioning, 95-97 (October, 1957).

George, H. H., Rodabaugh, E. C. , and Holt, M. , "Performance of 6061-T6 Aluminum Flanged-Pipe Assemblies Under Hydrostatic Pressure", ASME Paper No. 56 – PET-19 (1956).

Halford, D. E. , "Structural Procedure Report, Bolted Flanged Joints for Ducts", Convair Astronautics, General Dynamics Corp. , Report No. 7B 2326-1 (July 30, 1959) Contract AF 04(645)-104.

Hillmer, W. , "The Wedge-Ring Joint", Michelson Lab. Report, AD 260 021, 1-7 (June, 1961).

Kerkhof, W. P. , "New Stress Calculations and Temperature Curves for Integral Flanges", Procedures of World Petroleum Congress, Section VIII, The Hague, 146-168 (1951).

Labrow, J. , "Design of Flanged Joints", Proc. Inst. Mech. Eng. (London, 156, (1), 66-73 (1947).

Marin, Joseph, Discussion of Paper, "Formulas for Stresses in Bolted-Flanged Connections", ASME Transactions (1937).

Markl, A. R. C. , George, H. H. , "Fatigue Tests on Flanged Assemblies", Transactions of ASME, 77-87 (January, 1950).

Roberts, Irving, "Gaskets and Bolted Joints", ASME Journal of Applied Mechanics, 169-179 (June, 1950).

Robinson, E. L., "Steam-Piping Designs to Minimize Creep Concentrations", ASME Transactions (1955).

Rodabaugh, Discussion of "Effects of Internal Pressure on Stresses and Strains in Bolted-Flanged Connections", ASME Transactions (1951).

Shannon, W. B., Discussion of "First Report of the Pipe Flanges Research Committee", Proceedings of the Inst. of Mech. Engrs., 132, 279 (1936).

Smoley, E. M., "Joint and Gasket Design", Machine Design, 83-89 (January 19, 1961).

Sperry, A. M., Jr., "Structural Test Results of Bolted Flanged Joints for Ducts", Convair Astronautics, General Dynamics Corp., Report No. 7B2326-2 (June 27, 1960).

Tapsell, H. J., "Second Report of the Pipe Flanges Research Committee", Proc. Inst. of Mech. Engrs., 433-471, 141.

Waters, E. O., "Analysis of Bolted Joints at High Temperature", ASME Transactions (1938).

Waters, E. O., Wesstrom, D. B., Rossheim, D. B., Williams, F.S.G., "Formulas for Stresses in Bolted-Flanged Connections", ASME Trans., 1937.

Wesstrom, D. B., and Bergh, S. E., "Effect of Internal Pressure on Stresses and Strains in Bolted-Flanged Connections", ASME Trans., 1951.

Materials

Air Weapons Materials Application Handbook, Metals and Alloys, ARDC TR 59-66, (December, 1959).

"AM-350/AM-355 Precipitation Hardening Stainless Steels", Allegheny Ludlum Steel Corporation, 1963.

Arcand, Lionel, "Materials Selection for the Hydrogen Rocket", Aircraft & Missiles, 32-35 (January, 1960).

"Armco Precipitation Hardening Stainless Steel – Armco 17-4 PH Bar and Wire", Armco Steel Corp., Middletown, Ohio, Product Data (November 3, 1958).

Armour Research Foundation of IIT, "Materials Acceptability With Various Chemical Compounds – 14 Data Sheets", Chicago, Illinois.

Baughman, R. A., "Gas Atmosphere Effects on 32367 Metals", General Electric Company Interim Progress Report No. 3R59AGT 137, Contract AF 33(616)-5667 (February 15, 1959).

Bloom, Ralph, Weeks, Loren E., Raleigh, Charles W., "Materials for Construction of Equipment in Use with Hydrogen Peroxide", Becco Chemical Division, Food Machinery and Chemical Corp. (1959).

Boyd, W. K. , and White, E. L. , "Compatibility of Rocket Propellants With Materials of Construction", Defense Metals Information Center, Memorandum No. 65 (September 15, 1960).

Campbell, J. E. , "Compilation of Tensile Properties of High-Strength Alloys", DMIC Memorandum 150, AD 275263 (April 23, 1962).

Christian, J. L. , "Physical and Mechanical Properties of Pressure Vessel Materials for Application in Cryogenic Environment", ASD-TDR-62-258 (March, 1962).

Churchill, J. L. , and Watson, J. F. , "Properties of R-41 Sheet, A Vacuum-Melted, Nickel Based Alloy", Rept. MGR-164, Convair Astronautics Division of General Dynamics Corporation (June 19, 1960).

"Compatibility of Materials with Demazine", Food Machinery and Chemical Corp. , Inorganic Research and Development Department.

Corruccini, R. J. , "Properties of Materials at Low Temperatures, Part I", Chemical Engineering Progress, 53 (6), 262-267 (June, 1957).

Corruccini, R. J. , "Properties of Materials at Low Temperatures, Part II", Chemical Engineering Progress, 53 (7), 342-346 (July, 1957).

Corruccini, R. J. , "Properties of Materials at Low Temperatures, Part III", Chemical Engineering Progress, 53 (8), 397-402 (August, 1957).

Croucher, T. R. , and Nickols, R. C. , "The Use of Alloys at Cryogenic Temperatures", HD. 6593D Test Group, Edwards AFB, California, Memo I (August, 1961).

Cunningham, G. W. , and Spretnak, J. W. , "A Study of the Effect of Applied Pressure on Surface Contact Area", Int. J. Mech. Sci. , Pergamon Press Ltd. , 4, 1962.

"Effect of Creep-Exposure on Mechanical Properties of Rene 41", University of Michigan, ASD TR 61-73 (August, 1961).

Engineering Data Bulletin VM-107, Rene 41, Metallurgical Products Dept. , General Electric Co. , Detroit, Michigan (May, 1958).

Favor, R. J. , Deel, O. L. , Achbach, W. P. , "Design Information on AM-350 Stainless Steel for Aircraft and Missiles", DMIC Report 156, July 26, 1961.

Favor, R. J. , Deel, O. L. , Achbach, W. P. , "Design Information on 17-7 PH Stainless Steel for Aircraft and Missiles", DMIC Report 137, OTS PB 151096 (September 23, 1960).

Fink, F. W. , White, Earl L. , "Corrosion Effects of Liquid Fluorine and Liquid Oxygen on Materials of Construction", Corrosion, 17 (2) 58t-60t (February 1961).

Finnie, Iain, Heller, W. R. , Creep of Engineering Materials, McGraw-Hill Book Company, New York (1959).

Grigger, J. C., and Miller, H. C., "The Compatibility of Materials with Chlorine Trifluoride, Perchloryl Fluoride & Mixtures of These", Pennsalt Chem. Corp. Report, AD 266391, 1-100 (April, 1961).

Headquarters Office Instruction Data Sheets, HOI 74-30-1 through HOI 74-30-13, 6598 Test Group Development, Edwards Air Force Base, California.

"Integrated Pressure Systems and Components (Portable and Installed)", Air Force Technical Manual T. O. 00-25-223 (February 1, 1962).

Jaffee, Leonard D., and Rittenhouse, John B., "Behavior of Materials in Space Environments", ARS Journal 320-346 (March, 1962).

M. W. Kellogg Co. R&D Rept. SPD 121, "6000 Pound Thrust Jet Propulsion Unit, Part II, Materials Corrosion Data", Special Projects Dept., Jersey City, N. J.

Liberto, R. R., "Titan II Storable Propellant Handbook", Bell Aerosystems Company, AFFTC TR61-32 (June, 1961).

Liberto, Ralph R., "Storable Propellant Data for the Titan II Program", Bell Aerospace Systems Company, Rept. No. AFBMD-TR-61-55, Contract AF 04 (647)-846, (July, 1961).

Liberto, Ralph R., "Storable Propellant Data for the Titan II Program", Bell Aerospace Systems Company Contract AF 04(694)-72 (March, 1962).

Liquid Propellants Manual, Liquid Propellants Information Agency, Contract NORD 7386.

Ludwigson, D. C., "Semiaustenitic Precipitation-Hardenable Stainless Steels", DMIC Report 164 (December 6, 1961).

Marin, Joseph, Engineering Materials, Prentice-Hall, Inc., New York (1952).

Military Handbook 5, "Strength of Aircraft Elements", (March, 1961).

Norton, H. W., "Compatibility of Materials", HOI 74-30, Edwards Air Force Base, California (November 15, 1961).

"Oxygen Difluoride (OF_2)", Product Data Sheet, Product Development Department, General Chemical Division, Allied Chemical Corporation (November, 1962).

Pan American World Airways, Manual, "Liquid Fluorine, N_2, N_2O_4, UDMH/N_2H_2", Pan American World Airways Guided Missile Range Division, Patrick Air Force Base, Florida, ASTIA 291244 (July, 1962).

Popov, E. P., "Correlation of Tension Creep Tests with Relaxation Tests", ASME Journal of Applied Mechanics (June, 1947).

"R 41 Allegheny Ludlum Nickel Base Alloy for High Temperatures", Allegheny Ludlum Steel Corporation (1961).

Rene' 41® — A General Electric Vacuum Melted Alloy", Metallurgical Products Department, General Electric Company (May, 1958).

Rinehard, John S., "The Behavior of Metal Under High and Rapidly Applied Stresses of Short Duration", Navord Report 1183 (September 27, 1949).

Sterner, C. J., and Singleton, Alan H., "The Compatibility of Various Metals With Liquid Fluorine", Air Products, Inc., WADD TR 60-819, AD 260087 (March, 1961).

Stewart, W. C., and Shreitz, W. G., "Thermal Shock & Other Comparison Tests of Austenitic and Ferritic Steels for Main Steam Piping — A Summary Report", Trans. of ASME, 1051-1072 (August, 1953).

Stamdler, I., "Hypersonic Fasteners Use Exotic Forms and Materials", Space/ Aeronautics, 56-62 (September, 1961).

Wagner, Herbert J. and Lund, Carl, Private communication, Battelle Memorial Institute.

Wetheimer, E. G., "Selecting Fastener Materials", Machine Design, 150 (February 4, 1960).

York, H. J., "Compatibility of Various Materials of Construction with Nitrogen Tetroxide N_2O_4", Aerojet-General Corp., Liquid Rocket Plant, Eng. Divn., Research & Materials Dept. Report RM-13 (October 22, 1958).

Manufacturing

Armco Steel Corp. Fabricating Data Bulletin, "Armco Precipitation Hardening Stainless Steels.Welding Armco 17-4PH Stainless Steel", Armco Steel Corp., Middletown, Ohio (September 15, 1958).

Barton, G. R., et al., "Tubular Joining by Induction Brazing and Fusion Welding Methods", SAE Aerospace Manufacturing Forum, The Ambassador Hotel, Los Angeles, California, October 8, 1962.

Carlson, R. J., Hanes, Hugh D., Hodge, E. S., Peterson, J. H., Simons, C. C., and Smith, E. G., Jr., "Joining Zircaloy-Stainless Steel and SAP Alloys By Friction Rolling and Explosive Techniques", Report to the AEC, BMI-1594 (September 4, 1962).

Douglass, John J., "Forming Practices with High Explosives", Du Pont Technical Information Bulletin (May 26, 1960).

Personal communication with Ronald J. Carlson and Charles C. Simons of the Department of Metallurgy and Physics, Battelle Memorial Institute.

Personal communications with Robert M. Evans of Metals Joining Division, Battelle Memorial Institute.

Johnson, P. C., Stein, B. A., and Davis, R. S., "Basic Parameters of Metal Behavior Under High Rate Forming", report to Watertown Arsenal Laboratories AD 271 401 (November, 1961).

Lepkowski, W. J., Monroe, R. E., "The Welding of Wrought Age-Hardenable Nickel-Base Alloys for Service at Elevated Temperatures", DMIC Memorandum 38, November 25, 1959.

"Metal Forming and Its Application in Today's Industries", Winchester-Western Division, Olin Mathieson Chemical Co., New Haven, Connecticut.

Mishler, H. W., Monroe, R. E. Rieppel, P. J., "Welding of High-Strength Steels for Aircraft and Missile Applications", DMIC Report 118, October 12, 1959

Olofson, C. T., Boulger, F. W., "Machining of Superalloys and Refractory Metals", DMIC Memorandum 134 (October 27, 1961).

Niemann, J. T., Sopher, R. P., Rieppel, P. J., "Arc Welding of High-Strength Steels for Aircraft and Missile Structures", DMIC Memorandum 27, July 31, 1959.

Paprocki, Stan J., Porembka, Stanley W., et al., "Joining Zircaloy-Stainless Steel and SAP Alloys by Friction, Rolling, and Explosive Techniques", report BMI-1594 to the AEC (September 4, 1962).

Pearson, J., "The Explosive Working of Metals", WADD TR 60-58, "Symposium on Processing Materials for Re-entry Structures", May 1960.

Pipher, F. C., Rardin, G. N., and Richter, W. L., "High Energy Rate Metal Forming", Lockheed Aircraft Corporation, California Division, Technical Report, AD 254 776 (October 18, 1957, to August 1, 1960).

Reason, R. E., "Surface Finish", Product Engineering (September 16, 1957).

Roth, Julius, "The Forming of Metals by Explosives", The Explosives Engineer (March-April, 1959).

Roth, Julius, "Metal Deformation by Explosives", Hercules Powder Co., Research Center (July, 1961).

Simons, Charles C., "Explosive Metalworking", DMIC Memorandum 71, OTS PB 161221 (November 3, 1960).

"Technical Data of Design and Production Interest - CM-R 41, Vacuum Melted Nickel Base Alloy", The Alloy Specialist, Cannon-Muskegon Corporation, undated.

"Tubular Joining by Induction Brazing and Fusion Welding Methods", SAE Aerospace Mfg. Forum (October 8, 1962).

Weisenberg, L., Morris, R. J., "Manufacture of René 41 Components", WADD TR 60-58, "Symposium on Processing Materials for Re-entry Structures", May, 1960.

Yernow, Dr. Louis, "Explosive Welding", Paper presented at New Bonding Methods Symposium of Annual ASM Metals Show, New York, New York, October 30, 1962.

Seals

Andrews, J. N., "Hollow Metallic O-Rings", United Aircraft Products, Inc., Dayton, Ohio (1962).

Ashmead, R. R., "Static Seals for Missile Applications", Jet Propulsion, 331-340 (July, 1955).

Beacham, T. S., and Towler, F. H., "Hydraulic Seals", Proc. Inst. Mech. Eng. (London), 532-569 (November, 1948).

Cass, E., McCuistion, T. J., "O-Ring Compression Force", Applied Hydraulics, 132-133 (October, 1959).

Dymkowski, J. V., "Pneumatic System Design", Aeronautical Engineering Review, 50-66 (March, 1958).

Eddy, R. W., "Low-Temperature Seals", Chrysler Corporation Missile Division Memorandum EDR 825, 1-31 (April, 1958).

Ellis, E. G., "Sealing Problems of High Speed High Altitude Aircraft and Guided Missiles", Scientific Lubrication, 10-14 (May, 1959).

Gilder, G., "Modular Hydraulic System Development", Chance Vought, AD 273 209 (August, 1961).

Hull, J. W., "Ring-Spring Design for High Performance Metal Static Seals", Hydraulics & Pneumatics, 122-126 (September 1960).

Jordan, J., "Extreme Temperature Sealing", Missile Design & Development (January, 1959).

Keefe, John H., Davis, Noah S., "Static Seals for Concentrated Hydrogen Peroxide", Symposium on Aircraft High Temperature Static Seals for all Media, Cleveland, Ohio, ASTIA 101652 (May 18-19, 1954).

Kenyon, R. L., "Pressure-Energized Seals", Rocketdyne, Divn. of NAA, AFBMD-TR-60-74 (July, 1960).

Logan, S. E., "Static Seal for Low-Temperature Fluids", Jet Propulsion, 334-340 (July, 1955).

Liberto, R. R. "Research and Development on the Basic Design of Storable High-Energy Propellant Systems and Components", Bell Aerosystems Company, AFFTC TR-60-61 (May 19, 1961).

Mayhew, "Design and Development of a 1000 F Hydraulic System", Republic Aviation, AD 257940 (June, 1960).

Middleton, R. E., "Hydraulic and Pneumatic Problems in High-Performance Aircraft", Applied Hydraulics, 98-101 (December, 1956).

Newell, G. C. , "Preliminary Results of All Metal Boss Evaluation & Development", presented to SAE Committee A6, Montreal, Canada, April, 1962, by Boeing Aircraft, Transport Division, 1-11 (September, 1961).

Niemeier, B. A. , "Seals to Minimize Leakage at Higher Pressure", Trans. of ASME, 369-379 (September, 1952).

Noonan, J. W. , "Dependencies in Seal Materials and Design for Environmental Extremes", Society of Automotive Engineers, National Aeronautic Meeting (April 3-6, 1962).

"Power Feed Seals for High Pressure High Temperature Helium", Electromechanical Design, 28-29 (April, 1962).

Richards, C. M. , "Missile Piping Methods", Convair Astronautics, General Dynamics Corp. , ERR-AN-120, 1-17.

Rossheim, D. B. , and Markl, A. R. C. , "Gasket Loading Constants", Mechanical Engineering, Vol. 65, 1943, Page 647.

Skinner Seal Co. , "Metal Seals Solve Missile Leakage Problems", Aviation Age, 49-51 (May, 1957).

Shaw, C. J. , "Laboratory Test and Evaluation of Seals Used in the Propellant Line Systems", Douglas Aircraft, Report DEV-3227 (March 30, 1960).

Symposium on Aircraft High Temperature Static Seals, Applied Hydraulics, 93-101 (November, 1954).

Whalen, J. J. , "How to Select the Right Gasket Material", Product Engineering, 52-56 (October 3, 1960).

Willis, W. W. , "An All-Metal Sealing Joint", Missile Design & Development, 18-19 (August, 1958).

Testing

"Avica Ferrule Type Tube Fittings", Douglas Aircraft, Technical Memorandum DM 18-P&M-L0567 (February 28, 1958).

"Avica 2" Ferrule-Type Tube Assemblies", Douglas Aircraft, Technical Memorandum DM 18-P&M-L0940, (September 24, 1958).

Carlson, A. F. , "Interim Report of Conical Seals for Flared Tubing", Convair Astronautics, General Dynamics Corp. , AN 59MD3008-1.

Cerbin, W. G. , "Performance Characteristics of Flareless and Flared Fittings", Weatherhead Company Report 1060, 1-9 (August, 1959).

Currie, W. E. , "Pressure & Pull Tests on Size 24 'Ferulok' 17-4 PH Ferrules", Parker Appliance Co. Report 4320 D-5214, 1-11 (April 17, 1959).

Currie, W. E. , "Industrial Hydraulic Tube Fittings Meet New Fields and Problems",
SAE Paper S317 (September, 1961).

Davies, R. H. , "The J.I.C. Performance Standards for Tubing and Tube Fittings",
Applied Hydraulics, 9-27 (November, 1949).

Dubrow, A. , "Investigation of the Effect of Pre-Stress on Fatigue-Vibration Life of
High Pressure Hydraulic System Tubing", Aeronautical Materials Laboratory,
Philadelphia, Pennsylvania, AML NAM AE 6272, 1-13 (April 5, 1955).

Floreen, E. D. , "Double Seal Conoseal Joints for High Temperature Gas Cooled
Reactor", Marman Division, Aeroquip Corporation (July, 1962).

"Freon Leakage Test of Avica Tube Coupling", DC8 P & M-L0094 (March 28, 1957).

Kupiec, H. P. , "Testing of Metal Boss Seals", Aircraft Equip. Testing Co. , AD 74-322,
1-61 (April, 1955).

Lenhart, H. G. , and Gartside, W. , "Flared Tubing Fatigue Test", Boeing Aircraft,
T 2-1432, 1-33 (November 11, 1957).

Lundback, A. V. , "Evaluation of Annealed Stainless Steel Tubing and 'AN' Fitting
Joints", Aerojet-General SCR 56 (June 21, 1961).

Oliva, J. , "Report on Test on Dynatube", Resistoflex Corp. , TRA-1490, 1-31 (July 15,
1960).

Oliva, J. , "Report of Test on Dynatube Assemblies — High Temperature", Resistoflex
Corp. , TRA-1491, 1-4 (August 17, 1960).

Oliva, J. , "Report of Test on Dynatube Assemblies — Air & Helium Test", Resistoflex
Corp. , TRA-1525, 1-4 (May 25, 1961).

Oliva, J. , "Report of Test on Dynatube Assemblies — Helium Testing", Resistoflex
Corp. , TRA-1562, 1-7 (April 9, 1962).

Parker, W. E. , "Fitting, Tubing, and Line Support Test Program Status Program",
North American Aviation, AD 131845.

Perkins, C. C. , "Testing of Seal Designs and Materials", Arnold Engr. Dev. Center,
AD 72503, 1-39 (February, 1955).

Pittiglio, C. L. , "Hydrostatic Tests of High-Pressure Steel Valves and Fittings", Navy
Department, AD 215 727 (May, 1949).

Popov, E. P. , "Correlation of Tension Creep Tests with Relaxation Tests", ASME
Journal of Applied Mechanics (June, 1947).

Seibel, L. L. , and McGillen, V. W. , "Hydraulic and Pneumatic Fitting and Tubing Test
Program", AD 235024, North American Aviation (November, 1959).

"Summary of Test Results of Various Configurations of Couplings with Gamah Metal
Seals", Gamah Corp. , 1-12 (December 17, 1960).

Whelan, J. S. , "Test of 6,000 psi Socket Weld Fittings", U. S. N. Engineering Experiment Station, AD 206 396 (January, 1958).

White, H. F. , "Missile Leak Report", Convair Astronautics, General Dynamics Corp. , AR 141-1-3 (March, 1962).

Threads

Almen, J. O. "Fatigue Durability of Prestressed Screw Threads", Product Engineering, 153-156 (April, 1951).

Bluhm, J. I. , and Flanagan, J. H. , "Procedure for the Elastic Stress Analysis of Threaded Connections Including the Use of an Electrical Analogue" Soc. for Experimental Stress, 85-100 (November, 1956).

Bronson, K. R. , and Faroni, C. C. , "Vibration Resistance of Thread Locking Devices", Product Engineering, 58-61 (October 10, 1960).

Brown, A. F. C. , and Hickson, V. M. , "A Photo-Elastic Study of Stresses in Screw Threads".

Gerstung, H. , "Friction as a Factor in Bolt Tension, Galling, Seizing, Part I", Assembly & Fastener Engineering, 32 (January, 1961).

Gerstung, H. , "Friction as a Factor in Bolt Tension, Galling, Seizing, Part II", Assembly & Fastener Engineering, 38 (February, 1961).

Goodier, J. M. , "The Distribution of Load on the Threads of Screws", Journal of Applied Mechanics, A10-A16 (March, 1940).

Hanneman, W. M. , "How Much Torque Tightens A Screw", Machine Design, 179-182 (October 13, 1960).

Heywood, R. B. , "Tensile Fillet Stresses in Loaded Projections", Proc. Inst. Mech. Engineers, 384-398 (October, 1947).

Heywood, R. B. , "Tensile Fillet Stresses in Loaded Projections", Proc. I. Mech. Engr. , 160, 124 (1949).

Inglesby, J. V. , "Strength of Screw Threads of Whitworth Form", Journal of the Royal Aeronautical Society, 710-717 (April, 1945).

Kalevitch, R. , "Pneumatic High Pressure Fitting Operational Test", Douglas Aircraft Report 2364, 1-11 (January 10, 1956).

Modes, E. E. , "Selection of Screw Thread for Maximum Axial Force", Product Engineering, 244-245 (March, 1946).

Schwartz, A. , "New Thread Form Reduces Bolt Breakage", Steel, 86 (September 4, 1950).

Smith, C. W., and Low, A. C., "The Effect of Fit and Truncation on the Strength of Whitworth Threads Under Static Tension", Machinery, 817-823 (June 16, 1949).

Sopwith, D. G., "The Distributions of Load in Screw Threads", Proc. Inst. Mech. Eng. (London), 373-383 (October, 1947).

Waltermire, W. G., "Coarse or Fine Threads", Machine Design 134-140 (March 17, 1960).

Walker, P. B., "Fatigue of a Nut and Bolt", Journal of the Royal Aeronautical Society, 62 (570), 395-407 (June, 1958).

DISTRIBUTION LIST

	Number of Copies		Number of Copies
National Aeronautics and Space Admin. Langley Research Center Langley Field, Virginia Attn: E. R. Gilman, Librarian	1	Bureau of Naval Weapons Department of the Navy Washington 25, D. C. Attn: RMMP-24	2
National Aeronautics and Space Admin. Lewis Research Center 21000 Brookpark Road Cleveland 35, Ohio Attn: Library	1	Bureau of Naval Weapons Department of the Navy Washington 25, D. C. Attn: RMMP-4	1
Office of the Director of Defense Research and Engineering Washington 25, D. C. Attn: D. B. Brooks		Bureau of Naval Weapons Department of the Navy Washington 25, D. C. Attn: RRRE-6	1
Office of Fuels & Lubricants	1	Commander Pacific Missile Range	
National Aeronautics and Space Admin. George C. Marshall Space Flight Center Huntsville, Alabama Attn: Library	1	Point Mugu, California Attn Tech. Library, Code 212	1
National Aeronautics and Space Admin. Goddard Space Flight Center Greenbelt, Maryland Attn: Library	1	Commander U. S. Naval Ordnance Test Station China Lake, California Attn: Code 45	2
National Aeronautics and Space Admin. Manned Spacecraft Center P. O. Box 1537 Houston 1, Texas Attn: Library	1	Commander Naval Ordnance Laboratory White Oak Silver Springs, Maryland Attn: Dr. J. R. Holden	1
Scientific and Technical Info. Facility P. O. Box 5700 Bethesda, Maryland Attn: NASA Representative	1	Director (Code 6180) U. S. Naval Research Lab. Washington 25, D. C. Attn: H. W. Carhart	1
Department of the Air Force Headquarters USAF, DCS/R&T Washington 25, D. C. Attn: AFRDR/AS	1	Department of the Navy Office of Naval Research Washington 25, D. C. Attn: Power Branch - Code 429	1
Commanding Officer Picatinny Arsenal Liquid Rocket Propulsion Laboratory Dover, New Jersey Attn: Technical Library	1	Commanding Officer ONR Branch Officer 1030 East Green Street Pasadena, California	1
Headquarters Air Force Flight Test Center Air Force Rocket Propulsion Laboratory Edwards Air Force Base California		Commanding Officer U. S. Naval Underwater Ordnance Sta. Newport, Rhode Island Attn: W. W. Bartlett	1
Attn: Mr. Roy A. Silver, DGRPD Contract No. AF 04(611)-8176	10	Superintendent U. S. Naval Postgraduate School Naval Academy Monterey, California	1

	Number of Copies		Number of Copies
Arnold Engr. Development Center Air Force Systems Command Tullahoma, Tennessee Attn: AEOIM	1	Space Systems Division Air Force Systems Command P. O. Box 262, AF Unit Post Office Los Angeles 45, California Attn: TDC	1
Aeronautical Systems Division Wright-Patterson AFB, Ohio Attn: ASNRPP	1	Air Force Missile Dev. Center Holloman AFB, New Mexico Attn: MDGRT	1
Commanding General Aberdeen Proving Ground Maryland Attn: Ballistic Res. Lab. ORDBG-BLI	1	Air Force Systems Command Andrews AFB Washington 25, D. C. Attn: SCTAP	1
Commander U. S. Army Missile Command Redstone Arsenal, Alabama Attn: Technical Library	2	Commander AFSC Foreign Technology Division Wright-Patterson AFB, Ohio Attn: RTD (TD-E3b)	1
U. S. Army Chemical Research and Development Labs. Army Chemical Center, Maryland Attn: K. H. Jacobsen, Medical Research Directorate	1	Defense Document Center Concord Station Alexandria, Virginia	20
Commanding Officer Diamond Ord. Fuze Lab. Washington 25, D. C. Attn: AMXDO-TI-B	1	Mr. E. Floreen, Sr., Project Engineer Marman Division Aeroquip Corp. 11214 Exposition Blvd. Los Angeles 64, California	1
Commanding Officer Army Research Office (Durham) Box CM, Duke Station Durham, North Carolina	1	Burton Z. Chertoh Metallurgical Processing Corp. 180 Michael Drive Syosset, L. I., New York	1
Commanding Officer Picatinny Arsenal Dover, New Jersey Attn: Librarian	1	Sealol Inc. Warwick Industrial Park Providence 5, Rhode Island	1
Commanding General White Sands Missile Range New Mexico Attn: ORDBS Technical Library	1	Air Force Systems Command Attn: SCTAP Andrews AFB Washington 25, D. C.	1
Commander Aeronautical Research Laboratory Wright-Patterson AFB, Ohio Attn: AFC, Mr. Karl Scheller	1	Research and Technology Division Air Force Systems Command Attn: RTA Bolling AFB, 25, D. C.	1
Aeronautical Systems Division Wright-Patterson AFB, Ohio Attn: ASRCEE-1	1	Product Engineering and Research Dept. Tube Turns Incorporated Louisville, Kentucy	1

DISTRIBUTION LIST
(Continued)

	Number of Copies		Number of Copies
Robert H. Cummins The Deutsch Company P. O. Box 61188 Los Angeles 61, California	1	Mr. Adrien Aitkin Stanford Research Institute Menlo Park, California	1
George A. Mahoff Gamah Corporation Box 685 Santa Monica, California	1	Mr. John C. Bloom, Test Group Engineer Hydromechanical Design Section Douglas Aircraft Co., Inc. Long Beach, California	1
Wm. C. Musham Imperial-Eastman Corporation 6300 West Howard Street Chicago 48, Illinois	1	Mr. L. Andrews, Supervisor Space Propulsion Group Douglas Aircraft Co., Inc. Santa Monica, California	1
Mr. R. H. Williams Harrison Manufacturing Corp. 2908 N. Naomi Street Burbank, California	1	Mr. W. E. Currie The Parker Appliance Co. 17325 Euclid Avenue Cleveland 12, Ohio	1
R. W. Muery Brown Engineering Mail Stop 13 P. O. Box 917 Huntsville, Alabama	1	Mr. Bruce Pauly The Weatherhead Company Cleveland, Ohio	1
Mr. Keith Chandler (M-S&M-PA) Redstone Arsenal Huntsville, Alabama	1	Mr. Jasper McKae, Chief Mechanical Testing Flexonics Co. Bartlett, Illinois	1
General Electric Co. Attn: R. C. Elwell General Engineering Lab. Bldg. 37-1020 Schnectady, New York	1	Mr. Glen Howell Space Technology Laboratory Radiation and Compton Blvds Los Angeles, California	1
Mr. Miles C. Abbott National Utilities Corporation 135 E. Railroad Avenue Monrovia, California	1	Mr. Sherwin Lewis Propulsion Engineer Aerospace Corp. Los Angeles, California	1
Mr. Ralph Middleton Lockheed Aircraft Corp. 2555 N. Hollywood Way Burbank, California	1	Mr. Richard Weiner Development Engineer Jet Propulsion Laboratory 4800 Oak Grove Drive Pasadena, California	1
Mr. J. B. Smith Systems and Controls Aerojet General Sacramento, California	1	Mr. C. M. Richards, Design Engineer Astronautics Division General Dynamics Corp. San Diego, California	1
.Mr. Marvin G. Luebben Dept. 64-62 Lockheed Missiles and Space Co. Sunnyvale, California	1		

Number of Copies

Mr. John F. Mayer
Department 596, Group 121
Rocketdyne Division
North American Aviation, Inc.
6633 Canoga Avenue
Canoga Park, California   1

Mr. Frank Brock
Resistoflex Corp.
Roseland, New Jersey   1

Mr. Paul Bauer
Project Engineer
Mechanics Research Division
Armour Research Foundation
10 West 35th Street
Chicago 16, Illinois   1

Mr. Ralph E. Robertson
M-P&VE-PM-HIC-3
Marshall Space Flight Center
Huntsville, Alabama   1

Mr. M. H. Weisman, Research Specialist
Metalic Materials Laboratory
Los Angeles Division
North American Aviation
Los Angeles 9, California   1